DEVELOPMENT OF DEGRADABLE POLYPROPYLENE USING ORGANIC ADDITIVES

Thesis

Submitted for fulfillment of the Degree

of

Doctor of Philosophy

By

Sable Sunil Satwaji
(Registration No.: 901701002)

Under the guidance of

Dr. Haripada Bhunia
Professor
Department of Chemical Engineering,
Thapar Institute of Engineering &
Technology (Deemed to be University),
Patiala

Dr. Sanjeev Kumar Ahuja
Associate Professor
Department of Chemical Engineering,
Thapar Institute of Engineering &
Technology (Deemed to be University),
Patiala

Department of Chemical Engineering
Thapar Institute of Engineering & Technology (Deemed to be University)
Patiala – 147004, Punjab (India)
www.thapar.edu

September 2020
April 2021

Dedicated

To

My Parents

Mr. Satwaji Sable & Mrs. Suwarna Sable

And

The most precious inspiration of my life

My wife and daughter

Mrs. Priyanka Sable and Ms. Shivneri Sable

Certificate

This is to certify that the thesis entitled "**Development of degradable polypropylene using organic additives"** being submitted by **Mr. Sable Sunil Satwaji** (Roll No. 901701002) to Department of Chemical Engineering, Thapar Institute of Engineering & Technology (Deemed to be University), Patiala in fulfillment of the degree of Doctor of Philosophy, is a record of bonafide research work carried out by him under our guidance and supervision and is worthy of consideration for the award of the degree of **Doctor of Philosophy** of the University.

The results embodied in the thesis have not been submitted in part or full to any other University or Institute for the award of any degree or diploma.

(Haripada Bhunia)
Professor
Department of Chemical Engineering
Thapar Institute of Engineering & Technology
(Deemed to be University), Patiala

(Sanjeev Kumar Ahuja)
Associate Professor
Department of Chemical Engineering
Thapar Institute of Engineering & Technology
(Deemed to be University), Patiala

Acknowledgements

I would like to express my sincere regards and gratitude to my supervisors **Dr. Haripada Bhunia,** Professor& Head and **Dr. Sanjeev Kumar Ahuja**, Associate Professor, Department of Chemical Engineering, Thapar Institute of Engineering & Technology (Deemed to be University) for providing me such a valuable research opportunity. They provided me with motivation, knowledge and the tools to carry out this research and for future success. I am thankful for their constant encouragement, intellectual generosity and valuable contribution of their time throughout the course of this work.

I am extremely thankful to **Prof. Prakash Gopalan**, Director, Thapar Institute of Engineering & Technology (Deemed to be University), **Shri Gurbinder Singh, Registrar,** Thapar Institute of Engineering & Technology (Deemed to be University), **Prof. Rafat Siddique**, Dean of Research & Sponsored Projects, Thapar Institute of Engineering & Technology (Deemed to be University) for giving the necessary approvals and kind support to perform this research work.

My sincerest thanks are to **Dr. P. K. Bajpai** (Ex-Distinguished Professor), Department of Chemical Engineering, Thapar Institute of Engineering and Technology, Patiala for providing scientific advice and technical knowledge through many insightful discussions. His valuable comments and suggestions helped me a lot to improve my manuscripts.

I would like to express the utmost thank to my doctoral committee members **Dr. Rajeev Mehta**, Professor, Department of Chemical Engineering, Thapar Institute of Engineering & Technology (Deemed to be University); **Dr. Raj K. Gupta**, Professor, Department of Chemical Engineering, Thapar Institute of Engineering & Technology (Deemed to be University) and **Dr. Susheel Mittal,** Senior Professor, School of Chemistry & Biochemistry (DST-FIST Sponsored), Thapar Institute of Engineering & Technology (Deemed to be

University) for providing their expertise and vast experience throughout the course of this research in a patient and encouraging manner. The generous support of all the staff members of Department of Chemical Engineering, Thapar Institute of Engineering and Technology, Patiala (Deemed to be University) is greatly appreciated.

I am also grateful to **Dr. Veena Choudhary,** Ex-Professor, Centre of Polymer Technology, Indian Institute of Technology, Delhi for her kind support, guidance and constructive comments which have been of immense value in improving the quality of my research work.

Also, my sincere thanks are to **Dr. Vishal Goel,** IOCL, Faridabad, Haryana, India for extending the compounding facilities used for this study.

I express deep sense of gratitude to my senior **Dr. Gaurav Madhu**, and **Dr. Dev Kumar Mandal**, my colleagues **Mrs. Balpreet Kaur** and **Mr. Saudagar Dongare** for providing all the encouragement and support at various stages of work. I express my deepest gratitude to my parents **Mr. Satwaji Sable** and **Mrs. Suwarna Sable**, my brother **Mr. Balasaheb Sable**, and my wife and daughter **Mrs. Priyanka Sable** and **Shivneri Sable** for their love, never ending support, and encouragement and would like to dedicate this thesis to them. I am the first engineer in the family and my village, who has been able to attend college and go this far to receive my Ph.D.

Finally, I would like to gratefully acknowledge the financial support and Research Associateship from **Council of Scientific and Industrial Research (CSIR), Government of India, Delhi** through research project.

Above all, I express my indebtedness to the **"ALMIGHTY"** for all his blessing and kindness.

Sable Sunil Satwaji

Abstract

Polyolefins like polypropylene (PP) are extensively used for packaging applications because they are economical and convenient. However, PP is not eco-friendly because of its non-biodegradable nature. Consequently, its disposal and management at the end of the service life are a cause of significant global concern. These factors have led to the development of environmentally degradable polymeric material that can degrade under composting. The main objective of this study was to develop biodegradable PP by compounding with pro-oxidant. Cobalt stearate remained the focus because it exhibited promising results for initiating thermo-oxidative degradation and hence biodegradation in earlier studies. Before and after abiotic pretreatment (accelerated weathering), the influence of pro-oxidant loading on the molecular weight changes, morphological, physical, thermal, chemical, and biodegradability characteristics of packaging films was studied. Before abiotic pretreatment, the rheological properties of packaging films were also studied. The biodegradation kinetic modelling of oxidants (two different types) loaded PP films without and with abiotic pretreatment was then carried out. The effect of the biodegradation intermediates on the environment has also been evaluated by different ecotoxicity tests. This work has two parts, the first in which CoSt is used, and the second in which modified CoSt is used as pro-oxidant.

In the first part of this work, PP filled with different proportions (0 to 2 phr) of CoSt were prepared in a twin-screw extruder by compounding technique. Eight films of these compounds were prepared using compression moulding. Subsequently, abiotic pretreatment (accelerated weathering) was conducted to investigate the effect of accelerated weathering of CoSt filled PP composite films. These films were characterized for molecular weight changes, chemical, physical, thermal, and morphological properties (before and after abiotic and biotic treatments). Rheological properties of the CoSt filled PP composites were investigated. The biodegradation (biotic treatment) of the CoSt filled PP films without and after abiotic pretreatment were studied as per ASTM D 5338 under controlled composting conditions. The biodegradation kinetic modeling of CoSt filled PP films without and after abiotic pretreatment was then carried out. The biodegradation intermediates were subsequently evaluated for their eco-toxicological impact. The presence of CoSt and other oxygen products after degradation of composite PP by abiotic pretreatment was confirmed by Fourier transform infrared spectroscopy. The highest carbonyl index (0.83) was found in the film with 2 phr CoSt sample after abiotic pretreatment. As the addition of CoSt was progressively increased from 0 to 2 phr, the tensile strength (before

abiotic pretreatment) decreased from 35 to 14.5 MPa thermal stability also decreased as shown by TGA. Before and after abiotic pretreatment, the crystallinity of CoSt filled PP decreased with increase in CoSt from 0.2 to 2 phr, as indicated by DSC and XRD. Rheological studies confirmed the pseudo plastic nature of all the modified composites. Without and after abiotic pretreatment, the maximum biodegradation by the film having 2 phr CoSt was shown to be 19.80%, and 36.42 % respectively. SEM results of biotically treated films also showed erosion, several small pits and increased roughness on the modified PP films. The surface morphology of the films supported the biodegradation results. The significant decrease in molecular weight proved that chain scission mechanism occurred leading to the formation of intermediates, which further led to microbial assimilation. The overall results indicated that the addition of CoSt and abiotic treatment significantly enhanced the biodegradation of PP.

This work was also aimed at modeling the kinetics of biodegradation of PP loaded with CoSt as pro-oxidant without and after abiotic pretreatment. The experimental data were analyzed using an eight-parameter Komilis model containing a flat lag phase. The model formulations involved hydrolysis of primary solid carbon and its subsequent mineralization. The first step was rate controlling and it included hydrolysis of slowly (C_s), moderately (C_m), and readily (C_r) hydrolysable carbon fractions in parallel. The model parameters were evaluated by means of nonlinear regression technique. The model parameters and un-degraded/hydrolysable/mineralizable carbon evolutions followed only one kinetic regime in both without and with abiotic pretreatment. All the films involved moderately, and readily hydrolysable carbons but the absence of slowly hydrolysable carbon. For the films without abiotic pretreatment, the rate of degradation reached its maximum (0.223-0.740 % per day) at around 5-11th day. With abiotic pretreatment, the rate of degradation reached its maximum (0.322-0.897 % per day) at around 12-39th day. For all the films, readily hydrolysable carbon fractions and their hydrolysis rate constants (k_r) appreciably increased with increasing pro-oxidant loading. All the films showed the presence of growth phase because of their high initial readily hydrolysable carbon fractions. The methods presented here can be used for the design and control of other similar systems. The eco-toxicity tests of the degraded material, namely, microbial test, plant growth test, and earthworm acute-toxicity test demonstrated that the biodegradation intermediates were nontoxic. Hence, CoSt filled PP has high industrial potential to make biodegradable flexible packaging.

In the second part of this work, the changes in the properties of PP after loading of modified-CoSt pro-oxidant were studied. A master batch containing 10 phr of cobalt stearate in PP (PP100CoSt10) was made in a co-rotating twin-screw extruder at a speed of 150 rpm under a N_2 blanket and pelletized. This masterbatch was aged at 110 ^oC for 48 h. After that, it was crushed into powder, sieved, and used as a modified pro-oxidant (designated as T). Different proportions of modified-CoSt pro-oxidant were filled (5-30 phr) in PP, and composites were prepared. Five films of these composites were prepared using hot press moulding. These films were studied as in the first part. Before and after pretreatment, the carbonyl index of the films increased to (1.1 maximum) with modified pro-oxidant loading and time of abiotic pretreatment. The tensile properties (before abiotic pretreatment) of the modified pro-oxidant loaded PP films decreased. The thermal stability (before and after abiotic pretreatment) of the modified pro-oxidant filled PP films reduced as indicated by TGA. After abiotic pretreatment, the DSC results confirmed that the addition of modified pro-oxidant reduced the crystallinity of the PP films from 63 to 42.53 % (and 77 to 40.5% from XRD data). This led to enhanced degradation of PP. Before abiotic pretreatment, pseudo plastic behavior of all the modified-CoSt loaded PP films was confirmed by rheological studies. The highest biodegradability (28.87%) was obtained in the film containing 30 phr of modified pro-oxidant without abiotic pretreatment. With abiotic pretreatment, the maximum biodegradability (38.78%) was obtained in an abiotically treated film containing 30 phr of modified pro-oxidant in it. After the biodegradability test, SEM results also revealed several small pits, erosion, as well as enhanced roughness on the PP film samples. Decrease of molecular weight is higher in the case of modified pro-oxidant compared with CoSt pro-oxidant.

The kinetic modeling of the biodegradation was carried out in the same manner as was done above in the first part. The same Komilis model with a flat lag phase was used to correlate the experimental data. The model parameters and un-degraded/hydrolysable/mineralizable carbon evolutions followed only one kinetic regime in both before and after abiotic pretreatment. All the films involved moderately, and readily hydrolysable carbons but the absence of slowly hydrolysable carbon. For the films without abiotic pretreatment, the rate of degradation reached its maximum (0.407-0.730 % per day) at around 18-23th day. With abiotic pretreatment, the rate of degradation reached its maximum (0.408-0.920) % per day) at around 15-25th day. For all the films, readily hydrolysable carbon fractions and their hydrolysis rate constants (k_r) appreciably increased with increasing modified pro-oxidant loading. All the films showed the presence of growth phase because of their high initial readily hydrolysable carbon fractions.

All the eco-toxicity tests of the degraded product materials demonstrated that the degraded products were nontoxic. Hence, the prepared composites can be effectively used as biodegradable flexible packaging materials. A schematic of the overall thesis work is shown in Fig. 1.

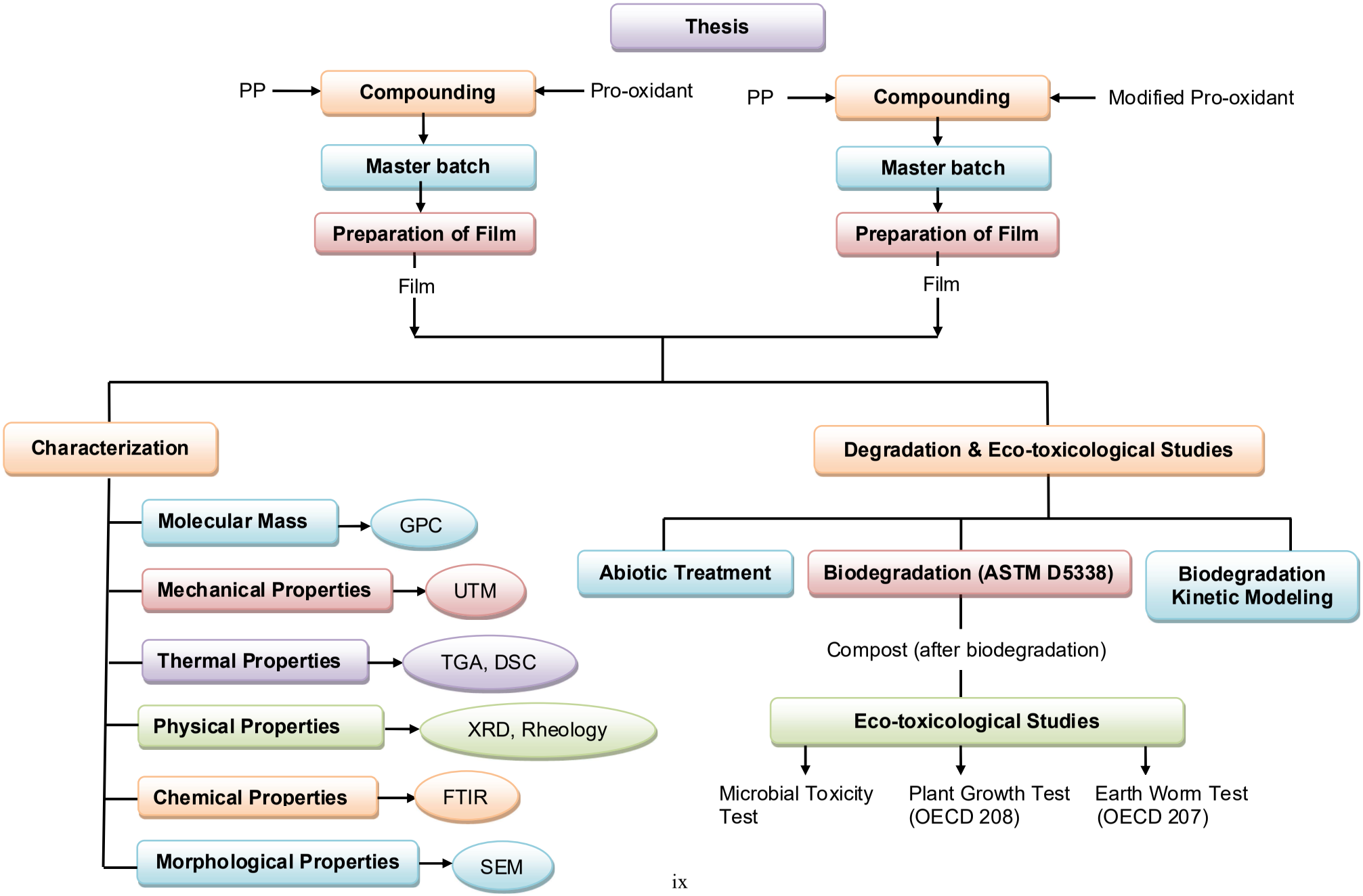

Fig. 1 Schematic of overall thesis work

Table of Contents

LIST OF FIGURES

LIST OF TABLES

LIST OF SYMBOLS

c	Duration of lag phase during the initial phase of biodegradation before the onset of CO_2 production
C_{aq0}	% of initial mineralizable intermediate carbon
C_{m0}	% of initial moderately hydrolysable solid carbon
CO_2	Carbon dioxide
$CO_2(Th)$	Theoretical carbon dioxide
C_{r0}	% of initial readily hydrolysable solid carbon
C_{s0}	% of initial slowly hydrolysable solid carbon
Da	Dalton
G'	Storage modulus
G''	Loss modulus
ΔH_c	Enthalpy of crystallization
ΔH_f	Enthalpy of fusion
k_{aq}	Rate constant for mineralizable water – soluble C-CO_2
k_m	Moderately first-order hydrolysis rate constant
k_r	Readily first-order hydrolysis rate constant
k_s	Slowly first-order hydrolysis rate constant
$\overline{M_n}$	Number average molecular weight
$\overline{M_w}$	Weighted average molecular weight
MPa	Mega pascal
T	Absolute temperature (K)
T_c	Crystallization temperature
T_g	Glass transition temperature
T_i	Initial degradation temperature
T_m	Melting temperature
T_{max}	Maximum degradation temperature
T_f	Final degradation temperature
X_c	Degree of crystallinity

LIST OF ABBREVIATIONS

ASTM	American Society for Testing and Materials
AAc	Acrylic acid
AgSt	Silver stearate
CAGR	Compound annual growth rate
CaSt	Calcium stearate
CEL	Microcrystalline cellulose
CFU	Colony forming units
CrSt	Chromium stearate
CoSt	Cobalt stearate
CuSt	Copper stearate
DDR	Draw-down ratio
DSC	Differential scanning calorimetry
DTA	Differential thermal analysis
DTG	Differential themogravimetry
EB	Elongation at break
EPA	Environmental protection agency
ESC	Environmental stress cracking
FeSt	Iron stearate
FMCG	Fast moving consumer goods
FTIR	Fourier transform infrared
HDPE	High density polyethylene
HT-GPC	High temperature gel permeation chromatography
ISO	International Organization for Standardization
LDPE	Low density polyethylene
LLDPE	Linear low-density polyethylene
MA	Maleic anhydride

MA-g-PP	Maleic anhydride grafted polypropylene
MFI	Melt flow index
MgSt	Magnesium stearate
MMT	Montmorillonite
MMTA	Million metric ton per annum
MnSt	Manganese stearate
MTA	Metric ton per annum
MSW	Municipal solid waste
MWD	Molecular weight distribution
NiSt	Nickel stearate
OECD	Organization for Economic Cooperation and Development
PCL	Poly(ε-caprolactone)
PDI	Polydispersity index
PE	Polyethylene
PDI	Polydispersity index
PHA	Poly(hydroxyalkanoates)
PHB	Poly(3-hydroxybutyrate)
phr	Parts per hundred of resin
PLA	Polylactic acid/polylactide
PMMA	Poly (methyl methacrylate)
POM	Polyacetal
PP	Polypropylene
PP-g-AAc	Polypropylene grafted acrylic acid
PS	Polystyrene
PSW	Plastic solid waste
PVA	Poly (vinyl acetate)
PVC	Poly (vinyl chloride)

RID	Refractive index detector
SEM	Scanning electron microscopy
TG	Thermogravimetry
TGA	Thermogravimetric analysis
TOC	Total organic carbon
TPD	Tons per day
UNEP	United nations environment program
USD	US Doller
UV	Ultraviolet
VSt	Vanadium stearate
WEF	World economic forum
XRD	X-ray diffraction
ZnSt	Zink stearate

Chapter 1-Introduction

History of Polymers

Polymers are macromolecules, which are made up through the linking together of large numbers of much smaller molecules called monomers. The chemical reactions responsible for this process are known as polymerizations. Currently, the term “polymer” is utilized in plastic and composite industry, and it is frequently utilized to include the meaning of “plastic” or “resin”. Polymeric materials involve different polymers like polystyrene (PS), polyethylene (PE), polytetrafluoroethylene (Teflon), polypropylene (PP), poly (vinyl chloride) (PVC), poly (methyl methacrylate) (PMMA), and poly (vinyl acetate) (PVA). Polymers attained reputation during the 1500s as the British investigators found out a rubber ball in ancient Mayan city in Central America. Leo Hendrik Baekeland invented the first commercial synthetic plastic material phenol-formaldehyde “Bakelite” [1]. In World War-I, the first synthetic rubber known as methyl rubber was formed. Paul Flory carried out a lot of theoretical and experimental work in the polymer chemistry and was awarded the Nobel Prize for Chemistry. German chemist Hermann Staudinger had also accepted a similar felicitation for his polymer research work [2]. The first paper on polymerization was published by Staudinger in 1920. Polystyrene was invented in 1930, followed by the invention of Nylon in 1938, PE in 1941, and PP in 1954.

Polymers are classified in different ways like their line structure, origin, physical characteristics, and various applications, crystallinity, method of formation, degradation, as well as thermal behavior. Some polymeric materials that consist of mainly carbon and hydrogen are polystyrene, polybutylene, polyethylene, and polypropylene. These materials have found very convenient applications in packaging, building, transportation, agricultures, medical appliances, and communication. Several varieties of polymers with various characteristics are now produced through utilization of additives namely, fillers, antioxidants, coloring agents, flame retardants, plasticizers, etc. It gives required functionality to these products. Plastic materials have provided high performance goods and made life very easy in various ways. Commodity plastics are plastic materials that are utilized in large volumes and have an extensive range of applications. Fig. 1.1 shows the global demand in 2018-19 for major commodity plastic materials and it can be found that PE, PP, and PVC contribute more toward the use of plastics. The Indian demands for major

commodity plastics are shown in Fig. 1.2. PP, PE, and PVC again contribute more to the use of plastic materials.

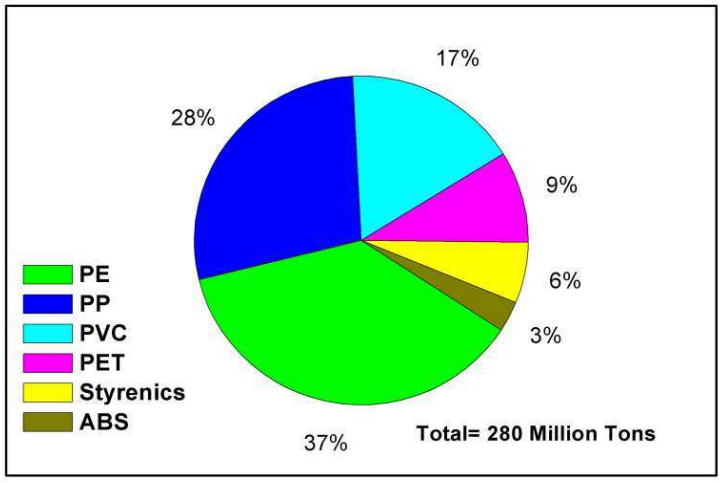

Fig. 1.1 Global demand for major commodity plastics in 2018-19 [3]

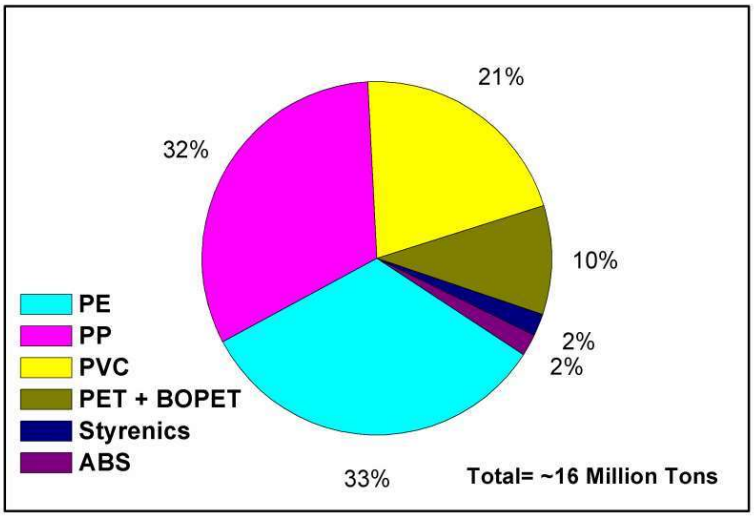

Fig. 1.2 Indian demand for major commodity plastics in 2018-19 [3]

The utilization and production of polymeric materials are as per the demand and supply. But in India, the demand and supply of different polymeric materials are not at par. In India, plastic utilization is 9.7 kg per person. Fig. 1.3 presents the consumption and production of various polymeric materials in the year 2017.

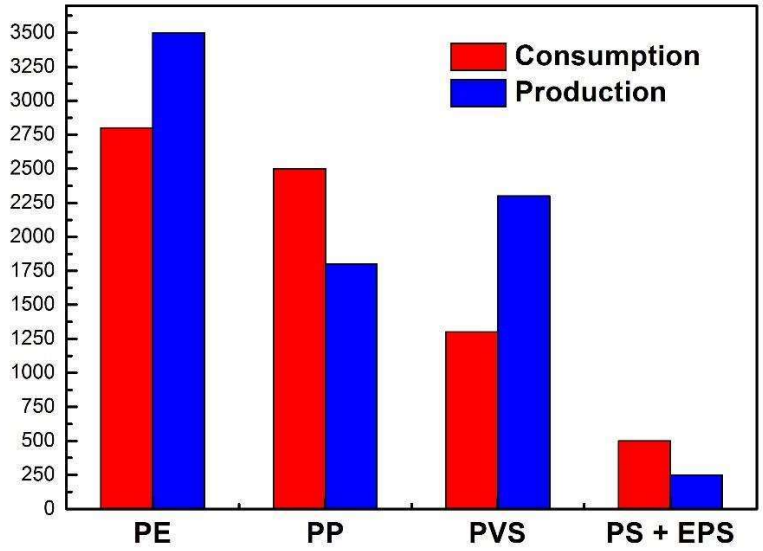

Fig. 1.3 Statistics on utilization and making of various polymeric materials in the year 2017 [4]

Today, we are using plastics that are made-up of petroleum resources. The development of new polymeric materials is a never finishing task. In the era of sustainability, researchers are mainly focused on developing biodegradable and compostable polymeric material. These biopolymeric materials are derived from natural resources and have characteristics almost the same as petroleum-based polymers and are eco-friendly. A polyolefin like polypropylene is a member of this group. After the development of PP, researchers have focused on improving its physico-chemical characteristics. PP is a thermoplastic polymeric material composed of long hydrocarbon chains of carbon and hydrogen atoms. According to its chemical structure and molecular weight, it will have various physical characteristics. PP has become the most desirable material due to its physical and chemical properties, involving its lightweight, durability, cost, high resistance, and the fact that it can be prepared easily and molded into different types of materials. It has been utilized in all sectors of life, including food packaging, and many other applications [5].

1.1 Polymeric materials in flexible packaging

The flexible packaging market is the fastest growing industry having a diversified market in the world. Globally, the market value for flexible packaging is reaching USD 31.7 billion in 2020. It is predicted to increase at a compound annual growth rate (CAGR) of 6.4% to around USD 59.6 billion by 2025 due to growing demand in foremost Asian markets like India and China [4, 6]. On an average, the production of plastic worldwide is crossing 150 million tons/year [7]. It is widely used in wrapping materials, packaging films, liquid containers, shopping, and garbage bags, building construction materials, toys, household, and industrial products, as well as clothing. The main part or ~ 44% of the worldwide plastic materials is utilized in the packaging industry [8]. The rapid population, urbanization, as well as industrial growth in emergent economies, has been driving governments to raise their construction expenditure to provide for growing infrastructure requirements. Rising construction spending by governments, particularly in China and India, will drive the demand for plastic polymers in infrastructure and construction applications. Food and soft drinks industry will have the maximum packaging markets share (in units) in the period 2016-2021 with a growth rate of 1.3% and 3.4%, respectively. During the same period 2016-2021, the rigid plastic materials will be the next gainers with the share progress rate of 0.6%. The flexible packaging market in India is set to rise by $ 9.76 bn in 2020-2024 expanding at a CAGR of 12% during the forecast period. In India, the packaging industry is poised to rise at 18% yearly including flexible (25%) and rigid (15%) packaging. The packaging is the 5th major area in Indian economy. It is one of the maximum growing areas in the country. As per packaging industry association of India (PIAI), the area is increasing at 22% to 25% each year. The main contributions of flexible packaging are in food packaging, cosmetics and toiletries, and the household care industry. This progress is mainly determined through its flexibility to match suitability (zip-locks, plastic closures), various sizes and shapes as well as low carbon footprint on the atmosphere in comparison to rigid plastic materials [9]. The worldwide and Indian packaging industry is emerging and growing every day. Today, this development is largely driven through the reasons such as increasing manufacturing, food processing, and pharmaceutical industries, fast-moving consumer goods (FMCG), healthcare section, as well as a subsidiary in the developing economies such as China, India, Brazil, Russia, and also some East European countries. Worldwide, plastics include 42 % of packaging with the combination of rigid and flexible plastic materials in packaging. Plastic materials are utilizing a lot for packaging applications because of innovative

visual demand for buyer attractiveness plus facility. Moreover, they increase the cleanliness quotient as well as lifetime of the products, particularly in the beverages with the food section. Flexible plastics remain the dominant packaging format in India. The move from application of rigid to flexible packaging has been a slow process as flexible packaging is visibly attractive, inexpensive, as well as strong. Customers prefer flexible packaging over rigid packaging because they are light weight, disposable, with their influence on the atmosphere being significantly lesser. Conventional polyolefin such as polyethylene (PE), polypropylene (PP), low-density polyethylene (LDPE), linear low-density polyethylene (LLDPE), as well as high-density polyethylene (HDPE) are very inexpensive and hence utilized broadly in packaging industries and in the manufacture of daily household goods.

A polymeric material shows unique properties and, therefore, has different packaging applications. PP has been a widely used plastic material and fastest-growing thermoplastic in the area of packaging, wrapping materials, clothing, fluid containers, building materials, household, and industrial products, shopping, and garbage bags, medical, and automotive industries. It is widely used in the packaging industry because of their cost-effectiveness, lighter, water resistance, good mechanical properties, durability, flexibility, and ease of processing. PP has excellent mechanical and water resistance properties and therefore is utilized in containers for shampoo, detergents, milk, deodorants, caps, bleach for bottles, and flexible packaging for ketchup bottles, yogurt cups, cereals, snacks, and crackers [7, 10]. Fig. 1.4 shows that 62 % of polymeric materials used in packaging (flexible) industry are PE and PP [11].

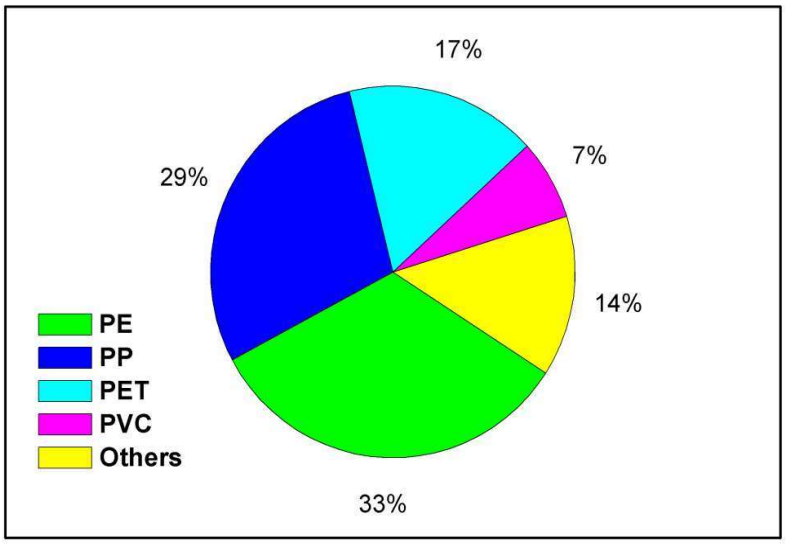

Fig. 1.4 Application of different plastic polymer products (%) [11]

1.1.1 Waste from packaging materials

Daily, large quantity of waste polymeric packaging material is dumped which ends up in to landfill, resulting in the number of urban wastes [6, 12]. Globally, as per World Bank, polymeric waste accounted for 8–12 % of total municipal solid waste (MSW) produced in various countries [13]. Barnes studied a statistical analysis and stated that about 10 % of municipal solid wastes (MSW) are only plastic-based and they are non-degradable in the environment [5, 14]. The real % changes in accordance with the earnings of the citizens in that country. The worldwide plastic solid waste (PSW) production in 2025 will rise to 9–13 % of the total MSW. In order to mitigate the negative consequences of PSW, attempts have been made for the recuperation of PSW by reprocessing. In Europe, about 50% of the produced PSW is reused and the remaining is discarded for landfill.

In India, the production of PSW was 5.6 million metric tons per annum by 2012 [4, 15]. According to the studies, the production of PSW would become nearly 16.5 million metric tons per annum (MMTA) in 2030. Also, polymeric material utilization in India is 16.5 MMTA in 2017-18. The polymeric material utilization of India's per capita was determined to be 9.7 kg in the financial year 2012-13. However, utilization and generation of different PSW are not the same in India [4]. The report prepared by Tata strategic on consumption and production of different PSW in 2017 is

shown in Fig. 1.3. Approximately 40% of contributions are from the packaging industries out of the total PSW. Every year, 500 billion to 1 trillion polymeric material bags are utilized globally, that is, over 1 million polymeric material bags consumed/minute in each year [16]. The second biggest source with a share of 20.3% of the total PSW is building and construction. The automobile sector is the 3rd sector having a share of 8.5%. The electrical and electronic equipment render 5.6% of PSW and is strongly followed by agricultural uses that have a share of 4.3%. Other application areas namely equipment, domestic and consumer goods, medical material as well as furniture make an overall of 21.7% of PSW [17].

One of the evilest effects of PSW is that it ends up in the sea. Each year, between 8 to 14 (MMTA) of PSW arrives at our sea, and the situation is getting worse [18]. Asia is the world leader in plastic pollution. As declared in the additional record reported in 2017 in Environmental Science and Technology journal, globally, 3 of the 10 rivers which transfer 90% of plastics to the world's seas are in India: the Brahmaputra, Ganga, and the Indus. Governments across Asia are waking up to the devastating environmental and monetary expenses of contaminated rivers as well as seas. The United Nations Environment Program (UNEP) has made marine plastic materials a crucial problem, highlighting the effects and finding the gaps in addressing marine plastic materials at every stage of the value chain. UNEP started a Clean Seas campaign in February 2017 to connect the public sector, the private sector, as well as governments, in a battle with marine plastic contamination. There was 1 kg plastic in the sea per 5 kg of fish in 2014. In terrestrial as well as aquatic coastal atmosphere, the synthetic plastic materials accumulated at a rate of 25 MTA. The overall quantity of plastic materials in the sea is probable to rise from 50 MT in 2015 to 150 MT by 2025 [6]. A World Economic Forum (WEF) study found that there will be more plastics than fish in the sea in weight by 2050. Plastic packaging accounts for 62% of all items recovered in coastal cleanup efforts. In 2014, the world's oceans about 2,68,940 tons of plastics materials were present and this value increases day by day [19]. Each year, India's contribution to plastic material waste that is discarded at the world level seas is a massively 60%. As per report of 2017-18, Central Pollution Control Board (CPCB) has estimated that India produced around 9.4 MMTA (26,000 tons per day) plastic polymer waste, new Delhi contributes 9,600 TPD [18]. Also, the Swachh Bharat Abhiyan or Clean India Mission was a country worldwide campaign from 2014 to 2019 to remove open defecation and improved waste management in urban and rural India.

1.1.2 Environmental impact of plastic waste

Presence of plastics in environment has become a worldwide problem [20]. Plastic pollution unfavorably affects wildlife, wildlife habitat, or humans [21]. This plastic waste may categorize into micro- and macro-plastic, based on its size [20, 22]. The eminence of plastic pollution is interrelated with plastic materials being of mechanical integrity, low-cost, flexibility, durability, and light weight, which is responsible for the high-levels of polymeric products utilized by humans [23, 24]. But it is degraded very slowly. Plastic pollution can adversely impact oceans, lands, and waterways. The enhanced collection of PSW on the ocean has caused more grave issues. Pollution due to PSW in the marine environment can be credited to the discarding of plastics directly/indirectly, through the persons into the ocean, involving actions for example cruise shipping, oil rigs, fishing, as well as actions on the land. From more human-occupied areas everywhere the plastic materials are brought to the ocean through water runoff, wind, etc.[20].

The large quantities of plastic fragments in the marine environment correspond to the increased utilization of plastic materials, particularly disposable/non-disposable, such as polypropylene (PP), polyethylene (PE), and polyethylene terephthalate (PET) polymeric products. Nearly 90 % of polymeric material debris that polluted seawater, which amounted to 5.6 million tons, comes from sea-based resources. Wastewater, utilized medicinal devices, mercantile ships banish cargo and another type of wastes introduce plastics into the marine. These polymeric substances can also by mistake end up into water during careless management. The biggest sea-based source of polymeric material contamination is waste fishing gear, accountable for 90 % of polymeric waste in a few zones. This apparatus involves different snares as well as nettings. Each year, a small above 10 % of polymeric material fragments in sea water comes from land-based resources, accounts to the tune of 0.8 MTA. A resource that has significant anxiety is landfill sites. Mostly, the waste in landfill sites is single utilized materials or packaging. Disposal of plastic materials this way results in its accrual [14]. The disposal of waste in landfill sites has low gas emissions risks than the disposal by incineration, since the former has space limits. Globally, approximately 83 % of tap water was contaminated due to plastics in the year 2017. This was the first research on worldwide drinking water pollution. After study, it was found that with a pollution rate of 94% and tap water in the United States was mostly contaminated, followed by Lebanon and India. European countries namely, France, Germany, and the United Kingdom had the highest pollution rate of

72%. This indicates that peoples can be consuming 3,000-4,000 micro-particles of polymeric material through tap water yearly. By studying the caloric intake of 15% Americans, Cox, et al. [25] recently estimated the annual exposure as 74,000 to 1,21,000 microplastics per person via inhalation and ingestion. Ocean tortoises are also influenced by plastic contamination.

The effects of worldwide changes on the seas were reported in the research project [26]. Plastic materials contamination does not only influenced animals in seas but also seabirds. Gulls in the North Sea, had an average of thirty parts of plastics in their belly in 2004 [27]. The smallest pieces of polymer waste material are eaten by fish. Seabirds frequently feed on fish on the surface of oceans and in this way the plastics are transferred to sea birds. This leads to decreasing their digestive capability as well as can lead to starvation, malnutrition, and death [5]. Gregory [28] reported that almost 260 species of different mammals, reptiles, insects, and birds have exhibited a discernible abnormality in physical movements and eating habits, sterility, as well as death because of swallowed plastic materials.

1.2 Apparent solutions for plastic waste management

Fig. 1.5 shows the concept of 4 Rs for polymeric materials waste management. The 4 Rs includes reduce, reuse, recycle, and redevelopment of plastic waste and to reduce environmental issues. The Environmental Protection Agency (EPA) promotes reduce, reuse, and recycle as an anticipated plan to manage the plastic materials wastes. In reduce; if every person rejects plastics for packing material, then industries will reduce their manufacturing and the related issues like the use of energy, contamination, and adverse impact on health will reduce. In reuse, if the refillable plastic containers can be re-used repeatedly, it can lead to a significant decrease in the demand for disposable polymeric materials and decreased utilization of energy, materials, and environmental effects. In recycling, the waste of plastic materials is recycled to yield new useful products. However, several factors can affect the recycling of waste of plastic material, for example, the collection of waste of plastic materials, separation of various types of plastic materials, cleaning of the waste, and probable contamination of the plastic materials. Another complicated factor is the lower value of most of the product materials that can be produced from recycled plastics. After recycling, most of the products losing a few of its properties such as stability, strength, etc. [4]. However, recycled product materials are more detrimental to the atmosphere as this includes different additives as well as colours. A minor quantity of total plastic generation (< 10%) is

successfully recycled, the rest being thrown to landfill sites. Therefore, recycling is not a secure or a permanent solution for PSW disposal [18].

In redevelop, the plastic is biotically degraded down to manure to revitalize the Earth. The degradability of polymeric materials depends on its shelf life as well as the physical, chemical conditions under O_2, light, temperature, as well as particular microbes. The most important alternatives for degradable polymeric materials are:

- Recycling and reprocessing
- Incineration as recovery options
- Biological treatments, including composting and anaerobic digestion
- Landfilling

In majority of the cases, the appropriate end of life management practice depends on nature of the biodegradable material. Composting is a useful alternative to the conventional disposal of biodegradable materials in landfills. The composting conditions such as pH, humidity, temperature, aeration, etc., must be checked and controlled regularly for attaining appreciable results [29, 30]. Degradability of the polymeric materials can be improved by (a) compounding with pro-oxidant like calcium stearate, cobalt stearate, iron stearate, magnesium stearate, etc. [5, 31-33], (b) blending with natural polymers like cellulose [30, 34, 35], starch [36-40], PLA [30, 41-43], poly(ε-caprolactone) [30, 44-46], etc., nanoclay [47], and (c) grafting with hydrophilic monomer like methacrylic acid acrylamide, acrylic acid, etc. [48, 49].

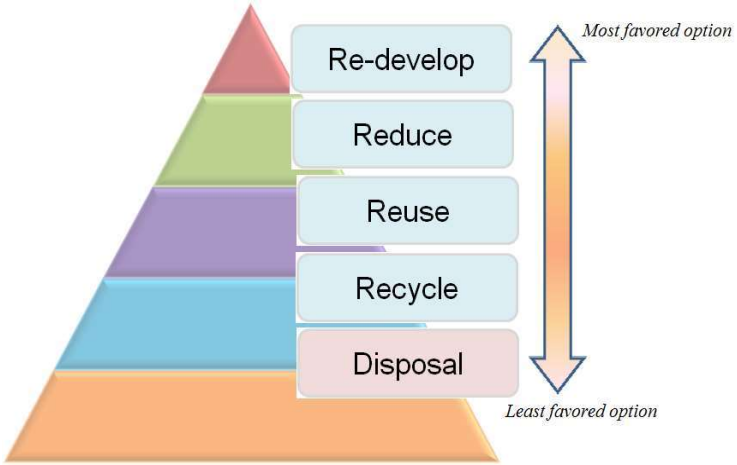

Fig. 1.5 Options for handling polymeric materials waste [50]

Biodegradable polymers

Bio-based materials involve natural polymeric materials. These polymeric materials are synthesized through all living organisms like animals, microbes, and plants and extracted as polymeric materials. These materials are synthesized from biobased monomers in research laboratory/industry and they are eco-friendly. Natural polymeric materials derived from biomass (without microbes) are renewable and available in the abundance in the environment [51]. They are also biodegradable, and, hence, they can decrease the strain on the landfill sites. These polymeric materials occur in the form of polysaccharides (like cellulose, chitin/chitosan, starches, and hyaluronic acids) [45, 52] proteins (plant proteins), lignin, natural rubber, and polyesters. Poly (lactic acid) (PLA), microcrystalline cellulose (CEL), polycaprolactone (PCL), starch, and chitosan, etc., are generally utilized biopolymers that would be replacing conventional polymers. The literature reported that PLA, CEL, and PCL are both degradable and compostable polymeric materials and have different applications ranging from packaging to commodity-based consumption [45, 53, 54]. The well-known degradable polymer is PLA which is derived from corn (maize). Fig. 1.6 presents the worldwide production of bioplastics.

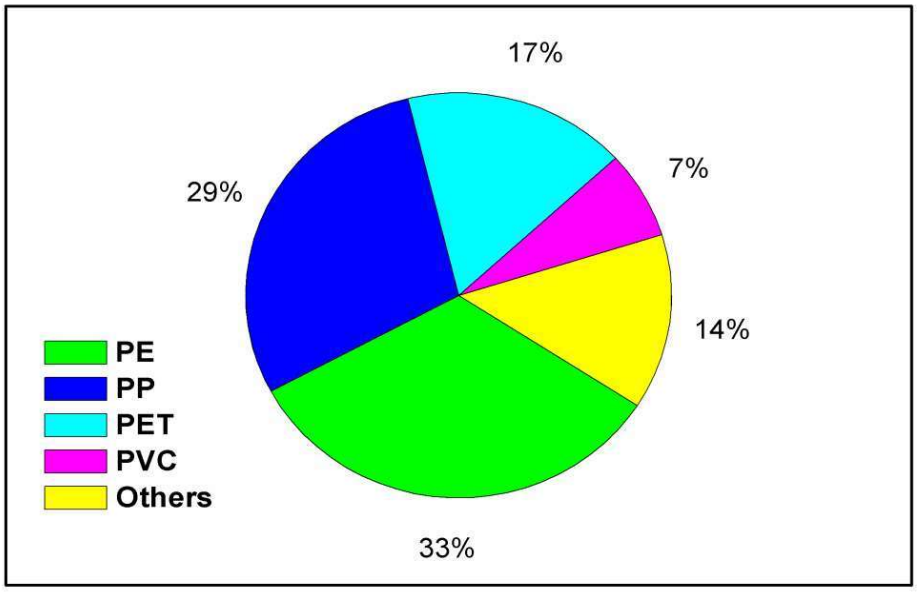

Fig. 1.6 Worldwide production of bioplastic in 2018 *[Source: European bioplastics, institute for bioplastics and biocomposites, nova-institute (2014)]*

1.3 Accelerating the degradability of polymeric materials

Polymeric materials degradability can be defined as "a deleterious change in the chemical structure, physical properties, or appearance of a polymer, which may result from chemical cleavage of the macromolecules, regardless of the mechanism of chain cleavage" [55, 56]. After degradability, some changes appear in a polymeric material such as mechanical, electrical, or optical properties, during erosion, phase separation, crazing, discoloration, and cracking. Generally, polymer degradability can occur in two steps: The first stage is abiotic and the second stage is biotic [57]. Abiotic degradation involves the chemical as well as physical processes that involve intermolecular degradability in the polymeric material [58, 59]. The degradability of polymeric materials can be classified as hydrolytic, photo-oxidative, ozone-induced, thermo-oxidative, mechano-chemical, catalytic, and biotic, depending upon the mechanism [60]. Polymeric materials suffer photooxidation or thermooxidation on UV irradiation/ heat, respectively. Generally, the thermoplastic polymeric materials like LDPE and PP are filled with pro-oxidant which can start the degradability. The amorphous nature of the modified PP makes it prone to microbial attack [5]. Microorganisms are consuming it as a source of energy and emitting carbon dioxide, water, and biomass [30]. It is found that the smaller molecules are eaten faster than the larger ones. To facilitate biodegradability of the polymeric materials, the first stage is photooxidation or thermo-oxidation. The oxidation of polymeric materials takes place and results in the creation of carbonyl residues. These carbonyl residues are consumed through non specific microorganism populations.

Standards for mechanical failure

Polymeric materials should conform to the failure of mechanical standards; and their energy for fracture has to decrease to the prescribed fraction of the initial value. During the life span of polymeric materials, this prescribed set point changes. For instance, in PP, the mechanical failure is the point at which the fracture energy arrives at half of the starting value [61]. However, this value may still be higher than the required for practical applications. Determination of elongation at break is also a method to evaluate the failure of polymeric material. If this value decreases by 5 % of the ultimate elongation determined under tension, the material cannot yield and will fail in a brittle form when force is applied. Direct evaluation of actual fracture toughness is also useful because the energy dissipation at the crack tip can be followed [61].

Polymer lifetime estimation

The polymer lifespan or shelf life evaluation is done by accelerated aging utilizing enhanced temperature or high radiation intensities. This method determines the rate of degradability under controlled conditions. The time used to attain the degree of degradability in proportion to the breakdown in these conditions can be calculated [62]. The reciprocating relation can be used to extrapolate the data back to the working condition.

Degradation by photo-oxidation

In photo-oxidative degradation, decomposition of a polymer occurs through the action of UV rays or visible light under the ambient condition. These radiations can initiate the degradation of polyolefins since these possess enough energy to break the chemical bonds. The degradability mechanism of polypropylene in the presence of UV light and O_2 was summarised by Rajakumar and Sarasvathy [63]. Carbonyl groups like esters, ketones, peroxides, and hydroperoxides are produced on the polymer surface due to photo-degradation [33, 60, 64]. The organic pro-oxidants can be integrated into the polymeric material chains to catalyze the decay of the hydroperoxides produced through photo-degradation. The hydroperoxides are unstable in both photolytic and thermal oxidation process [65]. Normally, some photosensitizing agent is also used. Photo-degradation includes the absorption of ultraviolet light and free radicals are formed during the process [66]. After that, autooxidation takes place that causes the final fragmentation of the polymeric material.

Thermal degradation

The thermal degradation of polyolefins is their molecular decay because of heat. The long-chain backbone of the polyolefins can start breaking at higher temperatures and their physico-mechanical properties degrade. The degradation is based on the same principles in the thermal and photo-oxidation process only exception is that photo-oxidation process proceeds at a faster rate than thermal degradation [57, 67]. However, former is slower than the latter. Temperature increases the rate of thermal degradation [68, 69]. The pro-oxidants can also increase both the thermal as well as thermo-oxidative degradation of polymeric materials.

Chemical degradation

Chemical decomposition brings a variation in the physical and chemical properties of the polymeric material. Chemical transformation is the most essential parameter during abiotic deterioration. Atmospheric contaminants can react with polymeric materials to vary their molecular structure [70]. Oxygen is mainly responsible for causing the degradability. The atmospheric O_2 breaks the covalent bonds of the polymer thus generating free radicals. The oxo-degradation depends on the presence of unsaturated bonds, and branched chains. The oxo-degradation is enhanced in the presence of light since more free radicals are generated.

Mechanical degradation

Mechanical degradability includes the degradation of polymeric material under mechanical stresses. The use of mechanical stress can also increase the speed of aforesaid methods of polymer degradation. Occasionally, mechanical degradation also takes place in polymeric material if they are exposed to mechanical stress more than the permitted value. The best example of mechanical degradation is during the processing of plastics, for example, during their preparation in a screw extruder, the polymeric materials are exposed to more shear stress because of which micro alkyds are created which leads to their enhanced oxidation [57, 71]. Mechanical features are not very essential in the biodegradability test but mechanical damages can be activating or accelerating it [70].

Degradation by irradiation

The maximum energy sources of radiation are X-rays and γ-rays. They decompose the polymeric material to a higher level as compared to the ultraviolet radiation. Although, γ-rays are electromagnetic radiations similar to ultraviolet, their energy level is higher than that of ultraviolet [72].

Degradation during environmental stress cracking (ESC)

Environmental stress cracking is the occurrence of cracks in a polymeric matrix by contact with external substances such as polar vapors and detergents. Chemical degradation is not taking place. But these agents increase the impact of stress by a purely physical mechanism thus resulting in microscopic crazes, which finally develop cracks and then the failure of the component.

Biodegradation

Biodegradation is defined as the degradation of the physical and chemical characteristics of the polymeric material along with a reduction in its molecular mass that is accompanied by the formation of carbon dioxide, water, methane, and other byproducts. Biodegradation is influenced by the action of microbes, either anaerobically or aerobically, and it is aided by abiotic treatments such as photodegradation, thermal degradation, oxidation, and hydrolysis [56, 67]. Petroleum-based synthetic plastics are not degraded biotically and are highly influencing our earth because of their hydrophobic nature, increased shelf-life, discarding issues, lack of degradability, high molecular weight, resistance to microbial attack, and unavailability of functional groups for hydrolysis [5, 73, 74]. Two steps are included in the biodegradation process of organic carbon in polymers [35, 75]. The first step is the external cell degradation involving solid hydrolysis and microorganisms attached on the polymer surface and then use polymer as a sole carbon source. Afterwards, the creation of low molecular weight products like dimers and monomers takes place. In the second step, mineralization of carbon takes place, that also involves internal cell degradation, in which the intermediate solid carbon is mineralized to CO_2, water, and biomass, [30]. To attain the biodegradability in a significant time, the average molecular weight of oxidizing polymers should be lower than 5000 Da [76]. Design of a degradable system as per ASTM D 5338 is a good technique for the estimation of the degradability of polymers [30].

Toxicity of degraded polymeric materials

Polymeric materials are inert and their biodegradability is increased after loading with pro-oxidant during their preparation. It is essential to identify the impact of biodegradation intermediates and organic additives on the atmosphere to confirm that they are non-toxic to the environment. Any toxic impact of degraded metabolites of the polymer can have an adverse impact on animal life, and plant growth. Hence, it is essential to evaluate the effects of those species and remaining polymer species as well as metabolites. Eco-toxicity tests are utilized to evaluate the toxic effect of degraded products through microbial, plant growth, and earthworm acute toxicity tests [57, 77, 78]. According to the guideline of OCED 208, plant growth tests are preformed and different types of plants are utilized during this test to find the eco-toxicity [47, 79-82]. Earthworm acute toxicity tests are performed as per the guideline of OCED 207 [54]. Currently, several researchers are working on the development of degradable as well as compostable polymeric materials to counter

the concerns influencing our atmosphere. Also, several researches are mainly focusing on the development of degradable polymers by blending technique. Blends of synthetic polymers with biopolymers are prepared to increase the biodegradability. However, to our knowledge, there is a lack of studies on the biodegradability and eco-toxicological effect of degradable intermediate products of pro-oxidant filled PP composites.

1.4 Thesis motivation and objectives

Petroleum-based synthetic polymers have been extensively utilized for packaging and agricultural products. These polymers are characterized by resistance to deterioration in environmental conditions. The plastic waste accumulation in nature burdens the environment and societies alike. Growing anxiety for environmental pollution and increasing wastes in nature has spurred research on the production of biodegradable polymeric materials.

Many investigators tried to resolve the plastic waste management issues through developing degradable polymeric materials, including naturally occurring biodegradable polymeric materials and increasing biodegradability of polymeric materials by blending with biodegradable polymeric materials. There are huge opportunities to explore the development of degradable and compostable polymeric materials that are inexpensive and nontoxic. Degradable polymers are gaining higher attention for the investigation in academics and industries because of eco-friendly. The blending of synthetic polymers with biodegradable polymeric material is much reported but very little focus has been there to the development of degradable polymeric material using organic additives. Moreover, it is essential to study the eco-toxicological effect of degraded intermediates after biodegradation. To overcome these gaps, cobalt stearate filled polypropylene composites are developed and their biodegradability and eco-toxicological effect of biodegraded products are evaluated.

The overall objective of the investigation is to develop biodegradable organic additives filled polypropylene that can sustain its functionality during its utilization life on one hand, and degrades faster thereafter on the other hand. The main objectives of the thesis are:

i. To develop biodegradable organic additives filled polypropylene.

ii. To investigate the effects of composition of organic additives filled PP to obtain optimum physico-mechanical properties.

iii. To study the degradation kinetics of abiotic and biotic degradability of organic additives filled polypropylene and its modeling.

iv. To study the eco-toxicity (after biodegradation) of the organic additives filled polypropylene.

1.5 Thesis overview

Cobalt stearate, one of the organic additives, remained in focus in earlier studies because it exhibited promising results for initiating thermo-oxidative degradation, and, hence, biodegradation of plastics. In this thesis, cobalt stearate pro-oxidant and modified pro-oxidant filled PP composites were prepared by compounding technique. Characterization was done by different characterization techniques to study the mechanical, chemical, thermal, and surface morphological properties before and after abiotic pretreatment. Biodegradability of modified PP composites was determined as per ASTM D 5338 standard under controlled composting conditions at thermophilic temperature. The biodegradation kinetic modeling of cobalt stearate and modified pro-oxidant filled PP films without and after abiotic pretreatment (accelerated weathering) was carried out. Eco-toxicological tests such as microbial, plant growth, and earthworm acute toxicity were performed to determine the toxicological impact of biodegradable intermediates of modified PP films. A schematic of the overall thesis work is shown in Fig. 1. The thesis has been divided into **six chapters** as described below.

Chapter-1 is the introduction that highlights the recent environmental issues of plastic waste management and their adverse effect on the environment. A brief explanation of the problems related to plastic waste management has been given. The main focus is on different applications of PP films in packaging, and its effects on the environment. Various approaches of reduction in the plastic waste are enumerated.

Chapter-2 presents the review of literature in which different physical, chemical, and biochemical approaches have been discussed that can be adopted to increase the biodegradability. The compounding method and the preparation of degradable polymeric materials using different organic additives, without any pretreatment and after abiotic pretreatment (accelerated weathering) are discussed. More emphasis has been laid on the development of oxo-degradable polypropylene by compounding method.

Chapter-3 (Materials and methods) discusses the specifications of materials, chemicals, experimental procedures, calculation methods, characterization, model formulations, and statistical analysis. The experimental procedures were utilized for the composite and film preparations, accelerated weathering testing (abiotic treatment), biodegradability determination as per ASTM D 5338, and eco-toxicological studies as shown in Fig. 1. The characterization of pro-oxidant (cobalt stearate) filled PP films without any treatment, after abiotic treatment, and after biotic treatment are then described. UTM, FTIR, TGA, DSC, XRD, Rheometer, HT-GPC, and SEM were employed to analyze the physico-chemical properties of modified PP films. Further, material balance, stoichiometric analysis, kinetic modelling, model constraints, initial conditions, a solution to the model, and statistical analysis using nonlinear regression of biodegradation results are elaborated. An eight-parameter Komilis model containing a flat lag phase was used to correlate the experimental results. The mechanism employed involved hydrolysis of primary solid carbon and its subsequent mineralization. The first step was rate controlling and it included hydrolysis of slowly (C_s), moderately (C_m), and readily (C_r) hydrolysable carbon fractions in parallel. A non-linear regression procedure was utilized in MS Excel Solver to analyze the biodegradation experiments and make model predictions. The biodegradation experiments were carried out for pro-oxidant loaded PP films under controlled composting conditions without and after abiotic pretreatments.

Chapter-4 (Pro-oxidant loaded PP composites): In this chapter, the results of experiments, modeling, and characterization of pro-oxidant loaded PP films have been discussed. PP has been modified by progressive addition of CoSt from 0.2 to 2 phr. These results are compared for the two cases corresponding to before and after abiotic pretreatments. These are elucidated for the biodegradation, biodegradation kinetic modeling, and eco-toxicological studies on biodegraded compost, each for without and after abiotic pretreatments. Detailed characterization and eco-toxicological tests (microbial, plant growth, and earthworm acute toxicity) were carried out to determine the toxicity impact of biodegradable intermediates of modified PP composites.

Chapter-5 (Modified pro-oxidant filled PP composites) presents the results for the modified pro-oxidant. A master batch containing 10 phr of cobalt stearate in PP (PP100CoSt10) was made in a co-rotating twin-screw extruder under a nitrogen blanket and pelletized. This masterbatch was aged at 110 ^{o}C for 48 h. After that, it was crushed into powder, sieved, and used as a modified pro-

oxidant (T). After addition of this pro-oxidant, double peroxide groups are formed and increase the dispersion of pro-oxidant particles in the PP matrix. This modified pro-oxidant was progressively added to PP from 5 to 30 phr. This chapter describes the characterization, biotic degradation, biodegradation kinetic modeling, and eco-toxicological studies of modified pro-oxidant filled polypropylene composites without and after abiotic pretreatment. All the details are discussed in the same manner as mentioned above for Chapter-4.

Finally, chapter-6 (Conclusions and recommendations) summarizes the conclusions derived from the experimental and theoretical data and also presents the scope of future work.

In the last part of the thesis, a list of cited references has been given.

Chapter 2-Literature Review

Chapter 1 introduced plastic applications, resulting waste generation, its environmental implications, the possible solutions, and the methods of accelerating the degradability of polyolefins. The rate of plastic materials buildup in the atmosphere is seen to be to the tune of 25 MMT/year. Polypropylene is mostly used in packaging applications, which are generally wasted after single utilization. Single utilization plastics bags are one of the packaging materials that accumulated in the environment because of their low degradability. Their accumulation in the environment makes a lot of pollution problems. These unwanted plastic wastes are not eco-friendly and give rise to a major worldwide issue related with environmental and health anxieties. Approximately, 80% of the waste that accumulated on the seashores, sea surface and sea-bed is plastics. Plastic contamination rises from both terrestrial and marine resources. Substituting plastic bags with degradable materials could be helpful to resolve the plastic contamination issues. Therefore, there is a dire need for the development of easily degradable polymeric material to replace these non-biodegradable polymeric materials.

In flexible packaging industry, compounding synthetic polymeric materials with organic additives is a useful technique for the preparation of degradable polymer. These composites on one hand keep well their physical and tensile properties throughout their lifelong utilization. On the other hand, nevertheless, these are easily biodegraded in the natural environment after their utilization.

2.1 Enhancing biodegradability

2.1.1 Blends with natural polymeric materials

There are many natural polymeric materials for blending and direct integration into polyolefin materials. Natural polymeric materials such as cellulose, starch, and chitosan are commonly used for this. Their content affects the physico-mechanical characteristics of the blends. They are extensively utilized to maximize the degradability of polymeric materials. Consumption of natural polymeric materials by the microorganism in blends was seen to improve the surface area of artificial bulk materials as well as to make them more vulnerable to biodegradation [83, 84]. The blending of polyolefin materials with different biodegradable polymeric materials is reviewed below.

Cellulose

Cellulose is an abundantly available and renewable biopolymer. In the cellulose structure, a long chain having monosaccharide glucose units is connected end to end by beta acetyl linkage. It has high strength and excellent mechanical characteristics that depend on the chain length [85-87]. After pre-irradiation, the degradability of PP loaded with 5 to 30% cellulose was determined under composting garden soil by Kaczmarek et al. [88]. They observed that photo- and bio-induced modifications in PP/cellulose proportions increased in comparison to pristine PP. They also found that the tensile properties of the modified sample are lower than those of PP.

Starch

Starch-based materials have received attention since 1970s. Starch is a renewable and biodegradable polymeric material, which can be obtained from various renewable resources and is extensively utilized in several sectors because it is inexpensive and easily available [89]. Starch is a combination of two glucans, amylopectin and amylose. Most starches consist of amylose (10-20%) and amylopectin (80-90 %) depending on the source. But amylose is water soluble and amylopectin is water insoluble. These polysaccharides are collected from units of D-glucose [90]. Starch is produced from different sources like sunlight, carbon dioxide, and water through photosynthesis and is utilized as a degradable material [90, 91]. Most of the degradable polymeric materials derived from renewable resources possess faster degradation, poor tensile characteristics, and hydrophilic character. These characteristics limit the use of starch as materials. Because of these demerits, starch should be blended with petroleum-derived polyolefins. It has mostly been utilized for the preparation of partly degradable polymeric materials by blending with synthetic polymers [89, 91, 92]. The first utilization of starch in plastic materials film samples was noted by Shulman and Howarth [93]. Different starch-based blends with various polymeric materials were prepared in 1970s and 1980s and they were mostly non-biodegradable.

Several studies have reported the enhancement of degradability by blending PP with starch. Al-Salem et al. [94] contrasted the mechanism of thermal degradation of PP with that of starch blended PP (30 to 70 weight ratio) under the influence of photo-degradation due to natural weathering. They found changes in the degradation mechanism due to the presence of starch [95]. Starch along with weathering conditions influenced the thermal stability and kinetic parameters of the degradation reaction. The influence on mechanical properties of the starch loaded PP blends has

been studied by Obasi and Igwe [96]. Different blends of PP filled with different proportions (0 - 50 wt. %) of starch were prepared using an injection molding machine. During the process, temperature and screw speed was 160 - 190°C and 50 rpm, respectively. They reported that the mechanical properties (tensile strength and elongation at break) were reduced, whereas weight loss (%), water absorption, and Young's modulus enhanced with enhancing starch concentration. The SEM results revealed the degradation of fractured surfaces.

Polylactic acid (PLA)

PLA is a thermoplastic polyester derived from a linear aliphatic monomer. It can be prepared from renewable resources and is easily biodegradable. The fermentation of natural sources such as sugarcane, wheat, and rice makes lactide and lactic acid monomers [97, 98]. PLA is a prominent biodegradable aliphatic polyester among others of the kind, namely, polyglycolic acid, polyhydroxy butyrate, and polycaprolactone. It is degraded biotically through the activity of fungi, algae, bacteria, etc. [45]. PLA is a popular biobased polymer material that has fascinated many from the last few decades. A wide range of research has been carried out on this polymeric material. These findings have been demonstrated in several books as well as review articles. Especially, the synthetic features [99], easy processing [100], structure [101], physical characteristics [101, 102], and decomposition processing [103], of PLA and its copolymers have been systematically studied. PLA and their blends have lots of applications in the decomposable packaging material, biomedical & pharmaceutical, and textile fields. PLA has the highest saleable possibility because of its biocompatibility, degradability, and easy processing. The blending of PLA with polyolefins (e.g. PP, PE, etc.) and other polymeric materials helps to optimize the thermal stability, mechanical properties, and melt processability of the composites and blends for various applications [43, 104-106]. It is now broadly utilized in packaging applications.

Blends of PP/PLA have an extremely important disadvantage of compatibilizing, because of which blends have low tensile characteristics. The enhancement in the tensile characteristics of the PP/PLA blends has been accomplished through the utilization of useful compatibilizers suitable for specific applications [42, 107, 108]. Compatibilizers are often utilized as an additive to solve immiscibility problems and to enhance their compatibility and, hence, mechanical properties. Commonly, maleic anhydride (MA) is grafted as an essential compatibilizer on PP to increase compatibility [108]. For blending PP with polar polymers, grafting is the most suitable for

accomplishing interfacial change of polymer blends/composites [104, 109, 110]. The influence of PLA with compatibilizer on the characteristics of PP/PLA materials was reported by Ploypetchara et al. [109]. FTIR results verified the interface between compatibilizer and polymeric materials. Addition of PLA loading from (40 to 60 wt%), reduced the crystallinity and melting temperature from 38 to 31% and 158 to 154 °C, respectively. With the addition of PLA to pristine PP, the modulus of tensile strength enhanced whereas the value of elongation at break significantly reduced from a high value of 500 % to as low as 50%. Blends of PP/PLA revealed a typical immiscibility in the polymer blend.

Yoo et al. [111] studied the influences of compatibilizers and hydrolysis on the surface morphology, interfacial tension, and tensile and impact strengths of the PP/PLA (80/20) blends. Before hydrolysis, the highest tensile strength of these blends was accomplished with 3 phr of polypropylene-g-MA copolymer. After hydrolysis, however, there was not much change in their tensile strength. Nevertheless, with the use of styrene-ethylene-butylene-styrene-g-MA compatibilizer, their tensile strength reduced for both the cases of before and after hydrolysis. Utilizing the Pelerine and Choi-Schowalter models, the interfacial tension was computed from the reduction time. They validated 3 phr as the optimum loading of polypropylene-g-MA. The loading of styrene-ethylene-butylene-styrene-g-MA compatibilizer after hydrolysis led to a more pronounced enhancement of impact strength.

Mandal et al. [47] investigated the influence of MA compatibilizer in PP/PLA/MA (85/15/4) blends. They concluded that their tensile strength, compatibility, and thermal stability improved at 4 phr compatibilizer loading. The loading of MA in blends enhanced the complex viscosity as measured by the rheological studies.

Polycaprolactum (PCL)

Polycaprolactone is a semicrystalline linear polyester. PCL is a polymeric material made of hexanoate repeat units belonging to the class of aliphatic polyesters. PCL is miscible with many polymers and has been systematically studied for its tensile characteristics and degradability. The mechanical, thermal, as well as physical characteristics of PCL mostly depends on its molecular weight and crystallinity. It decays through hydrolysis of its ester linkages. PCL is powerfully semicrystalline, highly soluble, easily processable, and hydrophobic because of the low melting

point and excellent blend compatibility, so motivating investigators to examine probable applications.

Chitosan

Chitosan is natural polymeric material with high molecular weight and it can be utilized for the production of translucent films [112-118]. In the blends, chitosan is used as a degradable additive and produces antimicrobial properties. The blending of chitosan enhanced the impact strength and Young's modulus but decreased the mechanical characteristics of petroleum-based polymers. It was also seen that chemically treated PP/chitosan composite films had higher tensile characteristics in comparison to pristine PP. TGA and DSC results also revealed the enhancement of the thermal stability and crystallinity of the PP/chitosan composites. This may be caused by the increased best dispersion and interface adhesion of the chitosan in the PP matrix [119]. The biodegradability of chitosan added LDPE films was reported by Sunil kumar et al. [120]. *Aspergillus niger* caused their degradation on a medium of potato dextrose agar after aging at 25 °C for 21 days. They found biodegradability enhancement with chitosan loading in the films.

2.1.2 Blends with synthetic biopolymers

Nowadays, synthetic aliphatic polyesters have been used for getting biodegradable blends due to the following factors.

(i) Although most biologically derived degradable polymeric materials are biocompatible, many may start an immune response in the human body, probably one that could be prevented through the utilization of a suitable synthetic biopolymers
(ii) Chemical changes in degradable these materials are problematic
(iii) Chemical changes can cause modification of the bulk characteristics of these materials

A diversity of characteristics can be attained and more changes are probable with well-developed synthetic biopolymers without changing the bulk characteristics. Aliphatic polyesters, for example, PLA, poly (glycolic acid), PCL, and their copolymers, are widely used due to their degradability and biocompatibility. These have generated much research interest due to their trimmable characteristics, namely, hydrophilicity, degradability, bioadhesion, moiety attachment, etc. Many studies [47, 99, 121, 122] have been reported on the blends of degradable polymeric

materials with the traditional polymers. These blends are partly miscible/immiscible as well as properly compatibilized to enhance the miscibility and interfacial adhesion. PLA blending with conventional polymeric materials namely polyacrylates, poly (ethylene glycol), polypropylene, poly (4-vinylphenol), poly (ethylene oxide), and poly (vinyl acetate) can change the tensile and thermal characteristics, permeability, and degradability rate [47, 123, 124].

2.1.3 Hydrophilic grafts

Another possible approach to improve the degradability of plastics is the grafting technique [125]. The two ways of radiation grafting techniques are simultaneous (mutual method) and pre-irradiation grafting (post-irradiation grafting) [126]. In the simultaneous technique, the monomers and the polymers are irradiated concurrently and to create free radicals as well as subsequent addition. In the pre-irradiation technique, firstly, the polymer films are subjected to ionizing radiation in vacuum (an inert atmosphere) to form free radicals before being subjected to a monomer. The simultaneous radiation grafting technique is very much effective as compared to pre-irradiation because of the higher radicals available through the direct method. Grafting polymerization is a famous technique for the alteration of the chemical as well as physical characteristics of polymers [110, 127, 128]. Grafting copolymerization modifies the size, shape, and polymeric material structure by various techniques [129], namely, γ-radiation [130, 131], chemical means [132], thermal [133], and photo-irradiation [134]. Out of the above, the γ-radiation is one of the most significant techniques because it rapidly forms free radicals, and effectively penetrates the polymer matrix. In a few studies, gamma irradiation has been used to graft acrylic acid (AAc) to the surface of the polymer to increase hydrophilicity, which can make the polymer more effective to microbial attack [48, 135]. The amount of additive used in the grafting solution can improve the degree of grafting as well as lower the radiation dose [48]. The degree of grafting depends on the selected solvent. The degree of grafting gets enhanced due to water content in a water-methanol mixture [136]. Acik et al. [137] reported the synthesis of polypropylene-graft-poly(L-lactide) copolymers with two grafting densities by copper (I)-catalyzed azide-alkyne cycloaddition and studied its biodegradation through enzymatic degradation experiments. They found that the weight loss for the grafted copolymers was up to 22.1%, which was only about 4% for a commercial chlorinated polypropylene sample.

Kaur et al. [138] studied acrylamide/methacrylic acid-grafted polyethylene (PE) film by a pre-irradiation technique utilizing benzoyl peroxide as a radical initiator. In the soil burial test, they have shown degradability during 50 days [138]. Raj et al. [139] showed the modification of pectin through grafting of vinyl monomers (tert-butyl acrylate and methacrylamide), and ammonium nitrate was used as the initiator. The modified pectin was blended with low-density polyethylene (LDPE) and was studied for its biodegradability. In the soil burial test, they found that the degradability rose to 23% after 45 days. Rosli et al. [140] investigated the degradability behavior of cellulose-graft-polymethylmethacrylate (cell-g-PMMA) with poly(lactic acid)-natural rubber/liquid natural rubber blends. Their results found that the physico-mechanical characteristics for composites improved due to the integration of cell-g-PMMA. Their degradation rate increased up to (72%) [140]. Sharma et al. [141] studied the synthesis of conducting hydrogels based on poly(acrylamide-aniline)-grafted gum ghatti [Gg-cl-poly(AAm)] by ɣ-irradiation technique and N, N'-methylene-bis-acrylamide was used as a crosslinker. Their degradability studies were carried out by soil burial test. They showed that biodegradability increased up to 78% in 60 days.

The grafted PP films have been studied in our earlier research [48, 49, 142]. Their synthesis and optimized physicomechanical characteristics have been studied for flexible packaging by various characterization techniques. The grafting conditions were optimized by using 4 factors and 5 levels of central composite design as per the response surface method. After 33.8% degree of grafting, no improvement in biodegradation was found. Successful grafting of acrylic acid onto PP film samples as shown by Fourier transform infrared spectroscopy (FTIR) and colorimetric analysis quantitatively confirmed the carboxylic groups on the film surface. The results of UTM, TGA, and DSC confirmed that the grafting of acrylic acid (AAc) on pristine PP decreased their mechanical properties by 60.57%, initial decomposition temperature by 33.44%, and crystallinity by 58.85%, which improved their biodegradability.

2.1.4 Nanoclay addition

Generally, nanoclays (NC) are utilized as nanoparticles for flame-retardance. They can be natural or synthetic, cationic, or anionic materials. The main advantage of NC is that the lamellas on their structure can exfoliate raising the interfacial contact with the polyolefin matrix [143, 144]. Most of the work has been done in the development of melt compounding PP with montmorillonite (MMT). MMT has been the most utilized organically modified natural clay mineral and it exhibits

excellent biocompatibility and degradability in combination with excellent tensile characteristics. In some studies, a coupling agent (MA-g-PP) was utilized to increase the dispersion of the particle of clay in the PP matrix [145-147]. The best characteristics of the PP film samples were attained due to the addition of clay and coupling agents. These increased characteristics are found at a significantly higher cost and it decreases their range of applications, such as in the automotive sector [148-150]. The influence of resistance of PP/clay composite was reduced, after loading of high concentrations of coupling agent.

Mandal et al. [47] studied the effect of NC on the characteristics of PP/PLA blends and nanocomposites. They concluded that NC improved the amorphous nature of composite films, which was useful in the biodegradability. An enhanced storage modulus with the loading of nanoclay in composite films was verified by rheological studies. The presence of NC increased the degradability of the composite films [151].

2.1.5 Abiotic pretreatment

Before biodegradation, abiotic pretreatment of the polymeric material has been utilized to increase the biodegradation significantly. The different pretreatment methods are described here.

Ultraviolet (UV) light

Sunlight is a source of UV radiation. Photo-degradation involves the usual propensity for most polymeric materials to undergo a slow reaction with atmospheric O_2 and in light. Normally a photosensitizing agent is used to increase the speed of this natural propensity. The mechanism of photo-degradation includes the absorption of UV light and subsequently resulting in the production of free radicals. Photo-oxidation is controlled through the intensity of the light. These radicals disseminate making more radicals in the polymeric materials thus enhancing its reactivity. This pretreatment leads to decrease in the average molecular weight of the polymeric materials. During the degradation process, the main products are hydroperoxides, that can photolyse or thermolyse in the presence of catalyst causing chain cleavage and accompanied by the generation of lower molecular weight hydrocarbons and oxidation products like ketones, carboxylic acid, alcohols [57, 152], which are then biologically degradable through the microbes aerobically [153] and anaerobically [154]. During the photoinitiation, peroxides and hydroperoxides absorb UV light in the wavelength range of 290 to 400 nm causing the homolytic chain breakdown [155].

Subramaniam et al. [5] investigated the effect of UV on oxo-degradation of PP compounded with different pro-oxidants. It includes irradiation at 0.68 W/m^2, UV lamp A at 60 ºC, water spraying for 5 min, and then condensation. The experiment was conducted for 1200 h with time interval of 400 h and after that sample weight was measured. They found the degradation of pro-oxidant filled PP samples faster as compared to without pro-oxidant. Crystallinity of the samples decreased and it showed a higher degradability. The degradation rate was very much depended on the concentration and type of pro-oxidant. Arraez et al. [156] studied the impact of weathering on PP with a pro-oxidant concentration of up to 3% w/w. The degradation studies were carried out in accelerated weathering tester for 40 h at 60 ºC. During the exposure time, pristine PP did not show significant change, however, PP with pro-oxidant samples showed the changes speedily in the higher concentration of pro-oxidant. Their FTIR results showed the presence of carbonyl and hydroxyl groups. DSC demonstrated that the crystallization and melting temperatures decreased as a result of the chain cleavage and during exposure, oxidation reactions have taken place. The photodegradation rate of PP was more in the presence of 3% cobalt 12-hydroxyl oleate, and its biodegradability increased up to 24% in 45 days [157].

Thermal

Thermal pretreatment makes the polymeric material more effective to microorganism attacks. By its very definition, this degradation is directly dependent on the temperature conditions. The main distinction between the oxidation prompted by heat and light is that whereas the ketone products formed are steady to heat, they are not steady to light [57]. Thermal pretreatment oxidizes the chain through introducing carboxyl, hydroxyl, as well as hydroperoxyl groups. The creation of oxidized products also made the polymeric material more hydrophilic and is more favorable to attachments of the organism. Previous studies demonstrated the demerits of thermal oxidation on the biodegradability of PE and PP [158, 159]. They reported that thermally treated low-density polyethylene for 120 h at 150°C increases the carbonyl index by 23%. Fungi *Phanerochaete chrysosporium* caused increase in carbonyl index in 3 months with decrease in chain length [155].

Hayoune et al. [160] studied the impact of iron stearate (0.2 % w/w) on the thermal decomposition of PP/PLA (1:1 weight ratio) blend compatibilized through 3% PP-grafted-MA, after artificial aging at 70 °C for 21 days. TGA analyses were conducted at different heating rates of 5, 10, 15, 20, and 25 °C/min and showed a two-stage decomposition mechanism for the samples. They found

that both FeSt, as well as artificial aging, decreased the degradation temperatures (onset and max) for every decomposition step. The presence of FeSt during thermal decomposition can decrease eco-toxicity.

Chemical

Different chemicals can change the elasticity, surface appearance, weight, mechanical strength, and colour of polymeric materials. Chemicals can attack the polymeric material as follows:

(i) Chemicals attack the chain of the polymer and reduce physical properties
(ii) Chemicals reacts/oxidizes the functional groups. Also, depolymerization can occur
(iii) Production of radicals
(iv) Carry out physical modifications, involving absorption of solvents; effect on its electrical characteristics, strength, and colour resulted in softening plus swelling of the polymer.
(v) Permit solvent to penetrate during the polymer leading to its dissolution, and
(vi) Cause stress cracking because of the interface of the "stress-cracking agent"

At room temperature, PP does not react with all the acids and bases in dilute concentration. Nitric acid, sulphuric acid, as well as chromic acid, oxidize PP. Hydrochloric acid (HCl) modifies the colour from light to dark brown of PP and is dependent on the acid concentration as well as the reaction temperature. This is because of the reaction between hydrochloric acid and the stabilizers loaded to the polymeric material. After H_2SO_4 acid (conc. 70%) treatment, PP does not reveal any changes. But, H_2SO_4 (with 80%), reduces its weight as well as mechanical strength [155]. The acid reacts with the amorphous parts of the polymer structure and give rise to cracks on the surfaces.

2.1.6 Addition of pro-oxidants

Naturally, the degradation of plastic materials is very slow. Different potential approaches are available to enhance the rate of biodegradation; the organic additives filled polyolefins like PE and PP are more suitable than others because they accelerate photooxidation and thermal oxidation in the polymer chain. The presence of organic additives leads to the fragmentation of the polyolefin matrix [5, 57, 64]. The utilization of pro-oxidants is an old technology. Patents on the science of pro-oxidant additives and biodegradable polyolefin materials have dated since the early 1940s. In patents dated 1941 and 1950 to Bayer and Du Pont, the first production of biodegradable polyolefin materials started through the integration of photosensitive unsaturated fractions into the polymer

[161]. Early patents in 1970s were due to Guillet on photosensitive carbonyl groups. These are formed during polymerization of ketones to give vinyl ketone copolymers. The subsequent patent was from Scott et al. in 1978, which were on the transition metal ion complex sensitizers [162].

Amongst many approaches used to make biodegradable polyolefins is the utilization of specific additives termed as pro-oxidants. Commonly, pro-oxidants are transition metal ions which are in the form of stearates. Some metal ions initiate the formation of radicals during the photo-oxidation, whereas some metal ions work as a catalyst in the lack of light for the decay of peroxides leading to chain cleavage. The pro-oxidants with molecular oxygen atoms are existing in the amorphous area of the polyolefin chains and hence the oxidation predominantly takes place [5, 155]. Pro-oxidants hasten abiotic oxidation and subsequently chain scission making the polymers prone to the microbial action [56, 84]. These special additives or pro-oxidants promote biodegradability and their utilization will be discussed in the following section.

2.1.6.1 Mode of pro-oxidant activity

Currently, transition metals are the most extensively studied pro-oxidant additives. The attractions of these pro-oxidants lie in their capability in catalyzing degradation of hydroperoxides to form free radicals as presented in Fig. 2.1. Transition metal ions of cobalt stearate (Co^{2+}), magnesium stearate (Mn^{2+}), and iron stearate (Fe^{3+}) are mostly used in the polyolefin materials to initiate the thermo-oxidation and photo-oxidation processes [57, 84, 163]. Among them, iron stearate (Fe^{3+}) initiates photooxidative degradation process. Cobalt stearate (Co^{2+}) and magnesium stearate (Mn^{2+}) initiate the process of thermo-oxidative degradation [164].

$$ROOH + M^{+} \rightarrow RO^{\bullet} + OH^{-} + M^{2+} \quad (2.1)$$

$$ROOH + M^{2+} \rightarrow ROO^{\bullet} + H^{+} + M^{+} \quad (2.2)$$

$$2ROOH \rightarrow RO^{\bullet} + ROO^{\bullet} + H_2O \quad (2.3)$$

Fig. 2.1 Degradation mechanisms of hydroperoxides in the presence of pro-oxidants

2.1.6.2 Commercially available pro-oxidants

Different advanced organic additives use a higher range of metal ions complex sensitizers, and are blended with degradable components as well as utilize pro-oxidants with stabilizers and antioxidants to alter the degradability reports. Scholars utilized several popular pro-oxidants for improving biodegradation and these are described here.

The mostly utilized pro-oxidants are complexes of transition metal stearates like zinc (ZnSt), copper (CuSt), calcium (CaSt), [152, 165], silver (AgSt), manganese (MnSt) [166], chromium (CrSt), nickel (NiSt), vanadium (VSt), magnesium (MgSt) [167], cobalt (CoSt) [5, 168, 169], or iron (FeSt) [170]. Pro-oxidant present in the polymer increases the oxidation through free radical chain reaction with oxygen that helps to reduce the molecular weight of the polymeric matrix which can be easily utilized by the microorganisms. Thermal oxidations of the materials have been investigated with the help of FTIR and luminescence method. Metal ions in pro-oxidants were found to act as catalyst [171, 172]. There are very few studies on the organic additives filled PP as shown in Table 2.1. A literature review has shown that very limited research work has been done to prepare degradable PP using pro-oxidants/organic additives. Biodegradation of pro-oxidants filled PP follows a two-stage process. During first stage, high molecular weight polymeric material produces low molecular weight monomers and oligomeric products like alcohols, ketones, carboxylic acid, aldehydes, etc. under abiotic conditions. During second stage, low molecular weight monomers and oligomeric products are utilized by the microbes as the sole carbon and energy source [173, 174] and lead to formation of carbon dioxide, H_2O, and biomass as ultimate degradation product [30, 155].

Degradation involves chemical, physical, and biological changes in the presence of air, high energy radiation, light, temperature, moisture, and microbial action. Sometimes the rate of chemical or physical degradation is higher than biological degradation. Chemical and physical degradation facilitate the biological degradation or biodegradation [175]. In the complete biodegradation process, high molecular weight polymer chains break down into low molecular weight monomers and degrade into CO_2, H_2O, and biomass due to the activities of the microorganism.

Table 2.1 Preparation of degradable polypropylene with pro-oxidant/organic additives

Sr. No.	Polypropylene with additives	Additive/Pro-oxidant	Conditions/Parameters	Observations	References
1.	PP with pro-oxidant	Mn, Mn/Fe or Co	Biodegradability, abiotic pre-treatment at 60 ± 1 °C by photooxidation and thermo oxidation about 3-4 years of outdoor weathering, 3-4 months of exposure to daylight and 3 years in soil.	Degradability of PP film is low as compared to PE film. The PP film loading pro-oxidant based on Mn and Mn+Fe gave useful outcomes for the biotest.	[153]
2.	PP with pro-oxidant	CoSt, CaSt	Pro-oxidants 0.2 to 2 phr, film prepared at 185°C, biodegradability of 45 days at 58°C, eco-toxicity.	The maximum biodegradation was found in CaSt and CoSt containing PP films. Both microbial and plant growth test shown that degradation intermediate products were nontoxic.	[84]
3.	PP with pro-oxidant	Polyacetal (POM) or d_2w)	Pro-oxidants POM is 0 to 2 phr and d_2w® 0-1 phr, film prepared at 190°C with compression pressure 2000psi	The two additives (POM and d_2w®) increased the oxidative thermal degradation of PP and the degradability of the PP/POM combination controlled by POM.	[176]
4.	PP with an organic additive	1, 2-Oxo-hydroxy group	Biodegradation, pro-degradant 1, 2, 3 wt%, film molded at 140-160°C	PP samples modified with organic pro-degradant presented higher CO_2 evolution, and consequently these samples revealed better weight loss in comparison to pristine PP.	[177]
5.	PP with organic pro-degradant	Benzoin (1,2-oxo-hydroxy group free of transition metals)	Degradation rate of PP under biotic and abiotic conditions. Plate prepared by using molding press at 220°C	Modified PP exposure to abiotic and biotic degradation shows reduced molecular weight and enhanced crystallinity, after degradation in the natural atmosphere for 120 days.	[167]

6.	PP with additives	(Cobalt 12-hydroxyl oleate)	Photo degradation, biodegradation, composition of pro-oxidant 1, 2, 3 wt %, blends prepared at 150-230 °C and 0 to 700 bar.	Fragmentations occur in the biodegradation of photo- degraded films. The biodegradation test results show that the Co 12-hydroxyl oleate gives 24% of biodegradability on photo degraded PP film samples in 45 days.	[157]
7.	PP with pro-oxidant	MnSt	Pro-oxidant 0.1 wt%.	A higher degradation rate was found due to addition of pro-oxidants.	[34]
8.	Isotactic PP/Ethylene-PP rubber blend with pro-oxidant	Calcium stearate	Film is prepared at 220°C	The addition of combination of calcium stearate shown an enhancement in the notched Izod impact strength over that of the unfilled iPP/EPR blend.	[178]
9.	PP with pro-oxidant	Starch and another component	Biodegradability, pH 7	The process of biodegradation essentially takes place in starch and does not significantly affect PP.	[37]
10.	PP with pro-oxidant/pro-degradant additive	Fe, Co, Mn	The oxo-degradation process of PP films loaded with pro-oxidants additives.	Synergistic effect of abiotic degradation and biotic degradation promoting the range of the whole degradation of the PP films containing pro-oxidant additives.	[154]
11.	PP with pro-oxidants	d_2w	Pro-oxidant d_2w is 0-3 phr	The addition of polyacetal polymer (POM) and the additive d_2w has opposite influences on the activation energy of PP.	[179]
12.	PP with pro-oxidant	Ca and Fe	Microorganism was isolation from soil utilizing a culture medium involving low molecular weight PP as a sole carbon source.	High degradability action toward PP whose molecular weight was as high as 228,000.	[73]
13.	PP, PE with pro-oxidant	Co, Mn, Cr, Ni and Fe, Mo	Rate of degradation of blends in three different environments, namely under direct sunlight, buried in soil	Higher rate of degradation in starch blended PP put under direct sunlight and 10.0% weight loss in 60 days in	[180]

			and immersed in marine waters for 150 days.	comparison to pro-oxidant blended HDPE and LDPE.	
14.	PP with pro-oxidant	Mn, Mn/Fe or Co	Biodegradability	PP films loaded with pro-oxidants provide positive results for the biotest. The degradability of oxidized PP film is less effective as contrast to oxidized PE film samples	[153]
15.	PP with pro-oxidant	CaSt, CoSt	Film preparation at 185°C and 400 kN/m^2 pressure, pro-oxidant 0 to 2 phr, Biodegradability at 58 °C (45days), eco-toxicology study	Optimum content of pro-oxidant = 0.2 phr. The maximum biodegradation of pro-oxidants containing films was 7.65 and 8.34% respectively. Ecotoxicity test indicated that biodegradation intermediates were nontoxic.	[165]
	Blends	**Pro-oxidants/ Additives**	**Conditions/Parameters**	**Observations**	**References**
01.	PP blends with starch blends and organic pro-oxidant	Calcium, magnesium stearate	Plates are prepared at 210 ± 5 °C,	The incorporation of plasticized starch (TPS_{plas}) to iPP has decreased the mechanical characteristics of iPP.	[181]
02.	PP/biodegradable polyester blends with additives	Cobalt, calcium or magnesium stearate	Pro-oxidants 0.2 %, at 190°C to 210°C, biodegradation	All the pro-oxidants enhanced the fluidity of PP and increased the degradability of polymer at higher temperature.	[121]
03.	PP/PLA blends with organic additive	Iron stearate	Pro-oxidant 0.2 %, PP/PLA (50:50 wt.%) blend and PP-grafted-maleic anhydride (3%), at 70 °C for 21 days.	The presence of FeSt decreased the properties of PP and thermal decomposition of PP/PLA blends	[160]

2.2 Biodegradation kinetic modelling

Composting is a useful alternative to the conventional disposal of biodegradable materials in landfills [182]. The composting experiments, in general, show different hydrolysable carbon fractions that decompose to the mineralizable carbon at different rates [182, 183]. These experiments demonstrate that their kinetics follow a first-order mathematical model under controlled composting conditions of temperature, cell population, nutrients, and moisture. The degradation mechanism of organic carbon in polymers may follow two stage [35, 75]. The first stage is the external cell degradation involving solid hydrolysis and the second stage is the carbon mineralization. The first stage proceeds by means of three parallel paths involving the solid hydrolysis of readily, moderately, and slowly hydrolysable carbon fractions. Here, the name of each path represents the rate at which it is occurring, the fastest being the readily hydrolysable fraction and the slowest being the slowly hydrolysable fraction. The second stage involves internal cell degradation, in which the intermediate solid carbon is mineralized to carbon dioxide. Solid hydrolysis was the rate controlling stage during biodegradation process. The different kinetic model parameters like initial slowly, moderately, and readily hydrolysable fraction, intermediate solid carbon fraction, mineralization, and its rate constant were computed after correlating with the experimental data using nonlinear regression analysis. During composting, the degradability curves of the CO_2 emission include three phases such as lag phase, growth phase, and stationary phase.

Recently, some studies have been reported on the kinetics of various types of organic and plastic waste using an aforesaid composting technique based upon the abiotic and biotic steps [35, 75, 184, 185]. The kinetic parameters were obtained from the model analysis. These estimated parameters were used to compute carbon mineralization. Leejarkapai et al. [35] introduced a flat lag phase into the model for the study of the kinetics of PP/starch, cellulose, and PLA. Stloukal et al. [184, 186], Stloukal and Kucharczyk [187] studied the kinetics of biodegradation of PLA/clay nanocomposites using the same model.

2.3 Toxicity of degraded metabolites

Biodegradation of polymers depends on their origin, nature, synthesis, type of additive used, but when they are degraded, they should not generate harmful substances for the environment [188] and not affect the life of other living organisms. After degradation, some polymers degrade into small monomers that are not visible to the naked eye and are toxic for living organisms [189]. Several authors studied the toxic effect of nanostructure poly(ester-imide)s containing a tyrosian-based diol [190], amino acid based diacids with 3,5-diamino-N-(thiazola-2-yl) bensimide [188], poly(urethane-imide)s based on alpha-amino acid [191], chiral poly(amide-imide)s loading various amino acids linkages [77] and concluded that PP is non-toxic for the environment. There were three types of toxicity tests reported (a) earthworm toxicity test [192-194], (b) plant toxicity test [194-196], and (c) microbial toxicity test [77, 188]. Worldwide researches have been working on the development of biodegradable polymeric materials as a waste management option by blending techniques. Until recently, most of the efforts were given to synthesizing the polymer by pro-oxidant/organic additives filled polyolefins. There is much effort needed for the development of non-toxic biodegradable polymers with their biodegradation under standard test conditions.

2.4 Gaps identified

There are immense opportunities to develop degradable and compostable polyolefins of inexpensive and nontoxic in the environment. Degradable polymers as a packaging material are getting considerable attention for the investigation in academics and industries because they are degradable under specific controlled composting conditions and in real composting environments. Blending of conventional polymers with biodegradable additive/polymer is a growing trend, however very little focus has been provided on the development of degradable polyolefins using organic additives and biodegradation kinetics of polymeric materials under controlled composting conditions. Numerous studies have investigated the degradability behavior of polyolefins other than PP and none of the researchers has described the biodegradation of PP. The kinetics of biodegradation and its modelling without and with abiotic (accelerated weathering) pretreatment of organic additives filled PP compounding for packaging application has not been validated in the literature. After biodegradability studies, the biotic treatment intermediates in the environment must be nontoxic. Therefore, it is essential to evaluate the ecotoxicological impact, which has not been studied. On the basis of literature survey, the following specific conclusions are drawn.

(i) A lot of literature is devoted to the degradation of polyethylenes, viz., polyethylene, high density polyethylene, linear low-density polyethylene, and low-density polyethylene. However, only some studies are devoted to the biodegradability of polypropylene.

(ii) Kinetic studies on the abiotic and biotic treatment steps for the case of organic additives filled PP composites still remain invalidated.

(iii) The toxicity of the end products of biodegradation is imperative, but this aspect has been seriously ignored. Consequently, the eco-toxicity investigation of the resulting compost is needed to be carried out.

Chapter 3-Materials and Methods

3.1 Materials

The commercial polypropylene of grade 1030FG (homopolymer pellets) with density 0.9 g/cm^3, $\overline{M}_n$ = 69500, $\overline{M}_w$ = 560900, *polydispersity index (PDI)* = 8.07, melting temperature 165 °C, and MFI = 11g/10 min, were received from Indian Oil Corporation Ltd, India, and were used as the matrix material to prepare the compounds [197]. Pellets of pro-oxidant (cobalt stearate) (Co, 9–10%) were obtained from Alfa Aesar-Johnson Matthey Chemical India Pvt. Ltd. Hydrous barium hydroxide (of molecular weight = 315.47) and microcrystalline cellulose powder (particle size ≤ 20 μm) were procured from S. D. Fine Chemicals Ltd. Mumbai, India. Hydrochloric acid (35% strength) and nutrient agar were procured from Hi-Media Laboratories Pvt. Ltd., India. The *Mung* bean and wheat seeds were purchased from Arman Seed Farm, Patiala, Punjab, India; the ethanol was procured from Changshu Yangyuan Chemicals (China). Earth worms were procured from a local farmer, Patiala, Punjab (India).

For biodegradation study, digested municipal solid waste (matured compost) was collected from Green-Tech Fuel Processing Plant (organic compost plant) at Chandigarh, India. The physical and chemical characteristics of compost were determined as per American Public Health Association [198]. The inorganic materials were separated from the compost by using < 4 mm mesh sieve. The compost contained total nitrogen 1.64%, phosphate 0.70%, potash 0.51%, and total organic carbon 31.11%. The pH measured as per the procedure of Singh et al. [199] was 6.70. The bulk density was 0.79 g/cm^3, and C:N ratio was 18.96.

3.2 Methods

3.2.1 Preparation of composites

The ingredients were mixed manually before filling them in the extruder. The compounding for CoSt filled PP was done in co-rotating twin-screw extruder (M/s Labtech Engineering Co., Ltd. Thailand) at a speed of 150 rpm under a nitrogen blanket and pelletized. The extruder temperature of the feed through die varied from 170 to 230 °C. After extrusion, the continuous compound was

cut into small pellets. Then, the prepared compounds were dried in the oven at 70 ºC for 2 h to remove moisture.

3.2.2 Preparation of PP films and sheets

The films of pro-oxidants filled PP were casted by compression moulding for 2 min. The pressure and temperature during the film preparation were 400kN/m^2 and 185 ºC, respectively. The films were 80–85 μm thick. The material was sandwiched between two Teflon sheets to prevent the sticking of melt with plates. Tap water was used to cool the plates. The sheets for rheological testing were prepared by injection moulding. The temperature during the sheet preparation was 165 ºC. The sheets were 1 mm thick.

3.2.3 Abiotic pretreatment (accelerated weathering)

All PP films were subjected to abiotic pretreatment (accelerated weathering) in a Q-Lab Corporation, USA (QUV model) machine which uses eight fluorescent lamps. It reproduces the damages on modified PP films that can take place in an outside atmosphere by rain, temperature, and sunlight. Films were cut into 50 mm width with 120 mm length and subjected to radiation of 340 nm wavelength and 0.63 W/m^2 intensity to assess the degradation phenomenon. The films were exposed in two cycles (UV irradiation and condensation) as per standard ASTM D 4329 [200]. The weathering cycle (12 h) was utilized which included continuous 8 h of UV exposure at 60 ºC, followed by 4 h of condensation at 50 ºC of water on the sample. The cycle was repeated in the same order up to 40 h and weight loss of the films was recorded after 12, 24, and 40 h.

3.2.4 Characterization

3.2.4.1 Mechanical testing

The mechanical properties of the prepared films before abiotic pretreatment were measured using a universal testing machine (UTM) (Z010, Zwick-Roell, Germany), according to the ASTM D 882-91 standard [32]. The rectangular specimens were prepared for the tensile test by the strip-sample cutter. The cross-head speed of 12.5 mm/min was selected in accordance with the standard. The distance between the clamps was 100 mm. Five specimens of each film were tested for elongation at break and the tensile strength. The average results have been reported.

3.2.4.2 Fourier transform infrared (FTIR) spectroscopy

The chemical and structural changes in the PP films before and after abiotic pretreatment (accelerated weathering) were investigated using spectrometer (Agilent Pro Cary 660). The scanning frequency range was 500 to 4000 cm^{-1} through a resolution of 4 cm^{-1}. A total of sixteen scans/sample were taken. To analyze the measured spectra, spectrum 100 software was used.

3.2.4.2.1 Carbonyl index

FTIR results were utilized to determine the carbonyl index (CI) after abiotic pretreatment (accelerated weathering), which characterizes the degradability of PP. It is the ratio of the intensity of signals (maximum carbonyl peak absorption) to internal constant band at 1454 cm^{-1}. These have been estimated by using the baseline method [64].

$$\text{Carbonyl Index (CI)} = \frac{\text{Absorption at the maximum of carbonyl peak}}{\text{Absorption at 1454 cm}^{-1}\text{ internal thickness band}} \qquad (3.1)$$

3.2.4.3 Thermogravimetric analysis (TGA)

TGA of the modified PP films before and after abiotic pretreatment (accelerated weathering) was performed under pure nitrogen condition (at a flow rate of 50 mL/min) with a TA Instruments TGA Q-500 series, USA. The sample weights were 5–10 mg, the heating rate was 20 °C/min in a temperature range of 30-650 °C, and the thermal profiles of samples were recorded. The initial decomposition temperature (T_i) of the samples is considered at 5% weight loss in polymeric material films and the final degradation temperature (T_f) is considered when 5% residual is left, after which no loss is possible.

3.2.4.4 Differential scanning calorimetry (DSC)

DSC analysis was performed in a Setaram DSC 131 evo DSC, France. Samples in the film form before and after abiotic pretreatment (accelerated weathering) were weighed to approximately 5-10 mg and were put in a 120 µL aluminum pan to evaluate the thermal behavior. All the films were pretreated before analysis at 25 °C for 10 min in the chamber. The films were heated from room temperature to 200 °C in a nitrogen atmosphere. After that, films were cooled from 200 °C to room temperature. Heating/cooling thermograms were recorded with a heating rate of 10 °C/min.

Thermal properties such as melting enthalpy (ΔH_m), melting temperature (T_m), crystallinity (%), and crystallization temperature (T_c) were determined. The area under the thermograms (melting) was utilized to calculate the melting enthalpy (ΔH_m). The melting enthalpy ($\Delta H_{m(\text{crys})}$) values of 100% crystalline PP is considered to be 163 J/ g [201]. The crystallinity (%) of the films has been estimated using the equation given below.

$$\mathrm{X}_c\ (\%) = \frac{\Delta \mathrm{H}_m}{\Delta \mathrm{H}_{m\,(\text{crys})}} \times 100 \qquad (3.2)$$

Where, ($\Delta H_{m(\text{crys})}$) designates the enthalpy for melting of 100% crystalline PP, and ΔH_m designates the melting enthalpy of modified PP samples.

3.2.4.5 X-ray diffraction (XRD)

The XRD analysis of the films before and after abiotic pretreatment (accelerated weathering) was carried out in X-ray diffractometer (Philips Xpert Almelo, Netherlands) with automatic recording and processing of the experimental data. The diffraction angle range was 5° to 60°. The impact of CoSt on the crystallographic structure of modified PP samples was evaluated by XRD. The XRD was run at 20 mA and 40 kV with monochromatic Cu-Kα radiation (λ = 1.54 A°). The scanning rate (5°/min) through 2θ values reproduced within ± 0.02° variation. The crystallinity (%) was determined from the ratio of the area of the crystalline zone (2θ=14°-18°) to a total area of the XRD pattern, i.e., the sum of the area of the amorphous region and the crystalline zone was 2θ = 14°-28° according to Eq. (3.3) [202].

$$Crystallinity\ (\%) = \frac{A_{crystalline}}{A_{crystalline} + A_{amorphous}} \times 100 \qquad (3.3)$$

Where, $A_{crystalline}$ and $A_{amorphous}$ are the area of crystalline zone and amorphous region, respectively.

3.2.4.6 Scanning electron microscopy (SEM)

The morphological structures of the films before abiotic, after abiotic, and after biotic treatment were analyzed with a JEOL scanning electron microscope instrument (JSM 6510-LV, Tokyo,

Japan). Before analysis, to avoid the charging, 15 nm thick gold film was coated using a high vacuum automatic sputter coater (model JFC-1600, Japan) through an electron beam. To reveal all changes into the film, surfaces were seen and compared.

3.2.4.7 Rheological testing

An instrument Anton Paar parallel plate rheometer (MCR 102) was utilized to determine the rheological behavior of PP and CoSt loaded PP composites at a test temperature of 165 °C. The geometry consisted of plate-plate of 25 mm diameter with a gap of 1 mm. The films were directly loaded in nitrogen atmosphere. The linear viscoelastic (LVE) region of each film sample was determined from the initial strain value of 0.01 to the final value of 1000% with a constant frequency of 1 rad/s. After that, frequency sweep test was carried out in the LVE region ($\gamma = 1\%$). The frequency range was 0.01 to 500 rad/s.

3.2.4.8 Molecular weight analysis

A few milligrams of each film were taken in 4 mL vials. After that, 1,2,4-trichlorobenzene (TCB) solvent was added to the vials. A concentration of approximately 0.5 mg/mL was obtained. The vials were placed on a heating and shaking plate at 150 °C for about 2 h. After dissolution, the vials were transferred into the carrousel of the chromatograph auto sampler. The number-averaged molecular weight ($\overline{M_n}$) and weighted-averaged molecular weight ($\overline{M_w}$) in terms of the polydispersity index (PDI) of pristine PP, modified PP samples without any treatment, after abiotic pretreatment, and after biotic treatment were determined with a high temperature gel permeation chromatography (HT-GPC) system (Polymer Char model GPC-IR). A three-column set was employed which consisted of PL gel 300 × 7.5 mm Agilent columns. The solvent (1,2,4-trichlorobenzene) flow rate used was 1.0 mL/min and the temperature was fixed at 160 °C using a IR5 MCT infrared detector for molecular weight analysis. The injection volume was 200 µL. The system was previously calibrated using solutions of polystyrene molecular weight standards.

3.2.5 Biodegradability study (Biotic treatment)

The biodegradability of different samples such as microcrystalline cellulose powder (MCE), PP, and modified PP films (before and after abiotic pretreatment) was determined under controlled composting conditions. In general, polymers are degraded in a two-step process. In the beginning,

abiotic degradation takes place which is followed by biotic degradation. In the abiotic degradation process, mainly the degradation of polymers takes place due to chain cleavage of the ester groups by hydrolysis and oxidation reaction. Molecular weight of polymeric material decreases through cleavage of chain length into some smaller chains. In the biotic degradation step, short polymer chains after abiotic degradation are assimilated by microorganisms and finally converted into biomass, water, CO_2, and residue [35, 45, 203].

Some of the standards are widely utilized for the evaluation of the biodegradability of degradable polymers in various environments. These standards were developed by certifying agencies like the American Society for Testing and Materials (ASTM) and the International Organization for Standardization (ISO). ASTM standard has set rules and different protocols for designating a plastic material biodegradable. ASTM D5338 is an important standard and it was commonly utilized to measure the degradability of polymer films during thermophilic phase of the composting process [204]. As per ASTM D5338, if 90% of carbon is converted into carbon dioxide then plastic can be marked as compostable. This standard again clarified the procedure that has to be followed for conducting a biodegradability test of the biodegradable polymer under controlled composting conditions. Fig. 3.1 shows the schematic diagram of the aerobic biodegradability testing system.

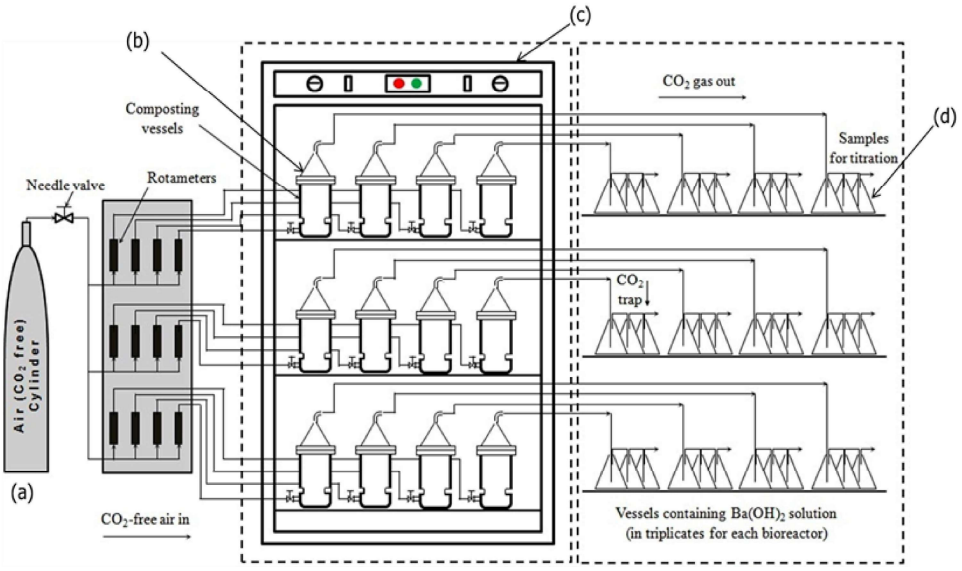

Fig. 3.1. A schematic diagram of biodegradation testing under composting conditions (ASTM D 5338-15). (a) Zero air supply and arrangement of rotameters, (b) Composting vessels, (c) temperature controlling chamber (58 ± 2 °C, and (d) Carbon dioxide trapping vessels containing $Ba(OH)_2$ solution

3.2.5.1 Preparation and standardization of $Ba(OH)_2$ and HCl solutions

Preparation of 0.024N barium hydroxide solution: Took $Ba(OH)_2.8H_2O$ (4 g) to dissolve it in deionized water (1 L). The normality of the prepared solution was confirmed by standardizing it against HCl. The primary standard sodium carbonate (Na_2CO_3) was utilized for HCl standardization as HCl is a secondary standard.

3.2.5.2 Positive, negative, and blank control

The inoculum without sample was used as blank control in the composting vessel (bioreactor). The inoculum with microcrystalline cellulose powder was used as a positive reference, and the inoculum material with pure PP sample was used as a negative reference.

3.2.5.3 Biodegradation procedure

In the composting vessels (bioreactors), four different mixtures/materials were added (1) blank control (only inoculum), (2) positive control (inoculum + CEL), (3) negative control (inoculum + pristine PP), and (4) (inoculum + modified PP film). Biodegradation test was conducted by measuring the CO_2 emitted from the samples without and after abiotic pretreatment. All the films were incubated for 45 days in 1 L reactors at 58 ± 2 ^oC in three replicates and their average results were reported. Before starting the test, the moisture was made 50-55% by the addition of deionized water. During the test, temperature, humidity, and aeration were monitored regularly and closely controlled as per the guidelines of ASTM D 5338. The reactors were shaken occasionally to ensure that air and moisture were circulated uniformly within the reactor. The flow rate of CO_2 free air was 60-70 mL per minute during the test period to maintain an oxygen level in the reactor. Petric and Selimbasic [205] reported that aeration gives enough oxygen to the oxidation of organic matter and removes extra moisture from the basic material. Sufficient porosity of inoculum was also maintained during the test.

The CO_2 emitted during the biodegradation was trapped in conical flasks containing 0.024N barium hydroxide and consequently precipitated as barium carbonate. The remaining barium hydroxide from each trap was titrated with a standard solution of 0.05 N HCl to the phenolphthalein end-point. The cumulative carbon dioxide evolution was calculated by acid-base titration at every 2-3 days interval as per the standard volumetric procedures.

3.2.5.4 Theory and calculations

The total theoretical mass of CO_2 (CO_2th), in grams per films, was computed using Eq. (3.4)

$$CO_2th = W_{sample} \times C_{sample} \times \frac{44}{12} \tag{3.4}$$

Where, W_{sample} = the total weight of dry solids (g) in the test sample before starting the test; C_{sample} is the amount of total organic carbon present in the dry solid's films (g/g); molecular weight of CO_2 is 44 and the atomic weight of carbon is 12, respectively (g/mol).

The theoretical mass of carbon dioxide (CO_2th(g)) was measured from the total organic carbon (TOC) analyzer [206], TOC-V_{CPH} (solid module) from Shimadzu, Japan, which utilizes heating at 900 ^oC. CO_2 was identified by an NDIR gas analyzer. NDIR detects the analog signal, generates a peak and its area is estimated by a software (TOC-Control V).

Biodegradation (%) of the sample has been determined by using Eq. (3.5).

$$(\%)\ \text{Biodegradation} = \frac{CO_2(test) - CO_2(blank)}{CO_2(th)} \times 100 \tag{3.5}$$

Where, CO_2*(test)* = the cumulative amount of CO_2 emitted (g) from the test sample containing inoculum, CO_2*(blank)* = cumulative amount of CO_2 emitted (g) from the bioreactor containing only inoculum (blank).

3.2.6 Biodegradation kinetic modelling

3.2.6.1 Material balance & stoichiometric analysis

For the total change in species amounts, the material balance computations were carried out using Eq. (3.6):

$$X_{in} - X_{out} = X_{accumulation/removal} \tag{3.6}$$

Where, X_{in} and X_{out} designate the input mass and output mass, $X_{accumulation/\ removal}$ designates the mass accumulation or removal.

However, for the instantaneous transient mass balance, the following equation, in general, was used

$$r_{in} + r_{formation} - r_{disappearance\ by\ reaction} - r_{out} = r_{accumulation/removal} \quad (3.7)$$

Where, r_{in} and r_{out} designate the rates of mass input and output of feed material, $r_{formation}$ designates the rate of mass formation by reaction, $r_{disappearance}$ designates rate of mass disappearance by reaction, and $r_{accumulation/removal}$ designates the rate of mass accumulation or removal of feed.

In the biodegradation tests, the carbon present in the samples was converted into the CO_2, biomass, water, and carbon residues by microbial respiration as given in Eq. (3.8) [207].

$$C_{sample} + O_2 \rightarrow CO_2 + C_{biomass} + C_{residue} \quad (3.8)$$

3.2.6.2 Material balance and kinetic modeling

Material balance for carbon

The different terms of Eq. (3.6) become

X_{in} = Initial carbon (g) in feed, X_{out} = C evolved as CO_2 (g), and $X_{accumulation}$ = Undegraded carbon (g) left

Now,

$$X_{in} = Initial\ carbon\ (g) = \frac{12}{44} \times CO_2(th) \quad (3.9)$$

The value of $CO_2(th)$ is given by Eq. (3.5). Now, X_{out} can be calculated by the stoichiometry of Eq. (3.8). As per stoichiometry, 1mol of carbon disappeared will form 1 mol CO_2. Hence,

X_{out} = Carbon evolved as CO_2 =
CO_2 emitted from the test sample - CO_2 emitted from the blank reactor

$$X_{out} = CO_2(test) - CO_2(blank) \quad (3.10)$$

Thus, using Eqs. (3.6), (3.9), and (3.10) the undegraded carbon remaining at any instant (t) is given by Eq. (3.11) as:

$$X_{accumulation} = \text{Undegraded carbon (g)} = \left\{CO_2(th) - \left(CO_2 test - CO_2 blank\right)\right\} \times \frac{12}{44} \qquad (3.11)$$

Kinetic modeling

The kinetic modelling of biodegradation was carried out by applying the instantaneous mass balance Eq. (3.6) for carbon and carbon dioxide. This is done considering the following mechanism of biodegradation study. In general, the two-stage degradation of organic carbon in polymers takes place as shown in schematic Fig. 3.2 [35, 75]. First, the main carbon backbone of the polymer chain is oxidized and forms smaller fragments abiotically. This causes creation of short polymer chains and different functional groups like carboxylic acid, aldehydes, esters and alcohols that can be readily assimilated by microbes. The hydrophobic polymer films become hydrophilic; hence hydrolysis occurs. Second, the biodegradation of the oxidation products occurs under aerobic conditions by the microorganisms, thus forming CO_2, H_2O, and biomass [24, 35].

The first step includes primary solid carbon hydrolysis and external cell degradation. This step is further sub-divided as per the rate of solid carbon hydrolysis of readily, moderately, and slowly hydrolysable carbon fractions. The second step is the ultimate carbon mineralization involving internal cell degradation [75]. This step involves the mineralization of the intermediate water soluble carbon to CO_2 [35]. The biodegradation can be postulated as first-order plus flat lag kinetics [35].

In the first step, the hydrolysis of the readily (C_r), moderately (C_m), and slowly (C_s) is shown in Eqs. (3.13), (3.14), and (3.15). Their corresponding hydrolysis rate constants are k_r, k_m, and k_s, respectively. In the ultimate carbon mineralization, the changes of intermediate solid carbon (C_{aq}) into C_{CO_2} and their rate constant (k_{aq}) are presented in Eqs. (3.18) and (3.21); the rate of cumulative carbon dioxide generation is also represented in Eq. (3.21).

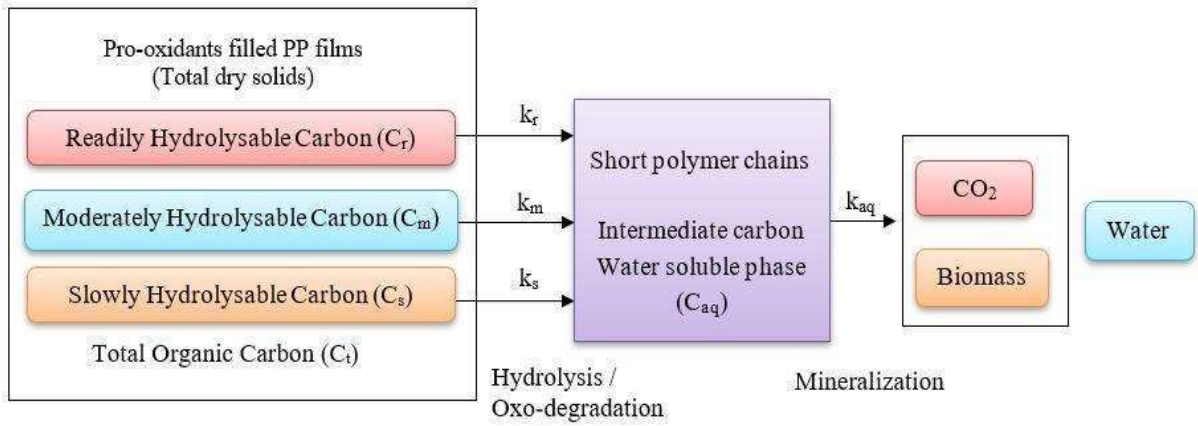

Fig. 3.2 Schematic of biodegradation pathway during aerobic composting [75].

Instantaneous carbon balance

Using Eq. (3.7), the mass balance for slowly hydrolysable carbon is given as:

$$\overset{0}{\cancel{r_{in}}} + \overset{0}{\cancel{r_{\text{formation by reaction}}}} - \overset{0}{\cancel{r_{\text{disappearance by reaction}}}} - r_{out} = r_{\text{accumulation/removal}} \tag{3.12}$$

Rate of accumulation of slowly hydrolysable carbon = rate of its disapperance

$$\frac{dC_s(t-c)}{dt} = -k_s.C_s(t-c) \tag{3.13}$$

The mass balance for moderately hydrolysable carbon is given as:

Rate of accumulation of moderately hydrolysable carbon = rate of its disapperance

$$\frac{dC_m(t-c)}{dt} = -k_m.C_m(t-c) \tag{3.14}$$

The mass balance for readily hydrolysable carbon is given as:

Rate of accumulation of readily hydrolysable carbon = rate of its disapperance

$$\frac{dC_r(t-c)}{dt} = -k_r.C_r(t-c) \tag{3.15}$$

Instantaneous mineralizable intermediate carbon balance

Using Eq. (3.7), the mineralizable intermediate carbon balance is given as:

$$\cancel{r_{in}}^{0} + r_{\text{formation by reaction}} - r_{\text{disappearance by reaction}} - \cancel{r_{out}}^{0} = r_{\text{accumulation/removal}} \tag{3.16}$$

$$r_{\text{accumulation/removal}} = r_{\text{formation by reaction}} - r_{\text{disappearance by reaction}} \tag{3.17}$$

The rate of accumulation of mineralizable intermediate carbon = The sum of the rates of its formation from slowly, moderately, and readily hydrolysable carbons – The rate of its disappearance in the mineralization step

$$\frac{dC_{aq}(t-c)}{dt} = k_r.C_r(t-c) + k_m.C_m(t-c) + k_s.C_s(t-c) - k_{aq}.C_{aq}(t-c) \tag{3.18}$$

Instantaneous carbon dioxide balance

Using Eq. (3.7), the mass balance for CO_2 is given as:

$$\cancel{r_{in}}^{0} + r_{\text{formation by reaction}} - \cancel{r_{\text{disappearance by reaction}}}^{0} - \cancel{r_{out}}^{0} = r_{\text{accumulation/removal}} \tag{3.19}$$

$$r_{\text{accumulation/removal}} = r_{\text{formation by reaction}} \tag{3.20}$$

Also, from the mineralization step in Fig. 3.1, the rate of formation of CO_2 = rate of disappearance of C_{aq}, which gives,

$$\frac{dC_{CO_2}(t-c)}{dt} = k_{aq}.C_{aq}(t-c) \tag{3.21}$$

In the above Eqs. (3.13), (3.14), (3.15), (3.18), and (3.21) the independent variable time (t) is shifted by the flat lag phase c (day). This is the starting phase before carbon to carbon dioxide emission.

3.2.6.3 Initial conditions

The Laplace transform technique was applied for solving the above model Eqs. (3.13), (3.14), (3.15), (3.18), and (3.21) for computing the production of C-CO_2 and rate of production C-CO_2 [208]. Initial conditions respectively in Eqs. (3.13), (3.14), (3.15), and (3.18) are ($C_s = C_{s0}$), ($C_m = C_{m0}$), ($C_r = C_{r0}$), and ($C_{aq} = C_{aqo}$) at $t = c$, where C_{s0} is fraction of initial slowly-hydrolysable carbon, C_{m0} is fraction of initial moderately, C_{r0} is fraction of initial readily, and C_{aq0} is fraction of initial water-soluble carbon. The initial condition in Eq. (3.21) is $C_{co_2} = 0$ at $t = c$, since no C-CO_2 is evolved before polymer degradation. Initial condition for the mineralizable intermediate carbon (C_{aq}) is $C_{aq} = 0$, $t = 0$ as seen in Eq. (3.25). The initial values of other parameters are ($C_r = 0$), ($C_m = 0$), and ($C_s = 0$) at $t = 0$. Hence, at $t = c$, jump discontinuities occur in the values of C_s, C_m, C_r, and C_{aq} from 0 to C_{s0}, 0 to C_{m0}, 0 to C_{r0}, and 0 to C_{aq0}, respectively. Chapter 4 shows these discontinuities. In our previous works, methods for formulating correct initial conditions for different systems involving discontinuities have been established [208-210].

3.2.6.4 Solution to the model

The solution to Eq. (3.13) leads to,

$$\left.\begin{aligned} C_r(t) &= C_{ro}.e^{-k_r.(t-c)}, \quad t \geq c \\ C_r(t) &= 0 \qquad\qquad\quad , \quad t < c \end{aligned}\right\} \tag{3.22}$$

The solution to Eq. (3.14) leads to,

$$\left.\begin{aligned} C_m(t) &= C_{mo}.e^{-k_m.(t-c)}, \quad t \geq c \\ C_m(t) &= 0 \qquad\qquad\quad , \quad t < c \end{aligned}\right\} \tag{3.23}$$

Similarly Eq. (3.15) gives,

$$\left.\begin{aligned} C_s(t) &= C_{so}.e^{-k_s.(t-c)}, \quad t \geq c \\ C_s(t) &= 0 \qquad\qquad\quad , \quad t < c \end{aligned}\right\} \tag{3.24}$$

Combining Eqs. (3.18), (3.21), and using Eqs. (3.22) -(3.24), the solutions for C_{aq}, C_{co_2}, and $\frac{dC_{co_2}}{dt}$ respectively, are,

$$C_{aq}(t) = \begin{cases} \left[\begin{array}{c} C_{aqo}.e^{-k_{aq}.(t-c)} \\ +C_{ro}.k_r.\dfrac{\left(e^{-k_r.(t-c)} - e^{-k_{aq}.(t-c)}\right)}{k_{aq} - k_r} \\ +C_{mo}.k_m.\dfrac{\left(e^{-k_m.(t-c)} - e^{-k_{aq}.(t-c)}\right)}{k_{aq} - k_m}, \quad t \geq c \\ +C_{so}.k_s.\dfrac{\left(e^{-k_s.(t-c)} - e^{-k_{aq}.(t-c)}\right)}{k_{aq} - k_s} \end{array} \right] \\ 0 \quad , \quad t < c \end{cases} \tag{3.25}$$

$$C_{co_2}(t) = \begin{cases} \left[\begin{array}{c} C_{aqo}.\left(1 - e^{-k_{aq}.(t-c)}\right) \\ +\left[C_{ro}.\left(1 - \dfrac{k_{aq}}{k_{aq} - k_r}.e^{-k_r.(t-c)} + \dfrac{k_r}{k_{aq} - k_r}.e^{-k_{aq}.(t-c)}\right)\right] \\ +\left[C_{mo}.\left(1 - \dfrac{k_{aq}}{k_{aq} - k_m}.e^{-k_m.(t-c)} + \dfrac{k_m}{k_{aq} - k_m}.e^{-k_{aq}.(t-c)}\right)\right] \\ +\left[C_{so}.\left(1 - \dfrac{k_{aq}}{k_{aq} - k_s}.e^{-k_s.(t-c)} + \dfrac{k_s}{k_{aq} - k_s}.e^{-k_{aq}.(t-c)}\right)\right] \end{array} \right] \quad , \quad t > c \\ 0 \quad , \quad t \leq c \end{cases} \tag{3.26}$$

$$\frac{dC_{co_2}}{dt} = K_{aq} \begin{cases} \left[\begin{array}{c} C_{aqo}.e^{-k_{aq}.(t-c)} \\ +C_{ro}.k_r.\dfrac{\left(e^{-k_r.(t-c)} - e^{-k_{aq}.(t-c)}\right)}{k_{aq} - k_{hr}} \\ +C_{mo}.k_m.\dfrac{\left(e^{-k_m.(t-c)} - e^{-k_{aq}.(t-c)}\right)}{k_{aq} - k_m}, \quad t \geq c \\ +C_{so}.k_s.\dfrac{\left(e^{-k_s.(t-c)} - e^{-k_{aq}.(t-c)}\right)}{k_{aq} - k_s} \end{array} \right] \\ \frac{dC_{co_2}}{dt} = 0 \quad , \quad t < c \end{cases} \tag{3.27}$$

3.2.6.5 Constraints

Constraints used during the non-linear regression procedure were reported by Komilis [75]. The initial total carbon (%) C_{t0} comprises of the initial readily, moderately, and slowly hydrolysable solid carbon, as well as the initial percentages of intermediate carbon, that is given in Eq. (3.28),

$$C_{to} = C_{ro} + C_{mo} + C_{so} + C_{aqo} \tag{3.28}$$

A similar equation can be written for final conditions,

$$C_{tfinal} = C_{rfinal} + C_{mfinal} + C_{sfinal} + C_{aqfinal} \tag{3.29}$$

As per the assumptions of the model, the various rate constants should follow,

$$0 \le k_s < k_m < k_r < k_{aq} \tag{3.30}$$

During the lag phase, all the rates and emission of C-CO_2 is presumed to be 0 in the model, therefore

$$C_r,\ C_m,\ C_s,\ C_{aq} \text{ and } C_{CO_2} = 0, \qquad t < c \tag{3.31}$$

All the kinetic constants are positive, hence

$$k_r,\ k_m,\ k_s,\ k_{aq},\ c,\ C_r,\ C_m,\ C_s,\ C_{aq} \text{ and } C_{CO_2} \ge 0 \tag{3.32}$$

3.2.6.6 Statistical analysis of experimental data

Each experimental procedure was completed in triplicate. Mean as well as standard deviation (S.D.) of the results were computed in Origin Pro 8.0. The eight parameters set, namely, k_{aq}, k_r, k_m, k_s, C_{r0}, C_{m0}, C_{s0}, C_{aq0}, and c in Eq. (3.26) were computed for the set of constraints of Eqs. (3.28)-(3.32). This was accomplished using non-linear regression analysis for each film and correlating experimental and simulated data. The MS Excel Solver was used for minimizing the sum of squares of the residuals (SSE) in the quasi-Newton method.

3.2.7 Eco-toxicological studies

After the biodegradability test (45 days), three replicate vessels were detached with care, and the content of each was thoroughly mixed. The effect of intermediates of biodegradation on compost quality was evaluated by conducting the microbial, plant growth, and earthworm toxicity tests.

3.2.7.1 Microbial toxicity test

3.2.7.1.1 Procedure

For testing the microbial toxicity after biodegradation, one gram of degraded compost was added in 10 mL sterilized distilled water and *vortexed* for one minute then kept it untouched for half an hour. The compost suspension was sequentially diluted to a factor (10^{-3}) and 100 µL of every dilution factors (10^{-1}, 10^{-2} and 10^{-3}) was used to inoculate the nutrient agar plates. The plates after inoculation were incubated at 37 ºC for 24 hours (in NSW-152 model incubator of Narang Scientific Works Pvt. Ltd., India). The colony forming units on the agar-plates were counted for determining the number of colonies per mL [47].

3.2.7.1.2 Calculation

The microbial populations on the compost samples were calculated (CFU per mL of suspension) using Eq. (3.33)

$$\frac{\text{CFU}}{\text{mL}} = \frac{\text{Number of colonies per mL plated}}{\text{Total dilution factor}} \tag{3.33}$$

In control, only digested municipal digested solid waste (without any polymer sample) was utilized.

3.2.7.2 Plant growth test

3.2.7.2.1 Medium preparation

For testing the plant growth toxicity, a mixture of soil, compost material post biodegradation test, and perlite were used in the ratio of 2:1:1.

3.2.7.2.2 Procedure

Plant growth test was completed as per the guidelines of the organization of economic co-operation and development (OECD 208) [79]. Two plants *Mung* bean (*Phaseolus Aureus*) and wheat (*Tritleum Aestivum*) were used for this test. In this test, 30 *Mung* bean seeds, and 30 wheat seeds plants were used. Experiments were conducted in triplicates. The conditions maintained during experiments are 22±10 ºC, 70±25% humidity and 8 h dark/ 16 h light cycle. The test was continued for 3 weeks. The seedlings grown during 3 weeks test were counted. Both the types of plants were dried at 75 ºC to a constant weight and calculated the total weight of each plant.

3.2.7.3 Earthworm acute toxicity test

3.2.7.3.1 Procedure

The compost material after biodegradation test was used for the earthworm toxicity test as per the guidelines of OECD 207 for earthworm toxicity test [211]. Three adult earthworms were placed in each plastic pot of 250 mL. Tap water was added to increase the moisture of the compost up to 35%. The compost sample for each test was taken 75 g on wet wt. basis. Tests were conducted in triplicates with the compost of each sample and the control. The pots were incubated at 25±2 ºC, with continuous illumination for 2 weeks. After 14 days, the worms were removed and mortality of worms in each pot was recorded. The worms were considered dead when they did not respond to a gentle mechanical stimulus.

3.3 Softwares used

Application software Origin Pro 8 was utilized for fitting of different kinetic data as well as drawing the curves of pristine PP and modified PP films in XRD, FTIR, DSC, TGA, SEM, etc. The non-linear regression analysis was done in MS Excel Solver and it was used for minimizing the sum of squares of the residuals (SSE) in the quasi-Newton method.

Chapter 4- Pro-oxidant Filled Polypropylene Composites

4.1 Preparation of composites

The composition and sample designation of cobalt stearate filled PP composites are given in Table 4.1. The ingredients were mixed manually before filling them in the extruder. The compounding for CoSt filled PP was done in co-rotating twin-screw extruder (M/s Labtech Engineering Co., Ltd. Thailand) at a speed of 150 rpm under a nitrogen blanket and pelletized. The extruder temperature of the feed through die varied from 170 to 230 °C. After extrusion, the continuous compound was cut into small pellets. Then, the prepared compounds were dried in the oven at 70 °C for 2 h to remove moisture.

Table 4.1 Composition of PP and cobalt stearate filled PP samples

Sr. No.	Polymer Samples	Sample Number	Composition	
			PP (phr)	CoSt (phr)
1	PP	S1	100	0
2	PP100CoSt0.2	S2	100	0.2
3	PP100CoSt0.4	S3	100	0.4
4	PP100CoSt0.6	S4	100	0.6
5	PP100CoSt0.8	S5	100	0.8
6	PP100CoSt1.0	S6	100	1.0
7	PP100CoSt1.5	S7	100	1.5
8	PP100CoSt2.0	S8	100	2.0

4.2 Preparation of PP films

The films of CoSt filled PP were casted by compression moulding for 2 min. The pressure and temperature during the film preparation were 400 kN/m^2 and 185 °C, respectively. The films were 80–85 μm thick. The material was sandwiched between two Teflon sheets to prevent the sticking of melt with plates. Tap water was used to cool the plates.

4.3 Abiotic pretreatment

The eight PP samples prepared for the study were coded as S1 (PP), S2 (PP100CoSt0.2), S3 (PP100CoSt0.4), S4 (PP100CoSt0.6), S5 (PP100CoSt0.8), S6 (PP100CoSt1.0), S7 (PP100CoSt1.5), and S8 (PP100CoSt2.0). The abiotic treatment of the films was performed to study the behavior of films under temperature, humidity, and UV exposure. The impact of irradiation time of 12, 24, and 40 h on the weight loss (%) of the modified PP samples was computed. Fig. 4.1 shows the results of the weight loss of modified PP film samples of different formulations. The weight loss of the S8 film was more significant in comparison with other films after UV irradiation. In case of most of the modified PP films, weight loss increased slowly with time. The weight loss of S8 film increased to about 0.1, 0.2, and 0.4 % after 12, 24, and 40 h, respectively.

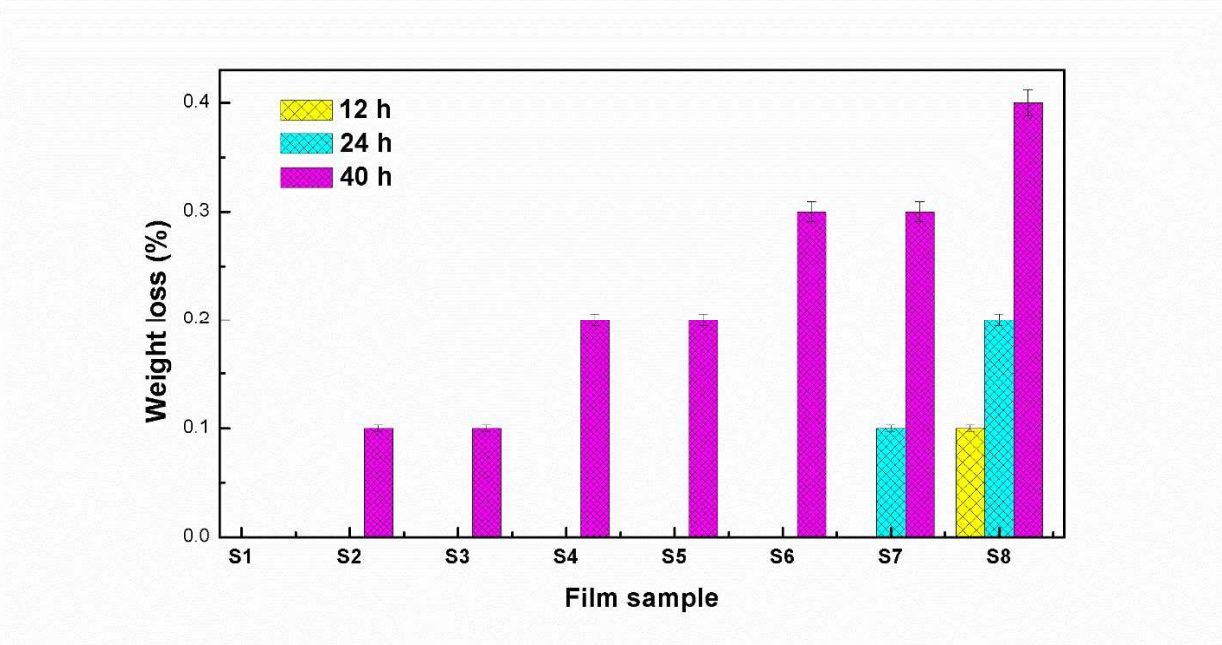

Fig. 4.1 Weight loss in CoSt filled PP samples after abiotic pretreatment (accelerated weathering) for different times ($n = 3$)

4.4 Characterization of samples before and after abiotic pretreatment

4.4.1 Mechanical properties

Before abiotic pretreatment, tensile strength and elongation at break (E_b) of pristine PP obtained were 35 MPa and 3.5%, respectively. On increase in addition of CoSt in the film, significant decrease in tensile strength and elongation at break was observed as shown in Fig. 4.2. This

happened due to the compounding; cobalt stearate might be oxidizing the PP and resulting in lower tensile strength [64, 84]. When cobalt stearate proportion was increased from 0.2 to 2.0 phr, the tensile strength as well as elongation at break decreased from 30.2 to 14.5 MPa, and 3.2 to 1.2 %, respectively probably due to some changes occurring in the polymer matrix because of the influence of CoSt in the PP [5, 206]. The film of PP100CoSt2.0 has a lowest tensile strength as compared to other films. Addition of 0.2 phr CoSt into the PP, the tensile strength reduced up to 30.2 MPa. However, further raising the concentration of CoSt, up to 0.4 phr, the tensile strength reduced significantly to 23.6 MPa. The film of PP100CoSt2.0 shows a lower value of E_b in comparison with PP and all other films as shown in Fig. 4.2. After abiotic treatment, we could not measure the mechanical properties of modified PP films because fragments were formed.

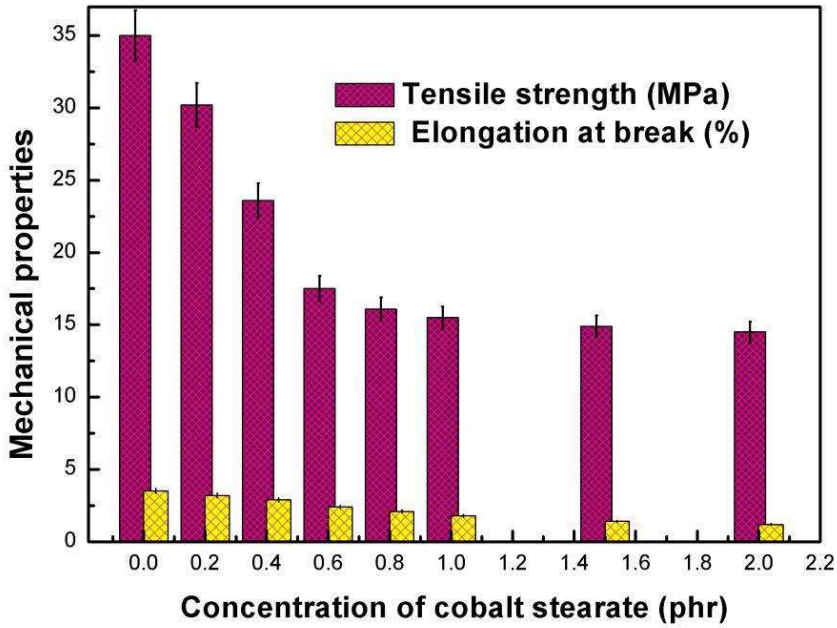

Fig. 4.2 Effect of CoSt concentration on mechanical properties of PP films.

4.4.2 Fourier transform infrared (FTIR) spectroscopy

The structural changes of PP samples were determined by FTIR spectroscopy before and after abiotic pretreatment (for 40 h) and shown in Fig. 4.3 (a). It shows the changes in FTIR peaks of the neat PP (S1), PP100CoSt0.2 (S3), PP100CoSt1.0 (S6), and PP100CoSt2.0 (S8) samples. The FTIR spectra of different formulations were investigated with respect to the time of exposure (Fig.

4.3 (a)). Fig. 4.3 (a) shows the comparison of FTIR peaks of the pristine PP (S1), S3, S6, and S8 samples before and after abiotic pretreatment. The peaks lying in the range of 2949-2866 cm^{-1} are attributed to C-H stretching, the peaks at 1454 cm^{-1} indicates CH_3 bending, and that at 1375 cm^{-1} shows C-H bending for the pristine PP. A small peak at 1735 cm^{-1} is exhibited due to the asymmetric stretching vibration in carbonyl group that is coordinated to Co^{2+} [165]. This substantiates that cobalt stearate has been incorporated in the modified PP film samples. A peak at 1800-1700 cm^{-1} is attributed to carbonyl groups [57, 158]. Before and after abiotic pretreatment, an increase of CoSt concentration did not have a significant effect.

In general, exposure of the films to the accelerated weathering pretreatment enhances the peak intensity due to new carbonyl groups generated on photo-degradation including the chain scission under the Norrish type-1 reaction [157]. In Fig. 4.3 (a) before and after abiotic treatment, a small change in the intensity is found due to low concentration of cobalt stearate. Substantial changes in the carbonyl (1780–1650 cm^{-1}), O-H region (3400 cm^{-1}), and amorphous region (1250-1050 cm^{-1}) are found after abiotic treatment. The absorption band around 1715 cm^{-1} may be assigned to the C=O stretch of ketones. Increases in its intensity and band broadening have also been seen, which indicate the appearance of several oxidation products on increase in CoSt concentration. The carbonyl band might be assigned to C=O stretching vibrations within esters, aldehydes (1734 cm^{-1}), γ lactones (1781 cm^{-1}), and carboxylic acid groups (1700 cm^{-1}). After the accelerated weathering treatment, little variation has been seen within the carbonyl peak (C=O). The carbonyl peak in the R3 film has been found from 1602 cm^{-1} to 1768 cm^{-1} and in the R8 film, from 1637 cm^{-1} to 1795.12 cm^{-1}. After UV exposure, the FTIR spectra show slight changes in the carbonyl group, and the extent of change depends on the pro-oxidant concentration [30, 36].

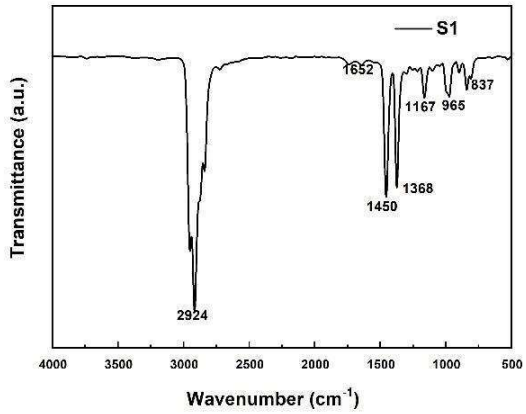

Before

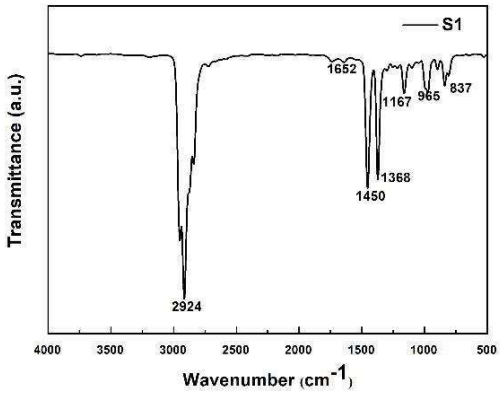

After

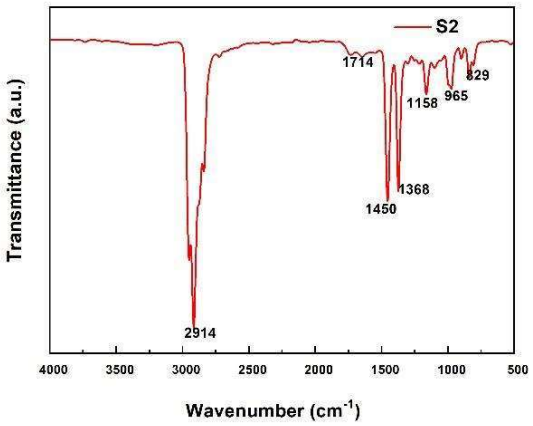

Before

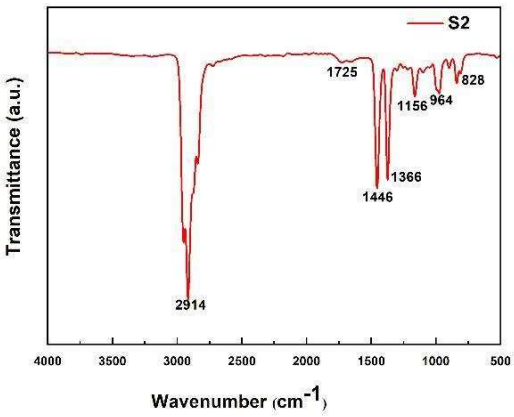

After

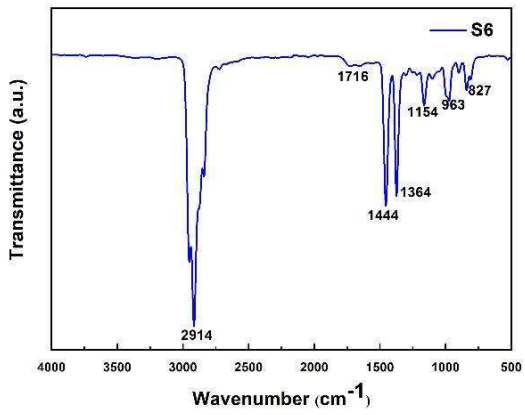

Before

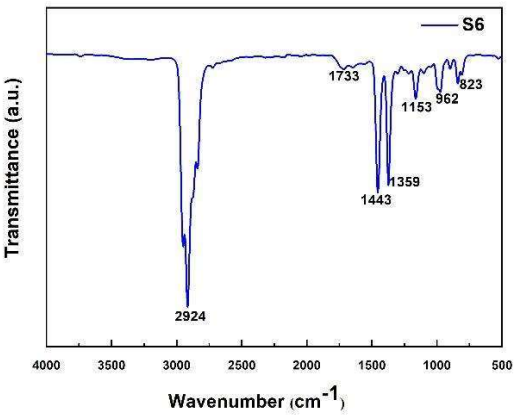

After

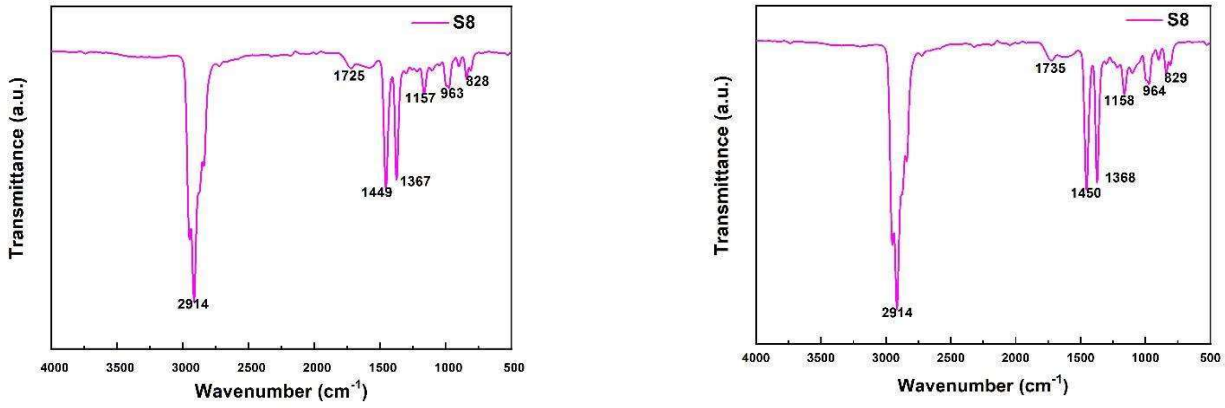

Before After

Fig. 4.3 (a) FTIR spectra of PP and CoSt filled PP samples before and after abiotic treatment (40 h)

4.4.2.1 Carbonyl index

Fig. 4.3 (b) presents the carbonyl index (CI) of PP films before and after abiotic treatment (for 40 h) as calculated from the FTIR data and using Eq. (3.1). The results showed that the highest carbonyl (0.83) index was found in PP100CoSt2.0 film sample after abiotic pretreatment (for 40 h). The increase in CI of modified PP films is proportional to the CoSt loading and time of exposure.

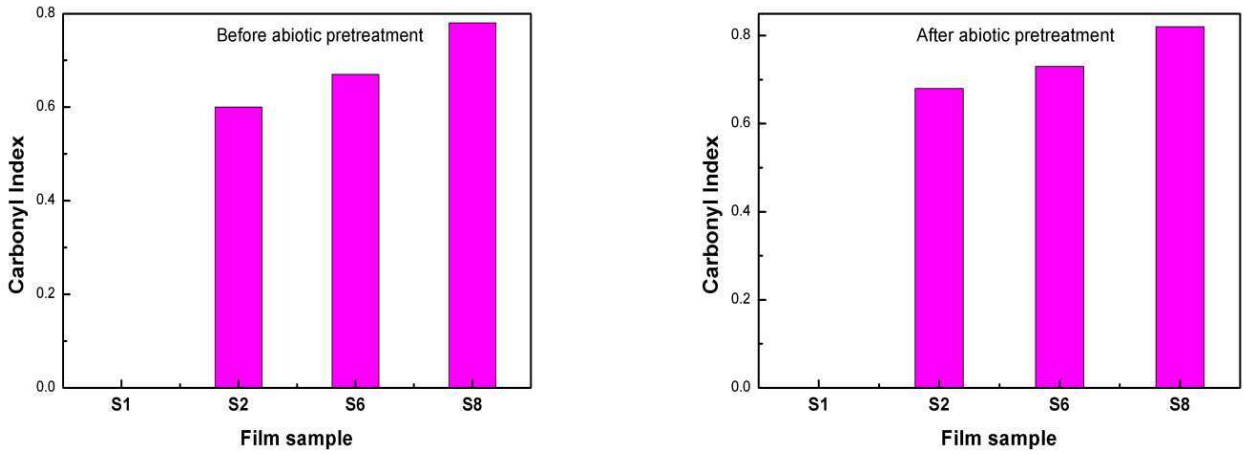

Fig. 4.3 (b) Carbonyl index (CI) of pro-oxidant PP films before and after abiotic treatment (for 40 h)

4.4.2.2 Mechanism of action

The degradation of the polymer takes place due to physical-chemical combined attack by light and atmospheric oxygen. The mechanism of the pro-oxidant catalyzed polyolefin degradation is a free radical chain reaction [172]. The pro-oxidant present in the polymer absorbs energy and transfer of electron in the 3d subshell of the cobalt which is leading to the formation of carboxylic acid-free radical (R'COO.). This radical again decarboxylates and forms R', which converts PP (PH) into free radical R. Then, O_2 reacts with free radicals, leading to hydroperoxide and peroxide which tend to breakdown to give oxygenated products of the PP chain scissions [212]. The oxidative reaction followed by the decay of peroxides and alkyl hydroperoxides leads to creation of carbonyl groups discoverable by FTIR [172, 213]. These carbonyl groups can abstract hydrogen from the PP chain and lead to the creation of radicals [152, 172, 214]. The reaction schemes of oxidative breakdown of the polymer chains are given below:

$$PH\ (heat, O_2, stress) \rightarrow POOH \tag{4.1}$$

$$POOH + M^{n+} \rightarrow PO^{\bullet} + M^{(n+1)+} + OH^{-} \tag{4.2}$$

$$POOH + M^{(n+1)+} \rightarrow POO^{\bullet} + M^{n+} + H^{+} \tag{4.3}$$

$$2POOH \xrightarrow{M^{n+}/M^{(n+1)+}} POO^{\bullet} + PO^{\bullet} + H_2O \tag{4.4}$$

Where, M represents cobalt metal and PH represents PP molecule. Sometimes, redox reactions reduce the activation energy of bimolecular peroxide decay. This decay by a transition metal in two oxidation states will be a factor in both light and heat-induced oxidation [64].

4.4.3 Thermogravimetric analysis (TGA)

The thermogravimetric analysis was performed for all the films before and after abiotic pretreatment (for 40 h). The thermogravimetric (TG) and differential thermogravimetric (DTG) analysis curves of all the films are shown in Fig. 4.4. It shows the comparison of TG and DTG curves before and after abiotic pretreatment of samples. After abiotic pretreatment, the weight loss is found to be more in modified PP samples. The weight-loss behavior of all the films was studied in a nitrogen atmosphere. Table 4.2 summarizes the values of T_i and T_f before and after abiotic pretreatment (accelerated weathering). The values of initiation degradation temperature (T_i) of

modified PP samples after abiotic pretreatment were lower than before abiotic pretreatment and pristine PP. It reveals that the loading of CoSt increases the degradation of PP because of metal ions in the CoSt and abiotic pretreatment [157]. The final degradation temperature (T_f) of the modified PP films before and after abiotic pretreatment was also lower than that of the pristine PP. This degradation has taken place due to UV exposure. It includes the chain scission and generation of carbonyl groups under the Norrish type-1 reaction [157]. The figure also shows that the thermal stability after abiotic pretreatment of S1, S2, S3, S4, S5, S6, S7, and S8 was upto 224.01, 190.17, 173.98, 167.83, 166.96, 165.24, 164.10, and 157.19 °C, respectively.

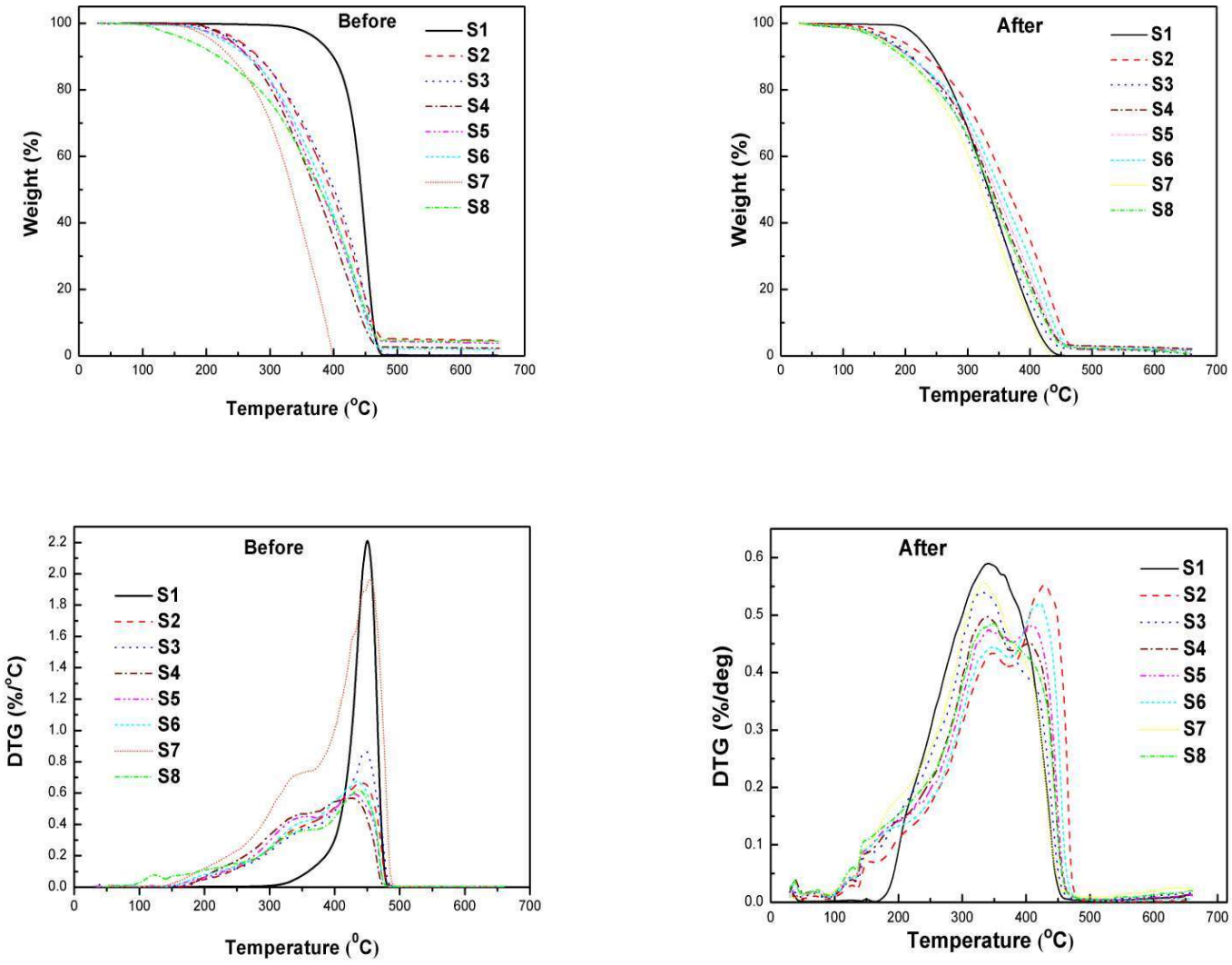

Fig. 4.4 TG and DTG curves of PP and CoSt filled PP films before and after abiotic pretreatment (for 40 h)

Table 4.2 TGA data of PP and CoSt filled PP samples before and after abiotic pretreatment (accelerated weathering)

Film sample	*Before* T_i (°C)	*After* T_i (°C)	*Before* T_f (°C)	*After* T_f (°C)	Weight loss (%)
S1	375.23	224.01	466.00	420.41	100
S2	248.66	190.17	549.03	457.96	100
S3	243.54	173.98	466.05	433.35	100
S4	236.43	167.83	458.41	443.67	100
S5	231.95	166.68	468.00	445.69	100
S6	225.11	165.24	462.04	449.76	100
S7	207.84	164.10	393.12	415.38	100
S8	169.81	157.19	470.49	441.21	100

4.4.4 Differential scanning calorimetry (DSC)

Before and after abiotic pretreatment, the film behavior through the cycle of heating and cooling in temperature from 30 to 200 °C was observed in DSC analysis. The results are shown in Fig. 4.5. The pristine PP is a semicrystalline thermoplastic polymeric material. The crystalline nature of the pristine PP film is destroyed and it undergoes a process of fusion by application of heat. The DSC data of all the films after accelerated weathering pretreatment (for 40 h) are presented in Table 4.3 and compared with those without any treatment. Table 4.3 also shows the comparison of T_m, T_c, and (ΔH_m) obtained from the DSC analysis before and after accelerated weathering pretreatment. The crystallinity of the film samples before and after accelerated weathering pretreatment is calculated by using Eq. (3.2), and listed in Table 4.2. The crystallinity $(X_c\%)$ and T_m of the pristine PP before and after accelerated weathering pretreatment is 63% and 166 °C, respectively.

The melting temperatures (T_m) of the modified PP films after accelerated weathering pretreatment are lower than those before accelerated weathering pretreatment and pristine PP due to the addition of functional groups [84, 167]. This could be because of the faster photo-degradation of modified PP samples. The CoSt pro-oxidant increases the susceptibility to thermal degradation [121]. The

crystallinity of the modified PP films after accelerated weathering pretreatment was also found to be lower than those before accelerated weathering pretreatment and pristine PP. The presence of cobalt stearate and accelerated weathering pretreatment decreases the crystallinity [5, 157], and consequently makes the modified PP films more prone to microbial attacks [84, 165].

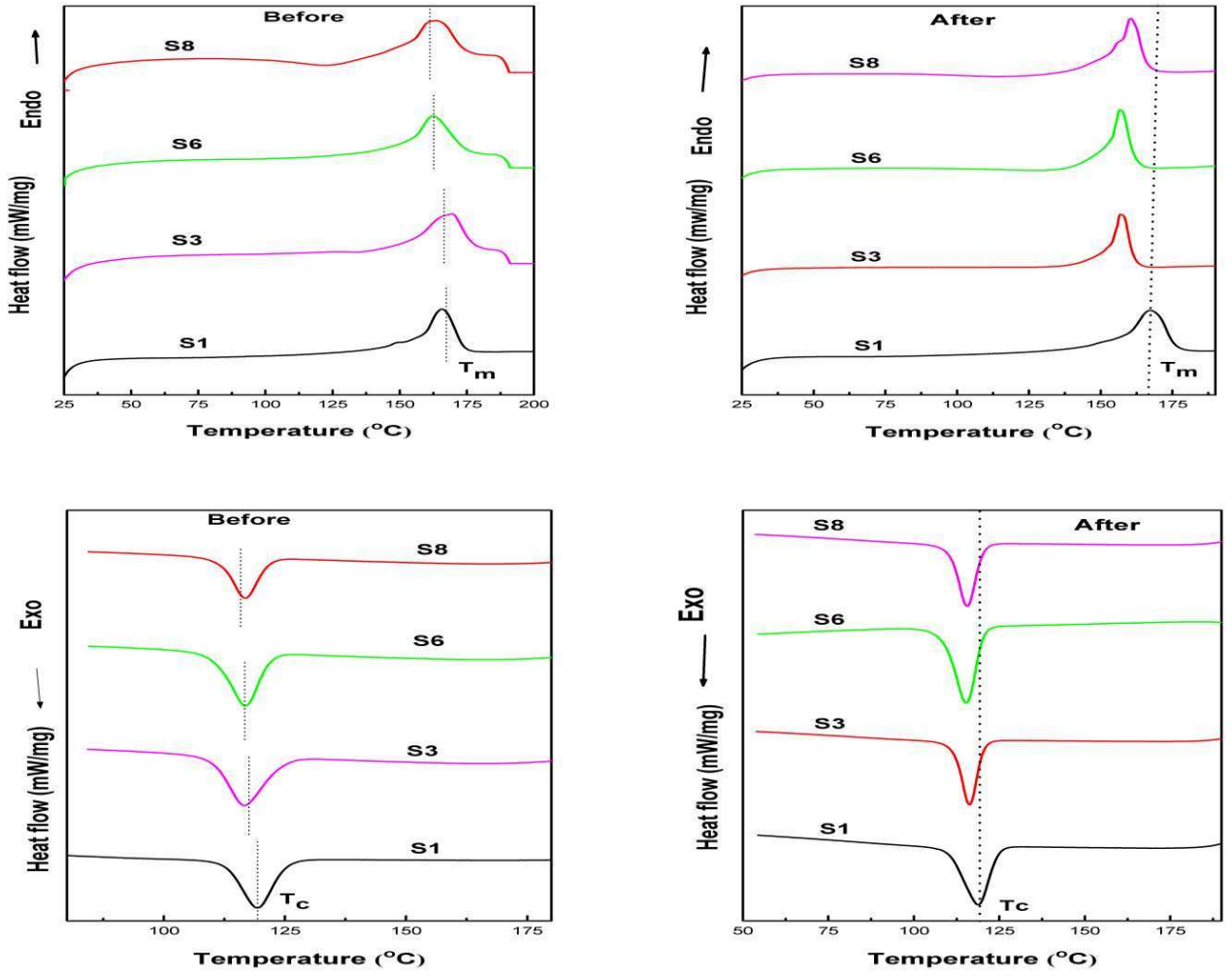

Fig. 4.5 DSC thermograms of PP and CoSt filled PP films before and after abiotic pretreatment (for 40 h)

Table 4.3 DSC melting and crystallization parameters of PP and CoSt filled PP films before and after abiotic treatment (accelerated weathering)

Film sample	*Before* T_m (°C)	*After* T_m (°C)	*Before* T_c (°C)	*After* T_c (°C)	*Before* ΔH_m (Jg^{-1})	*After* ΔH_m (Jg^{-1})	*Before* X_c (%)	*After* X_c (%)
S1	166.39	166.39	119.13	119.13	104	104	63.80	63.80
S3	165.21	157.66	116.68	116.09	78.25	78.05	48.00	47.88
S6	164.91	156.97	116.24	115.46	78	77	47.85	47.23
S8	164.12	156.14	116.06	114.71	77.5	76.40	47.54	46.87

4.4.5 X-ray diffraction (XRD)

Fig. 4.6 reveals the XRD patterns of all the samples before and after abiotic pretreatment (for 40 h). The diffraction peaks of the pristine PP indicated at 2θ = 14.1°, 16.8°, 18.6°, 21.1°, and 21.8° correspond to the α-monoclinic form of PP [42, 84, 165]. The addition of CoSt in the PP and due to abiotic pretreatment reduced the intensity of these peaks, it indicates decreased crystallinity [84]. The presence of CoSt did not change the diffraction angles [206]. Table 4.4 shows the comparison of percentage crystallinity of different films before and after abiotic pretreatment as determined by Eq. (3.3). The percentage crystallinity of pristine PP is 76.57% before and after abiotic treatment, it decreased to 64.2%.

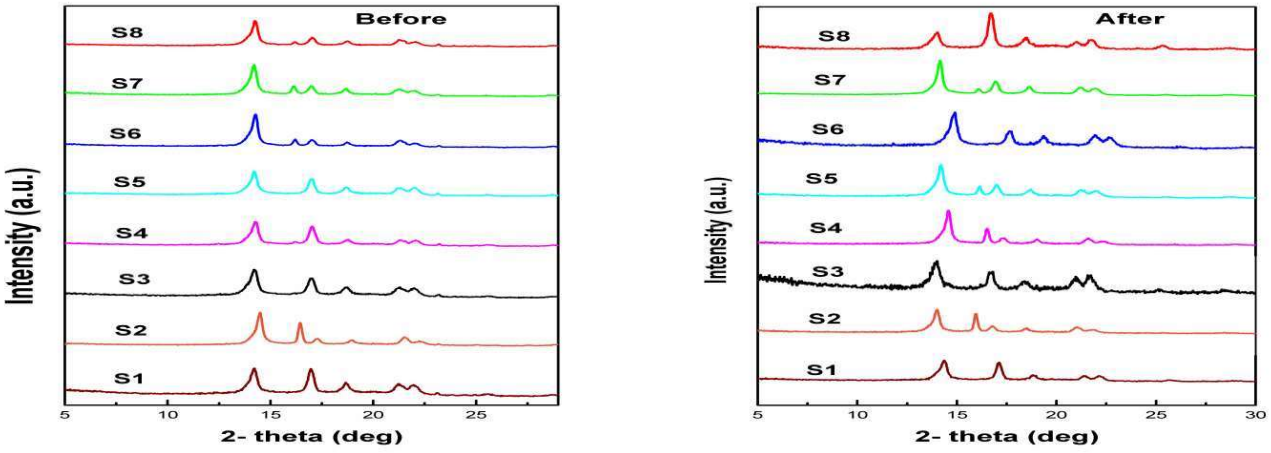

Fig. 4.6 XRD results of PP and CoSt filled PP films before and after abiotic pretreatment (for 40 h)

Table 4.4 Crystallinity (%) of different films as calculated from XRD analysis before and after abiotic pretreatment (accelerated weathering)

Film sample	Before	After
S1	76.57	76.57
S2	75.40	75.34
S3	73.41	72.36
S4	71.32	70.63
S5	69.74	68.96
S6	69.02	68.29
S7	67.63	66.14
S8	65.20	64.20

4.4.6 Scanning electron microscopy (SEM)

Fig. 4.7 shows a comparison of the morphology of film samples before any abiotic pretreatment and after abiotic pretreatment. The surface of the pristine PP (S1) films look smooth, clear, and dense before and after abiotic pretreatment as compared to that of the modified films. Before abiotic pretreatment, it was found that presence of CoSt did not significantly affect the morphology of the pristine PP [84, 121]. But, after abiotic pretreatment, the modified PP becomes rough and shows the formation of small cracks, erosion, and fractures (Fig. 4.7) [157, 215]. However, the extent of damage was much more prominent in the modified PP films with higher CoSt content.

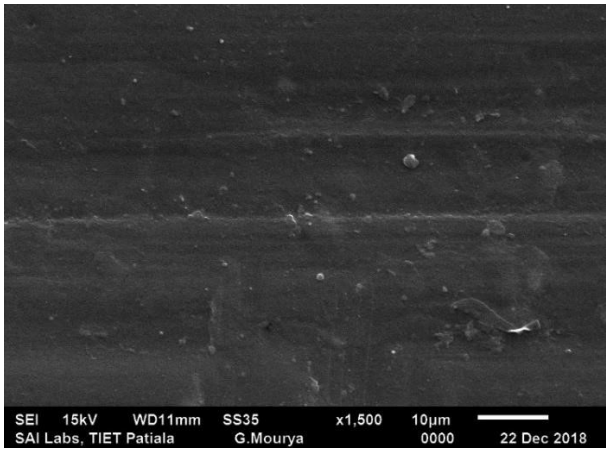

Before any pretreatment (S1)

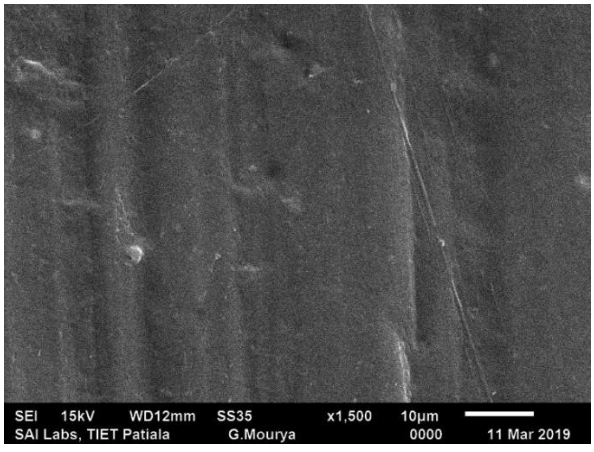

After abiotic pretreatment(S1)

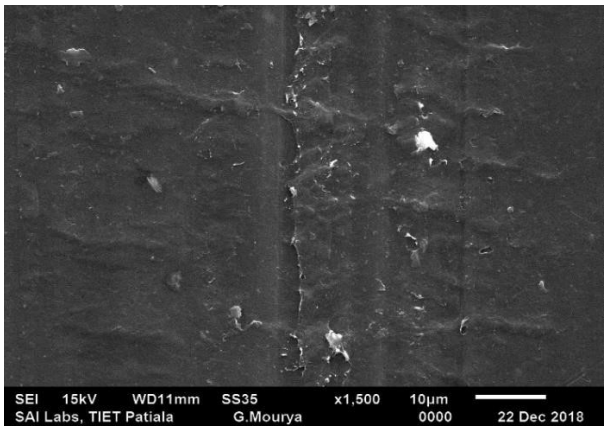

Before any pretreatment (S2)

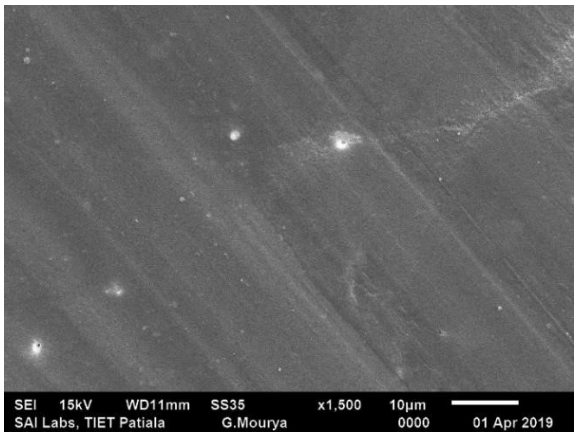

After abiotic pretreatment (S2)

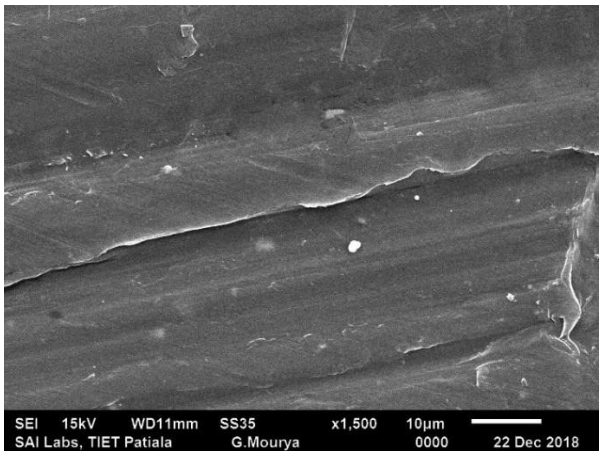

Before any pretreatment (S3)

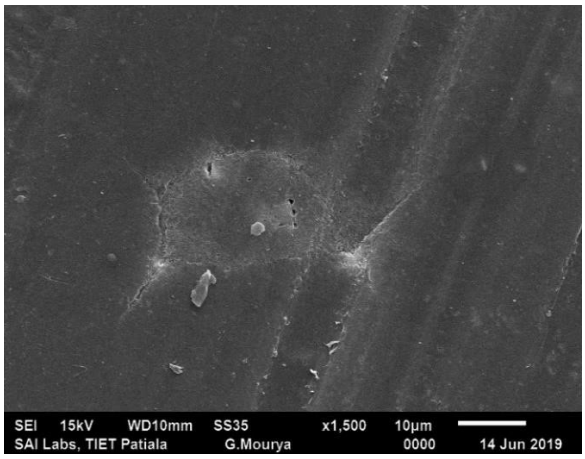

After abiotic pretreatment (S3)

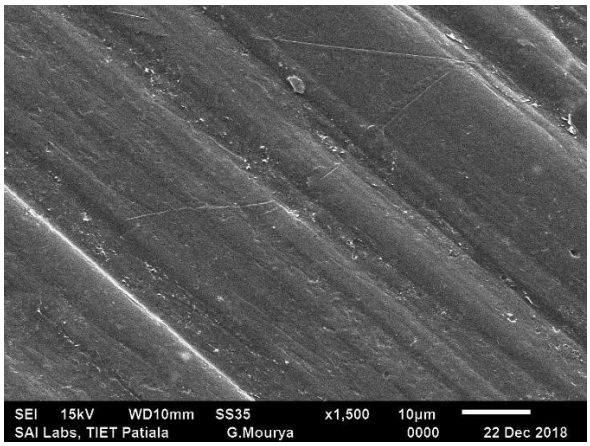

Before any pretreatment (S4)

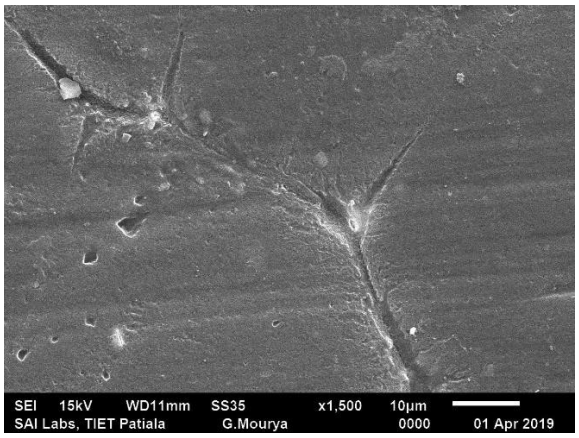

After abiotic pretreatment (S4)

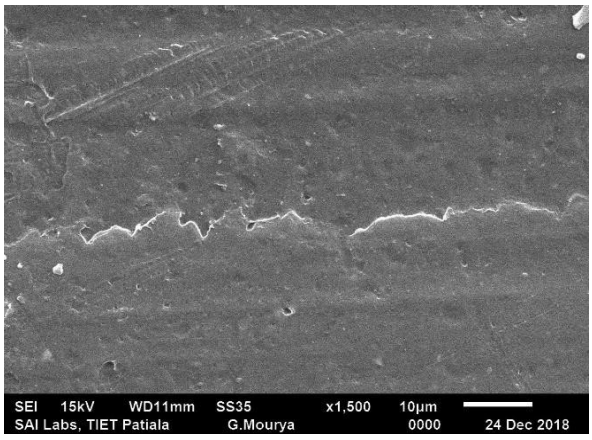

Before any pretreatment (S5)

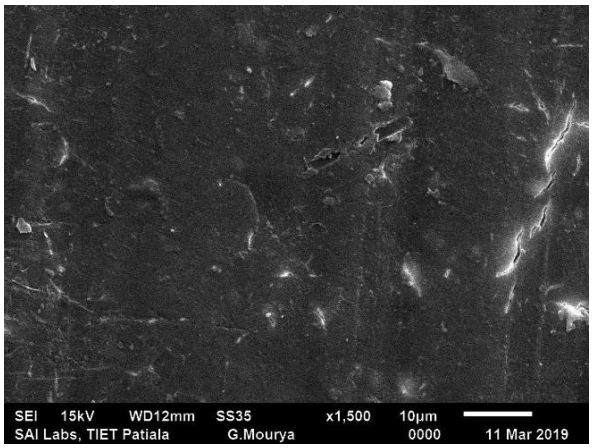

After abiotic pretreatment (S5)

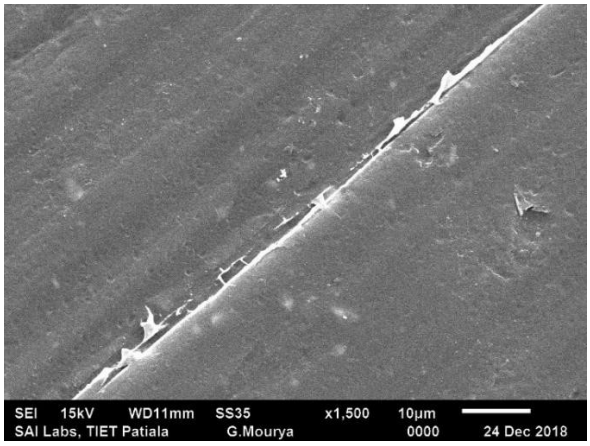

Before any pretreatment (S6)

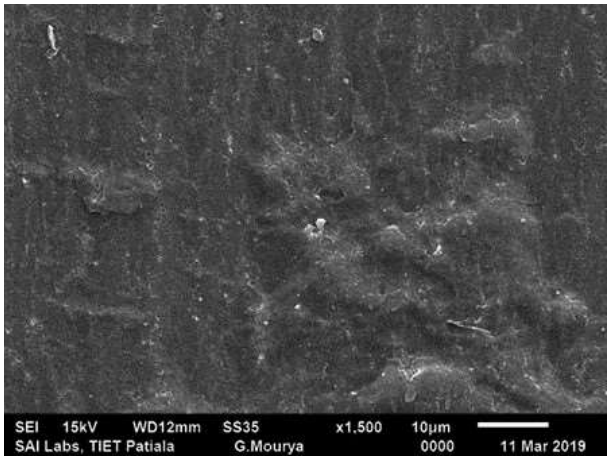

After abiotic pretreatment (S6)

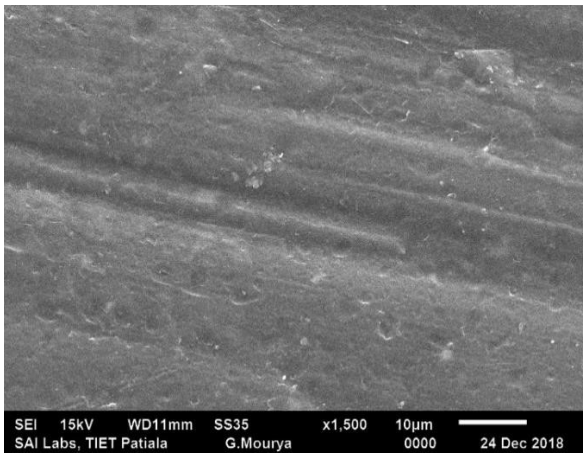

Before any pretreatment (S7)

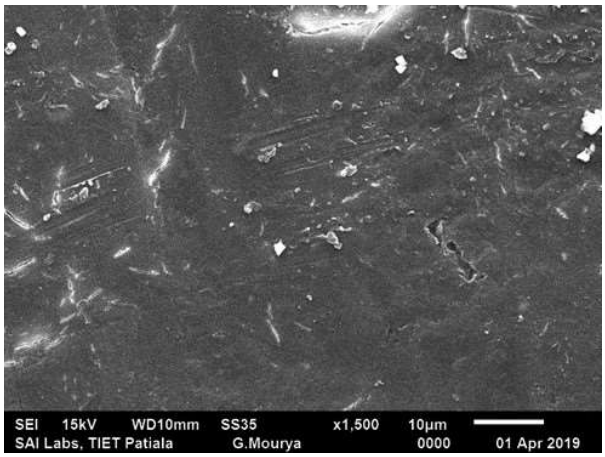

After abiotic pretreatment (S7)

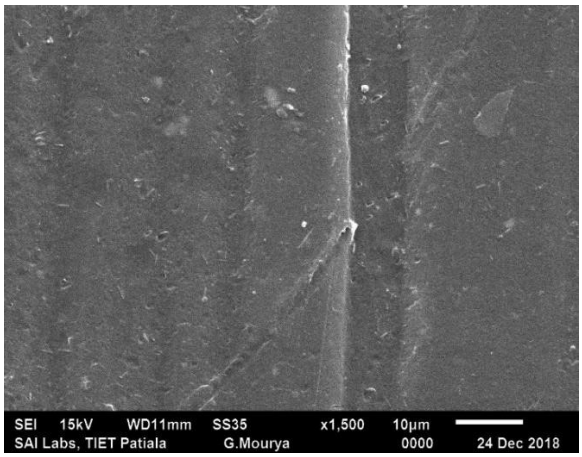

Before any pretreatment (S8)

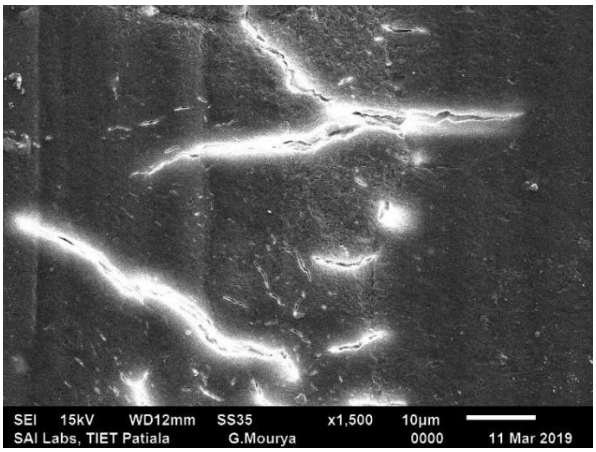

After abiotic pretreatment (S8)

Fig. 4.7 SEM images before any pretreatment and after abiotic pretreatment (for 40 h) of different samples (a) PP (S1), (b) PP100CoSt0.2 (S2) (c) PP100CoSt0.4 (S3), (d) PP100CoSt0.6 (S4), (e) PP100CoSt0.8 (S5) (f) PP100CoSt1.0 (S6) (g) PP100CoSt1.5 (S7), and (h) PP100CoSt2.0 (S8)

4.4.7 Rheological properties

The rheological study is necessary to know the structure–property relationship of materials, during the processing especially in the melt state. Dynamic shear strain sweep testing was applied to study the linear viscoelasticity region (VLE) of polymeric materials. Shear rheological behaviour is sensitive to the chain length as well as topologic structure. The storage modulus (G') is utilized to estimate the elastic behavior and the loss modulus (G") is utilized to know the viscous behavior of the polymers. The storage modulus is a more sensitive rheological function in contrast to the loss modulus for structural changes of the polymer composites. Fig. 4.8 shows the result of rheological studies of pristine PP (S1) and the PP composite with highest CoSt pro-oxidant loading S8. Fig. 4.8 (a, b) presents the dependance of storage modulus (G') and loss modulus (G") on the shear strain. The films revealed a linear behavior (Newtonian plateau) at lower shear strain and a nonlinear behavior at higher shear strain. The storage modulus as well as loss modulus of the modified PP film are lower than pristine PP.

The viscosity is a measure of the resistance to flow, especially the complex viscosity (η*). Fig. 4.8 (c) shows the complex viscosity (η*) v/s angular frequency (ω) curves for CoSt filled PP composites. For all the modified PP films, η* reduces monotonically with rise in angular frequency (shear thinning). The reduction in η* with rise in ω shows the pseudo-plastic behavior of all the modified PP films. As expected, with rise in shear rate, the viscosity reduced for pristine PP (S1)

and the PP composite with highest CoSt pro-oxidant loading S8. The presence of CoSt pro-oxidant in PP film reduced the complex viscosity but less significantly because of better mixing.

The elastic and viscous properties of pristine PP (S1) and the PP composite with highest CoSt pro-oxidant loading S8 are given in Figs. 4.8 (d) and 4.8 (e), showing the storage modulus as well as loss modulus as a function of angular frequency. The dependance of G' and G" on ω shows the relative motion of all the molecules in the bulk and can give vital information about the flow behavior of the melts [216]. Storage modulus of all the composites rises monotonously with rise in frequency. The loss modulus trends are quite same as that of storage modulus.

Fig. 4.8 (f) shows the dependency of loss angle (tan δ) on frequency of modified PP films. The loss angle is stated as the ratio of the loss to the storage modulus. It shows the viscoelastic damping behavior of a polymer system [84]. The loss angle value reduces with rise in frequency as observed in Fig 4.8 (f). A positive slope of tan δ curve would have displayed the elastic response of the viscoelastic samples. For pristine PP (S1) and the PP composite with highest CoSt pro-oxidant loading S8, the slope of the tan δ curve is negative from Fig. 4.8 (f). It exhibits that the composites behave as viscoelastic.

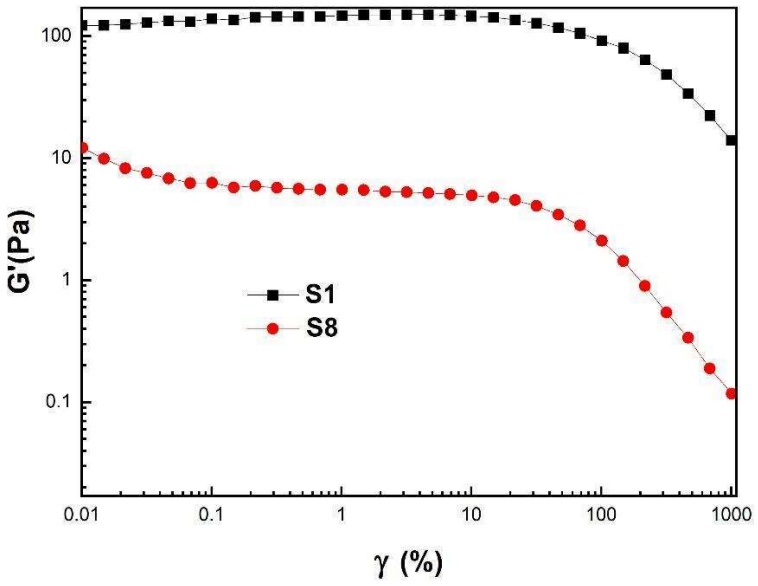

Fig. 4.8 (a) Storage modulus (G') as a function of shear strain (γ) of pristine PP and CoSt pro-oxidant filled PP film samples

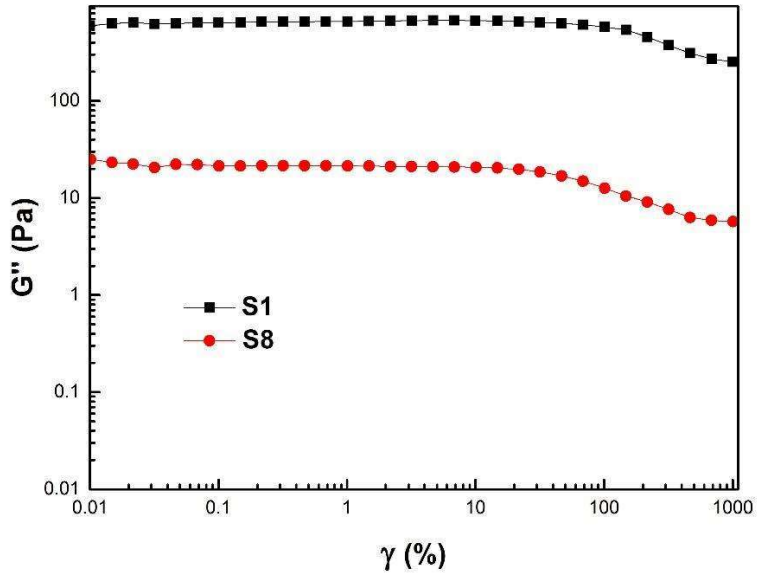

Fig. 4.8 (b) Loss modulus (G") as a function of shear strain (γ) of pristine PP and CoSt pro-oxidant filled PP film samples

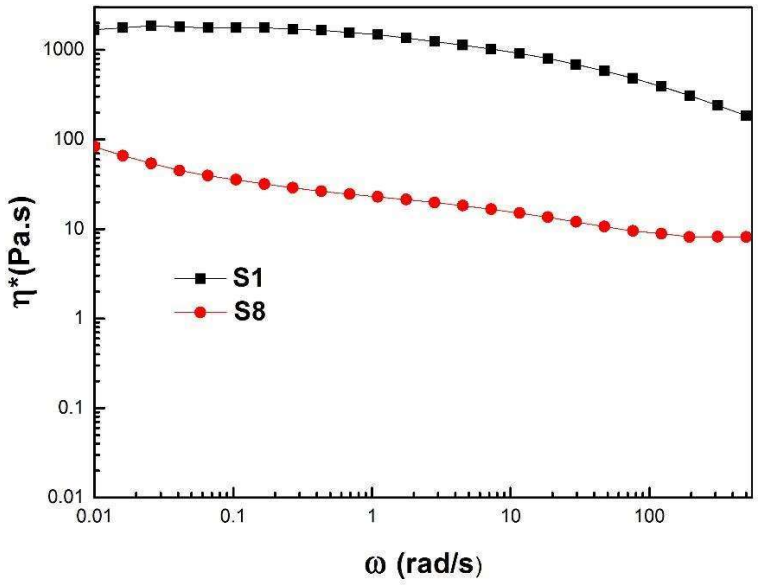

Fig. 4.8 (c) Complex viscosity (η*) as a function of angular frequency (ω) of pristine PP and CoSt pro-oxidant filled PP films

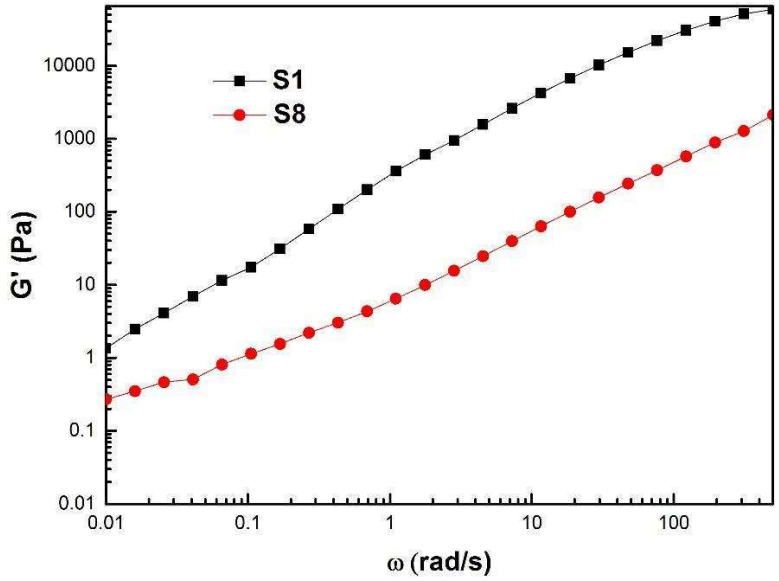

Fig. 4.8 (d) Storage modulus (G') as a function of angular frequency (ω) of pristine PP and CoSt pro-oxidant filled PP films

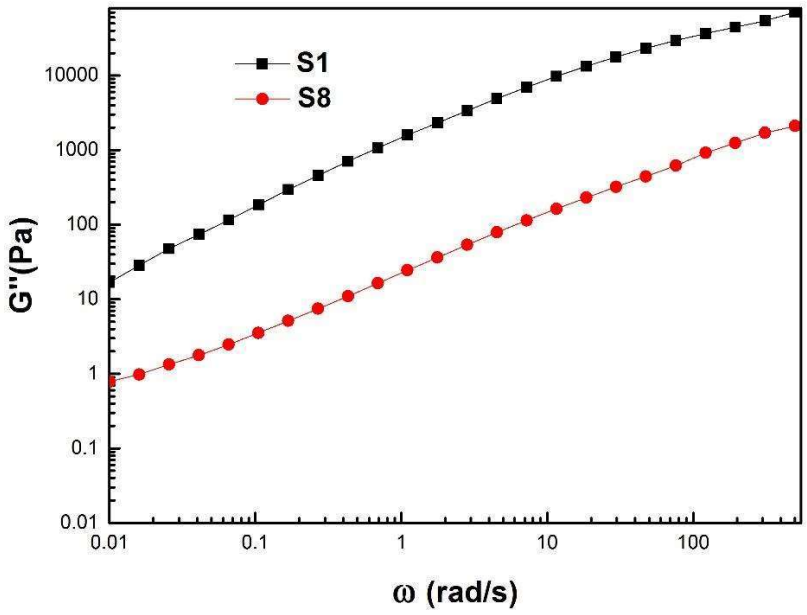

Fig. 4.8 (e) Loss modulus (G") as a function of angular frequency (ω) of pristine PP and CoSt pro-oxidant filled PP films

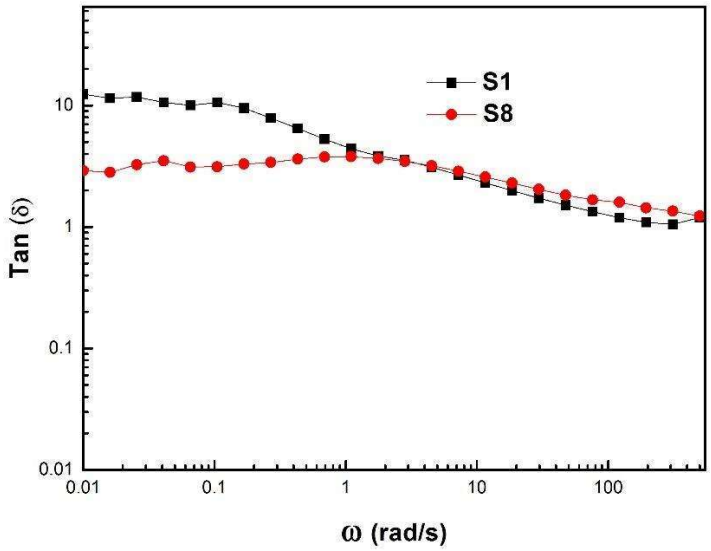

Fig. 4.8 (f) Tan (δ) as a function of angular frequency (ω) of pristine PP and CoSt pro-oxidant filled PP film samples

4.5 Biodegradability studies without and after abiotic pretreatment

The total organic carbon (TOC) of various composite films without and after abiotic pretreament were determined from TOC analyzer and used to compute the theoretical carbon dioxide (*$CO_2(th)$*), and presented in Tables 4.5 and 4.6, respectively.

Table 4.5 Total organic carbon (%) and theoretical CO_2 (g) emission from the films without abiotic pretreatment

Sample	TOC (%)	Wt. of carbon in 1 g of sample (g)	Th. CO_2 evolution (g)
Microcrystalline cellulose (CEL)	42	0.42	1.54
PP	96	0.96	3.52
PP100CoSt0.2	91	0.91	3.33
PP100CoSt0.4	89	0.89	3.26
PP100CoSt0.6	88	0.88	3.22
PP100CoSt0.8	87	0.87	3.19
PP100CoSt1.0	86	0.86	3.15
PP100CoSt1.5	85	0.85	3.11
PP100CoSt2.0	84	0.84	3.08

Table 4.6 Total organic carbon (%) and theoretical CO_2 (g) emission from the samples after abiotic pretreatment

Sample	TOC (%)	Wt. of carbon in 1 g of sample (g)	Th. CO_2 evolution (g)
Microcrystalline cellulose (CEL)	42	0.42	1.54
PP	96	0.96	3.525
PP100CoSt0.2	88	0.88	3.22
PP100CoSt0.4	88	0.88	3.22
PP100CoSt0.6	87	0.87	3.19
PP100CoSt0.8	86	0.86	3.15
PP100CoSt1.0	85	0.85	3.11
PP100CoSt1.5	84	0.84	3.08
PP100CoSt2.0	83	0.83	3.04

Example calculation for theoretical CO_2 (g)

CO_2 (*Th*) for PP100CoSt0.2 sample = $1 \times 0.91 \times \frac{44}{12} = 3.33$

The values of CO_2 generated (g) and the biodegradability (%) of every film was determined by Eqs. 3.4 and 3.5, respectively.

Example calculation for biodegradability (%)

Molecular weight of $Ba(OH)_2.8H_2O$ = 315.47

Water taken = 4 lit

Mass of $Ba(OH)_2.8H_2O$ taken = 16 g

Moles of $Ba(OH)_2.8H_2O$ = $\frac{16}{315.47} = 0.0507$

Therefore, molarity of $Ba(OH)_2.8H_2O$ = $\frac{0.0507}{4} = 0.0127$

Vol. of $Ba(OH)_2.8H_2O$ taken = 30 mL

Hence, mmols of $Ba(OH)_2.8H_2O$ taken = 30 × 0.0127 = 0.381 mmols

And,

Vol. of HCl used = 9.5 mL

Normality of HCl = 0.05

Molarity of HCl = 0.05 (as the basicity of HCl is 1)

Hence, mmols of HCl utilized = 9.5 × 0.05 = 0.475 mmols

Now,

$$\text{mmols of } CO_2 \text{ emitted} = \text{mmoles of } Ba(OH)_2 \text{ at start} - \frac{\text{mmol of HCl}}{2}$$

$$= 0.381 - \frac{0.475}{2} = 0.1435 \text{ mmols}$$

We know that,

1 mol of CO_2 = 44 g/L

Therefore, 1 mmol of CO_2 produced = 44×10^{-3} = 0.044 g/L

Hence, grams of CO_2 generated = 0.1435 × 0.044 = 0.0063 g

In this way, the readings were taken after 2-3 days of interval for 45 days and the cumulative sum of CO_2 emitted for PP100CoSt0.2 film was 3.55 grams.

Finally, using Eq. 3.5, we get,

$$(\%) \text{ Biodegradation} = \frac{3.55 - 3.29}{3.33} \times 100 = 7.65\%$$

The biodegradability of all the films, without and after accelerated weathering pretreatment (for 40 h), was determined under thermophilic composting conditions. The microorganisms present in the inoculum mineralize the CoSt filled PP films and formed CO_2, H_2O, and biomass [84]. The percentage biodegradability of modified PP films without and after abiotic pretreatment was computed using Eq. (3.5) based on the cumulative CO_2 emission after 45 days. The fragments appear gradually in the photo-degraded films in the biotic treatment. Fig. 4.9 presents the biodegradability of all the modified PP films without and after abiotic pretreatment. Without abiotic pretreatment, in the increasing order of their biodegradability, these are: PP(S1) 0%, PP100CoSt0.2(S2) 7.65%, PP100CoSt0.4(S3) 8.90%, PP100CoSt0.6(S4) 10.35%,

PP100CoSt0.8(S5) 11.52%, PP100CoSt1.0(S6) 14.38%, PP100CoSt1.5(S7) 17.11%, PP100CoSt2.0(S8) 19.78%, and cellulose (reference) 77.11%. Similarly, after abiotic pretreatment, in the increasing order of their biodegradability, these are: PP (S1) 0%, PP100CoSt0.2 (S2) 11.20%, PP100CoSt0.4 (S3) 14.90%, PP100CoSt0.6 (S4) 18.18%, PP100CoSt0.8 (S5) 23.19%, PP100CoSt1.0 (S6) 28.13%, PP100CoSt1.5 (S7) 32.23%, PP100CoSt2.0 (S8) 36.42%, and cellulose (CEL) 77.11% whereas the maximum biodegradability of S8 was only 19.78% when the film was not given any abiotic treatment.

The results showed that biodegradability has been enhanced by abiotic treatment because of the formation of functional groups, amorphous nature, weak linkages, and chain scission [165, 180]. The more amorphous nature of the modified PP makes it prone to microbial attack [5, 84]. Microorganisms are consuming it as a source of energy and releasing carbon dioxide, water, and biomass [174]. The higher biodegradation is attributed to their tendency for thermal degradation, enhancing the availability of short chains for the microbial attack [165].

The degradation process during composting proceeds in two steps. The first step involves the abiotic hydrolysis of solid and the second step involves the carbon biomineralization [75]. The degradation mechanism can be summarized as follows. During the first step, free radicals are generated by the reaction of PP with oxygen. The radicals are converted into hydroperoxides that further decompose to more radicals due to the metal salt by chain reaction mechanism [172]. Henceforth, the original polymer chain gets fragmented through microbial action.

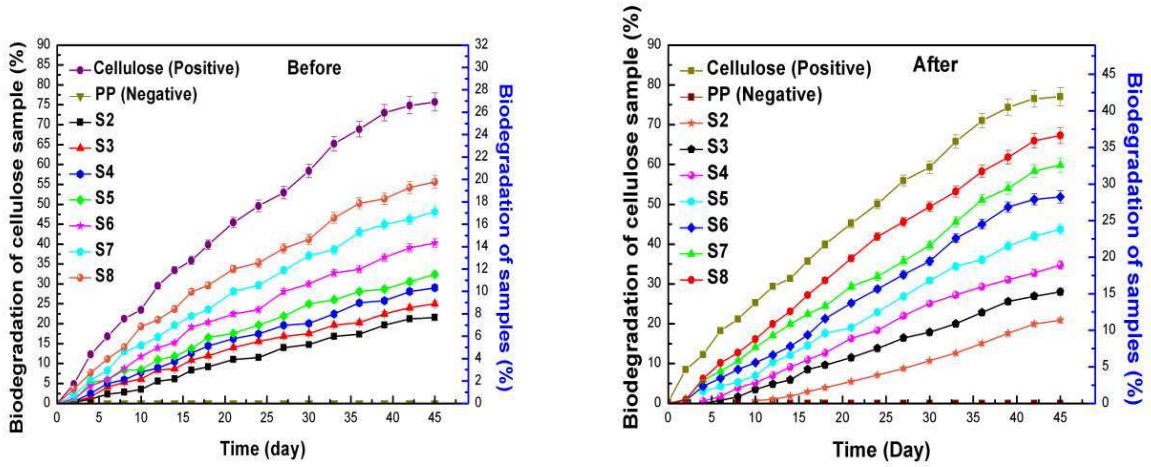

Fig. 4.9 Biodegradability (on biotic treatment) of different samples without (left) and after (right) abiotic (40 h) pretreatment

4.5.1 Scanning electron microscopy (SEM)

The surface morphology of the biotically treated films was observed. Fig. 4.10 shows morphology of different films without any pretreatment and after biodegradation test, abiotically treated and after biodegradation test under controlled composting conditions. Fig. 4.10 (a) shows the surface of pristine PP after the biodegradability test (for 45 days). After 45 days, the surface of the PP films does not change its morphology. It indicates that microbes have not attacked the PP film during biodegradability test.

Fig. 4.10 (b-h) shows the surface morphology of modified PP films without any pretreatment and after biotic treatment, after abiotic and biotic treatment. After composting test, distinct changes were found on modified PP films, with roughening, cavitation, and disintegration of the surface, which is clear confirmation of biodegradation results [35, 56]. The surface of modified PP films changed, indicating that it was attacked by the microorganisms under composting conditions. More pronounced exfoliation, peeling, and several small holes in the plate structure were found in comparison to pristine PP. It indicates a greater degree of surface deterioration of modified PP films. As the addition of CoSt pro-oxidant concentration and exposure time increases the roughness of the pristine PP increases. Finally, we concluded that SEM results of modified PP films after pretreatment and after biotic treatment are rougher than without any pretreatment and after biotic treatment.

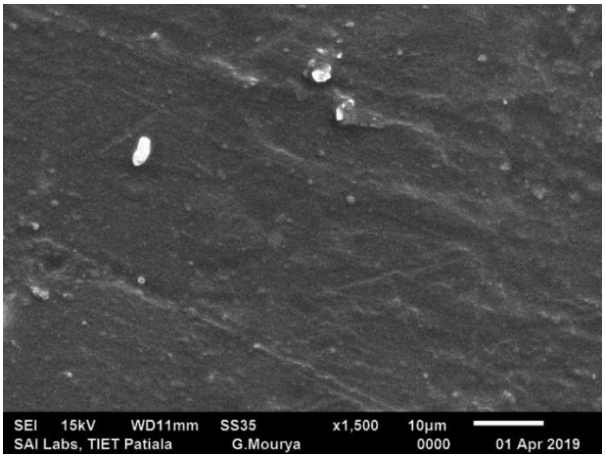

S1 (Without any treatment and after biotic treatment)

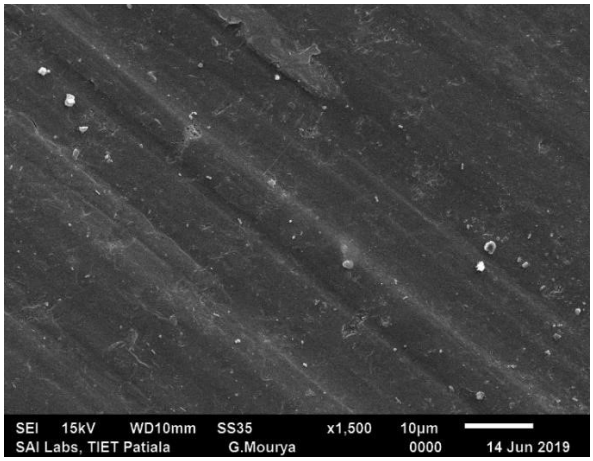

S1 (After abiotic and biotic treatment)

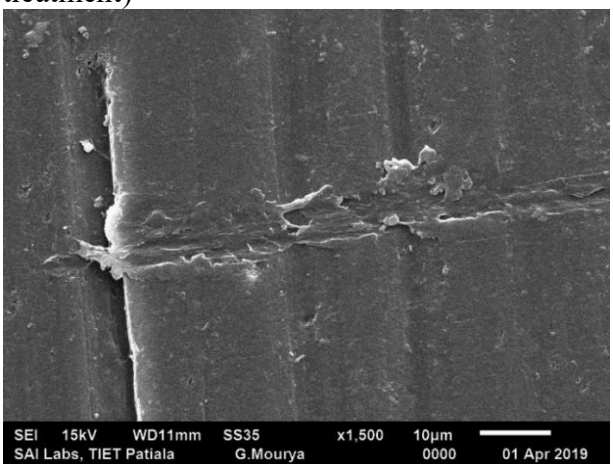

S2 (Without any treatment and after biotic treatment)

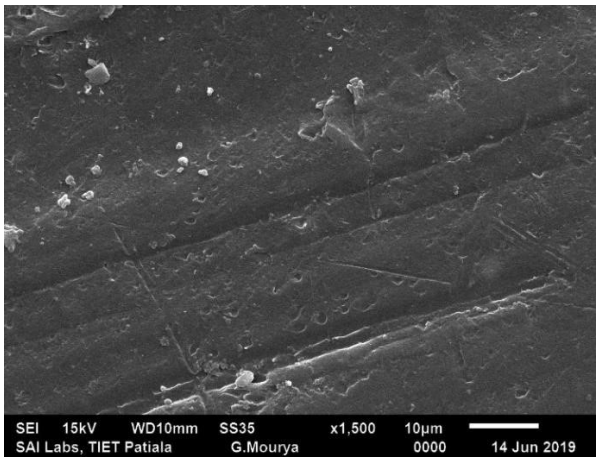

S2 (After abiotic and biotic treatment)

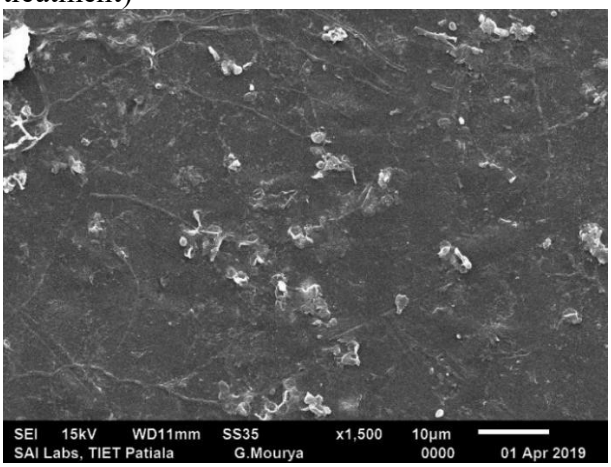

S3 (Without any treatment and after biotic treatment)

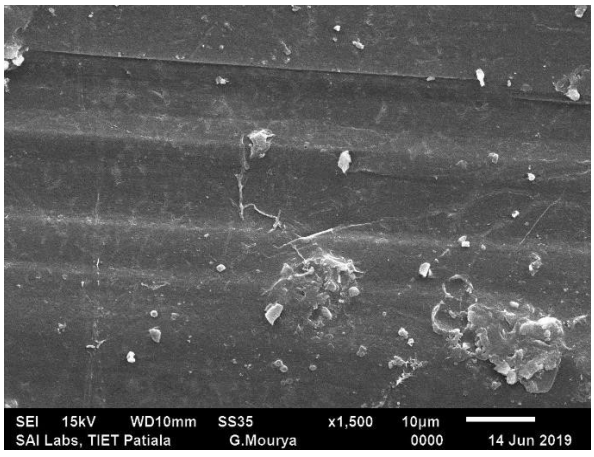

S3 (After abiotic and biotic treatment)

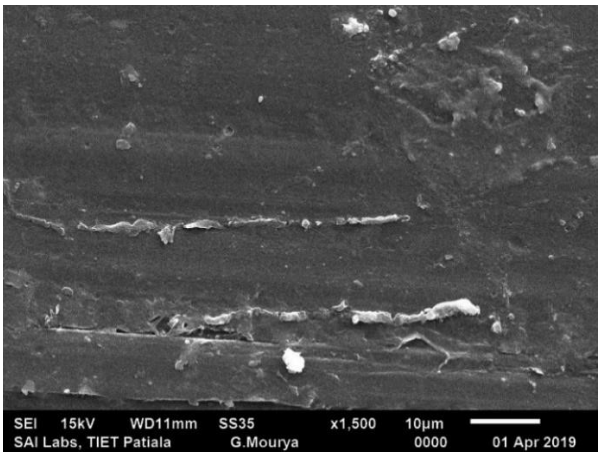

S4 (Without any treatment and after biotic treatment)

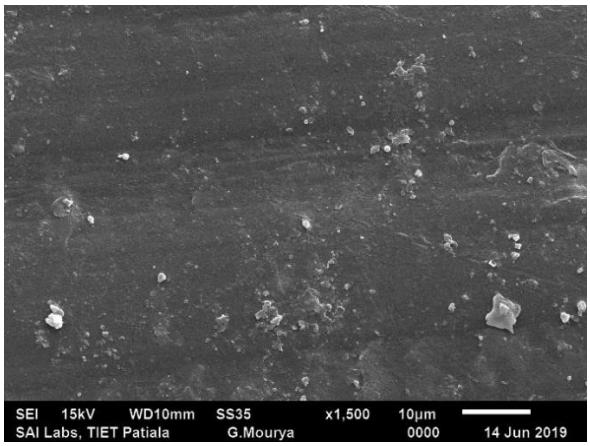

S4 (After abiotic and biotic treatment)

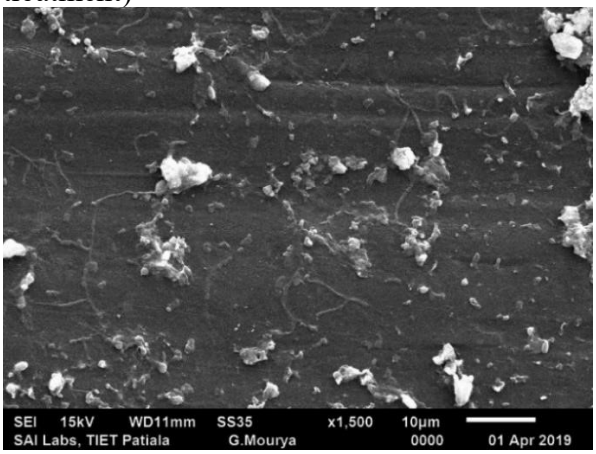

S5 (Without any treatment and after biotic treatment)

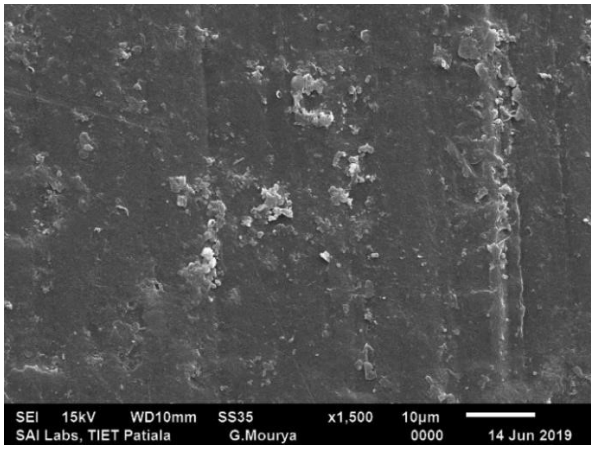

S5 (After abiotic and biotic treatment)

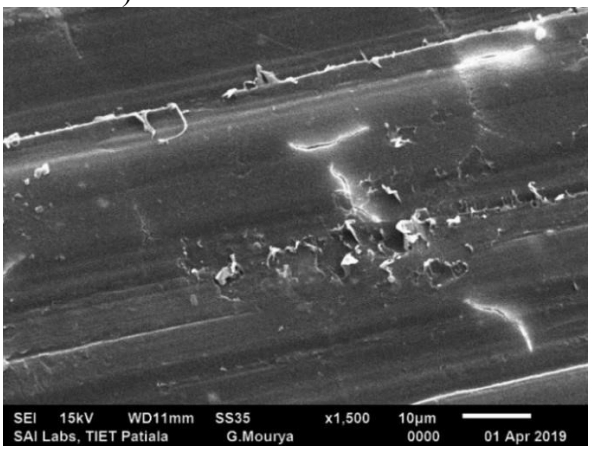

S6 (Without any treatment and after biotic treatment)

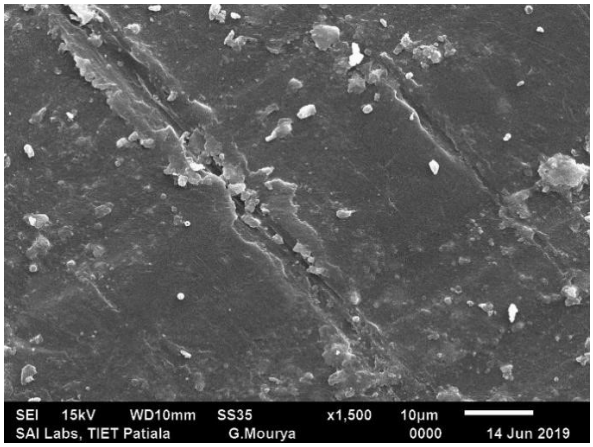

S6 (After abiotic and biotic treatment)

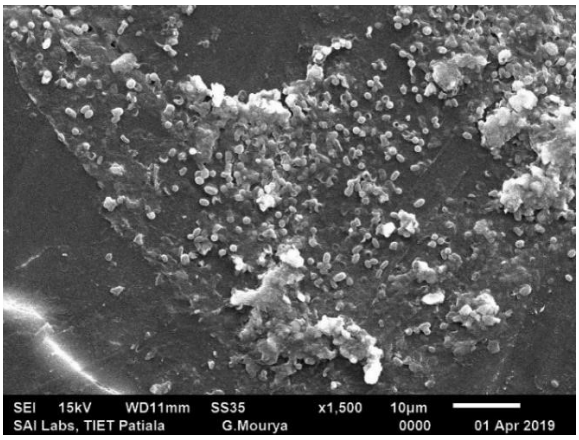

S7 (Without any treatment and after biotic treatment)

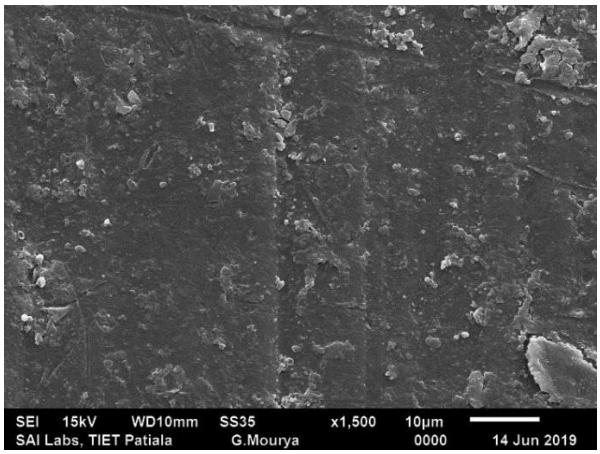

S7 (After abiotic and biotic treatment)

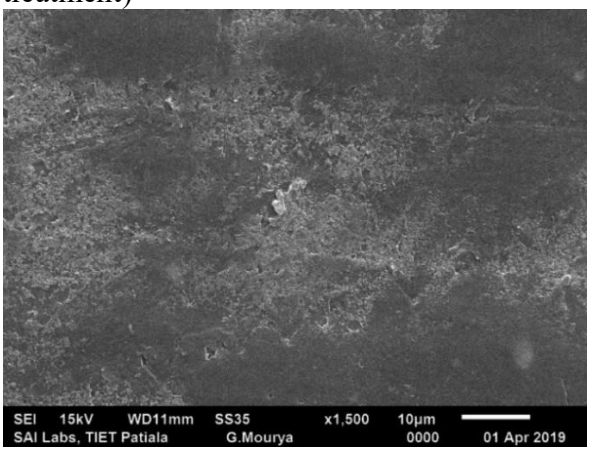

S8 (Without any treatment and after biotic treatment)

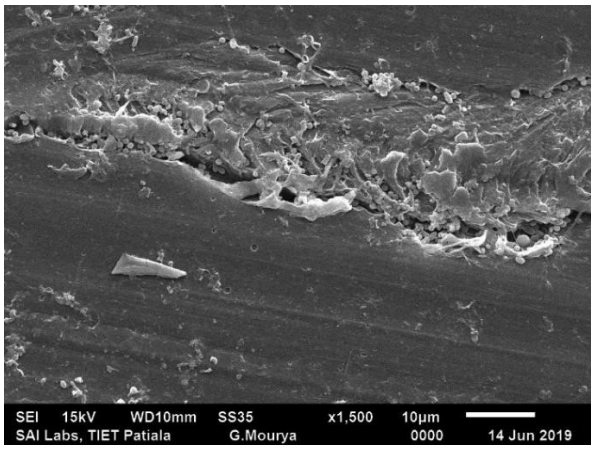

S8 (After abiotic and biotic treatment)

Fig. 4.10 SEM images without (left) any treatment and after biotic treatment (45 days), after (right) abiotic (for 40 h) and biotic (45 days) treatment of different film samples: (a) PP (S1), (b) PP100CoSt0.2 (S2) (c) PP100CoSt0.4 (S3), (d) PP100CoSt0.6 (S4), (e) PP100CoSt0.8 (S5) (f) PP100CoSt1.0 (S6) (g) PP100CoSt1.5 (S7), and (h) PP100CoSt2.0 (S8)

4.5.2 Molecular weight analysis

Reduction in molecular weight is one of the most consistent signs of biodegradation in biodegradable polymers in different environmental conditions. Abiotic pretreatment also results in abundant chain scission of PP because of hydroperoxides produced in the oxidation step. Significant amounts of volatile compounds such as acetic acid, acetone, and methanol have also been observed [153, 217]. The molecular weight analysis was carried out for the pristine PP samples and PP100CoSt2.0 samples that exhibit maximum biodegradability. Table 4.7 shows the average molecular weights ($\overline{M_n}$, $\overline{M_w}$), and PDI of the PP and modified PP films without any

treatment, after abiotic pretreatment and after biodegradation tests. After the abiotic (accelerated weathering) pretreatment, both the $\overline{M_n}$ and $\overline{M_w}$ values of the modified PP films (oxidized) are much lower than those of the pristine PP. $\overline{M_n}$ values are more sensitive to low molecular weights. The addition of CoSt pro-oxidant catalyses the breakdown of hydroperoxides and also improves the embrittlement of PP chains under abiotic pretreatment. This chain breakage increases the carbon mineralisation of the polymeric materials [30, 43]. The decrease of molecular weight of various modified PP films exposed to abiotic pretreatment is related to the degree of oxidation. It can be seen that the decrease of molecular weight is higher in the case of modified PP films compared with pristine PP [58, 153].

Table 4.7 Average molecular weights ($\overline{M_n}$ and $\overline{M_w}$) and polydispersity index (PDI) of the PP samples and CoSt filled PP samples before (without any pretreatment), after (abiotic treatment), without any pretreatment and after biotic treatment, and after abiotic and biotic treatment

Polymer sample		$\overline{M_n}$	$\overline{M_w}$	PDI
PP	Without any pretreatment	69500	560900	8.07
	Without any pretreatment and after biotic treatment	69500	560900	8.07
	After abiotic pretreatment	69500	560900	8.07
	After abiotic pretreatment and biotic treatment	69500	560900	8.07
PP100CoSt2.0	Without any pretreatment	78700	434100	5.51
	Without any pretreatment and after biotic treatment	5400	18500	3.42
	After abiotic pretreatment	5200	16100	3.08
	After abiotic pretreatment and biotic treatment	5300	17200	3.24

4.6 Biodegradation kinetic modeling of pro-oxidant filled PP composites without and after abiotic pretreatment

4.6.1 Kinetics and model parameters

The un-degraded carbon was calculated by using Eq. (3.11) utilizing the carbon to carbon dioxide conversion experimental data. The trajectory of the undegraded carbon reveals its kinetics. Fig. 4.11 shows the undegraded carbon vs. time plots for S2, S3, S4, S5, S6, S7, and S8 films without and after abiotic pretreatment. Without abiotic pretreatment, these seven films showed degradability in the range of 7.65-19.78% and after abiotic pretreatment showed biodegradability in the range of 11.20 - 36.42 % because of integration of CoSt and abiotic pretreatment as explained in Section 4.5. These figures demonstrate similar kinetic behavior as indicated by the shape of the curves. Therefore, these should fall into a similar kinetic regime. In previous work, a similar methodology has been used for the kinetic modelling of complex reaction systems [218].

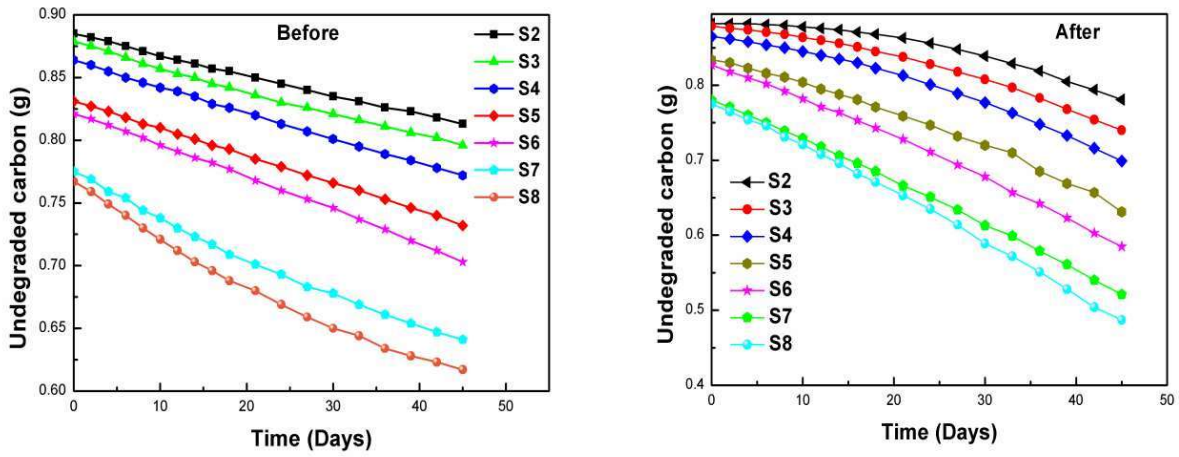

Fig. 4.11 Computed undegraded carbon profiles of different samples without (left) and after (right) abiotic pretreatment (accelerated weathering) (S2: PP100CoSt0.2, S3: PP100CoSt.4, S4: PP100CoSt0.6, S5: PP100CoSt0.8, S6: PP100CoSt1.0, S7: PP100CoSt1.5, S8: PP100CoSt2.0)

Tables 4.8 and 4.9 presents the kinetic parameters results with their determination coefficient (R^2). In all the experiments, the obtained data is well correlated as R^2 values are close to 1. Fig. 4.12 shows the kinetics of intermediate solid carbon into CO_2 production from the experimental and

model predictions without and after abiotic pretreatment. Fig. 4.13 presents C-CO_2 emitted data for the cellulose, blank, and PP controls during an experiment from the inoculum without and after abiotic pretreatment.

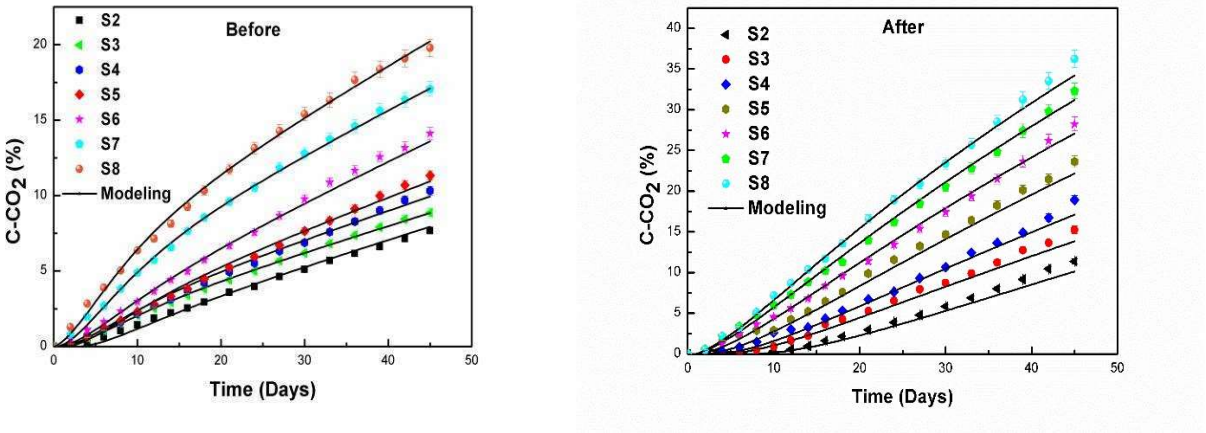

Fig. 4.12 C-CO_2 evolution profiles of different samples without (left) and after (right) abiotic pretreatment (accelerated weathering) (S2: PP100CoSt0.2, S3: PP100CoSt0.4, S4:PP100CoSt0.6, S5: PP100CoSt0.8, S6: PP100CoSt1.0, S7: PP100CoSt1.5, S8: PP100CoSt2.0). Error bars correspond to twice standard deviation (n = 3)

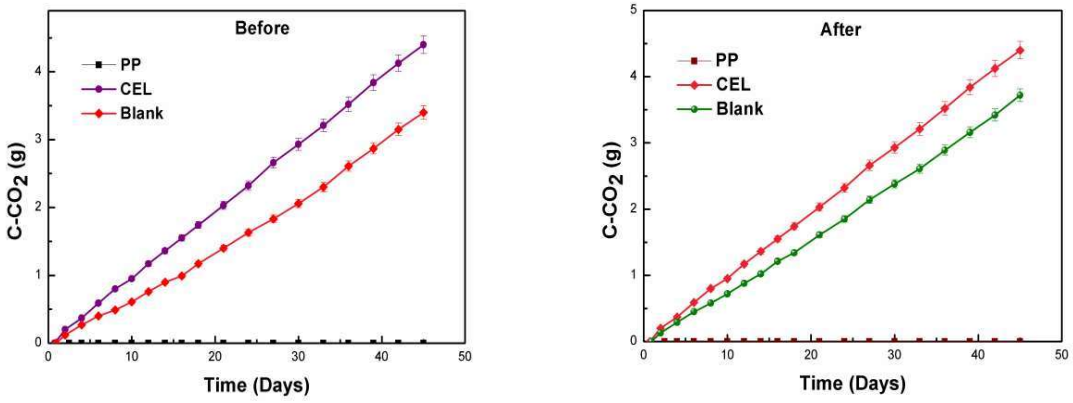

Fig. 4.13 C-CO_2 evolution for the blank, PP (without and after abiotic pretreatment), and cellulose from the compost. Error bars correspond to twice standard deviation (n = 3)

Table 4.8 Kinetic model parameters and coefficients of determination without abiotic pretreatment (accelerated weathering)

Parameters	PP	PP100CoSt0.2	PP100CoSt0.4	PP100CoSt0.6	PP100CoSt0.8	PP100CoSt1.0	PP100CoSt1.5	PP100CoSt2.0	Cellulose
	S1	S2	S3	S4	S5	S6	S7	S8	CEL
C-CO_2 evolution (%) ± s.d.	0.0	7.65 ± 0.32	8.90 ± 0.37	10.35 ± 0.3	11.52 ± 0.39	14.38 ± 0.48	17.11 ± 0.6	19.78 ± 0.65	77.11 ± 2.6
Biodegradability (%)	0.0	7.65	8.90	10.35	11.52	14.38	17.11	19.78	77.11
C_{aq0} (%)	-	0.084	0.7	0.65	0.23	0.25	0.61	0.87	9.5
C_{r0} (%)	-	1.2	1.2	1.6	2	2	4	4.85	6
C_{m0} (%)	-	98.71	98.1	97.75	97.77	97.75	95.39	94.28	84.5
C_{s0} (%)	-	-	-	-	-	-	-	-	-
k_{aq} (day^{-1})	-	0.21	0.22	0.22	0.22	0.22	0.23	0.24	0.24
k_r (day^{-1})	-	0.20324	0.21230	0.21632	0.21835	0.21942	0.22613	0.23821	0.15
k_m (day^{-1})	-	0.00190	0.00195	0.00216	0.00242	0.00312	0.00353	0.00432	0.035
k_s (day^{-1})	-	0	0	0	0	0	0	0	0
c (day)	-	2.92	1.77	1.42	1.54	0.623	0.515	0.05	0.75
R^2	-	0.9993	0.9996	0.9979	0.9974	0.9973	0.9990	0.9990	0.9997

Table 4.9 Kinetic model parameters and coefficients of determination after abiotic pretreatment (accelerated weathering)

Parameters	PP	PP100CoSt0.2	PP100CoSt0.4	PP100CoSt0.6	PP100CoSt0.8	PP100CoSt1.0	PP100CoSt1.5	PP100CoSt2.0	Cellulose
	S1	S2	S3	S4	S5	S6	S7	S8	CEL
C-CO_2 evolution (%) ± s.d.	0.0	11.20 ± 0.39	14.90 ± 0.48	18.18 ± 0.72	23.19 ± 0.98	28.13 ± 0.86	32.23 ± 1.1	36.42 ± 1.5	77.11 ± 2.6
Biodegradability (%)	0.0	11.20	14.90	18.18	23.19	28.13	32.23	36.42	77.11
C_{aq0} (%)	-	0.00001	0.00001	0.000016	0.62	1	2	2	9.5
C_{r0} (%)	-	0.00001	0.00001	0.00001	0.00045	0.531	0.535	1.47	6
C_{m0} (%)	-	99.99	99.99	99.99	99.37	98.46	97.46	96.53	84.5
C_{s0} (%)	-	-	-	-	-	-	-	-	-
k_{aq} (day^{-1})	-	0.13	0.18	0.18	0.18	0.18	0.18	0.18	0.24
k_r (day^{-1})	-	0.12111	0.17212	0.17521	0.17732	0.17812	0.17823	0.17921	0.15
k_m (day^{-1})	-	0.00361	0.00423	0.00515	0.00662	0.00796	0.00918	0.01432	0.035
k_s (day^{-1})	-	0	0	0	0	0	0	0	0
c (day)	-	7.04	3.6	2.8	2.23	1.31	1.08	0.96	0.75
R^2	-	0.9936	0.9946	0.9946	0.9972	0.9982	0.9987	0.9974	0.9997

Without and after abiotic pretreatment, the computed parameters and regression analysis are presented in Tables 4.8 and 4.9. All the samples have moderately hydrolysable carbon and readily hydrolysable carbon fractions that can be utilized by microbes and increase their degradability. The moderately hydrolysable carbon fractions (C_{m0}) and hydrolysis rates (k_m) are appreciably high in all the samples without and after abiotic pretreatment. The films do not include slowly hydrolysable carbon fractions. They show sigmoid behavior in Fig. 4.12 and also exhibit an initial flat lag phase as their '$_c$' values are non-zero (Tables 4.8 and 4.9). In all the samples, the values of initial intermediate hydrolysable carbon fraction C_{aq0} are significantly low, which shows the absence of short polymeric chains [35]. The results here show only one kinetic regime.

In Tables 4.8 and 4.9, the C_{r0} values decrease with progressive decrease in pro-oxidant concentration. Hence, the degradability progressively decreases with a decrease in initial readily hydrolysable solid carbon. Before abiotic pretreatment, the degradability of S8, S7, S6, S5, S4, S3 and S2 are 19.78%, 17.11%, 14.38%, 11.52%, 10.35%, 8.90%, and 7.65%, respectively. The model curves exhibit good correlation with the experimental ones having R^2= 0.9990, R^2= 0.9990, and R^2= 0.9973, R^2= 0.9974, R^2= 0.9979, R^2= 0.9996, R^2= 0.9993, respectively. Their C_{r0} values are 4.85 %, 4 %, 2 %, 2 %, 1.6 %, 1.2 %, and 1.2 %, respectively. The hydrolysis rates k_r of S8, S7, S6, S5, S4, S3 and S2 are 0.23821day^{-1}, 0.22613day^{-1}, 0.21942 day^{-1}, 0.21835 day^{-1}, 0.21632 day^{-1}, 0.21230 day^{-1}, and 0.20324 day^{-1}, respectively and their k_m values are 0.00432 day^{-1}, 0.00353 day^{-1}, 0.00312 day^{-1}, 0.00242 day^{-1}, 0.00216 day^{-1}, 0.00195 day^{-1}, and 0.00190 day^{-1}.

After abiotic pretreatment, the degradability of S8, S7, S6, S5, S4, S3, and S2 are 36.42%, 32.23%, 28.13%, 23.19%, 18.18%, 14.90%, and 11.20%, respectively. The model curves exhibit good correlation with the experimental ones having R^2= 0.9974, R^2= 0.9987, and R^2= 0.9982, R^2= 0.9972, R^2= 0.9946, R^2= 0.9946, R^2= 0.9936, respectively. Their C_{r0} values are 1.47 %, 0.535 %, 0.531 %, 0.00045 %, 0.00001 %, 0.00001 %, and 0.00001 %, respectively. The hydrolysis rates k_r of S8, S7, S6, S5, S4, S3 and S2 are 0.17921 day^{-1}, 0.17823 day^{-1}, 0.17812 day^{-1}, 0.17732 day^{-1}, 0.17521 day^{-1}, 0.17212 day^{-1}, and 0.12111 day^{-1}, respectively and their k_m values are 0.01432 day^{-1}, 0.00918 day^{-1}, 0.00796 day^{-1}, 0.00662 day^{-1}, 0.00515 day^{-1}, 0.00423 day^{-1}, and 0.00361 day^{-1}. All of these values depend on biodegradability and generally decrease with a decrease in the pro-oxidant loading and abiotic pretreatment. In all the films, slowly hydrolysable carbon (C_{s0}) fractions are absent since the presence of pro-oxidant and accelerated weathering (abiotic

treatment) has enhanced the hydrolysis rate of carbon. The values of all the parameters are consistent with earlier works on polyolefins [35]. Table 4.10 presents the kinetic modelling parameters evaluated by different researchers on biodegradation under controlled composting conditions.

Table 4.10 Reported parameter values from different studies on biodegradation kinetic modelling under controlled composting conditions

Polyolefins	Standard	C_{aq0} (%)	C_{r0} (%)	C_{m0} (%)	C_{s0} (%)	C_h (%)	k_{aq} (day^{-1})	k_r (day^{-1})	k_m (day^{-1})	k_s (day^{-1})	k_h (day^{-1})	c (day)	C-CO_2 (%)	Reference
Different municipal solid wastes (MSW)	-	8 to 11	0 to 8.5	16 to 90	0 to 82	-	10^{6}	0 to 0.1	0.005 to 0.06	0 to 82	-	-	-	[75]
Polyethylene (PE), PE/starch blend	ISO 14855-1	0 to 2.256	0	0 to 97.744	0	-	0 to 1.00000	-	0 to 0.00098	0	-	0	0.56 to 11.50	[35]
PLA/clay Nanocomposites	-	0	37.48 to 80.83	19.17 to 62.52	0	-	0.0489 to 0.1470	0.0262 to 0.0367	0.0121 to 0.0353	0	-	12.8 to 27.6	62.73 to 84.42	[184]
Polylactide (PLA) and carbodiimide additive	-	0	-	-	-	100	0.0330 to 0.1866	-	-	-	0.0150 to 0.0352	15.7 to 100	65.2 to 74.62	[186]
Polylactide (PLA) with poly(acrylic acid)/PLA hydrolysis additive	-	0	-	-	-	100	0.0542 to 0.0825	-	-	-	0.0542 to 0.0825	6.8 to 13.1	83.02 to 97.12	[187]
Polypropylene/CoSt composites	ASTM D 5338	0.084 to 9.5	1.2 to 6	94.28 to 98.71	-	-	0.21 to 0.24	0.20324 to 0.15	0.00190 to 0.00432	0	-	0.05 to 2.92	7.65 to 19.80	Present study without abiotic pretreatment
Polypropylene/CoSt composites	ASTM D 5338	0.00001 to 9.5	0.00001 to 6	96.53 to 99.99	-	-	0.13 to 0.18	0.12111 to 0.17921	0.00361 to 0.01432	0	-	0.96 to 7.04	11.20 to 36.42	Present study after abiotic pretreatment

4.6.2 Hydrolysable carbon profiles

Figs. 4.14 and 4.15 show the profile for the readily and moderately hydrolysable solid-carbon without and after abiotic pretreatment (accelerated weathering treatment). All the figures show initial discontinuity at $t = c$ as noted in Chapter 3, Section 3.2.6.3. The readily carbon decomposes rapidly in all the samples (S2-S8) as depicted in Fig. 4.14. The readily hydrolysable solid-carbon of films S7 and S8 reduces very rapidly in comparison to other films S6, S5, S4, S3, and S2 as the values of initial readily hydrolysable solid carbon C_r, as well as hydrolysis rate constant k_r for the other films are lower than S7 and S8 in Tables 4.8 and 4.9. Fig. 4.15 presents moderately hydrolysable solid carbon profiles for all the films without and after abiotic pretreatment. All the curves of S7-S8 films exhibit exponential decay and decrease very fast initially since their initial moderately hydrolysable solid carbon values are high as shown in Tables 4.8 and 4.9.

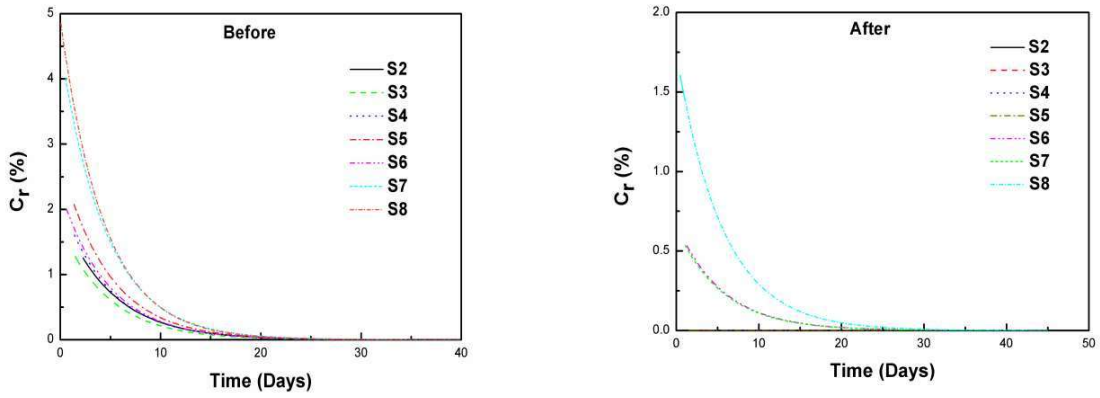

Fig. 4.14 Readily hydrolysable solid carbon profiles of different films without and after abiotic pretreatment (accelerated weathering) (S2: PP100CoSt0.2, S3: PP100CoSt0.4, S4: PP100CoSt0.6, S5: PP100CoSt0.8, S6: PP100CoSt1.0, S7: PP100CoSt1.5, S8: PP100CoSt2.0)

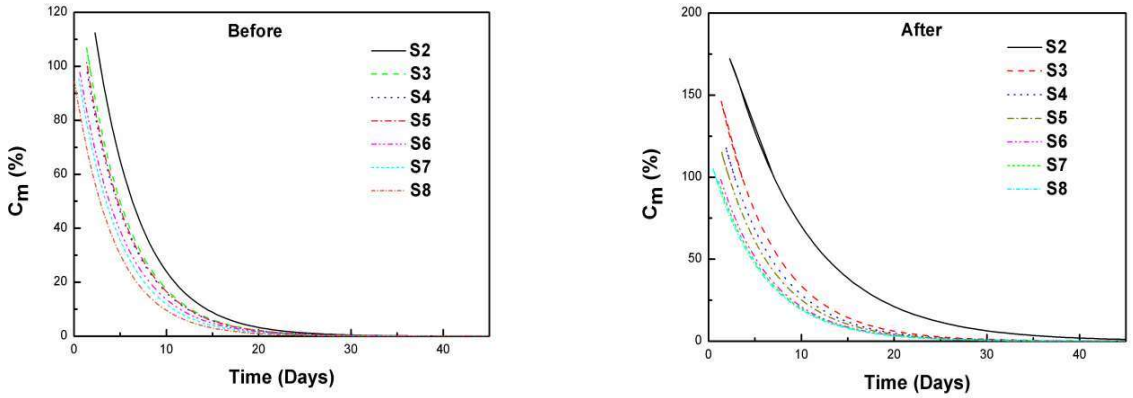

Fig. 4.15 Moderately hydrolysable solid carbon profiles of different films without and after abiotic pretreatment (accelerated weathering) (S2: PP100CoSt0.2, S3: PP100CoSt0.4, S4: PP100CoSt0.6, S5: PP100CoSt0.8, S6: PP100CaSt1.0, S7: PP100CoSt1.5, S8: PP100CoSt2.0)

4.6.3 Degradation curves

Without and after abiotic pretreatment (accelerated weathering treatment), all the degradation curves are presented combinatorially (Fig. 4.16) by calculating the rate of carbon to carbon dioxide emission using Eq. (3.27). All the sample curves S2-S8 exhibited two decay phases after the first phase (lag phase). The rate enhances rapidly in the second or growth phase, attains a peak, and then starts falling rapidly in the third (stationary) phase. This trend is attributed to sigmoid behavior of C-CO_2 evolution shown in Fig. 4.12. The second (growth) phase is because of the readily-hydrolysable carbon. The stationary phase is because of the moderately-hydrolysable carbon [75]. Before pretreatment, the highest rates of carbon to carbon dioxide production of the samples of PP100CoSt0.2 (S2), PP100CoSt0.4 (S3), PP100CoSt0.6 (S4), PP100CoSt0.8 (S5), PP100CoSt1.0 (S6), PP100CoSt1.5 (S7), and PP100CoSt2.0 (S8) are 0.226% per day, 0.269% per day, 0.310% per day, 0.337% per day, 0.390% per day, 0.599% per day, and 0.743% per day, respectively. These values depend on pro-oxidant loading. The highest rate is found at 11.36 days, 6.81 days, 7.27 days, 8.18 day, 7.72 days, 6.36 days, and 5.45 days, respectively.

After abiotic pretreatment (accelerated weathering), the highest rates of carbon to carbon dioxide production of the samples of PP100CoSt0.2 (S2), PP100CoSt0.4 (S3), PP100CoSt0.6 (S4), PP100CoSt0.8 (S5), PP100CoSt1.0 (S6), PP100CoSt1.5 (S7), and PP100CoSt2.0 (S8) are 0.322% per day, 0.382% per day, 0.462% per day, 0.581% per day, 0.698% per day, 0.797%

per day, and 0.897% per day, respectively. These values depend on pro-oxidant loading. The highest rate is found at 39.09 days, 25.90 days, 23.63 days, 20.45 day, 16.36 days, 14.09 days, and 12.27 days, respectively. Without and after abiotic pretreatment (accelerated weathering), the rate profiles of carbon to carbon dioxide emission for PP and cellulose are shown in Fig. 4.17.

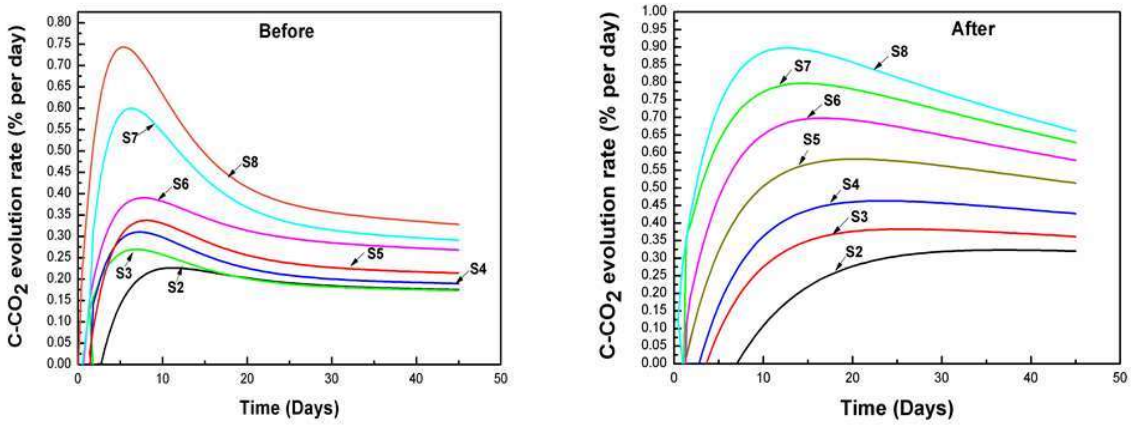

Fig. 4.16 C-CO_2 evolution rate profiles of different samples without (left) and after (right) abiotic pretreatment (accelerated weathering) (S2: PP100CoSt0.2, S3: PP100CoSt0.4, S4: PP100CoSt0.6, S5: PP100CoSt0.8, S6: PP100CoSt1.0, S7: PP100CoSt1.5, S8: PP100CoSt2.0)

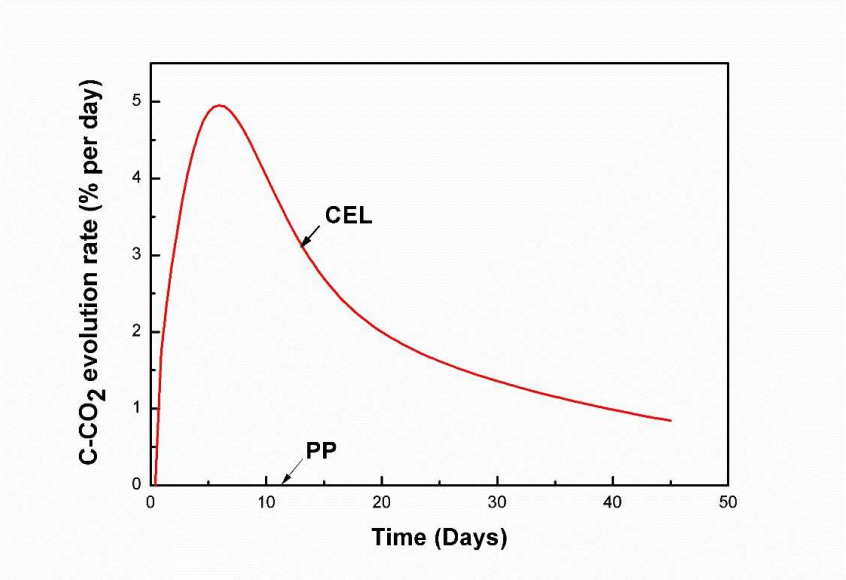

Fig. 4.17 C-CO_2 evolution rate profiles of PP (without and after abiotic pretreatment) and cellulose (without any abiotic pretreatment) samples

4.6.4 Mineralizable intermediate carbon

Without and after abiotic pretreatment (accelerated weathering), the curves for C_{aq} of all the samples are shown in Fig. 4.18. It shows a similar trend like in Section 4.6.3. This occurs because C_{aq} increases with the rate of carbon to carbon dioxide conversion noted in Eq. (3.21). The intermediate-carbon magnitude is a function of the difference between the rates of the second and first steps of the reaction path. This is equal to the rate of creation from the initial hydrolysable solid-carbon minus the disappearance rate in mineralization [in Eq. (3.18)].

All the evolutions from S8-S2 first rise because the rate of creation of C_{aq} was higher than its disappearance. This is so because the fractions of initial moderately and readily hydrolysable carbon are higher than the fraction of intermediate solid carbon C_{aq} as shown in Tables 4.8 and 4.9, and hence the first step over-rides the second step. These curves reach a maximum but subsequently come down because of the domination of the second step as a result of the sufficient buildup of intermediate solid carbon fraction.

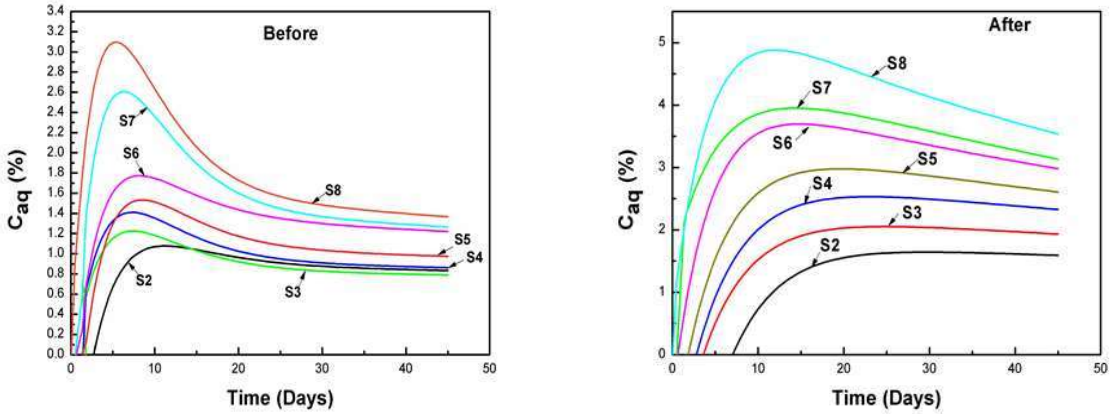

Fig. 4.18 Mineralizable intermediate carbon profiles of different samples without (left) and after (right) abiotic pretreatment (accelerated weathering) (S2: PP100CoSt0.2, S3: PP100CoSt0.4, S4: PP100CoSt0.6, S5: PP100CoSt0.8, S6: PP100CoSt1.0, S7: PP100CoSt1.5, S8: PP100CoSt2.0)

4.7 Eco-toxicological studies of biodegraded material before and after abiotic pretreatment

4.7.1 Microbial toxicity test

Table 4.11 presents the results of CFU count in water extract of compost containing different samples without and after abiotic pretreatment (accelerated weathering). It was found that cellulose gave the highest CFU count and the blank gave the lowest CFU count of 0.3×10^4. The CFU counts of all the modified PP films were more than the blank sample, which indicates increased bacteria in the compost samples. Hence, the biotically treated products from the films are considered nontoxic in nature.

Table 4.11 Number of bacterial colonies (CFUs) from water extract of compost containing different film samples before and after abiotic treatment

Film sample	Number of colonies, CFU/mL (Before)	Number of colonies, CFU/mL (After)
Control	3	3
Cellulose	Bacterial lawn	Bacterial lawn
S1	4	5
S2	9	8
S3	10	11
S4	11	12
S5	12	13
S6	13	15
S7	18	20
S8	23	25

4.7.2 Plant growth toxicity test

A medium-range of pH was used to verify the suitability of composted PP samples for plant growth. The suggested pH for the plants growth is 5.5 [84]. A pH value will affect the solubility as well as the availability of nutrients in the growth medium. In the present case, the pH was maintained at about 5.8-6.0, which is close to the suggested pH value for the plant growth test.

To identify the toxic impacts of biotically degraded intermediates of modified PP films without and after abiotic pretreatment and pristine PP on the medium, the plant growth test was performed on *Mung* bean and wheat plants [79]. After 3 weeks, the visual evaluations of both the seedlings in the growth medium showed that the average number of germinations was

100%. Without and after abiotic pretreatment (accelerated weathering), no differences were observed between test samples and the control in the growth of both the plants (Figs. 4.19, 4.20, 4.21, and 4.22). After 3 weeks of growth, plants were cut, dried, and weighed. The dry weight of *Mung* bean plants was almost the same within 2% in all the samples of compost. Similar was the case with the wheat plants.

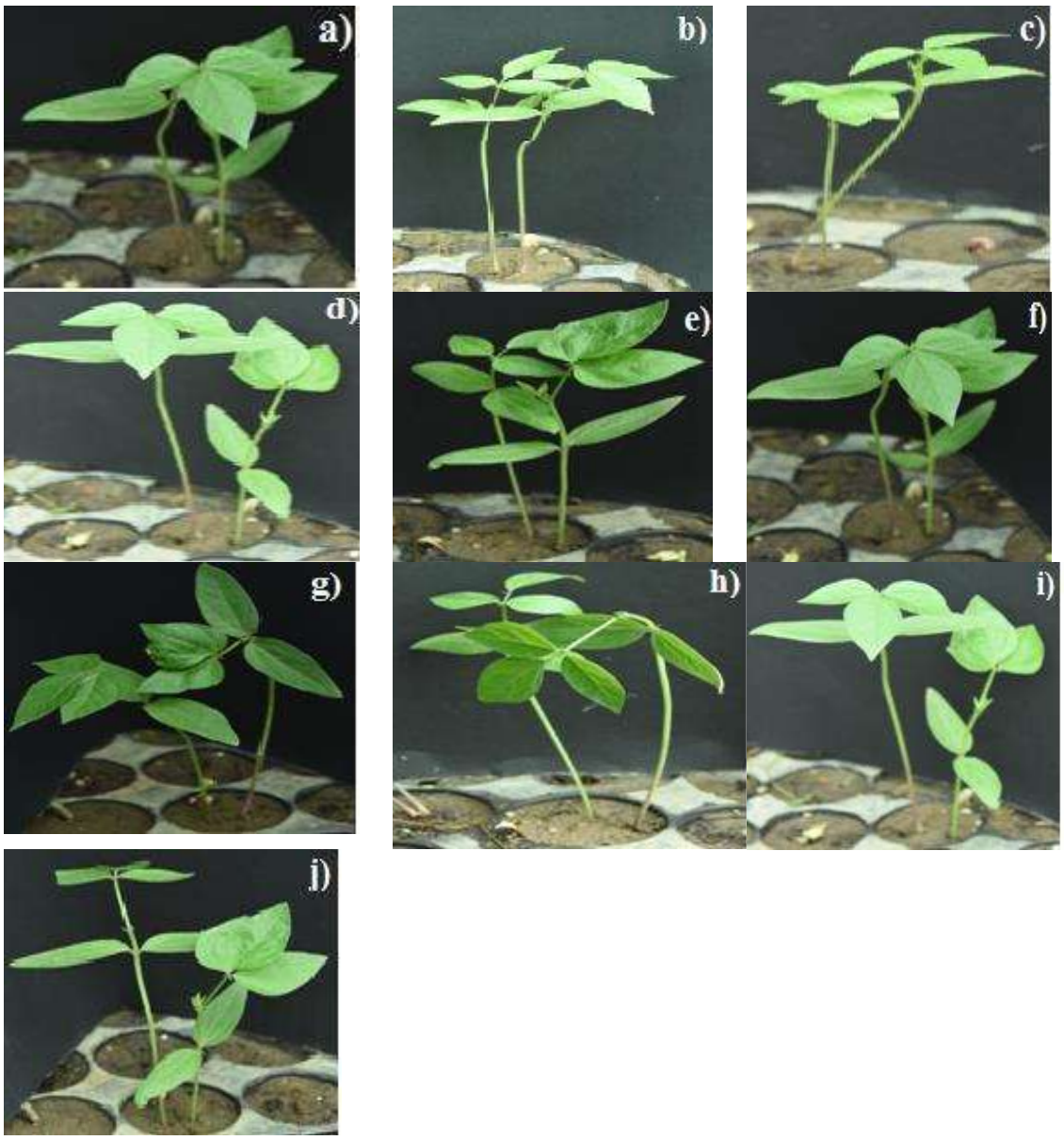

Fig. 4.19 Growth of *Mung* bean in compost (after 45 days biodegradation) of (a) control, (b) cellulose, (c) PP (S1), (d) PP100CoSt0.2 (S2), (e) PP100CoSt0.4 (S3), (f) PP100CoSt0.6 (S4), (g) PP100CoSt0.8 (S5), (h) PP100CoSt1.0 (S6), (i) PP100CoSt1.5 (S7), and (j) PP100CoSt2.0 (S8) without abiotic pretreated films

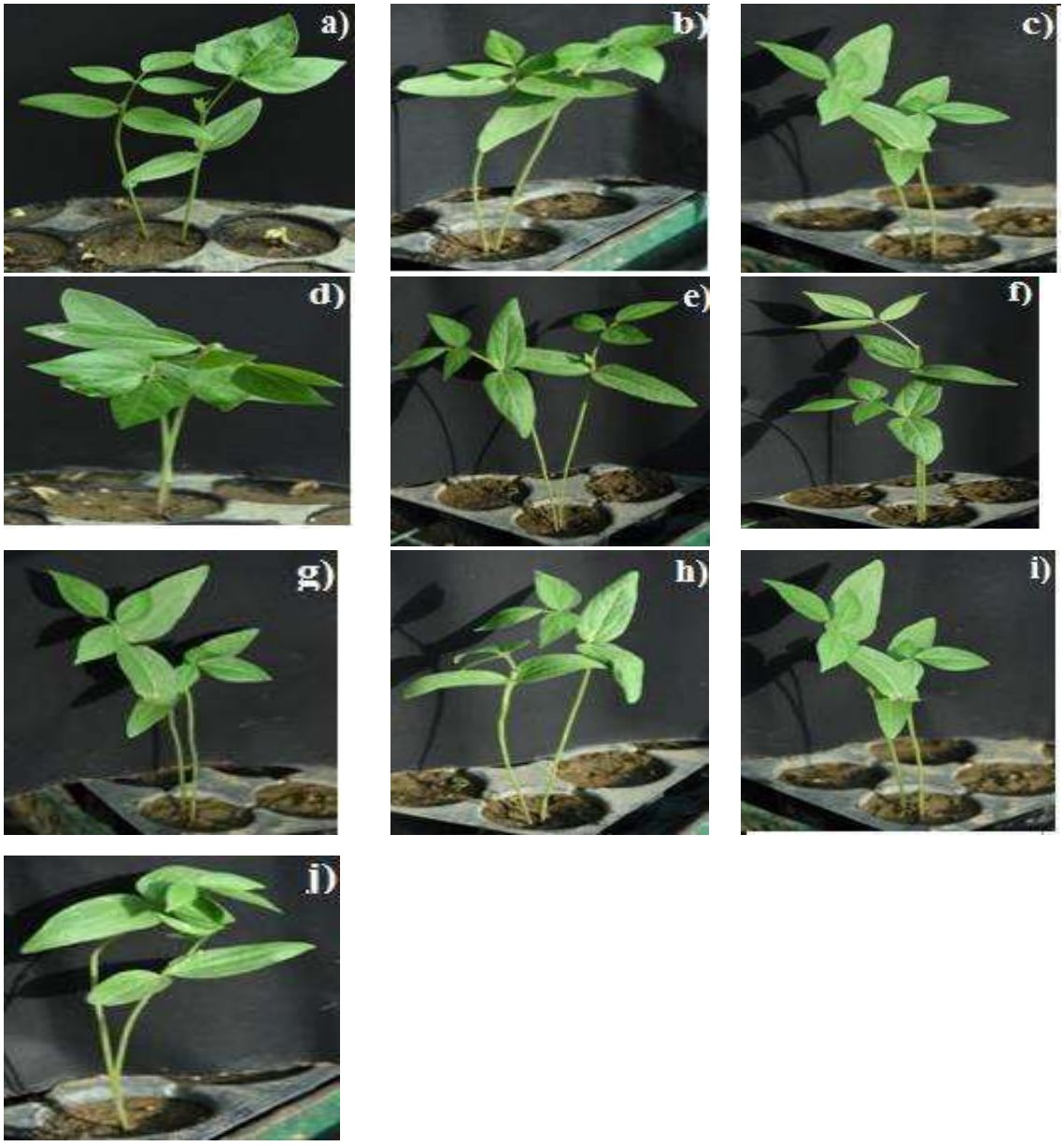

Fig. 4.20 Growth of *Mung* bean in compost (after 45 days biodegradation) of (a) control, (b) cellulose, (c) PP (S1), (d) PP100CoSt0.2 (S2), (e) PP100CoSt0.4 (S3), (f) PP100CoSt0.6 (S4), (g) PP100CoSt0.8 (S5), (h) PP100CoSt1.0 (S6), (i) PP100CoSt1.5 (S7), and (j) PP100CoSt2.0 (S8) after abiotic pretreated films

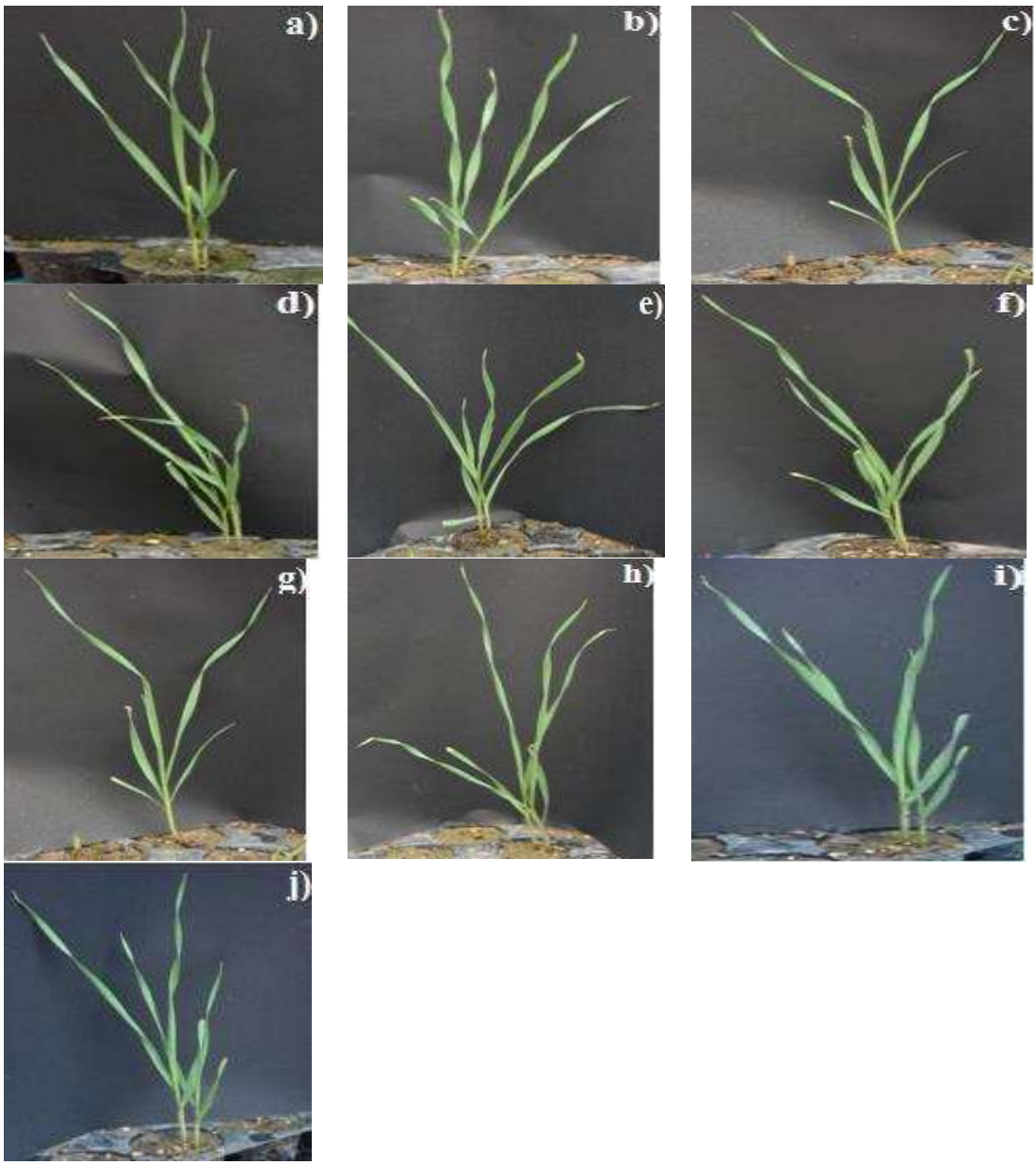

Fig. 4.21 Growth of wheat in compost (after 45 days biodegradation) of (a) control, (b) cellulose, (c) PP (S1), (d) PP100CoSt0.2 (S2), (e) PP100CoSt0.4 (S3), (f) PP100CoSt0.6 (S4), (g) PP100CoSt0.8 (S5), (h) PP100CoSt1.0 (S6), (i) PP100CoSt1.5 (S7), and (j) PP100CoSt2.0 (S8) without abiotic pretreated films

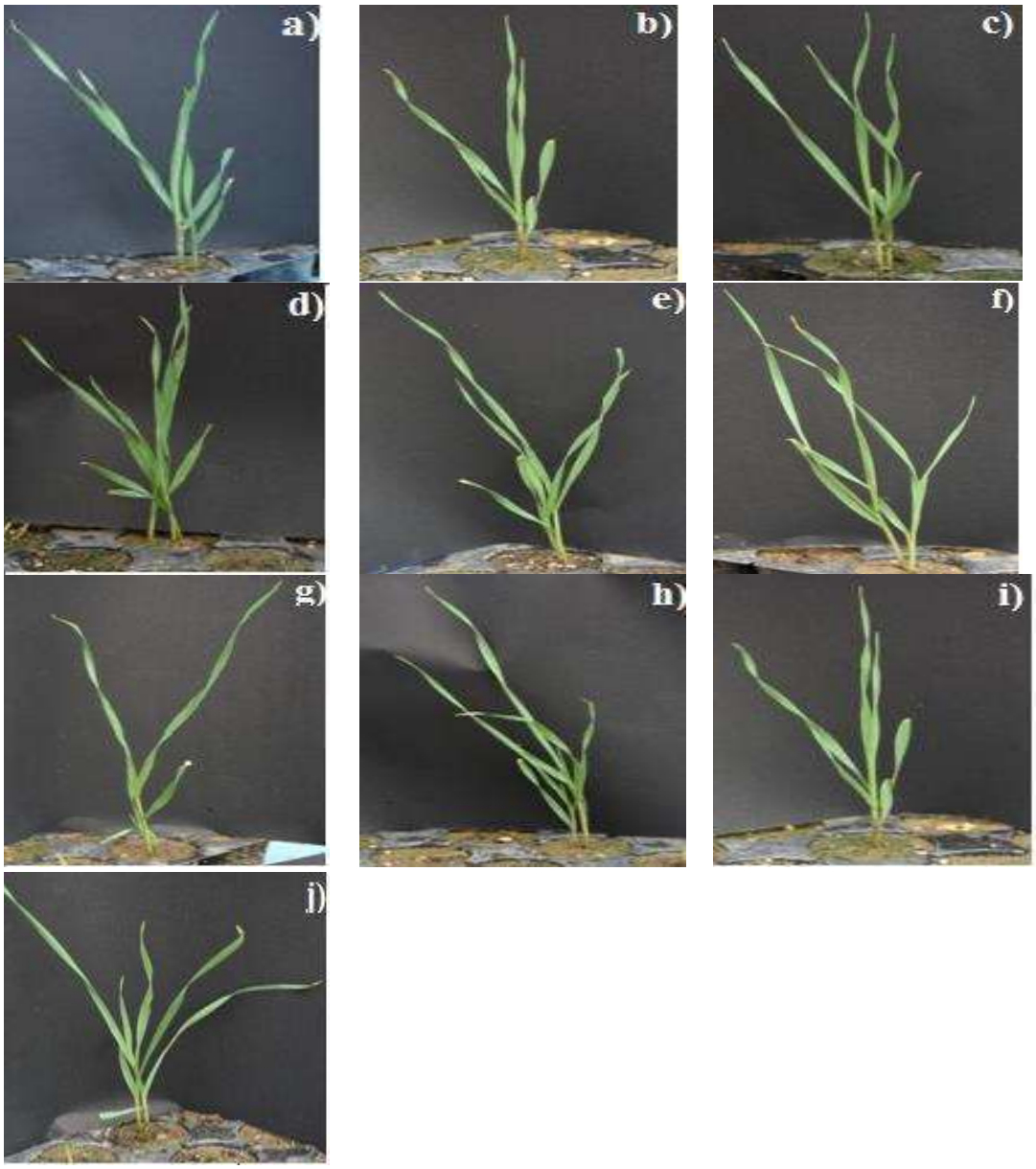

Fig. 4.22 Growth of wheat in compost (after 45 days biodegradation) of (a) control, (b) cellulose, (c) PP (S1), (d) PP100CoSt0.2 (S2), (e) PP100CoSt0.4 (S3), (f) PP100CoSt0.6 (S4), (g) PP100CoSt0.8 (S5), (h) PP100CoSt1.0 (S6), (i) PP100CoSt1.5 (S7), and (j) PP100CoSt2.0 (S8) after abiotic pretreated films.

4.7.3 Earthworm acute toxicity test

The value of mean percentage mortality of earthworm in post biodegradation compost for the blank (control), cellulose, PP, and different cobalt stearate filled PP film samples (for 14 days) without and after abiotic pretreatment was nil. This indicates that the degradation products of all the samples were non-toxic.

Chapter 5-Modified Pro-oxidant Filled PP Composites

5.1 Preparation of modified pro-oxidant

Masterbatch containing 10 phr of cobalt stearate in PP (PP100CoSt10) was made in a co-rotating twin-screw extruder (M/s Labtech Engineering Co., Ltd. Thailand) at a speed of 150 rpm under a nitrogen blanket and pelletized. This masterbatch was aged at 110 ºC for 48 h. After that, it was crushed in to powder, sieved, and used as a modified pro-oxidant (designated as T).

5.2 Composites Preparation

Table 5.1 summarizes the compositions of different prepared composites. For preparation of the composites, the procedure followed was the same as given in Section 4.1.

Table 5.1 Composition of PP composites loaded with T pro-oxidant

Sr. No.	Polymer Samples	Sample code	Composition	
			PP (phr)	T (phr)
1	PP	R1	100	0
2	PP100T5	R2	100	5
3	PP100T10	R3	100	10
4	PP100T20	R4	100	20
5	PP100T30	R5	100	30

5.3 Film preparation

After processing of composites, the different films were prepared through hot press moulding, following the same procedure as given in Section 4.2.

5.4 Abiotic pretreatment

The five modified pro-oxidant containing PP films, namely, PP, PP100T5, PP100T10, PP100T20, and PP100T30 were used to examine the behavior of film samples under UV exposure temperature, and humidity. In this test, the effect of exposure time (12 h, 24 h, 40 h) on the weight loss of the modified pro-oxidant containing PP films was determined and shown in Fig. 5.1. After UV exposure, the weight loss of the PP100T30 sample was more significant in contrast to others. The weight loss of the specimens was enhanced slowly with increasing

irradiation time. The weight loss of PP100T30 (R5) samples enhanced to about 0.1, 0.3, and 0.5 % after 12, 24, and 40 h, respectively.

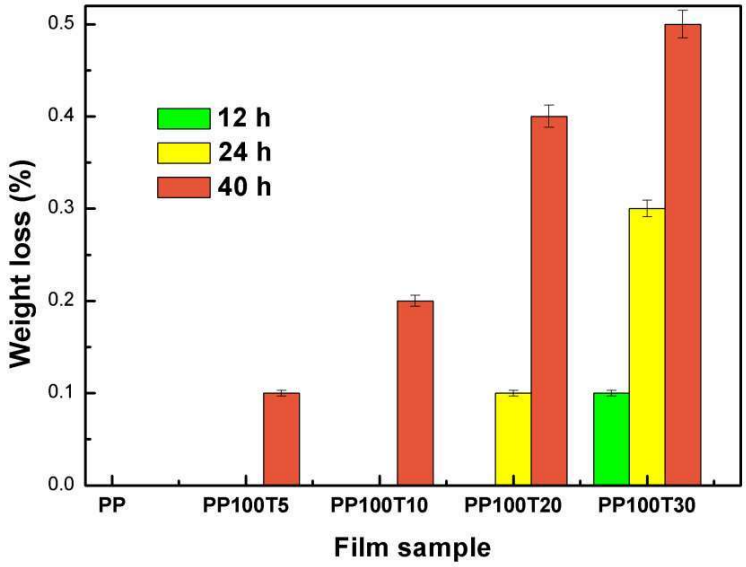

Fig. 5.1 Weight loss in modified pro-oxidant loaded PP films after abiotic pretreatment (accelerated weathering) for different times

5.5 Characterization of samples before and after abiotic pretreatment

5.5.1 Tensile properties

The mechanical properties (tensile strength and elongation at break) of the modified pro-oxidant containing PP and pristine PP film sample before abiotic pretreatment (accelerated weathering) are shown in Fig. 5.2. Compared with film 1, which is only pristine PP, adding the modified pro-oxidant could decrease the tensile strength significantly from 35 to 14 MPa. However, elongation at break (%) was decreased significantly from 3.5% to 1.1%. When the content of modified pro-oxidant was enhanced from 5 to 30 phr, a considerable decreased in tensile strength and elongation at break was found from 28.4 to 14 MPa and 2.7 to 1%, respectively. The film of PP100T30 (R5) observed the lowest value of tensile strength with elongation at break than all other films as presented in Fig. 5.2. At 5 phr concentration, maximum tensile strength and elongation at break were 28.4 MPa and 2.7%. This drop in the values might have occurred due to modifications in the PP matrix on the loading of modified pro-oxidant to the PP matrix. The decrease in tensile characteristics could be due to the

oxidation of PP by modified-CoSt pro-oxidant [64]. Mandal et al. [84] have also found that the addition of cobalt stearate 0.2 phr in PP reduced elongation at break and tensile strength 3.6 to 3.4% and 39 to 35 MPa, respectively.

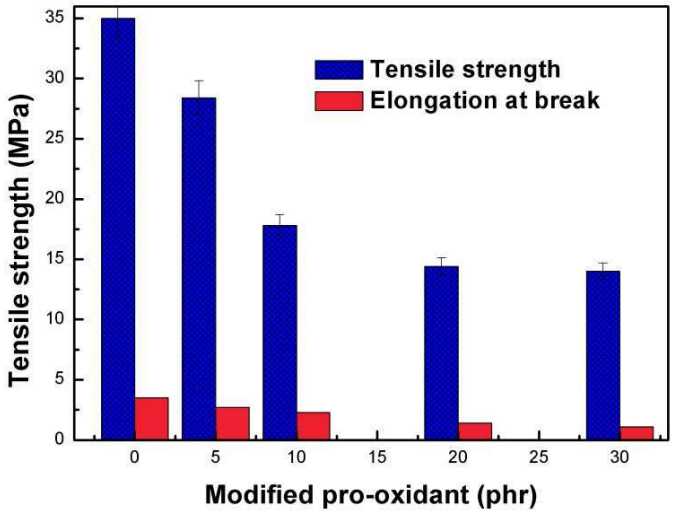

Fig. 5.2 Effect of modified pro-oxidant concentration on mechanical properties of PP films

5.5.2 Fourier transform infrared (FTIR) spectroscopy

The impacts of modified pro-oxidant and abiotic pretreatment (accelerated weathering) on PP structure were studied through FTIR spectroscopy. Fig. 5.3(a) presents the comparison of FTIR spectra of the neat PP, PP100T5, PP100T10, PP100T20, and PP100T30 films without any pretreatment and after abiotic pretreatment. Excluding PP100T20 and PP100T30 films, almost similar spectra were found for all other samples before and after abiotic pretreatment. However, after abiotic pretreatment, the peak intensity at 1715 cm^{-1} of PP100T20 and PP100T30 films increased and it confirmed that due to UV exposure new carbonyl groups are formed on the PP films. Peaks between 2949-2866 cm^{-1} are assigned to C-H stretching, peak at 1375 cm^{-1} shows C-H bending, and peak at 1454 cm^{-1} indicates CH_3 bending in the FTIR spectra of neat PP. A peak observed at 1715 cm^{-1} is recognized to modified pro-oxidant, which can be attributed to asymmetric vibration stretching of the carbonyl group attached to the metal ion [64]. A peak observed at 1715 cm^{-1} is recognized to modified pro-oxidant, that can be attributed as asymmetric vibration stretching of the carbonyl groups attached to the metal ion [64]. This confirmed that the modified pro-oxidant is present in the PP films. The carbonyl groups are present as a peak at 1800-1700 cm^{-1} [57, 158].

Exposure of the samples to abiotic pretreatment increases the peak intensity because of new carbonyl groups produced on photo-degradation containing the chain scission under the Norrish type-1 reaction [157]. After abiotic pretreatment, a slight change in the peak intensity was found because of the low concentration of modified pro-oxidant. After abiotic pretreatment, significant changes in the O-H region (3400 cm^{-1}), carbonyl (1780–1650 cm^{-1}), and amorphous region (1250-1050 cm^{-1}) are observed. The absorption band around 1715 cm^{-1} may be assigned to the C=O stretch of ketones. Increasing its peak intensity and band broadening has also been observed, which denotes the formation of some oxidized products on the increasing concentration of modified pro-oxidant. The carbonyl band might be assigned to C=O stretching vibrations inside esters, γ lactones (1781 cm^{-1}), carboxylic acid groups (1700 cm^{-1}), also aldehydes (1734 cm^{-1}). Small modifications have been observed inside the carbonyl peak (C=O). In the PP100T5 sample, the carbonyl peak has been observed from 1605 cm^{-1} to 1769 cm^{-1}. Similarly, in the PP100T30 sample, the carbonyl peak has been observed from 1640 cm^{-1} to 1791 cm^{-1}. The FTIR spectra confirm small modifications in the carbonyl group after UV irradiation, and the extent of modification depends on the amount of modified pro-oxidant added [30, 36].

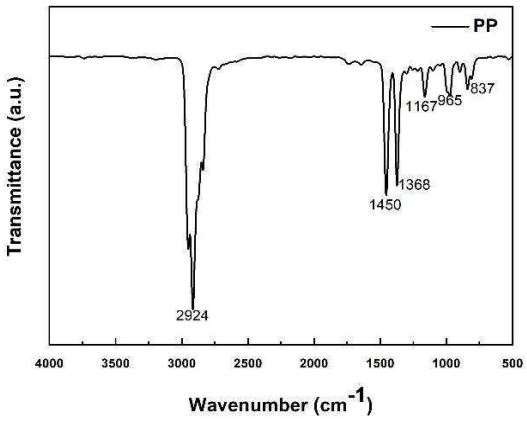

Before

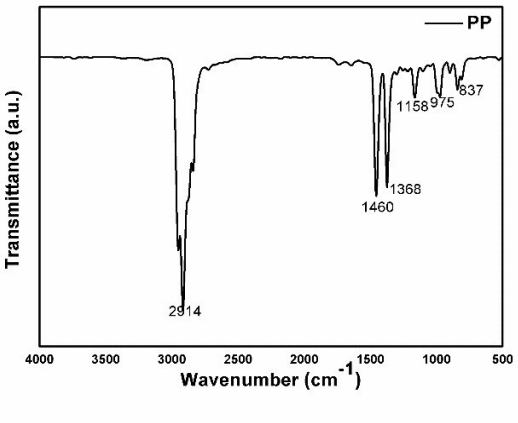

After

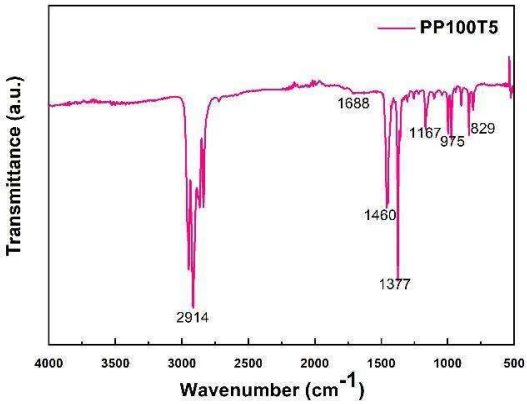

Before

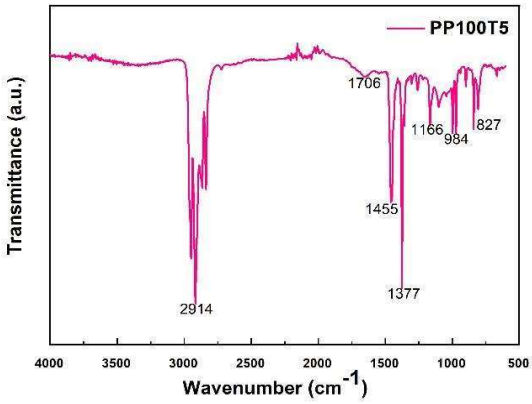

After

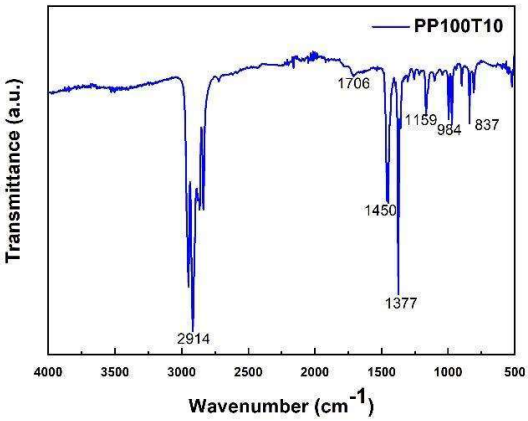

Before

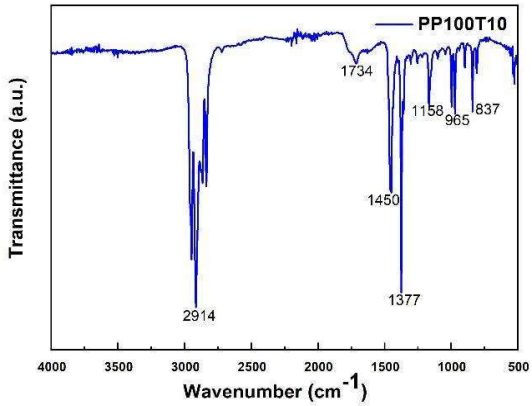

After

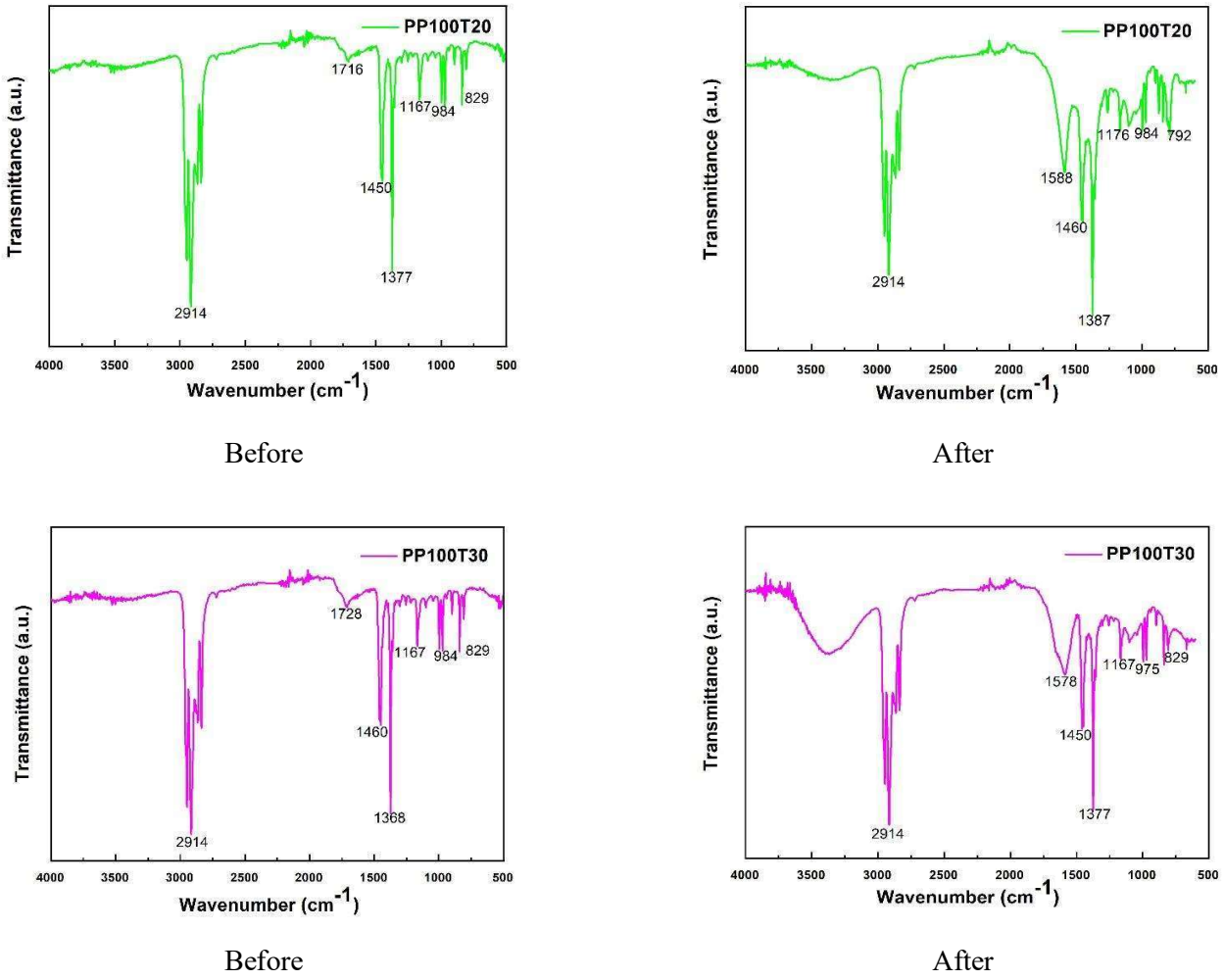

Fig. 5.3 (a) FTIR spectra of modified pro-oxidant loaded PP films before and after abiotic pretreatment (for 40 h)

5.5.2.1 Carbonyl index

Before and after abiotic pretreatment (for 40 h), the carbonyl index (CI) of all the modified pro-oxidant containing PP composites was computed from the FTIR data using Eq. (3.1) and shown in Fig. 5.3 (b) and compared to those of before abiotic pretreatment. The highest value of CI (1.1) was obtained in the PP100T30 (R5) film for 40 h. The increasing value in CI of modified pro-oxidant loaded PP samples is proportional to the amount of pro-oxidant loading and time of exposure.

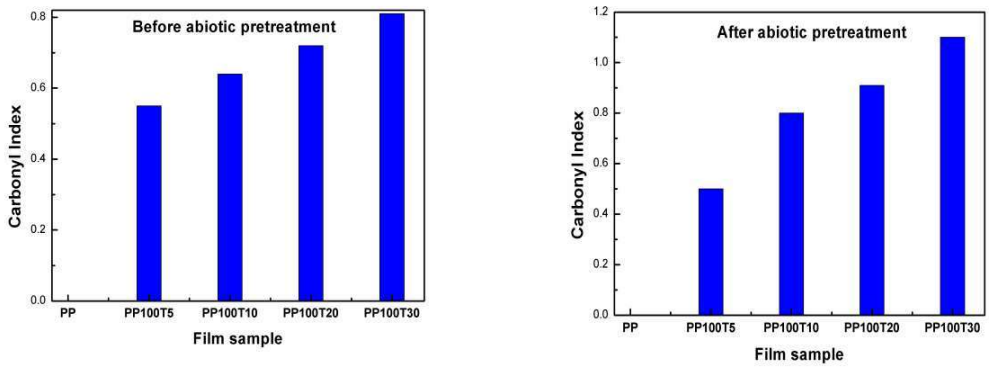

Fig. 5.3 (b) Carbonyl index (CI) of modified pro-oxidant loaded PP films before and after abiotic pretreatment (for 40 h)

5.5.3 Thermogravimetric analysis (TGA)

Fig. 5.4 presents the thermogravimetric (TG) and differential thermogravimetric (DTG) trends for pristine PP and modified PP composite films before and after abiotic pretreatment (for 40 h). The weight loss in modified pro-oxidant containing PP film samples after abiotic pretreatment (accelerated weathering) was observed to be more as compared to without any pretreatment samples. Table 5.2 summarizes the values of T_i and T_f before and after abiotic pretreatment. The values of T_i of the modified pro-oxidant containing PP film samples after abiotic pretreatment are lower in contrast to before abiotic pretreatment and the neat PP. It illustrates the progressive enhancement of thermal degradation in modified pro-oxidant loaded PP samples because of the increased double peroxide groups and abiotic pretreatment [5, 157]. This deterioration has occurred because of abiotic pretreatment (UV exposure). This involves the chain scission as well as the production of carbonyl groups under the Norrish type-1 reaction [219, 220]. After abiotic pretreatment, the thermal stability of different films of PP, PP100T5, PP100T10, PP100T20, and PP100T30 is up to 294.44, 207.30, 206.78, 199.59, and 194.11 °C, respectively.

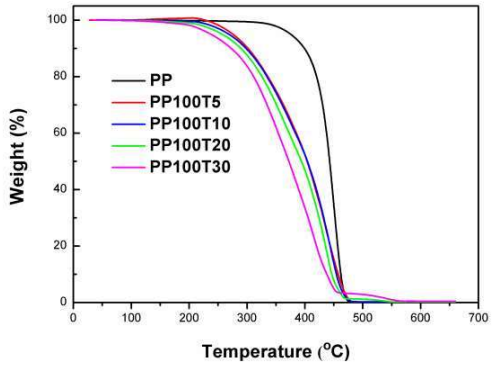

Before (TG)

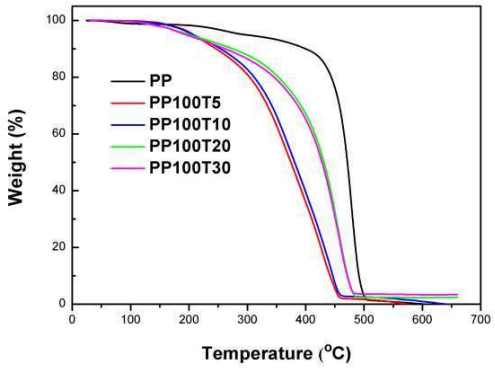

After (TG)

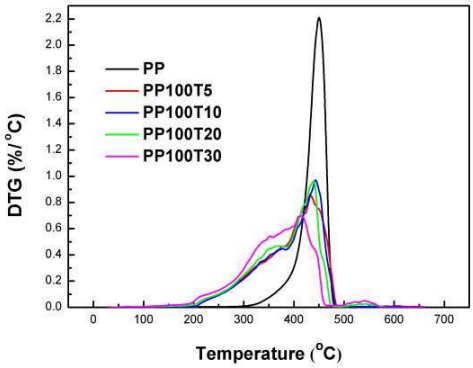

Before (DTG)

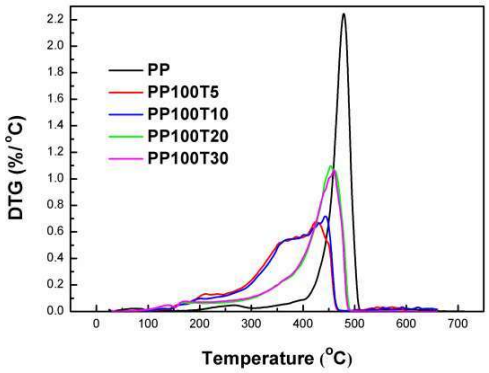

After (DTG)

Fig. 5.4 TG and DTG curves of modified pro-oxidant loaded PP films before and after abiotic pretreatment (for 40 h)

Table 5.2 TGA data of modified pro-oxidant loaded PP samples before and after abiotic pretreatment (accelerated weathering)

Film sample	*Before* T_i (°C)	*After* T_i (°C)	*Before* T_f (°C)	*After* T_f (°C)	Weight loss (%)
PP	375.50	294.44	466.0	496.26	100
PP100T5	275.63	207.30	464.14	450.11	100
PP100T10	268.47	204.78	460.35	454.28	100
PP100T20	257.19	199.59	447.05	478.82	100
PP100T30	237.47	194.11	454.07	478.83	100

5.5.4 Differential scanning calorimetry (DSC)

To monitor the effect of the modified pro-oxidant and UV exposure on the degradability of the pristine PP films, their percentage crystallinity was calculated from DSC analysis data (before and after abiotic pretreatment). During DSC analysis, cooling and heating cycles of modified pro-oxidant loaded PP films were found from atmospheric temperature to 200 °C. The results are presented in Fig. 5.5. The values of melting enthalpy (ΔH_m), melting temperature (T_m), and crystallization temperature (T_c), before and after abiotic pretreatment (for 40 h) were estimated from the curves and reported in Table 5.3. The crystallinity of all the films before and after abiotic pretreatment was estimated using Eq. (3.2) and given in Table 5.3. The percentage crystallinity and melting temperature of the pure PP before abiotic pretreatment is 63.80 % and 166.4 °C, respectively. However, after abiotic pretreatment the melting temperature of the pure PP decreased slightly. The T_m values of the modified pro-oxidant loaded PP samples after abiotic pretreatment are lower than those before abiotic pretreatment due to the presence of functional groups [84, 167]. It may be due to the rapid photo-oxidation taking place in the modified pro-oxidant containing PP films. These results indicate that modified pro-oxidant enhanced the sensitivity to thermal decomposition [121].

In general, the thermal characteristics and stability of the polymer film samples revealed that the PP films are highly resistant to thermal decomposition. The percentage crystallinity of the modified pro-oxidant loaded PP samples after abiotic pretreatment was observed to be lower than those of before abiotic pretreatment as well as the pure PP. The results clearly show that the film PP100T30 had the lowest percentage of crystallinity. This confirmed that the addition of modified pro-oxidant and abiotic pretreatment could decrease the crystallinity [5, 221]. Consequently, it made the modified pro-oxidant containing PP samples more prone to microbial attacks [84, 121, 165] as the rate of degradability is influenced by the crystallinity of the films.

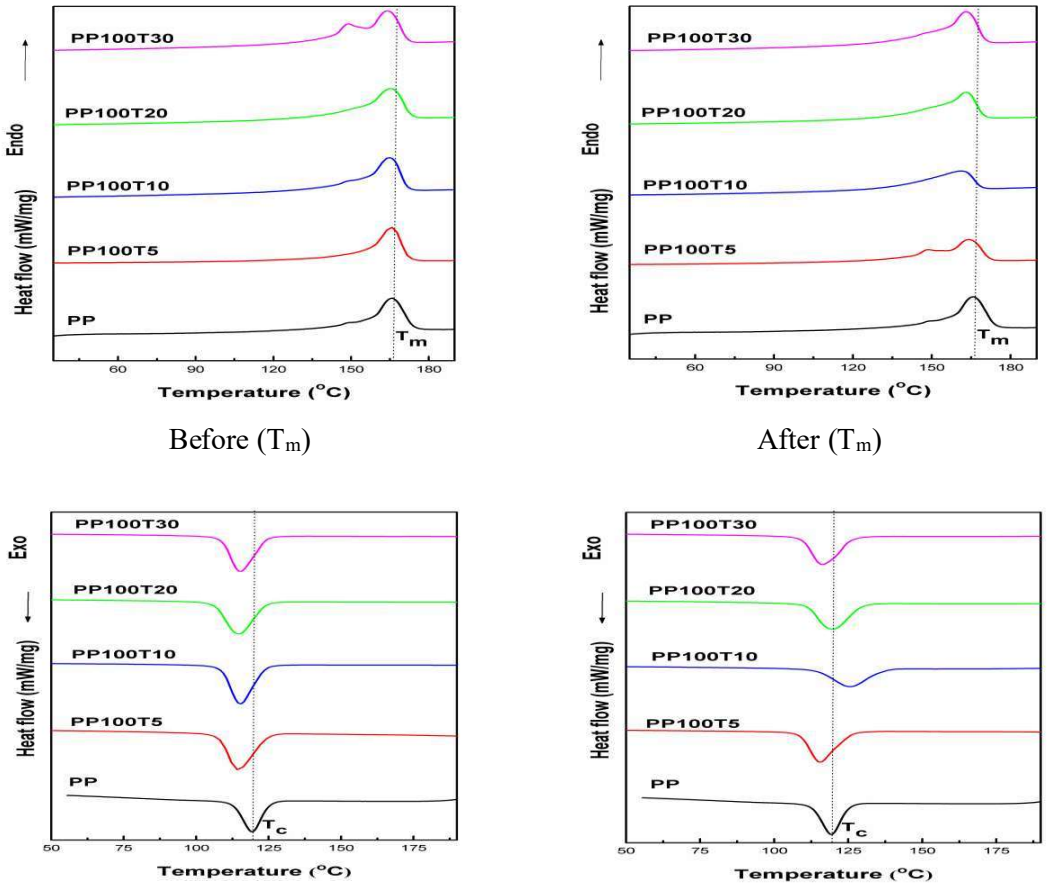

Before (T_m) After (T_m)

Before (T_c) After (T_c)

Fig. 5.5 DSC thermograms of modified pro-oxidant loaded PP films before and after abiotic pretreatment (for 40 h)

Table 5.3 DSC melting and crystallization parameters of modified pro-oxidant loaded PP films before and after abiotic pretreatment (accelerated weathering)

Film sample	*Before* T_m (°C)	*After* T_m (°C)	*Before* T_c (°C)	*After* T_c (°C)	*Before* ΔH_m (Jg^{-1})	*After* ΔH_m (Jg^{-1})	*Before* X_c (%)	*After* X_c (%)
PP	166.4	165.80	119.1	119.13	104	104	63.80	63.80
PP100T5	165.67	163.85	115.78	115.94	103.8	81.22	63.68	49.82
PP100T10	164.65	161.91	115.46	125.00	88.46	78.95	54.26	48.43
PP100T20	164.23	161.56	114.52	120.15	84.65	74.30	51.93	45.58
PP100T30	163.59	161.28	114.20	115.84	78.4	69.34	48.09	42.53

5.5.5 X-ray diffraction (XRD)

In Fig. 5.6, the XRD patterns of the pristine PP, and modified pro-oxidant loaded PP composites are presented before and after abiotic pretreatment. The peaks of the pristine PP correspond to the α-monoclinic form at 2θ = 14.1°, 16.8°, 18.6°, 21.1°, and 21.8° [42, 84, 165]. The presence of modified pro-oxidant in the PP reduced the peaks intensity indicating decreased crystallinity. Similar observations were also reported by Mandal et al [84]. The addition of the modified pro-oxidant did not shift the diffraction angles [206]. The comparison of percentage crystallinity of all the modified pro-oxidant loaded PP film samples before and after abiotic pretreatment (for 40 h) as determined by Eq. (3.3) are presented in Table 5.4. The value of the crystallinity of PP reduced from 76.65 to 40.50 % due to the effect of accelerated weathering.

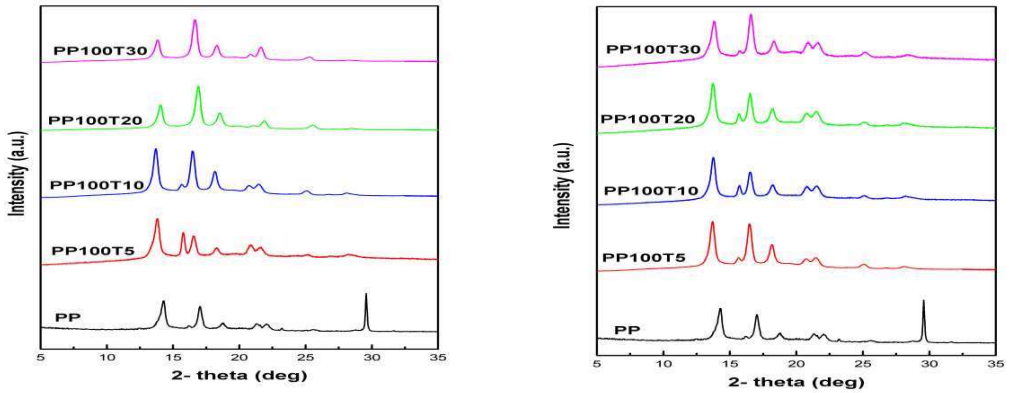

Before After

Fig. 5.6 XRD results of modified pro-oxidant loaded PP films before and after abiotic pretreatment (for 40 h)

Table 5.4 Crystallinity (%) of modified pro-oxidant loaded PP films as calculated from XRD analysis before and after abiotic pretreatment (accelerated weathering)

Film sample	Before	After
PP	76.57	76.57
PP100T5	66.8	65.91
PP100T10	65.33	42.06
PP100T20	62.52	41.20
PP100T30	58.00	40.50

5.5.6 Scanning electron microscopy (SEM)

Before any pretreatment and after abiotic pretreatment (accelerated weathering) changes in the surface morphology of the PP, PP100T5, PP100T10, PP100T20, and PP100T30 composite films were investigated using a scanning electron microscopy and reported in Fig. 5.7. The surface morphology of neat PP before any pretreatment and after abiotic pretreatment (for 40 h) looks clear, uniform, and smooth as compared to modified pro-oxidant containing PP films and as shown in Fig. 5.7. It revealed that the presence of modified pro-oxidant did not affect the surface morphology of pristine PP. The surface morphology of modified pro-oxidant containing PP film samples after abiotic pretreatment (accelerated weathering) becomes rough and reveals the creation of erosion, fractures, and small cracks [157, 219]. However, the surface roughness of modified pro-oxidant containing films increased and it depended on the content of modified pro-oxidant, which was helpful in the growth of the microbes [5].

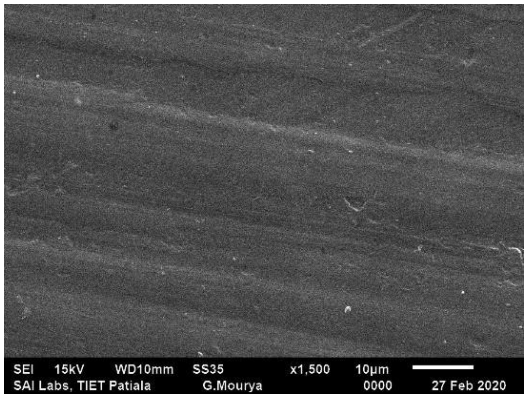

Before any pretreatment (PP)

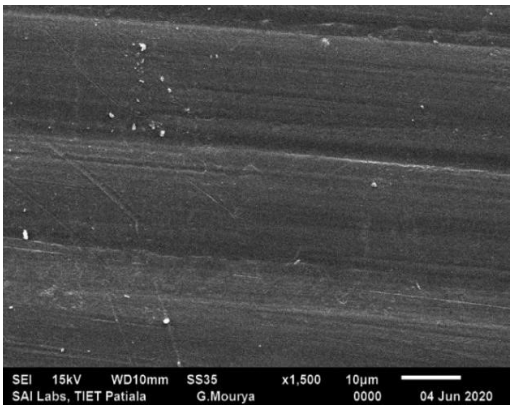

After abiotic pretreatment (PP)

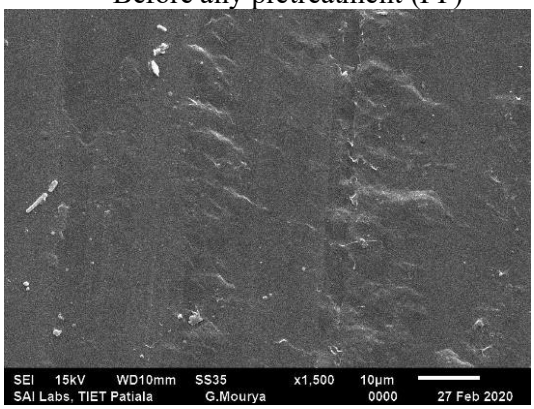

Before any pretreatment (PP100T5)

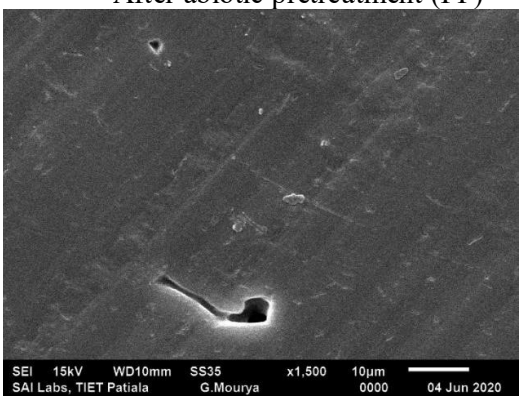

After abiotic pretreatment (PP100T5)

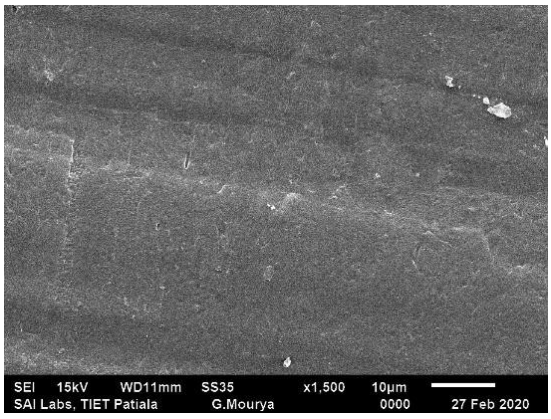

Before any pretreatment (PP100T10)

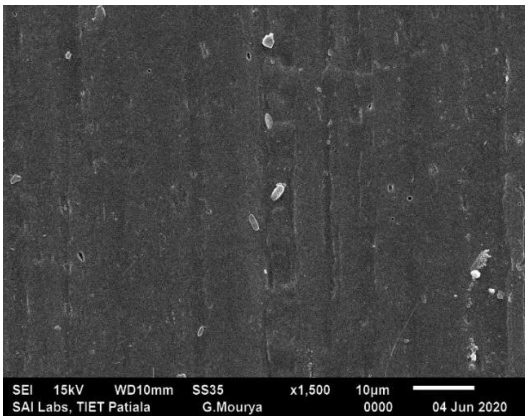

After abiotic pretreatment (PP100T10)

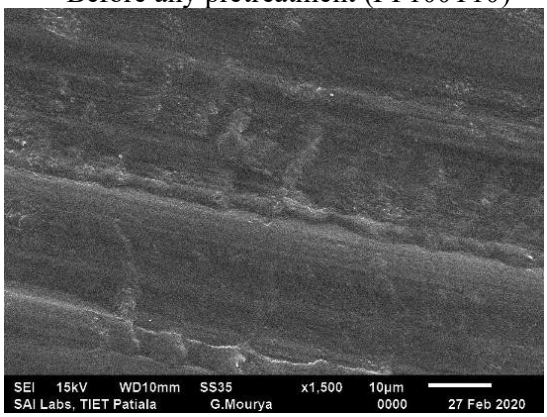

Before any pretreatment (PP100T20)

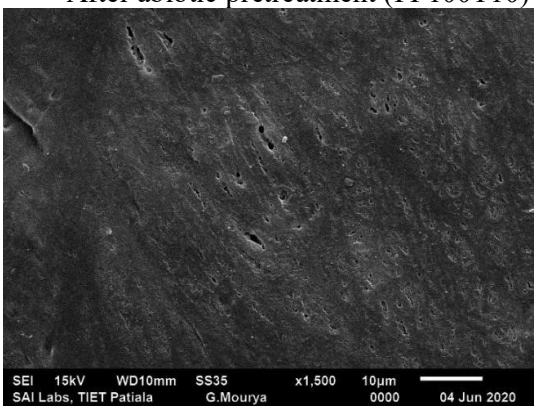

After abiotic pretreatment (PP100T20)

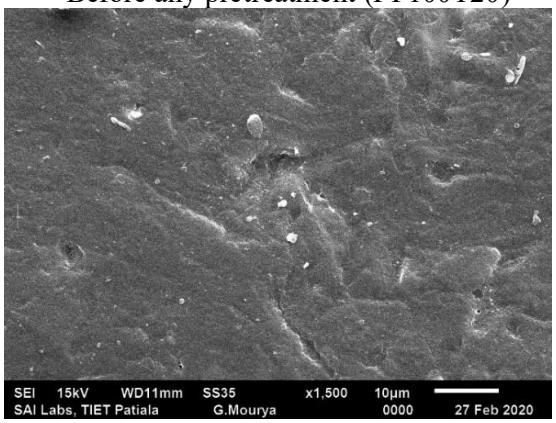

Before any pretreatment (PP100T30)

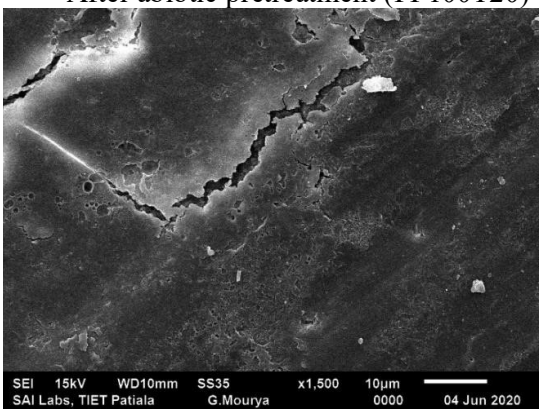

After abiotic pretreatment (PP100T30)

Fig. 5.7 SEM images of modified pro-oxidant loaded PP samples before any pretreatment and after abiotic pretreatment (for 40 h).

5.5.7 Rheological properties

The rheological study is necessary to know the structure–property relationship of materials, during the processing especially in the melt state. Dynamic shear strain sweep testing was applied to study the linear viscoelasticity region (VLE) of polymeric materials. Shear rheological behaviour is sensitive to the chain length as well as topologic structure. The storage

modulus (G') is utilized to estimate the elastic behavior and the loss modulus (G") is utilized to know the viscous behavior of the polymers. The storage modulus is a more sensitive rheological function in contrast to the loss modulus for structural changes of the polymer composites. Fig. 5.8 shows the result of rheological studies of pristine PP and the PP composite with highest modified-CoSt pro-oxidant loading PP100T30. Fig. 5.8 (a, b) presents the dependance of storage modulus (G') and loss modulus (G") on the shear strain. The films revealed a linear behavior (Newtonian plateau) at lower shear strain and a nonlinear behavior at higher shear strain.

The viscosity is a measure of the resistance to flow, especially the complex viscosity (η*). Fig. 5.8 (c) shows the complex viscosity (η*) v/s angular frequency (ω) curves for modified-CoSt filled PP composites. For all the modified PP films, η* reduces monotonically with rise in angular frequency (shear thinning). The reduction in η* with rise in ω shows the pseudo-plastic behavior of all the modified PP films. As expected, with rise in shear rate, the viscosity reduced for pristine PP and the PP composite with highest modified-CoSt pro-oxidant loading (PP100T30). The presence of modified-CoSt pro-oxidant in PP film reduced the complex viscosity but less significantly because of better mixing.

The elastic and viscous properties of pristine PP and the PP composite with highest modified-CoSt pro-oxidant loading (PP100T30) are given in Figs. 5.8 (d) and 5.8 (e), showing the storage modulus as well as loss modulus as a function of angular frequency. The dependance of G' and G" on ω shows the relative motion of all the molecules in the bulk and can give vital information about the flow behavior of the melts [216]. Storage modulus of all the composites rises monotonously with rise in frequency. The loss modulus trends are quite same as that of storage modulus.

Fig. 5.8 (f) shows the dependency of loss angle (tan δ) on frequency of modified PP films. The loss angle is stated as the ratio of the loss to the storage modulus. It shows the viscoelastic damping behavior of a polymer system [84]. The loss angle value reduces with rise in frequency as observed in Fig 5.8 (f). A positive slope of tan δ curve would have displayed the elastic response of the viscoelastic samples. For pristine PP and the PP composite with highest modified-CoSt pro-oxidant loading (PP100T30), the slope of the tan δ curve is negative from Fig. 5.8 (f). It exhibits that the composites behave as viscoelastic.

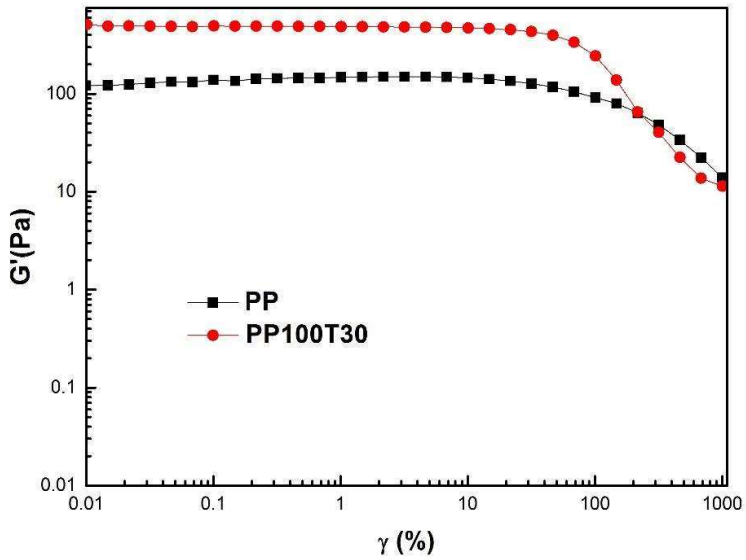

Fig. 5.8 (a) Storage modulus (G') as a function of shear strain (γ) of pristine PP and modified-CoSt pro-oxidant filled PP film samples

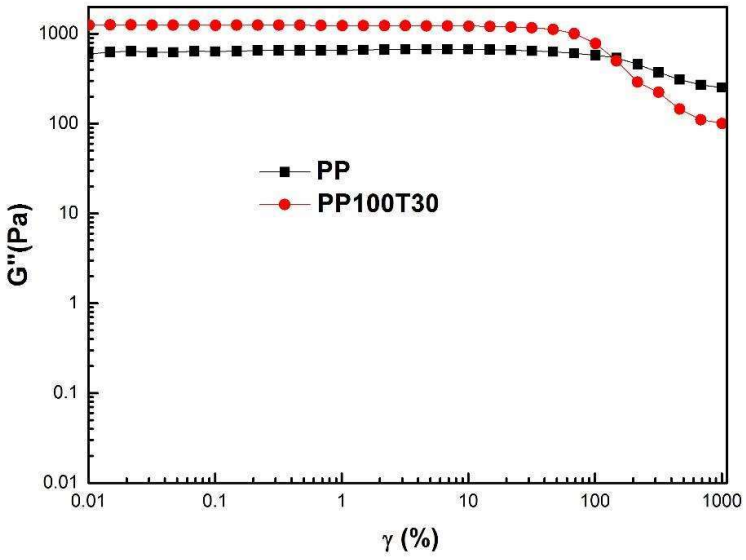

Fig. 5.8 (b) Loss modulus (G") as a function of shear strain (γ) of pristine PP and modified-CoSt pro-oxidant filled PP film samples

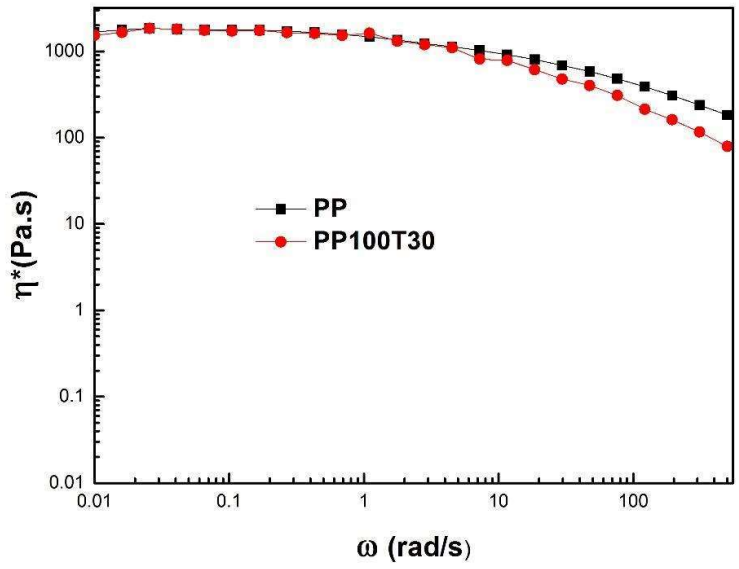

Fig. 5.8 (c) Complex viscosity (η*) as a function of angular frequency (ω) of pristine PP and modified-CoSt pro-oxidant filled PP films

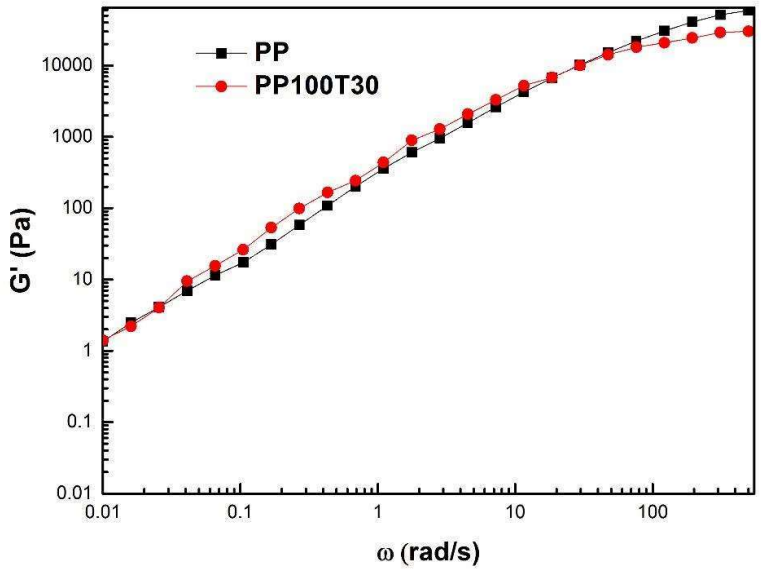

Fig. 5.8 (d) Storage modulus (G') as a function of angular frequency (ω) of pristine PP and modified-CoSt pro-oxidant filled PP films

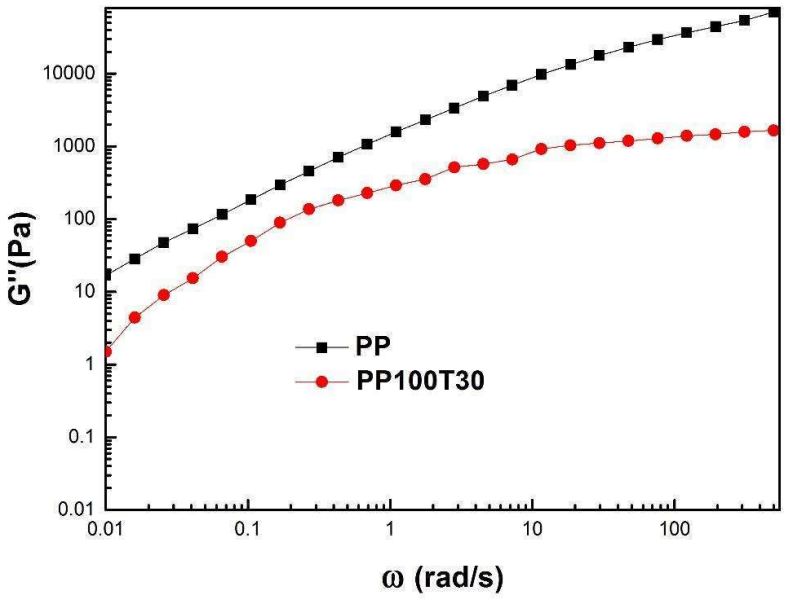

Fig. 5.8 (e) Loss modulus (G") as a function of angular frequency (ω) of pristine PP and modified-CoSt pro-oxidant filled PP films

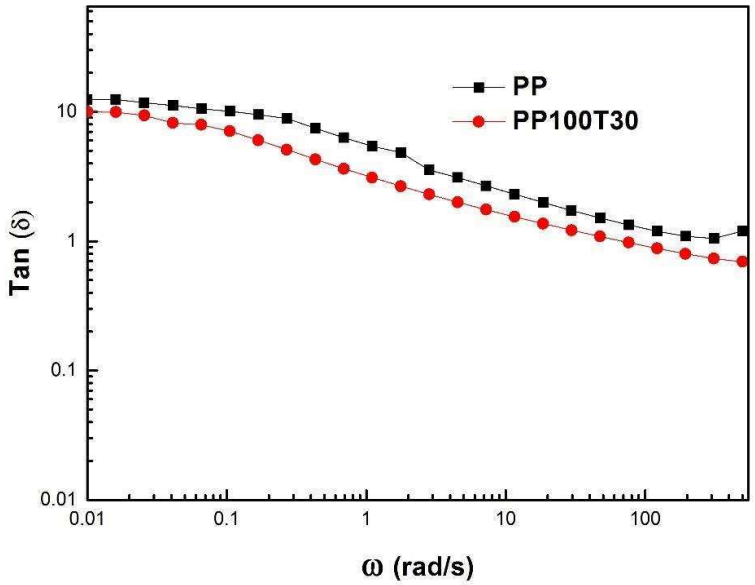

Fig. 5.8 (f) Tan (δ) as a function of angular frequency (ω) of pristine PP and modified-CoSt pro-oxidant filled PP film samples

5.6 Determination of biodegradability without and with after abiotic pretreatment

The total organic carbon (TOC) of various films without and with abiotic pretreatment were determined to make it possible to estimate the theoretical carbon dioxide ($CO_{2(th)}$) and are presented in Tables 5.5 and 5.6, respectively.

Table 5.5 Total organic carbon (%) and theoretical CO_2 (g) evolution from the samples before abiotic pretreatment

Sample	TOC (%)	Wt. of carbon in 1 g of sample (g)	Th. CO_2 evolution (g)
Microcrystalline cellulose (CEL)	43	0.43	1.56
PP	95	0.95	3.48
PP100T5	90	0.90	3.3
PPT0010	89	0.89	3.26
PP100T20	87	0.87	3.19
PP100T30	86	0.86	3.15

Table 5.6 Total organic carbon (%) and theoretical CO_2 (g) evolution from the samples with abiotic pretreatment

Sample	TOC (%)	Wt. of carbon in 1 g of sample (g)	Th. CO_2 evolution (g)
Microcrystalline cellulose (CEL)	43	0.43	1.56
PP	95	0.95	3.48
PP100T5	88	0.88	3.22
PPT00T10	88	0.88	3.22
PP100T20	86	0.86	3.15
PP100T30	85	0.85	3.11

The values of CO_2 generated (g) and the biodegradability (%) of every film was determined by Eqs. 3.4 and 3.5, respectively. The sample calculations from first principles are shown in Section 4.5 of Chapter 4. To evaluate the biodegradability without and with abiotic pretreatment (for 40 h), the composite films were subjected to a respirometry test using bioreactors. The percentage biodegradability of PP (R1), PP100T5 (R2), PP100T10 (R3), PP100T20 (R4), and PP100T30 (R5) without and with accelerated weathering was estimated based on ASTM D 5388-15 standard protocol. Determining the amount of CO_2 emitted through

microbial respiration after utilization of degradable plastic material as a nutrient source of carbon and energy in the polymer films makes it possible to estimate % biodegradability [219]. Using Eq. (3.5), the biodegradability was estimated in terms of C-CO_2 release. The present microbes present in the inoculum should mineralize the degradable substrate and convert 90% carbon content of the individual films into C-CO_2, H_2O, and biomass [30, 219, 222]. The biodegradation of all the modified pro-oxidant containing PP film samples without and with abiotic pretreatment are presented in Fig. 5.9. Before abiotic pretreatment, the percentage biodegradation of all the films in enhancing order are: PP (R1) 0%, PP100T5 (R2) 15.51%, PP100T10 (R3) 18.88%, PP100T20 (R4) 23.92%, PP100T30 (R5) 28.87% and cellulose (reference) 77.11%. After abiotic pretreatment, the biodegradation (%) of all the films in ascending order are PP (R1) 0%, PP100T5 (R2) 16.70%, PP100T10 (R3) 22.83%, PP100T20 (R4) 30.91%, PP100T30 (R5) 38.78% and cellulose (reference) 77.11% while the highest biodegradability obtained of PP100T30 film was only 28.87% when the sample was not given any abiotic pretreatment.

The biodegradability of modified pro-oxidant loaded PP composites has been increased by abiotic pretreatment. During abiotic pretreatment (accelerated weathering), polymeric material leads to free radicals' generation, which is mixed with atmospheric O_2 to form radicals (peroxides and hydroperoxide). Also, weak linkages, amorphous nature, chain cleavage, and different functional groups like ketones, alkenes, aldehydes, carboxylic acids, alcohols, linear-esters, alkanes, keto-acids, and lactones are created, which decreased the polymeric materials molecular weight, hydrophobicity and resulting into enhanced bioavailability for decomposition [165, 180, 219]. The modified pro-oxidant made the PP prone to microbial attack due to its amorphous nature [5, 84, 121]. Microbes have consumed biodegradable plastic material as a nutrient source of energy and emitted CO_2, biomass, and water [84, 219, 223]. The mechanism of action has been explained in Section 4.5 of Chapter 4.

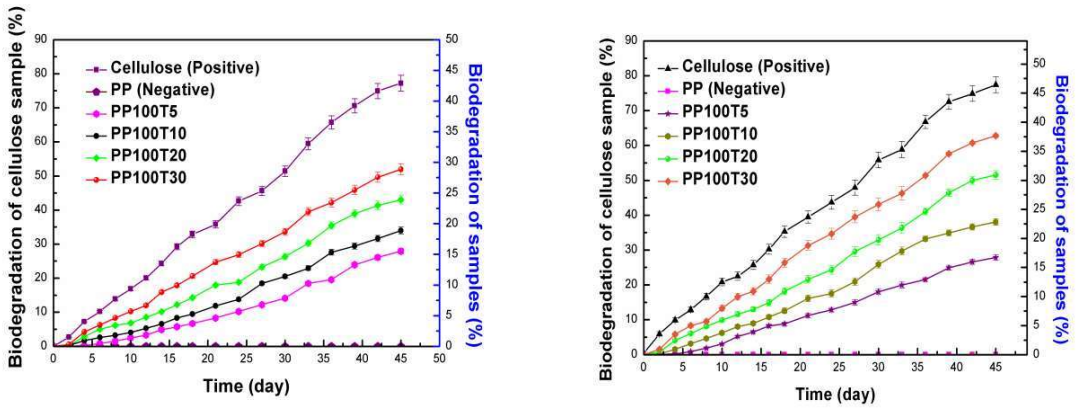

Before After

Fig. 5.9 Biodegradability (on biotic treatment) of different samples without (left) and with (right) abiotic (40 h) pretreatment (accelerated weathering)

5.6.1 Scanning electron microscopy (SEM)

Fig. 5.10 shows the morphology of different films without any pretreatment and after biotic treatment, after abiotic pretreatment (accelerated weathering) and after biotic treatment under controlled composting conditions. After 45 days, the surface of the PP film does not change its morphology. It indicates that microbes did not attack the PP film during biodegradability test. After composting test, distinct changes were found on modified PP films, with roughening, cavitation, and disintegration of the surface, which is clear confirmation of biodegradation [35]. The surface of modified PP films changed, indicating that it was attacked by the microorganisms under composting conditions. After abiotic pretreatment, more pronounced exfoliation, peeling, and several small holes in the plate structure were found in comparison to without any pretreatment and after biotic pretreatment and pristine PP. It indicates a greater degree of surface deterioration of modified PP films. This is due to addition of modified-CoSt pro-oxidant and UV exposure; these films became more fragile on biodegradation. Finally, it is concluded that the modified PP films on abiotic plus biotic degradation became rougher than those without any pretreatment but after biotic treatment.

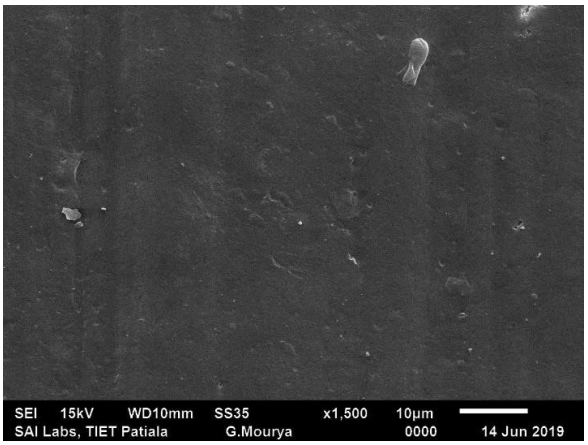

Without any pretreatment and after biotic treatment (PP)

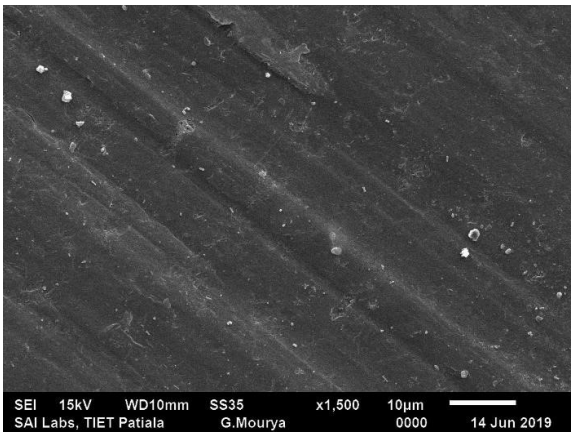

After abiotic pretreatment plus after biotic treatment (PP)

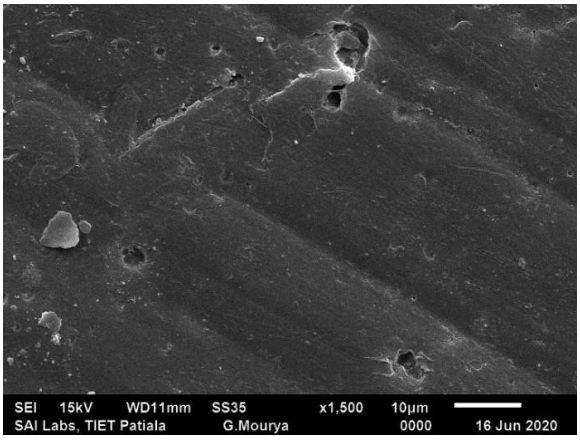

After abiotic pretreatment plus after biotic treatment (PP100T5)

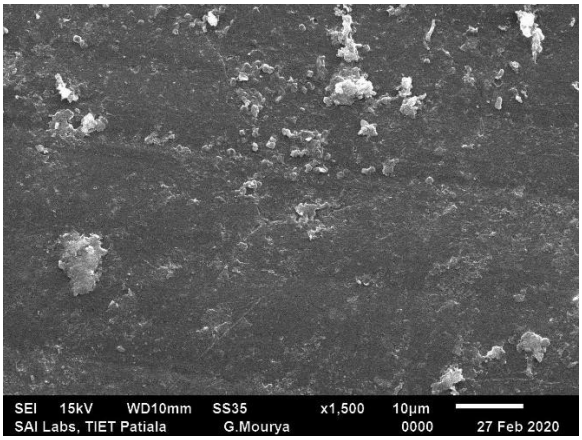

After abiotic pretreatment plus after biotic treatment (PP100T5)

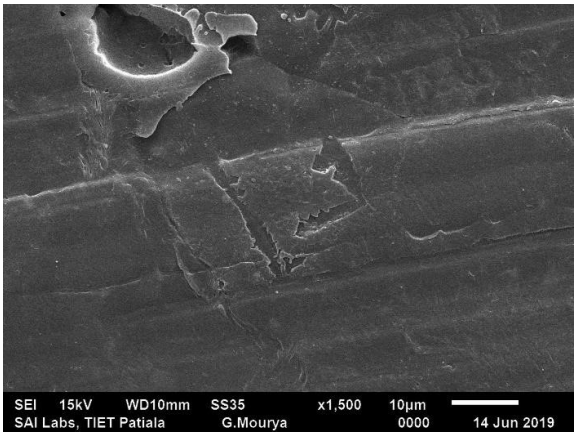

Without any pretreatment and after biotic treatment (PP100T10)

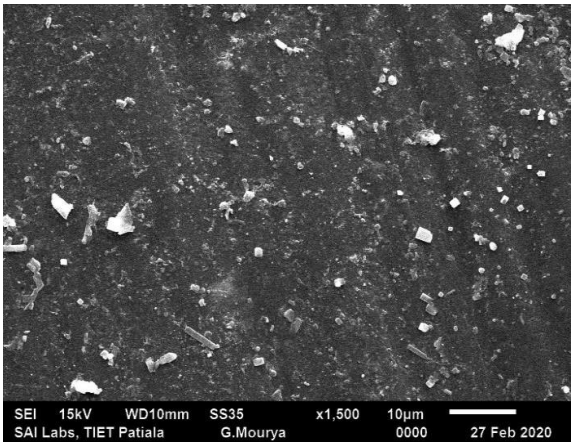

After abiotic pretreatment plus after biotic treatment (PP100T10)

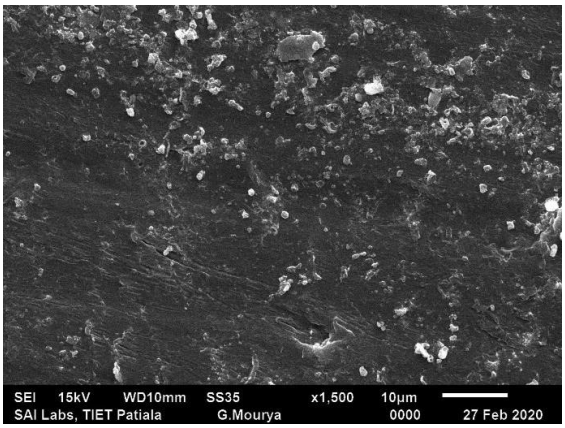

Without any pretreatment and after biotic treatment (PP100T20)

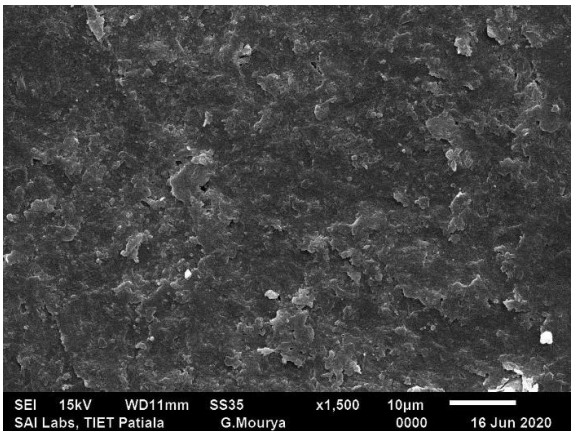

After abiotic pretreatment plus after biotic treatment (PP100T20)

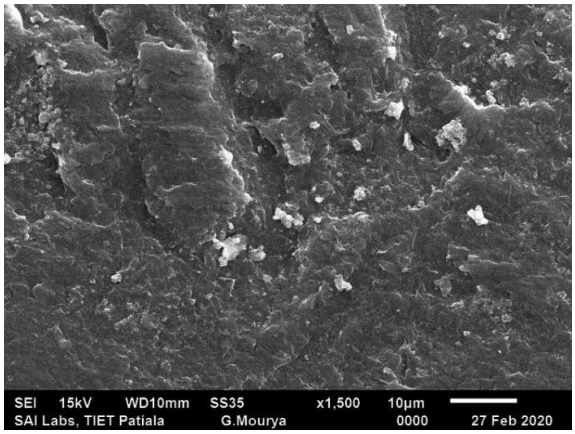

Without any pretreatment and after biotic treatment (PP100T30)

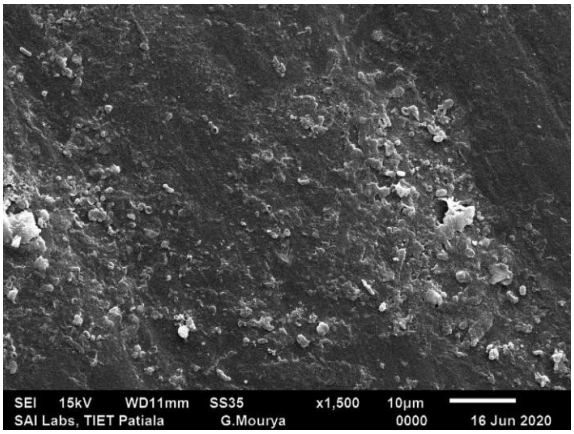

After abiotic pretreatment plus after biotic treatment (PP100T30)

Fig. 5.10 SEM images of modified pro-oxidant loaded PP samples- LEFT: before any pretreatment and after biotic treatment (45 days), and RIGHT: after abiotic (for 40 h) and biotic (45 days) treatment of different film samples

5.6.2 Molecular weight analysis

Reduction in molecular weight is one of the most consistent signs of biodegradation in biodegradable polymers in different environmental conditions. Abiotic pretreatment also results in abundant chain scission of PP because of hydroperoxides produced in the oxidation step. Significant amounts of volatile compounds such as acetic acid, acetone, and methanol have also been observed [153, 217]. The molecular weight analysis was carried out for the pristine PP samples and PP100T30 samples that exhibit maximum biodegradability. Table 5.7 shows the average molecular weights ($\overline{M_n}$, $\overline{M_w}$), and PDI of the PP and modified PP films without any treatment, after abiotic pretreatment and after biodegradation tests. After the

abiotic (accelerated weathering) pretreatment, both the $\overline{M_n}$ and $\overline{M_w}$ values of the modified PP films (oxidized) are much lower than those of the pristine PP. $\overline{M_n}$ values are more sensitive to low molecular weights. The addition of modified-CoSt pro-oxidant catalyzes the breakdown of hydroperoxides and also improves the embrittlement of PP chains under abiotic pretreatment. This chain breakage increases the carbon mineralisation of the polymeric materials [30, 43]. The decrease of molecular weight of various modified PP films exposed to abiotic pretreatment is related to the degree of oxidation. It can be seen that the decrease of molecular weight is higher in the case of modified PP films compared with pristine PP [58, 153]. Decrease of molecular weight is higher in the case of modified pro-oxidant compared with CoSt pro-oxidant.

Table 5.7 Average molecular weights ($\overline{M_n}$ and $\overline{M_w}$) and polydispersity index (PDI) of the PP samples and modified pro-oxidant filled PP samples before (without any pretreatment), after (abiotic treatment), without any pretreatment and after biotic treatment, and after abiotic and biotic treatment

Polymer sample		$\overline{M_n}$	$\overline{M_w}$	PDI
PP	Without any pretreatment	69500	560900	8.07
	Without any pretreatment and after biotic treatment	69500	560900	8.07
	After abiotic pretreatment	69500	560900	8.07
	After abiotic pretreatment and biotic treatment	69500	560900	8.07
PP100T30	Without any pretreatment	77500	412300	5.32
	Without any pretreatment and after biotic treatment	5100	11300	2.23
	After abiotic pretreatment	4800	9200	1.91
	After abiotic pretreatment and biotic treatment	4600	9100	1.98

5.7 Biodegradation kinetic modeling of pro-oxidant filled PP composites without and with abiotic pretreatment

5.7.1 Kinetics and model parameters

A comprehensive view of the computed un-degraded carbon data is reported in Fig. 5.11 for various samples without and with abiotic pretreatment shown in Table 5.1. The carbon left un-degraded was computed from Eq. (3.11) using the experimental data of C-CO_2 evolution obtained in the biodegradation runs. The temporal evolution of the undegraded carbon in these films reflects their kinetics in this figure. The kinetic data profiles for the undegraded carbon versus time are plotted together for samples R2, R3, R4, and R5 without and with abiotic pretreatment in Fig. 5.11. Without abiotic pretreatment, these four samples exhibited biodegradability in the range of 15.51-28.87% and with abiotic pretreatment showed biodegradability in the range of 16.70 - 38.78 % because of integration of modified pro-oxidant and abiotic pretreatment as explained in Section 4.5. It can be observed that these profiles show the same kinetic behavior as the curves are similar in shape. Hence, these must be governed by the same kinetic regime. The same methodology has been established in our earlier work on kinetic modelling of complex polymeric reaction systems [218].

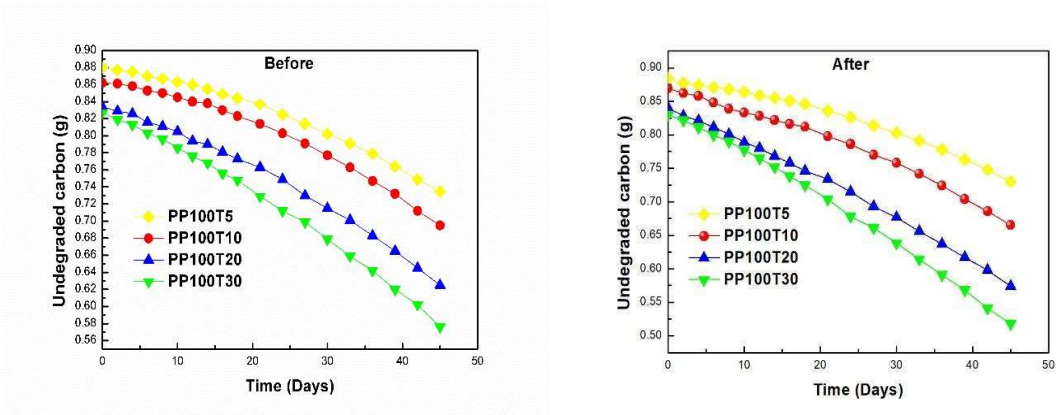

Fig. 5.11 Computed undegraded carbon profiles of different samples without (left) and with (right) abiotic pretreatment (accelerated weathering)

Without and with abiotic pretreatment, Tables 5.8 and 5.9 presents the kinetic parameters results with their determination coefficient (R^2). A very high correlation of the data is obtained in all the experiments. The value of R^2 approached 1 in all the cases. The kinetics of C-CO_2 evolutions during biodegradation of all the samples without and with abiotic pretreatments

from the experimental and model predictions are shown in Fig. 5.12. The corresponding experimental data of C-CO_2 evolved for the blank control, PP, and cellulose from the inoculum without and with abiotic pretreatment is shown in Fig. 5.13.

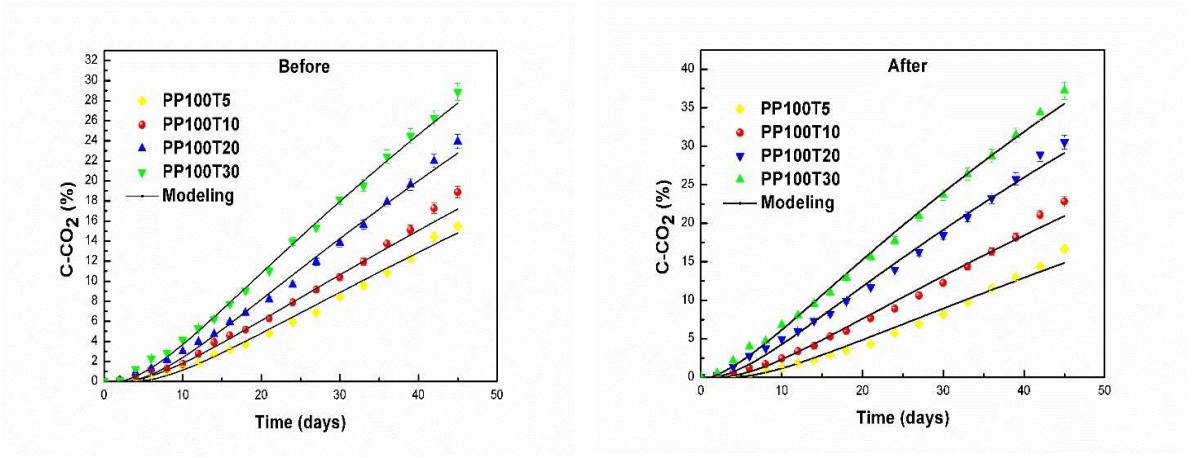

Fig. 5.12 C-CO_2 evolution profiles of different samples without (left) and with (right) abiotic pretreatment (accelerated weathering). Error bars correspond to twice standard deviation (n = 3)

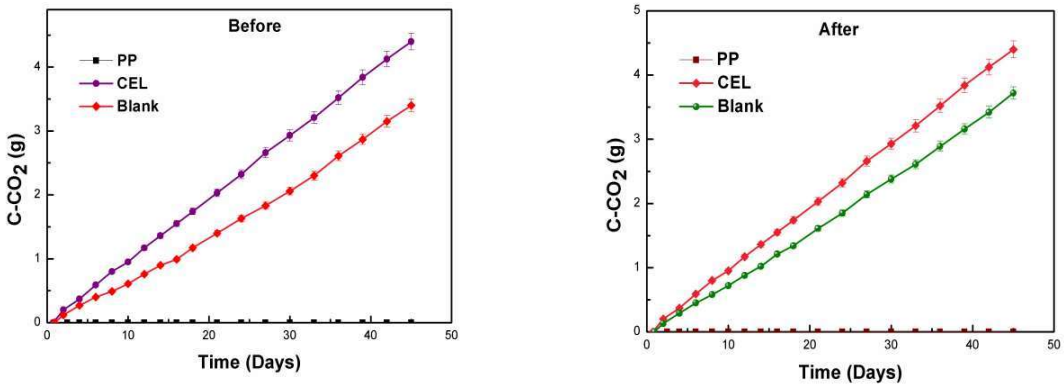

Fig. 5.13 C-CO_2 evolution for the blank, cellulose, and PP (without and with abiotic pretreatment) from the compost. Error bars correspond to twice standard deviation (n = 3)

Table 5.8 Kinetic model parameters and coefficients of determination without abiotic pretreatment (accelerated weathering)

Parameters	PP	PP100T5	PP100T10	PP100T20	PP100T30	Cellulose
	R1	R2	R3	R4	R5	CEL
C-CO_2 evolution (%) ± s.d.	0.0	15.51 ± 0.39	18.88 ± 0.52	23.92 ± 0.7	28.87 ± 0.88	77.11 ± 2.6
Biodegradability (%)	0.0	15.51	18.88	23.92	28.87	77.11
C_{aq0} (%)	-	0.00017	0.00031	0.095	0.83	9.5
C_{r0} (%)	-	0.00001	0.00027	0.11	0.15	6
C_{m0} (%)	-	99.99	99.99	99.79	99.06	84.5
C_{s0} (%)	-	-	-	-	-	-
k_{aq} (day^{-1})	-	0.17	0.18	0.18	0.18	0.24
k_r (day^{-1})	-	0.16621	0.17411	0.17510	0.17512	0.15
k_m (day^{-1})	-	0.00450	0.00511	0.00712	0.00852	0.035
k_s (day^{-1})	-	0	0	0	0	0
c (day)	-	3.6	2.39	2.01	1.94	0.75
R^2	-	0.9951	0.9919	0.9962	0.9974	0.9997

Table 5.9 Kinetic model parameters and coefficients of determination with abiotic pretreatment (accelerated weathering)

Parameters	PP	PP100T5	PP100T10	PP100T20	PP100T30	Cellulose
	R1	R2	R3	R4	R5	CEL
C-CO_2 evolution (%) ± s.d.	0.0	16.70 ± 0.42	22.83 ± 0.59	30.91 ± 0.94	38.78 ± 1.2	77.11 ± 2.6
Biodegradability (%)	0.0	16.70	22.83	30.91	38.78	77.11
C_{aq0} (%)	-	0.00018	0.029	0.71	2	9.5
C_{r0} (%)	-	0.0001	0.00044	0.03311	0.53510	6
C_{m0} (%)	-	99.99	99.97	99.25	97.46	84.5
C_{s0} (%)	-	-	-	-	-	-
k_{aq} (day^{-1})	-	0.18	0.18	0.18	0.18	0.24
k_r (day^{-1})	-	0.17211	0.17521	0.17532	0.17612	0.15
k_m (day^{-1})	-	0.00451	0.00630	0.00882	0.01121	0.035
k_s (day^{-1})	-	0	0	0	0	0
c (day)	-	2.5	2.01	1.16	1.45	0.75
R^2	-	0.9929	0.9951	0.9974	0.9979	0.9997

The regression analysis was used to compute the model parameters without and with abiotic pretreatment. Their values are shown in Tables 5.8 and 5.9. All the samples have moderately hydrolysable carbon and readily hydrolysable carbon fractions, which could be used by the microorganisms, thus resulting in their moderate biodegradability. The values of their moderately hydrolysable carbon fractions C_{m0} and their hydrolysis rates k_m are significantly high in all the samples without and with abiotic pretreatment. They show an initial flat lag phase along with sigmoid behavior (Fig. 5.12). The films do not include slowly hydrolysable carbon fractions (Tables 5.8 and 5.9). In all the samples, the initial intermediate hydrolysable carbon fraction C_{aq0} values are significantly lower that indicates the absence of short polymer chains [35].

In Tables 5.8 and 5.9, the C_{r0} values decrease with progressive decrease in modified pro-oxidant concentration. Hence, the degradability progressively decreases with a decrease in initial readily hydrolysable solid carbon. Without abiotic pretreatment, the degradability of R5, R4, R3, and R2 are 28.87%, 23.92%, 18.88%, and 15.51%, respectively. The model curves exhibit good correlation with the experimental ones (R^2= 0.9974, R^2= 0.9962, R^2= 0.9919, and R^2= 0.9951, respectively). Their C_{r0} values are 0.15 %, 0.11 %, 0.00027 %, and 0.00001 %,

respectively. The hydrolysis rates k_r of R5, R4, R3, and R2 are 0.17512 day^{-1}, 0.17510 day^{-1}, 0.17411 day^{-1}, and 0.16621 day^{-1}, respectively and their k_m values are 0.00852 day^{-1}, 0.00712 day^{-1}, 0.00511 day^{-1}, and 0.00450 day^{-1}.

With abiotic pretreatment, the degradability of R5, R4, R3, and R2 are 38.78%, 30.91%, 22.83%, and 16.70%, respectively. The model curves exhibit good correlation with experimental data (R^2= 0.9979, R^2= 0.9974, R^2= 0.9951, and R^2= 0.9929, respectively). Their C_{r0} values are 0.53510 %, 0.03311 %, 0.00044 %, and 0.00011 %, respectively. The hydrolysis rates k_r of R5, R4, R3, and R2 are 0.17612 day^{-1}, 0.17532 day^{-1}, 0.17521 day^{-1}, and 0.17211 day^{-1}, respectively and their k_m values are 0.01121 day^{-1}, 0.00882 day^{-1}, 0.00632 day^{-1}, and 0.00451 day^{-1}. All of these values depend on biodegradability and decrease with a decrease in the pro-oxidant loading. In all the films, slowly hydrolysable carbon (C_{s0}) fractions are absent since the presence of pro-oxidant and accelerated weathering (abiotic treatment) has enhanced the hydrolysis rate of carbon. The values of all the parameters are consistent with the earlier works on polyolefins [35]. Table 5.10 presents the kinetic modelling parameters evaluated by different researchers on biodegradation under controlled composting conditions.

Table 5.10 Reported parameter values from different studies on biodegradation kinetic modelling under controlled composting conditions

Polyolefins	Standard	C_{aq0} (%)	C_{r0} (%)	C_{m0} (%)	C_{s0} (%)	C_h (%)	k_{aq} (day^{-1})	k_r (day^{-1})	k_m (day^{-1})	k_s (day^{-1})	k_h (day^{-1})	c (day)	C-CO_2 (%)	Reference
Different municipal solid wastes (MSW)	-	8 to 11	0 to 8.5	16 to 90	0 to 82	-	10^{6}	0 to 0.1	0.005 to 0.06	0 to 82	-	-	-	[75]
Polyethylene (PE), PE/starch blend	ISO 14855-1	0 to 2.256	0	0 to 97.744	0	-	0 to 1.00000	-	0 to 0.00098	0	-	0	0.56 to 11.50	[35]
PLA/clay Nanocomposites	-	0	37.48 to 80.83	19.17 to 62.52	0	-	0.0489 to 0.1470	0.0262 to 0.0367	0.0121 to 0.0353	0	-	12.8 to 27.6	62.73 to 84.42	[184]
Polylactide (PLA) and carbodiimide additive	-	0	-	-	-	100	0.0330 to 0.1866	-	-	-	0.0150 to 0.0352	15.7 to 100	65.2 to 74.62	[186]
Polylactide (PLA) with poly(acrylic acid)/PLA hydrolysis additive	-	0	-	-	-	100	0.0542 to 0.0825	-	-	-	0.0542 to 0.0825	6.8 to 13.1	83.02 to 97.12	[187]
Polypropylene/modified pro-oxidant composites	ASTM D 5338	0.00017 to 9.5	0.00001 to 6	99.06 to 99.99	-	-	0.17 to 0.18	0.16621 to 0.17512	0.00450 to 0.00852	0	-	1.94 to 3.6	15.51 to 28.87	Present study without abiotic pretreatment
Polypropylene/modified pro-oxidant composites	ASTM D 5338	0.00018 to 9.5	0.00011 to 6	97.46 to 99.99	-	-	0.18	0.17211 to 0.17612	0.00451 to 0.01121	0	-	1.45 to 2.5	16.70 to 38.78	Present study with abiotic pretreatment

5.7.2 Hydrolysable carbon profiles

The above models are then used to see the evolution of the readily and moderately hydrolysable solid carbon profiles of different films. Figs. 5.14 and 5.15 show the profile for the readily and moderately hydrolysable solid-carbon without and with abiotic pretreatment (accelerated weathering treatment) of different films. All the figures show initial discontinuity at $t = c$. The readily hydrolysable carbon decomposes rapidly in all the samples PP100T5 (R2) –PP100T30 (R5) as depicted in Fig. 5.14. The readily hydrolysable solid-carbon of films PP100T20 (R4) and PP100T30 (R5) reduces very rapidly in comparison to other films (R3 and R2) as the values of initial readily hydrolysable solid carbon C_r, as well as hydrolysis rate constant k_r for the other films are lower than R4 and R5 (Tables 5.8 and 5.9). Fig. 5.15 presents moderately hydrolysable solid carbon profiles for all the films without and with abiotic pretreatment. All the curves of R4-R5 films exhibit exponential decay and decrease very fast initially since their initial moderately hydrolysable solid carbon values are high.

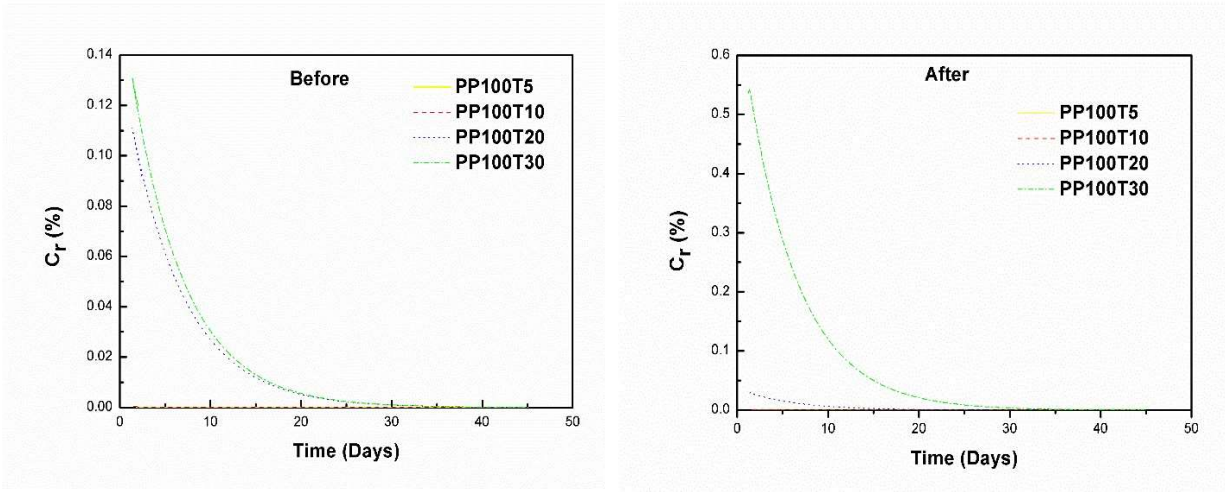

Fig. 5.14 Readily hydrolysable solid carbon profiles of different films without (left) and after (right) abiotic pretreatment (accelerated weathering)

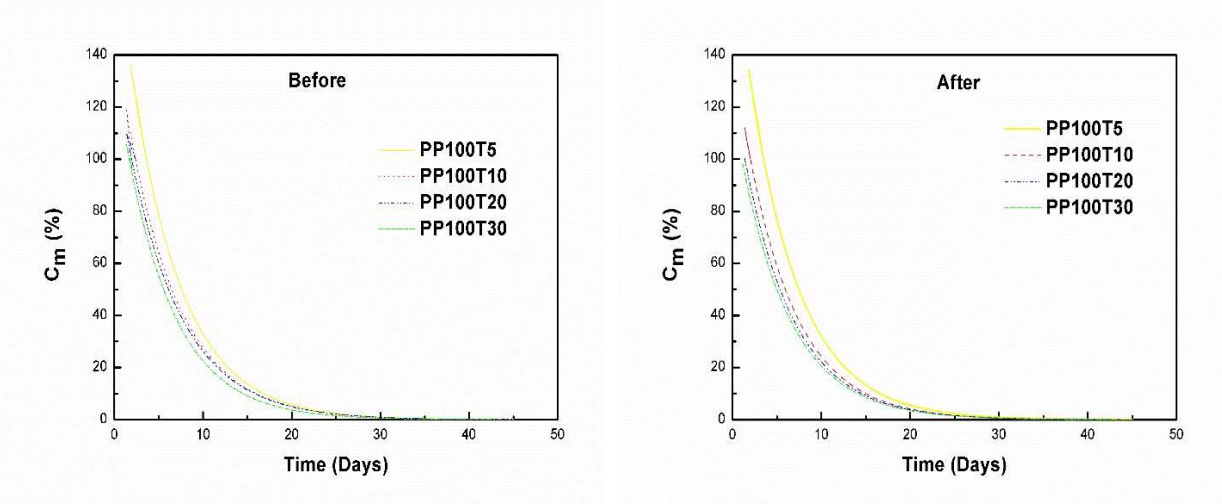

Fig. 5.15 Moderately hydrolysable solid carbon profiles of different films without (left) and after (right) abiotic pretreatment (accelerated weathering)

5.7.3 Degradation curves

Fig. 5.16 presents the degradation curves plotted together for all the films without and with abiotic pretreatment that show the rate of C-CO_2 production predicted from the model (Eq. (3.27)). All the sample curves PP100T5 (R2) -PP100T30 (R5) exhibited two decay phases after the first phase (lag phase). The rate enhances rapidly in the second or growth phase, attains a peak, and then starts falling rapidly in the third (stationary) phase. This trend is attributed to the sigmoid behavior of C-CO_2 evolution shown in Fig. 5.12. The second (growth) phase is because of the readily-hydrolysable carbon. The stationary phase is because of the moderately-hydrolysable carbon [75]. Without pretreatment, the maximum rates of C-CO_2 production of the samples of PP100T5 (R2), PP100T10 (R3), PP100T20 (R4), and PP100T30 (R5) are 0.407% per day, 0.456% per day, 0.612% per day, and 0.730% per day, respectively. These values depend on modified pro-oxidant loading. The maximum rate is found at 23.63 days, 23.18 days, 21.36 days, and 18.63 days, respectively.

With abiotic pretreatment (accelerated weathering), the maximum rates of C-CO_2 production of the samples of PP100T5 (R2), PP100T10 (R3), PP100T20 (R4), and PP100T30 (R5) are 0.408% per day, 0.557%, 0.763% per day, and 0.920% per day, respectively. These values depend on pro-oxidant loading. The maximum rate is found at 25 days, 21.36 days, 17.27 days, and 15.45 days,

respectively. Fig. 5.17 presents the degradation curves plotted together for PP and cellulose that show the rate of C-CO_2 production predicted from the model (Eq. (3.27)).

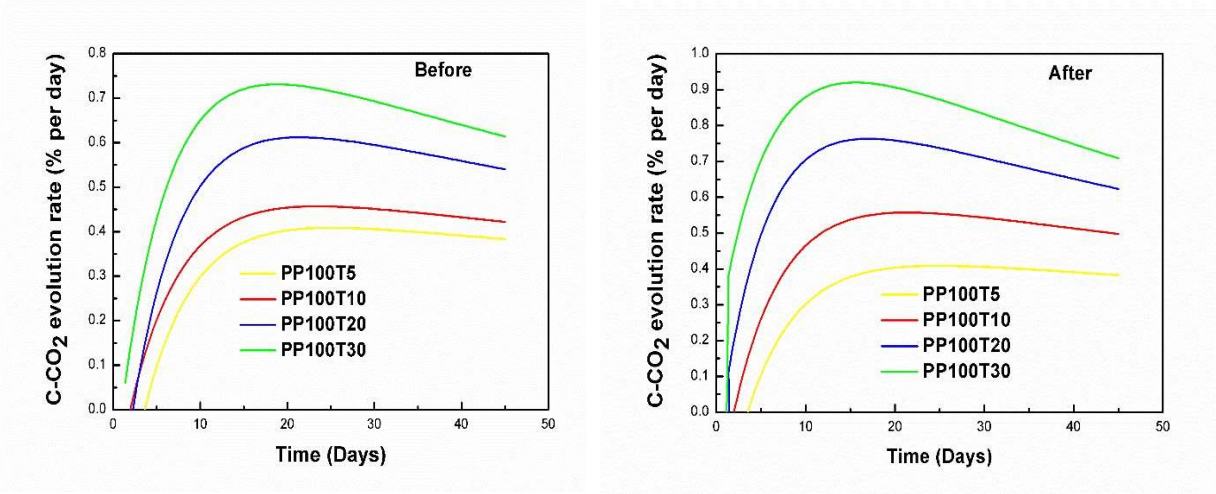

Fig. 5.16 C-CO_2 evolution rate profiles of different samples without (left) and after (right) abiotic pretreatment (accelerated weathering)

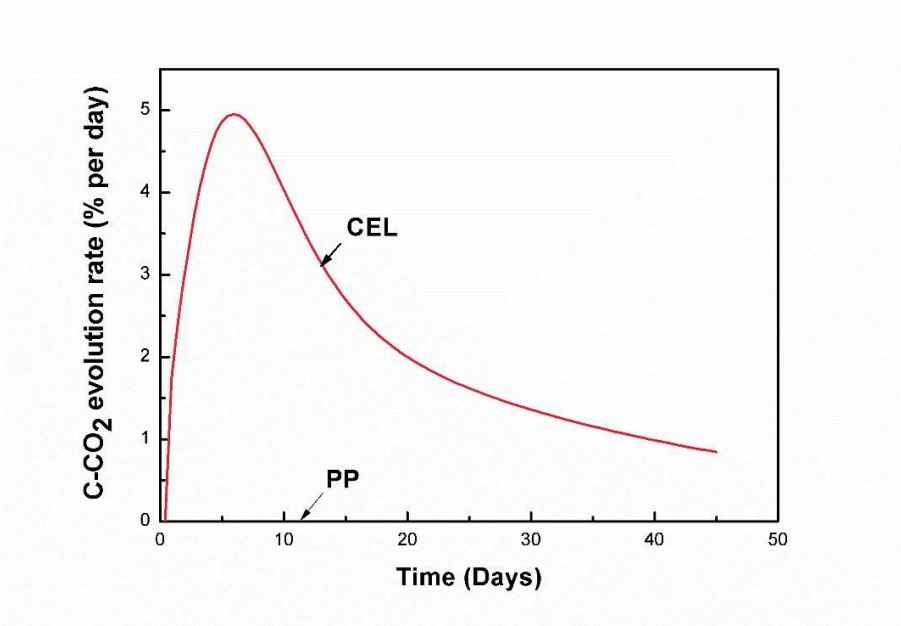

Fig. 5.17 C-CO_2 evolution rate profiles of PP (without and with abiotic pretreatment) and cellulose (without any abiotic pretreatment) samples

5.7.4 Mineralizable intermediate carbon

The evolution for the intermediate carbon C_{aq} is shown in Fig. 5.18. It exhibits the same behavior as that of the degradation curves. This is due to the fact that C_{aq} is directly proportional to the rate of C-CO_2 evolution as seen from Eq. (3.21). The intermediate carbon depends upon the difference between the first and second stages of the reaction pathway. That is, the rate of its formation from the initial hydrolysable carbon fractions minus the rate of its disappearance during mineralization in Eq. (3.18).

Curves PP100T5 (R2)-PP100T30 (R5) fall monotonically since the rate of the disappearance of C_{aq} is more than its formation. This is so because there are initially more readily and moderately hydrolysable carbon fractions than the intermediate carbon fraction as seen (Tables 5.8 and 5.9), and so the first stage dominates over the second stage. After reaching a maximum, however, these profiles start falling subsequently due to the dominance of the second stage caused by a sufficient buildup of C_{aq} by this time.

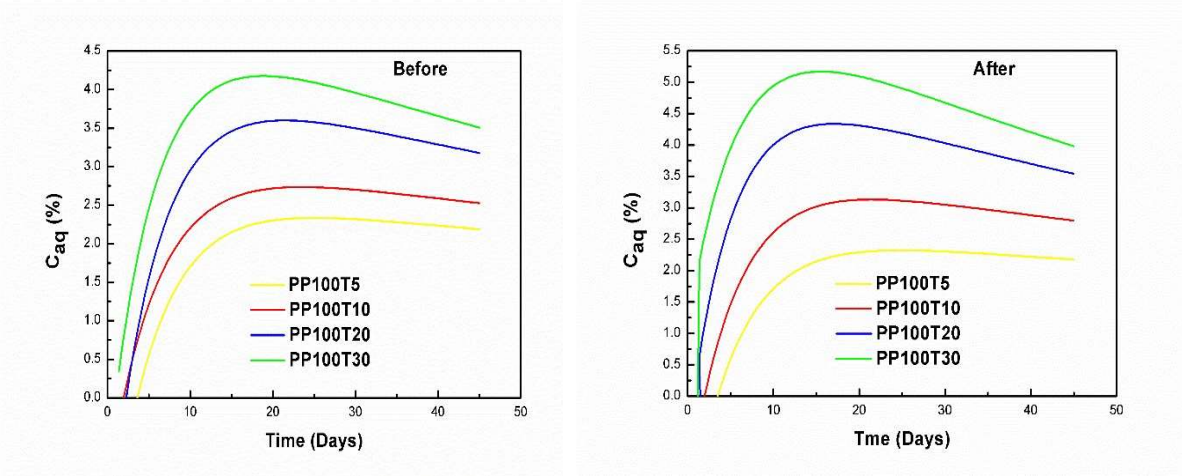

Fig. 5.18 Mineralizable intermediate carbon profiles of different samples without (left) and after (right) abiotic pretreatment (accelerated weathering)

5.8 Eco-toxicological studies of biodegraded material without and with abiotic pretreatment

5.8.1 Microbial toxicity test

Table 5.11 presents the numbers of colony-forming bacteria in the composted film material witout and with abiotic pretreatment (accelerated weathering). The blank sample gave CFU count of 0.3×10^4, and CEL gave the maximum CFU count (bacterial lawn). In all the modified pro-oxidant loaded PP films, the value of CFU count was more than that of the blank sample, which shows an enhanced bacterial growth in the composted samples. Therefore, the degraded intermediate products from all the film samples are considered as non-toxic.

Table 5.11 Number of bacterial colonies (CFUs) from water extract of compost containing different samples without (before) and after (with) abiotic pretreatment

Film sample	Number of colonies, CFU/mL (Before)	Number of colonies, CFU/mL (After)
Control	3	3
Cellulose	Bacterial lawn	Bacterial lawn
PP	3	5
PP100T5	14	16
PP100T10	16	18
PP100T20	19	20
PP100T30	24	26

5.8.2 Plant growth test

For this test, a middle range of pH was utilized to confirm the aptness of composted PP films. The suggested optimal range of pH is 5.5 [224] for the growth of plants. In the growth medium, a pH value very low or high will influence the solubility and the availability of nutrients. As per suggestions, in this case, the pH was kept at 5.8-6.0, which is close to the optimal range of pH.

Mung bean and wheat plants are utilized to know the toxic impacts of biodegraded intermediate products of modified pro-oxidant loaded PP samples without and with abiotic pretreatment [79]. After 21 days, the visual assessment of both the seedlings was done in the growth medium and the average number of plant growth was 100%. In Figs. 5.19, 5.20, 5.21, and 5.22, no differences were

seen in the tested films and control in case of both the plants before and after abiotic pretreatment (accelerated weathering). After 21 days of growth, both plants were cut, dried, and weighed. The dry weight of the wheat plants was nearly similar within 2% of all the composted samples. The same was the case for the plants of the *Mung*.

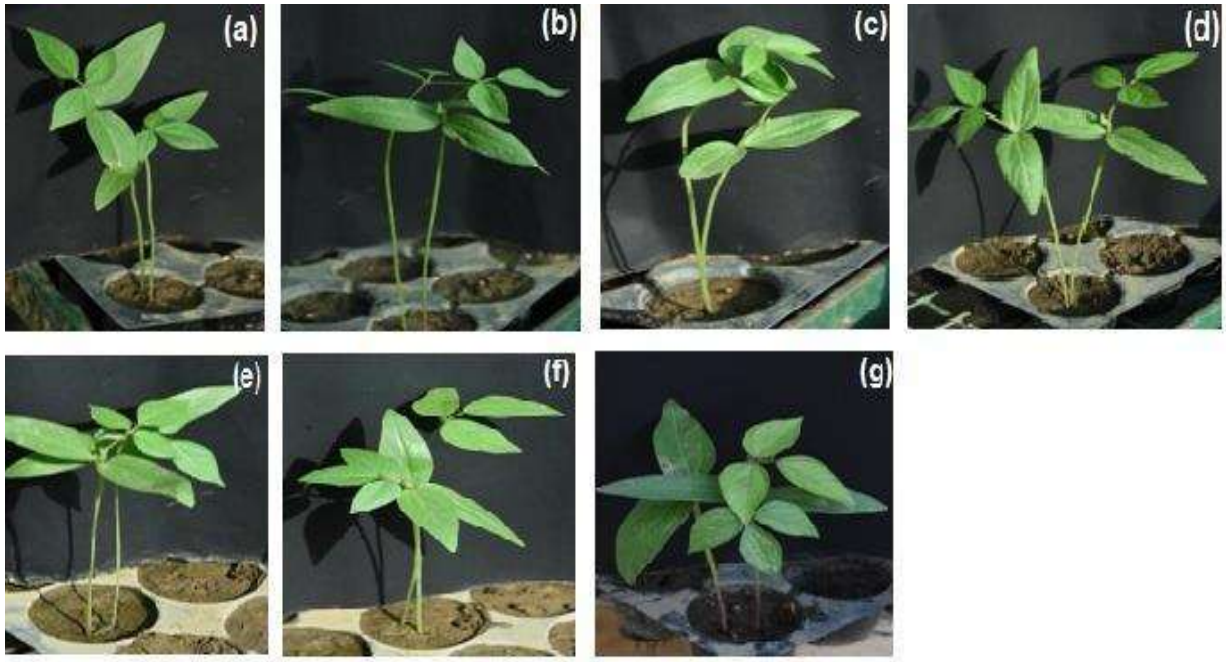

Fig. 5.19 Growth of *Mung* bean in compost (after 45 days biodegradation) of (a) control, (b) cellulose, (c) PP, (d) PP100T5, (e) PP100T10, (f) PP100T20, and (g) PP100T30 without abiotic pretreatment (accelerated weathering)

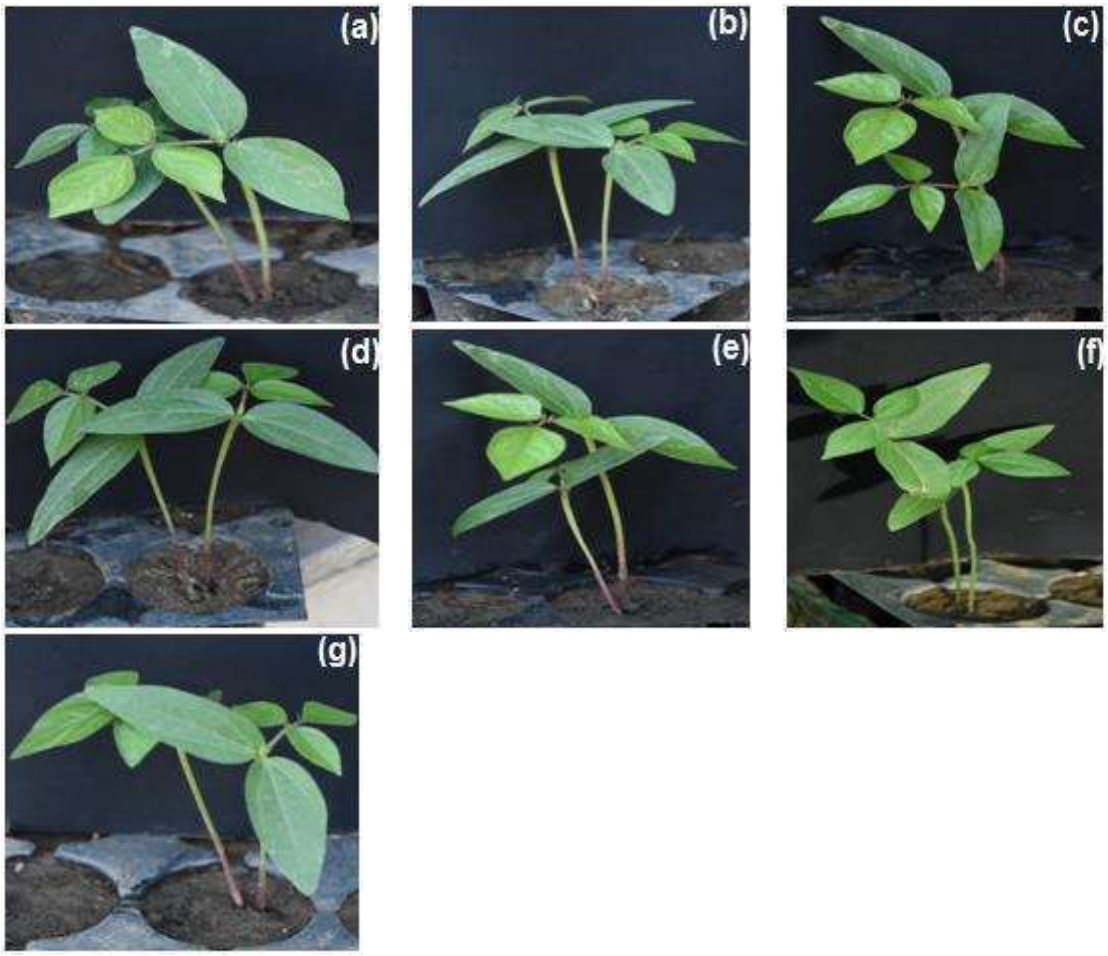

Fig. 5.20 Growth of *Mung* bean in compost (after 45 days biodegradation) of (a) control, (b) cellulose, (c) PP, (d) PP100T5, (e) PP100T10, (f) PP100T20, and (g) PP100T30 with abiotic pretreatment (accelerated weathering)

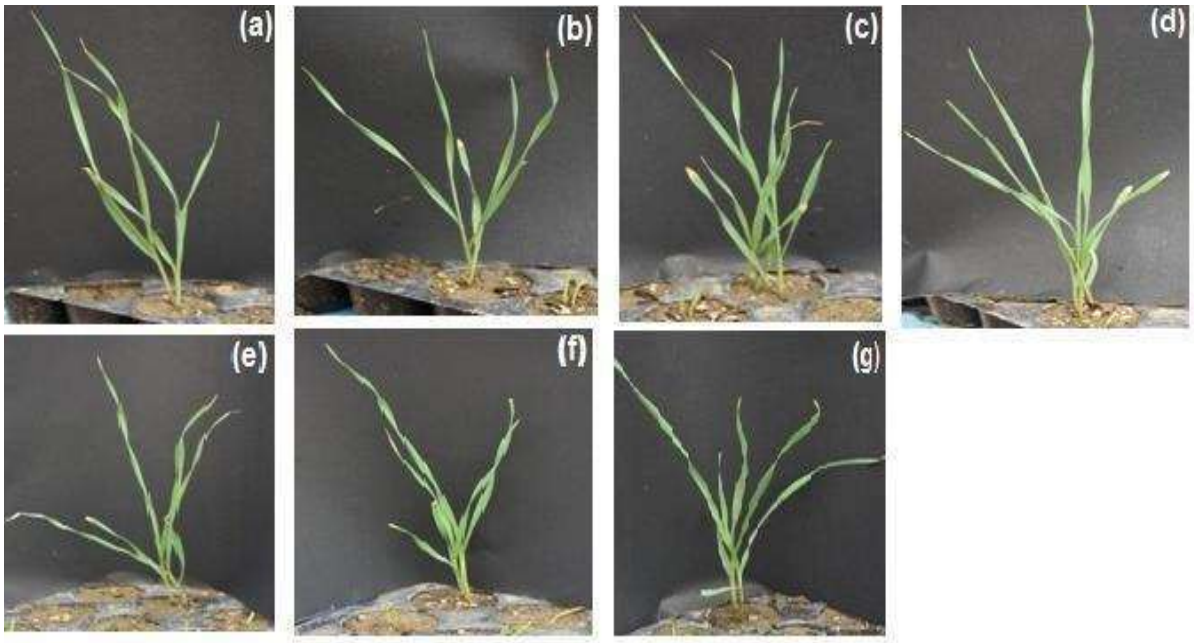

Fig. 5.21 Growth of wheat in compost (after 45 days biodegradation) of (a) control, (b) cellulose, (c) PP, (d) PP100T5, (e) PP100T10, (f) PP100T20, and (g) PP100T30 without abiotic pretreatment (accelerated weathering)

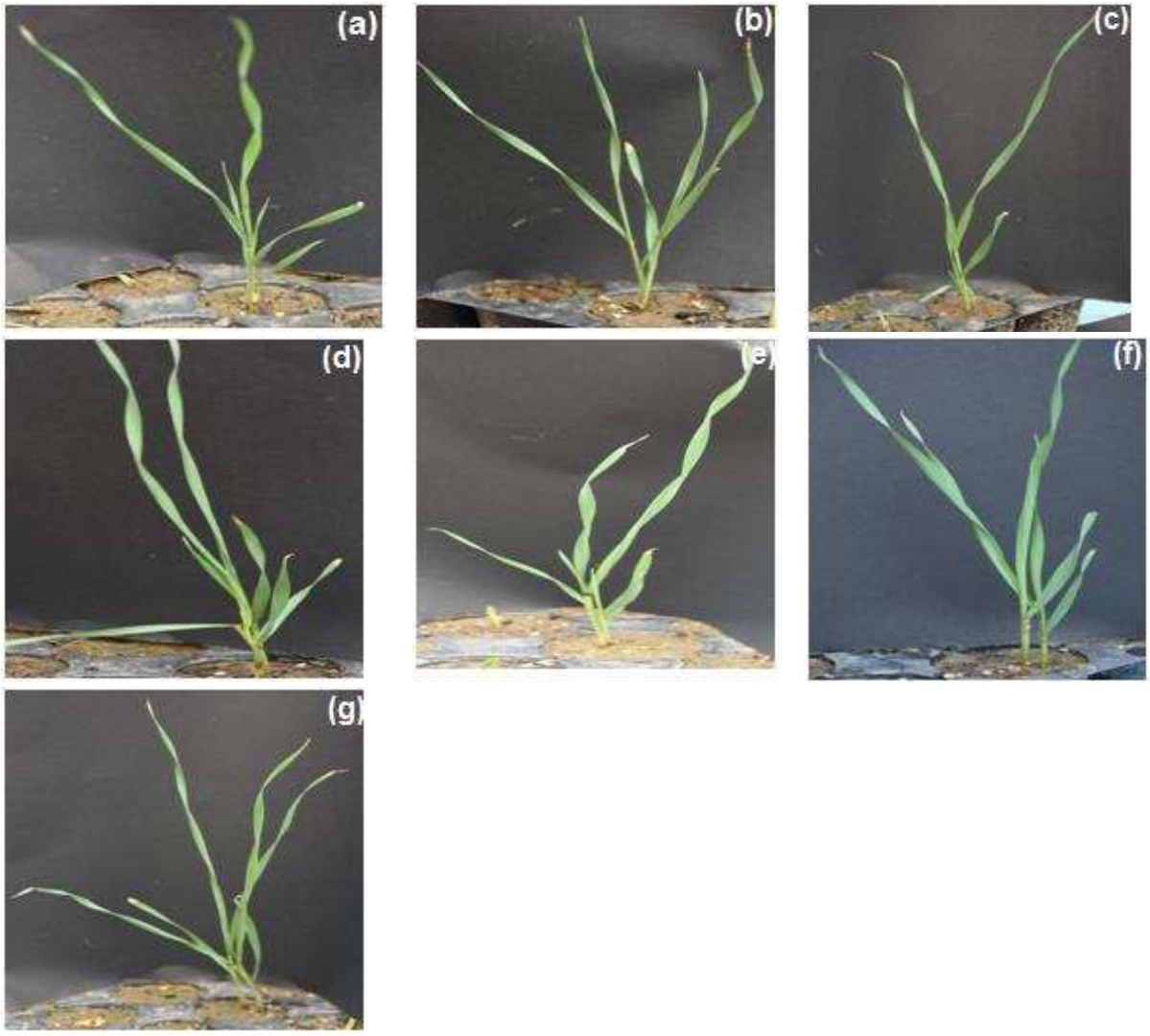

Fig. 5.22 Growth of wheat in compost (after 45 days biodegradation) of (a) control, (b) cellulose, (c) PP, (d) PP100T5, (e) PP100T10, (f) PP100T20, and (g) PP100T30 with abiotic pretreatment (accelerated weathering)

5.8.3. Earthworm acute-toxicity test

In the post biodegradation compost, the value of average percentage mortality of earthworms for the PP, CEL, blank (control), PP100T5, PP100T10, PP100T20, and PP100T30 was nil after the two-week test. This revealed that the biodegradation products of different film samples without and with abiotic pretreatment (accelerated weathering) were nontoxic.

Chapter 6-Conclusions and Recommendations for Future Work

6.1 Conclusions

In this work, cobalt stearate loaded PP composites have been successfully prepared by compounding technique. The study attempts to investigate the influence of CoSt loading and UV exposure on the morphological, physical, thermal, chemical, and biodegradability characteristics of packaging films. Without any abiotic pretreatment, the tensile strength has decreased from 35 to 14.5 MPa on increase in CoSt from 0 to 2 phr. The highest carbonyl index (0.83) has been found in PP100CoSt2.0 (S8) film sample after abiotic pretreatment. The addition of CoSt has reduced the crystallinity. After abiotic pretreatment, the thermal stability of the samples decreases. For example, T_i decrease from 170 to 157 ºC, and T_m from 166 to 156 ºC, in case of S8 sample. Addition of CoSt pro-oxidant reduces the complex viscosity and storage modulus. The loss angle vs frequency curve shows a negative slope thereby indicating that the composites behave as viscoelastic. The highest biodegradation of abiotically treated composite PP films has been shown to be 36.42% having 2 phr CoSt in it. Decrease in the molecular weight of the test samples proved the occurrence of chain scission mechanism, leading to the formation of intermediates, which resulted in microbial assimilation.

Modeling the kinetics of biodegradation of PP loaded with CoSt as pro-oxidant without and with abiotic pretreatment has been attempted. The experimental data have been analyzed using an eight-parameter Komilis model containing a flat lag phase. The model formulations involve hydrolysis of primary solid carbon and its subsequent mineralization. The first step is the rate controlling and it includes hydrolysis of slowly (C_s), moderately (C_m), and readily (C_r) hydrolysable carbon fractions in parallel. The model parameters and un-degraded/ hydrolysable/ mineralizable carbon evolutions follow only one kinetic regime in both without and with abiotic pretreatment. All the films involved moderately, and readily hydrolysable carbons but the absence of slowly hydrolysable carbon. For the films without abiotic pretreatment, the rate of degradation reaches its maximum (0.223-0.740 % per day) at around 5-11th day. With abiotic pretreatment, the rate of degradation reaches its maximum (0.322-0.897 % per day) at around 12-39th day. For all the films, readily hydrolysable carbon fractions and their hydrolysis rate constants (k_r) appreciably increased

with increasing pro-oxidant loading. All the films show the presence of growth phase because of their high initial readily hydrolysable carbon fractions. The methods presented here can be used for the design and control of other similar systems. The eco-toxicity tests of the degraded material, namely, microbial test, plant growth test, and earthworm acute-toxicity test demonstrate that the biodegradation intermediates were nontoxic. Hence, CoSt filled PP has high industrial potential to make biodegradable flexible packaging.

After addition of modified-CoSt pro-oxidant in PP, the mechanical properties (tensile strength and elongation at break) decreases significantly, this can be still suitable for the packaging applications. On abiotic pretreatment, the carbonyl index increases, reaching to a maximum value of 1.1 in PP100T30 film sample. After abiotic pretreatment, the crystallinity of the PP films has decreased to a greater extent on addition of modified pro-oxidant (from 77 to 40%). After abiotic pretreatment, the thermal stability of the modified pro-oxidant filled PP samples decreases (T_i decrease from 237 to 194 ºC and T_m from 166 to 161 ºC in case of PP100T30 film sample). The loss angle vs frequency curve shows a negative slope thereby indicating that the composites behave as viscoelastic. The maximum biodegradability (38.78%) has been obtained in an abiotically treated film containing 30 phr of modified pro-oxidant in it. Decrease of molecular weight is higher in the case of modified pro-oxidant compared with CoSt pro-oxidant.

The kinetic modeling of the biodegradation for the case of modified-CoSt pro-oxidant in PP has been carried out in the same manner as done in the first part. The model parameters and un-degraded/hydrolysable/mineralizable carbon evolutions follow only one kinetic regime in both without and with abiotic pretreatment. All the films involve moderately, and readily hydrolysable carbons but the absence of slowly hydrolysable carbon. For the films without abiotic pretreatment, the rate of degradation reaches its maximum (0.407-0.730 % per day) at around 18-23th day. After abiotic pretreatment, the rate of degradation reaches its maximum (0.408-0.920) % per day) at around 15-25th day. For all the films, readily hydrolysable carbon fractions and their hydrolysis rate constants (k_r) appreciably increase with increasing modified pro-oxidant loading. All the films show the presence of growth phase because of their high initial readily hydrolysable carbon fractions. SEM results have confirmed the results of the biodegradability and kinetic modeling of the modified PP films. The data obtained from the kinetic model study would be helpful in the design and control of aerobic biodegradation systems for degradable plastics.

The rate of biodegradation is dependent on concentration of pro-oxidants. Biodegradation products have been found to be nontoxic in nature as determined by the plant growth, earthworm acute-toxicity, and microbial growth tests. Hence, the prepared composites can be effectively applied for flexible packaging materials and reducing the plastic waste in the environment.

6.2 Recommendations for further study

Research, being an everlasting process, throws up a vast set of opportunities at each turn. Some of these are listed here.

1. Some part of the modified PP still remains un-degraded after composting that needs further research for its mitigation.
2. The relative biodegradability of novel pro-oxidant loaded polymeric material can be studied for combinations of methods, namely, simultaneous photo-degradation and biodegradation. The results of these degradations on the polymer matrix also needs to be characterized.
3. Specialized characterizations can further be employed for this purpose, such as, nuclear magnetic resonance, chromatography, matrix-assisted laser desorption/ionization time of flight, and GPC.
4. Leaching studies can be done to find out the metal toxicity of CoSt for food packaging applications.
5. Finally, the scale-up studies may also be performed to assess the techno-economic feasibility.

References

[1] L. Utracki, History of commercial polymer alloys and blends (from a perspective of the patent literature), Polymer Engineering & Science 35(1) (1995) 2-17.

[2] M.H. Nguyen, Biodegradation of polyethylene and functional polyethylene under controlled composting conditions in Soil, Ph.D. thesis,Texas Southern University (2017).

[3] P. foundation, Indian plastic industry report 2019, https://www.plastindia.org/plastic-industry-status-report.html (2019).

[4] N. Singh, D. Hui, R. Singh, I. Ahuja, L. Feo, F. Fraternali, Recycling of plastic solid waste: A state of art review and future applications, Composites Part B: Engineering 115 (2017) 409-422.

[5] M. Subramaniam, S. Sharma, A. Gupta, N. Abdullah, Enhanced degradation properties of polypropylene integrated with iron and cobalt stearates and its synthetic application, Journal of Applied Polymer Science 135(12) (2018) 46028.

[6] A. Chamas, H. Moon, J. Zheng, Y. Qiu, T. Tabassum, J.H. Jang, M. Abu-Omar, S.L. Scott, S. Suh, Degradation Rates of Plastics in the Environment, ACS Sustainable Chemistry & Engineering 8(9) (2020) 3494-3511.

[7] Ministry of Housing and Urban Affairs. Plastic waste management issues, solutions and case studies, Governmnt of India (March 2019).

[8] R. Geyer, J.R. Jambeck, K.L. Law, Production, use, and fate of all plastics ever made, Science Advances 3(7) (2017) 1700782.

[9] B. Wire, https://www.businesswire.com/news/home/20170509006321/en/Trends-Opportunities-Indian-Packaging-Industry-2017-Analysis.

[10] S.E. Selke, J.D. Culter, Plastics packaging: properties, processing, applications, and regulations, Carl Hanser Verlag GmbH Co KG (2016).

[11] Conference on Plastic Packaging - The sustainable choice, Tata strategic managment group http://ficci.in/spdocument/20690/Plastic-packaging-report.pdf.

[12] S. Sam, M.A. Nuradibah, H. Ismail, N. Noriman, S. Ragunathan, Recent advances in polyolefins/natural polymer blends used for packaging application, Polymer-Plastics Technology and Engineering 53(6) (2014) 631-644.

[13] D. Hoornweg, P. Bhada-Tata, What a waste: A Global Review of Solid Waste Management, Urban Development Series Knowledge Papers 15(2012) 1-95.

[14] D.K. Barnes, F. Galgani, R.C. Thompson, M. Barlaz, Accumulation and fragmentation of plastic debris in global environments, Philosophical Transactions of the Royal Society of London B: Biological Sciences 364(1526) (2009) 1985-1998.

[15] M. Sarker, M.M. Rashid, M.S. Rahman, Conventional naphtha chemical produced from municipal solid low density polyethylene (LDPE) waste plastic, International Journal of Applied Chemistry 8(3) (2012) 153-163.

[16] J. Clapp, L. Swanston, Doing away with plastic shopping bags: international patterns of norm emergence and policy implementation, Environmental Politics 18(3) (2009) 315-332.

[17] F.W. Mader, Plastics waste management in Europe, Macromolecular Symposia, Wiley Online Library, 1992, pp. 15-31.

[18] Plastic waste management issues, solutions, and case studies, Ministry of Housing and Urban Affairs, Government of India (March 2019) http://164.100.228.143:8080/sbm/content/writereaddata/SBM%20Plastic%20Waste%20Book.pdf.

[19] M. Eriksen, L.C. Lebreton, H.S. Carson, M. Thiel, C.J. Moore, J.C. Borerro, F. Galgani, P.G. Ryan, J. Reisser, Plastic pollution in the world's oceans: more than 5 trillion plastic pieces weighing over 250,000 tons afloat at sea, PloS one 9(12) (2014) 111913.

[20] A. Khoironi, H. Hadiyanto, S. Anggoro, S. Sudarno, Evaluation of polypropylene plastic degradation and microplastic identification in sediments at Tambak Lorok coastal area, Semarang, Indonesia, Marine Pollution Bulletin 151 (2020) 110868.

[21] C. Moore, Plastic Pollution, Encyclopaedia Britannica (2015), pp.76.

[22] J. Hammer, M.H. Kraak, J.R. Parsons, Plastics in the marine environment: the dark side of a modern gift, Reviews of environmental contamination and toxicology, Springer 2012, pp. 1-44.
[23] J.I. Allen, J.R. Stewart, J. Readman, K. Davidson, M. Moore, Marine pollution and human health, Royal Society of Chemistry 2011.
[24] S. Al-Salem, A. Al-Hazza'a, H. Karam, M. Al-Wadi, A. Al-Dhafeeri, A. Al-Rowaih, Insights into the evaluation of the abiotic and biotic degradation rate of commercial pro-oxidant filled polyethylene (PE) thin films, Journal of Environmental Management 250 (2019) 109475.
[25] K.D. Cox, G.A. Covernton, H.L. Davies, J.F. Dower, F. Juanes, S.E. Dudas, Human consumption of microplastics, Environmental Science & Technology 53(12) (2019) 7068-7074.
[26] F. Fernández-Armesto, Pathfinders: a global history of exploration, WW Norton & Company 2007.
[27] P. André, Hill, Marquita K., 1900. Understanding Environmental Pollution, Géographie Physique et Quaternaire 53(3) (1999) 415-415.
[28] M.R. Gregory, Environmental implications of plastic debris in marine settings—entanglement, ingestion, smothering, hangers-on, hitch-hiking and alien invasions, Philosophical Transactions of the Royal Society B: Biological Sciences 364(1526) (2009) 2013-2025.
[29] M. Ajmal, S. Aiping, S. Uddin, M. Awais, M. Faheem, L. Ye, K.U. Rehman, M.S. Ullah, Y. Shi, A review on mathematical modeling of in-vessel composting process and energy balance, Biomass Conversion and Biorefinery (2020) https://doi.org/10.1007/s13399-020-00883-y
[30] N.K. Kalita, S.M. Bhasney, A. Kalamdhad, V. Katiyar, Biodegradable kinetics and behavior of bio-based polyblends under simulated aerobic composting conditions, Journal of Environmental Management 261 (2020) 110211.
[31] P. Roy, P. Surekha, C. Rajagopal, V. Choudhary, Degradation behavior of linear low-density polyethylene films containing prooxidants under accelerated test conditions, Journal of Applied Polymer Science 108(4) (2008) 2726-2733.
[32] L. Montagna, A. Catto, K. Rossini, M. Forte, R. Santana, Evaluation of the effect of organic pro-degradant concentration in polypropylene exposed to the natural ageing, AIP Conference Proceedings, AIP, 2014, pp. 329-332.
[33] F. Bensaad, N. Belhaneche-Bensemra, Effects of calcium stearate as pro-oxidant agent on the natural aging of polypropylene, Journal of Polymer Engineering 38(8) (2018) 715-721.
[34] L. Burman, A.C. Albertsson, Evaluation of long-term performance of antioxidants using prooxidants instead of thermal acceleration, Journal of Polymer Science Part A: Polymer Chemistry 43(19) (2005) 4537-4546.
[35] T. Leejarkpai, U. Suwanmanee, Y. Rudeekit, T. Mungcharoen, Biodegradable kinetics of plastics under controlled composting conditions, Waste Management 31(6) (2011) 1153-1161.
[36] R. Steller, W. Meissner, Structure and properties of degradable polyolefin-starch blends, Polymer Degradation and Stability 60(2-3) (1998) 471-480.
[37] X. Ramis, A. Cadenato, J. Salla, J. Morancho, A. Valles, L. Contat, A. Ribes, Thermal degradation of polypropylene/starch-based materials with enhanced biodegradability, Polymer Degradation and Stability 86(3) (2004) 483-491.
[38] J. Morancho, X. Ramis, X. Fernández, A. Cadenato, J. Salla, A. Vallés, L. Contat, A. Ribes, Calorimetric and thermogravimetric studies of UV-irradiated polypropylene/starch-based materials aged in soil, Polymer Degradation and Stability 91(1) (2006) 44-51.
[39] Y. Orhan, J. Hrenovic, H. Buyukgungor, Biodegradation of plastic compost bags under controlled soil conditions, Acta Chimica Slovenica 51(3) (2004) 579-588.
[40] A. Kaushik, R. Kaur, Thermoplastic starch nanocomposites reinforced with cellulose nanocrystals: effect of plasticizer on properties, Composite Interfaces 23(7) (2016) 701-717.
[41] K. Jain, G. Madhu, H. Bhunia, P.K. Bajpai, M.S. Reddy, Kinetics of biodegradation of polypropylene/polylactide blends, Journal of Polymer Materials 31(1) (2014) 63-76.
[42] K. Jain, G. Madhu, H. Bhunia, P.K. Bajpai, G.B. Nando, M.S. Reddy, Physico-mechanical characterization and biodegradability behavior of polypropylene/poly (L-lactide) polymer blends, Journal of Polymer Engineering 35(5) (2015) 407-415.

[43] N.K. Kalita, M.K. Nagar, C. Mudenur, A. Kalamdhad, V. Katiyar, Biodegradation of modified Poly (lactic acid) based biocomposite films under thermophilic composting conditions, Polymer Testing 76 (2019) 522-536.
[44] M. Rutkowska, M. Jastrzębska, H. Janik, Biodegradation of polycaprolactone in sea water, Reactive and Functional Polymers 38(1) (1998) 27-30.
[45] N.K. Kalita, S.M. Bhasney, C. Mudenur, A. Kalamdhad, V. Katiyar, End-of-life evaluation and biodegradation of Poly (lactic acid)(PLA)/Polycaprolactone (PCL)/Microcrystalline cellulose (MCC) polyblends under composting conditions, Chemosphere 247 (2020) 125875.
[46] M. Nevoralová, M. Koutný, A. Ujčić, Z. Starý, J. Šerá, H. Vlková, M. Slouf, I. Fortelný, Z. Krulis, Structure characterization and biodegradation rate of poly (ε-caprolactone)/starch blends, Frontiers in Materials 7 (2020) 141.
[47] D.K. Mandal, H. Bhunia, P.K. Bajpai, C.V. Chaudhari, K.A. Dubey, L. Varshney, A. Kumar, Preparation and characterization of polypropylene/polylactide blends and nanocomposites and their biodegradation study, Journal of Thermoplastic Composite Materials (2019) https://doi.org/10.1177/0892705719850601.
[48] D.K. Mandal, H. Bhunia, P.K. Bajpai, J.P. Kushwaha, C.V. Chaudhari, K.A. Dubey, L. Varshney, Optimization of acrylic acid grafting onto polypropylene using response surface methodology and its biodegradability, Radiation Physics and Chemistry 132 (2017) 71-81.
[49] D.K. Mandal, H. Bhunia, P.K. Bajpai, C. Chaudhari, K. Dubey, L. Varshney, Radiation-induced grafting of acrylic acid onto polypropylene film and its biodegradability, Radiation Physics and Chemistry 123 (2016) 37-45.
[50] R. Headifen, Plastic Waste Solution, http://plasticwastesolutions.com/the-4rs-for-controlling-plastic-waste.
[51] Y. Lu, S. Ozcan, Green nanomaterials: On track for a sustainable future, Nano Today 10(4) (2015) 417-420.
[52] P.L. Kashyap, X. Xiang, P. Heiden, Chitosan nanoparticle based delivery systems for sustainable agriculture, International Journal of Biological Macromolecules 77 (2015) 36-51.
[53] S.M. Bhasney, P. Bhagabati, A. Kumar, V. Katiyar, Morphology and crystalline characteristics of polylactic acid [PLA]/linear low density polyethylene [LLDPE]/microcrystalline cellulose [MCC] fiber composite, Composites Science and Technology 171 (2019) 54-61.
[54] E. Castro-Aguirre, R. Auras, S. Selke, M. Rubino, T. Marsh, Enhancing the biodegradation rate of poly (lactic acid) films and PLA bio-nanocomposites in simulated composting through bioaugmentation, Polymer Degradation and Stability 154 (2018) 46-54.
[55] J. Pospíšil, Z. Horák, Z. Kruliš, S. Nešpůrek, The origin and role of structural inhomogeneities and impurities in material recycling of plastics, Macromolecular Symposia, Wiley Online Library, 1998, pp. 247-263.
[56] L.S. Montagna, M.M.d.C. Forte, R.M.C. Santana, Study on the accelerated biodegradation of PP modified with an organic pro-degradant additive, Journal of Applied Polymer Science 131(22) (2014).
[57] A. Ammala, S. Bateman, K. Dean, E. Petinakis, P. Sangwan, S. Wong, Q. Yuan, L. Yu, C. Patrick, K. Leong, An overview of degradable and biodegradable polyolefins, Progress in Polymer Science 36(8) (2011) 1015-1049.
[58] A. Benítez, J.J. Sánchez, M.L. Arnal, A.J. Müller, O. Rodríguez, G. Morales, Abiotic degradation of LDPE and LLDPE formulated with a pro-oxidant additive, Polymer Degradation and Stability 98(2) (2013) 490-501.
[59] B. Imre, B. Pukánszky, Compatibilization in bio-based and biodegradable polymer blends, European Polymer Journal 49(6) (2013) 1215-1233.
[60] B. Singh, N. Sharma, Mechanistic implications of plastic degradation, Polymer Degradation and Stability 93(3) (2008) 561-584.
[61] B. Fayolle, X. Colin, L. Audouin, J. Verdu, Mechanism of degradation induced embrittlement in polyethylene, Polymer Degradation and Stability 92(2) (2007) 231-238.

[62] M.C. Celina, Review of polymer oxidation and its relationship with materials performance and lifetime prediction, Polymer Degradation and Stability 98(12) (2013) 2419-2429.
[63] K. Rajakumar, V. Sarasvathy, A.T. Chelvan, R. Chitra, C. Vijayakumar, Natural weathering studies of polypropylene, Journal of Polymers and the Environment 17(3) (2009) 191-202.
[64] N.M. Islam, N. Othman, Z. Ahmad, H. Ismail, Effect of pro-degradant additives concentration on aging properties of polypropylene films, Polymer-Plastics Technology and Engineering 49(3) (2010) 272-278.
[65] D.M. Wiles, G. Scott, Polyolefins with controlled environmental degradability, Polymer Degradation and Stability 91(7) (2006) 1581-1592.
[66] T. Ojeda, A. Freitas, K. Birck, E. Dalmolin, R. Jacques, F. Bento, F. Camargo, Degradability of linear polyolefins under natural weathering, Polymer Degradation and Stability 96(4) (2011) 703-707.
[67] S. Nanda, S. Sahu, J. Abraham, Studies on the biodegradation of natural and synthetic polyethylene by Pseudomonas spp, Journal of Applied Sciences and Environmental Management 14(2) (2010) 57-60.
[68] T. Gerard, T. Budtova, Morphology and molten-state rheology of polylactide and polyhydroxyalkanoate blends, European Polymer Journal 48(6) (2012) 1110-1117.
[69] E. Corradini, L. Mattoso, C. Guedes, D. Rosa, Mechanical, thermal and morphological properties of poly (ε-caprolactone)/zein blends, Polymers for Advanced Technologies 15(6) (2004) 340-345.
[70] D. Briassoulis, The effects of tensile stress and the agrochemical Vapam on the ageing of low density polyethylene (LDPE) agricultural films. Part I. Mechanical behaviour, Polymer Degradation and Stability 88(3) (2005) 489-503.
[71] W.K. Busfield, P. Taba, Photo-oxidative degradation of mechanically stressed polyolefins, Polymer Degradation and Stability 51(2) (1996) 185-196.
[72] Y. Kodama, N.B. Lima, L.D. Machado, K. Nakayama, Investigation of gamma irradiated PCL/PLLA blend by wide-angle x-ray diffraction, International Nuclear Atlantic Conference (2014).
[73] H.J. Jeon, M.N. Kim, Isolation of mesophilic bacterium for biodegradation of polypropylene, International Biodeterioration & Biodegradation 115 (2016) 244-249.
[74] M. Dziadek, E. Stodolak-Zych, K. Cholewa-Kowalska, Biodegradable ceramic-polymer composites for biomedical applications: a review, Materials Science and Engineering: C 71 (2017) 1175-1191.
[75] D.P. Komilis, A kinetic analysis of solid waste composting at optimal conditions, Waste Management 26(1) (2006) 82-91.
[76] Y. Zheng, E.K. Yanful, A.S. Bassi, A review of plastic waste biodegradation, Critical Reviews in Biotechnology 25(4) (2005) 243-250.
[77] S. Mallakpour, K. Banihassan, M.R. Sabzalian, Novel bioactive chiral poly (amide–imide) s containing different amino acids linkages: studies on synthesis, characterization and biodegradability, Journal of Polymers and the Environment 21(2) (2013) 568-574.
[78] M.A. Bardi, M.M. Munhoz, R.A. Auras, L.D. Machado, Assessment of UV exposure and aerobic biodegradation of poly (butylene adipate-co-terephthalate)/starch blend films coated with radiation-curable print inks containing degradation-promoting additives, Industrial Crops and Products 60 (2014) 326-334.
[79] OCED 208. Terrestial plant growth test. OECD guidelines for testing of chemicals (1984).
[80] P. Gong, B.-M. Wilke, E. Strozzi, S. Fleischmann, Evaluation and refinement of a continuous seed germination and early seedling growth test for the use in the ecotoxicological assessment of soils, Chemosphere 44(3) (2001) 491-500.
[81] P. Maiti, C.A. Batt, E.P. Giannelis, Biodegradable polyester/layered silicate nanocomposites, MRS Online Proceedings Library Archive 740 (2002).
[82] M. Rani, A. Agarwal, Y.S. Negi, Chitosan based hydrogel polymeric beads–As drug delivery system, BioResources 5(4) (2010) 2765-2807.
[83] G. Scott, D.M. Wiles, Programmed-life plastics from polyolefins: a new look at sustainability, Biomacromolecules 2(3) (2001) 615-622.

[84] D.K. Mandal, H. Bhunia, P.K. Bajpai, C.V. Chaudhari, K.A. Dubey, L. Varshney, Morphology, rheology and biodegradation of oxo-degradable polypropylene/polylactide blends, Journal of Polymer Engineering 38(3) (2018) 239-249.
[85] D. Chiaramonti, Bioethanol: role and production technologies, Improvement of crop plants for industrial end uses, Springer 2007, pp. 209-251.
[86] A. Rani, S. Monga, M. Bansal, A. Sharma, Bionanocomposites reinforced with cellulose nanofibers derived from sugarcane bagasse, Polymer Composites 39 (2018) 55-64.
[87] M. Bansal, D. Kumar, G.S. Chauhan, A. Kaushik, Preparation, characterization and trifluralin degradation of laccase-modified cellulose nanofibers, Materials Science for Energy Technologies 1(1) (2018) 29-37.
[88] H. Kaczmarek, D. Ołdak, P. Malanowski, H. Chaberska, Effect of short wavelength UV-irradiation on ageing of polypropylene/cellulose compositions, Polymer Degradation and Stability 88(2) (2005) 189-198.
[89] G. Wang, S. Li, Y. Feng, Y. Hu, G. Zhao, W. Jiang, Effectively toughening polypropylene with in situ formation of core-shell starch-based particles, Carbohydrate Polymers 249 (2020) 116795.
[90] L. Avérous, C. Fringant, L. Moro, Plasticized starch–cellulose interactions in polysaccharide composites, Polymer 42(15) (2001) 6565-6572.
[91] S. Pokhrel, A review on introduction and applications of starch and its biodegradable polymers, International Journal of Environment 4(4) (2015) 114-125.
[92] L. Yu, K. Dean, L. Li, Polymer blends and composites from renewable resources, Progress in Polymer Science 31(6) (2006) 576-602.
[93] S. Joseph, J.T. Howarth, Waterproof plastic films of increased water vapor permeability and method of making them, Google Patents, 1964.
[94] S.M. Al-Salem, B.K. Sharma, A.R. Khan, J.C. Arnold, S.M. Alston, S.R. Chandrasekaran, A.T. Al-Dhafeeri, Thermal degradation kinetics of virgin polypropylene (PP) and PP with starch blends exposed to natural weathering, Industrial & Engineering Chemistry Research 56(18) (2017) 5210-5220.
[95] A. Saffar, P.J. Carreau, A. Ajji, M.R. Kamal, Development of polypropylene microporous hydrophilic membranes by blending with PP-g-MA and PP-g-AA, Journal of Membrane Science 462 (2014) 50-61.
[96] H. Obasi, I. Igwe, Effects of native cassava starch and compatibilizer on biodegradable and tensile properties of polypropylene, American Journal Engineering Research 3(2) (2014) 96-104.
[97] S.S. Ray, M. Okamoto, Biodegradable polylactide and its nanocomposites: opening a new dimension for plastics and composites, Macromolecular Rapid Communications 24(14) (2003) 815-840.
[98] O. Martin, L. Averous, Poly (lactic acid): plasticization and properties of biodegradable multiphase systems, Polymer 42(14) (2001) 6209-6219.
[99] R. Mehta, V. Kumar, H. Bhunia, S. Upadhyay, Synthesis of poly (lactic acid): a review, Journal of Macromolecular Science, Part C: Polymer Reviews 45(4) (2005) 325-349.
[100] R. Datta, M. Henry, Lactic acid: recent advances in products, processes and technologies—a review, Journal of Chemical Technology and Biotechnology 81(7) (2006) 1119-1129.
[101] S. Saeidlou, M.A. Huneault, H. Li, C.B. Park, Poly (lactic acid) crystallization, Progress in Polymer Science 37(12) (2012) 1657-1677.
[102] M.A. Abdelwahab, A. Flynn, B.-S. Chiou, S. Imam, W. Orts, E. Chiellini, Thermal, mechanical and morphological characterization of plasticized PLA–PHB blends, Polymer Degradation and Stability 97(9) (2012) 1822-1828.
[103] A. Södergård, M. Stolt, Industrial production of high molecular weight poly (lactic acid), In: Poly (Lactic Acid): Synthesis, Structures, Properties, Processing, and Applications (2010) pp. 27-41.
[104] N. Reddy, D. Nama, Y. Yang, Polylactic acid/polypropylene polyblend fibers for better resistance to degradation, Polymer Degradation and Stability 93(1) (2008) 233-241.
[105] K. Hamad, M. Kaseem, F. Deri, Rheological and mechanical characterization of poly (lactic acid)/polypropylene polymer blends, Journal of Polymer Research 18(6) (2011) 1799-1806.

[106] H. Rokbani, A. Ajji, Rheological Properties of Poly (lactic acid) Solutions Added with Metal Oxide Nanoparticles for Electrospinning, Journal of Polymers and the Environment 26(6) (2018) 2555-2565.
[107] H. Ebadi-Dehaghani, H.A. Khonakdar, M. Barikani, S.H. Jafari, Experimental and theoretical analyses of mechanical properties of PP/PLA/clay nanocomposites, Composites Part B: Engineering 69 (2015) 133-144.
[108] S.M. Bhasney, A. Kumar, V. Katiyar, Microcrystalline cellulose, polylactic acid and polypropylene biocomposites and its morphological, mechanical, thermal and rheological properties, Composites Part B: Engineering 184 (2020) 107717.
[109] N. Ploypetchara, P. Suppakul, D. Atong, C. Pechyen, Blend of polypropylene/poly (lactic acid) for medical packaging application: physicochemical, thermal, mechanical, and barrier properties, Energy Procedia 56 (2014) 201-210.
[110] P. Choudhary, S. Mohanty, S.K. Nayak, L. Unnikrishnan, Poly (L-lactide)/polypropylene blends: Evaluation of mechanical, thermal, and morphological characteristics, Journal of Applied Polymer Science 121(6) (2011) 3223-3237.
[111] T.W. Yoo, H.G. Yoon, S.J. Choi, M.S. Kim, Y.H. Kim, W.N. Kim, Effects of compatibilizers on the mechanical properties and interfacial tension of polypropylene and poly (lactic acid) blends, Macromolecular Research 18(6) (2010) 583-588.
[112] C. Vasile, R.N. Darie, C.N. Cheaburu-Yilmaz, G.-M. Pricope, M. Bračič, D. Pamfil, G.E. Hitruc, D. Duraccio, Low density polyethylene–chitosan composites, Composites Part B: Engineering 55 (2013) 314-323.
[113] A. Martínez-Camacho, M. Cortez-Rocha, A. Graciano-Verdugo, F. Rodríguez-Félix, M. Castillo-Ortega, A. Burgos-Hernández, J. Ezquerra-Brauer, M. Plascencia-Jatomea, Extruded films of blended chitosan, low density polyethylene and ethylene acrylic acid, Carbohydrate Polymers 91(2) (2013) 666-674.
[114] M. Kurek, C.-H. Brachais, C.M. Nguimjeu, A. Bonnotte, A. Voilley, K. Galić, J.-P. Couvercelle, F. Debeaufort, Structure and thermal properties of a chitosan coated polyethylene bilayer film, Polymer Degradation and Stability 97(8) (2012) 1232-1240.
[115] S. Ghosh, R. Chowdhury, P. Bhattacharya, Sustainability of cereal straws for the fermentative production of second generation biofuels: a review of the efficiency and economics of biochemical pretreatment processes, Applied Energy 198 (2017) 284-298.
[116] A. Bhowmick, S.L. Banerjee, N. Pramanik, P. Jana, T. Mitra, A. Gnanamani, M. Das, P.P. Kundu, Organically modified clay supported chitosan/hydroxyapatite-zinc oxide nanocomposites with enhanced mechanical and biological properties for the application in bone tissue engineering, International Journal of Biological Macromolecules 106 (2018) 11-19.
[117] A.R. Deshmukh, H. Aloui, C. Khomlaem, A. Negi, J.-H. Yun, H.-S. Kim, B.S. Kim, Biodegradable films based on chitosan and defatted Chlorella biomass: Functional and physical characterization, Food Chemistry 337 (1) (2020) 127777.
[118] A.R. Deshmukh, B.S. Kim, Chitosan-Vitamin C Nanoparticles, Korean Society for Biotechnology and Bioengineering Journal 34(4) (2019) 221-232.
[119] F. Amri, S. Husseinsyah, K. Hussin, Mechanical, morphological and thermal properties of chitosan filled polypropylene composites: The effect of binary modifying agents, Composites Part A: Applied Science and Manufacturing 46 (2013) 89-95.
[120] M. Sunilkumar, T. Francis, E.T. Thachil, A. Sujith, Low density polyethylene–chitosan composites: a study based on biodegradation, Chemical Engineering Journal 204 (2012) 114-124.
[121] D. Rosa, D. Grillo, M. Bardi, M. Calil, C. Guedes, E. Ramires, E. Frollini, Mechanical, thermal and morphological characterization of polypropylene/biodegradable polyester blends with additives, Polymer Testing 28(8) (2009) 836-842.
[122] D.K. Mandal, H. Bhunia, P.K. Bajpai, Thermal degradation kinetics of oxo-degradable PP/PLA blends, Journal of Polymer Engineering 39(1) (2019) 58-67.

[123] B. Liu, L. Jiang, H. Liu, J. Zhang, Synergetic effect of dual compatibilizers on in situ formed poly (lactic acid)/soy protein composites, Industrial & Engineering Chemistry Research 49(14) (2010) 6399-6406.
[124] S. Soni, H. Gupta, N. Kumar, D.K. Nishad, G. Mittal, A. Bhatnagar, Biodegradable Biomaterials, Recent Patents on Biomedical Engineering 3(1) (2010) 30-40.
[125] G. González-Hernández, V.H. Pino-Ramos, L. Islas, C. Alvarez-Lorenzo, A. Concheiro, E. Bucio, Radiation-grafting of N-vinylcaprolactam and 2-hydroxyethyl methacrylate onto polypropylene films to obtain a thermo-responsive drug delivery system, Radiation Physics and Chemistry 157 (2019) 6-14.
[126] M.M. Nasef, E.-S.A. Hegazy, Preparation and applications of ion exchange membranes by radiation-induced graft copolymerization of polar monomers onto non-polar films, Progress in Polymer Science 29(6) (2004) 499-561.
[127] D.K. Mandal, H. Bhunia, P.K. Bajpai, V.K. Bhalla, Thermal degradation kinetics and estimation of lifetime of radiation grafted polypropylene films, Radiation Physics and Chemistry 136 (2017) 1-8.
[128] V. Nikolic, S. Velickovic, A. Popovic, Biodegradation of polystyrene-graft-starch copolymers in three different types of soil, Environmental Science and Pollution Research 21(16) (2014) 9877-9886.
[129] M. Barsbay, O. Güven, Surface modification of cellulose via conventional and controlled radiation-induced grafting, Radiation Physics and Chemistry 160 (2019) 1-8.
[130] C. Chaudhari, K. Dubey, N. Goel, Y. Bhardwaj, L. Varshney, Correlation between surface energy and uptake behavior of radiation-grafted methacrylic acid-g-LDPE, Polymer Bulletin 69(7) (2012) 779-793.
[131] J.F. Madrid, L.V. Abad, Modification of microcrystalline cellulose by gamma radiation-induced grafting, Radiation Physics and Chemistry 115 (2015) 143-147.
[132] O.H. Kwon, Y.C. Nho, Radiation induced graft polymerization of methyl methacrylate onto ultrahigh molecular weight polyethylene in the presence of a metallic salt and acid, Journal of Applied Polymer Science 86(9) (2002) 2348-2356.
[133] J. Zhao, G. Geuskens, Surface modification of polymers VI. Thermal and radiochemical grafting of acrylamide on polyethylene and polystyrene, European Polymer Journal 35(12) (1999) 2115-2123.
[134] R. Guan, Study on compatibility of PP–STC blends functionalized by ultraviolet irradiation, Journal of Applied Polymer Science 77(1) (2000) 96-103.
[135] L. Wojnárovits, C.M. Földváry, E. Takács, Radiation-induced grafting of cellulose for adsorption of hazardous water pollutants: A review, Radiation Physics and Chemistry 79(8) (2010) 848-862.
[136] S.-H. Choi, Y.C. Nho, Radiation-Induced Graft Copolymerization of Mixture of Acrylic Acind and Acrylonitrile onto Polypropylene Film, Korea Polymer Journal 6(4) (1998) 287-294.
[137] G. Acik, C. Altinkok, M.A. Tasdelen, Synthesis and characterization of polypropylene-graft-poly (l-lactide) copolymers by CuAAC click chemistry, Journal of Polymer Science Part A: Polymer Chemistry 56(22) (2018) 2595-2601.
[138] I. Kaur, N. Gupta, V. Kumari, Swelling, ion uptake and biodegradation studies of PE film modified through radiation induced graft copolymerization, Radiation Physics and Chemistry 80(9) (2011) 947-956.
[139] M. Raj, R. Savaliya, S. Joshi, L. Raj, H. Keharia, Biodegradability, thermal, chemical, mechanical and morphological behavior of LDPE/pectin and LDPE/modified pectin blend, Polymer Bulletin 76(10) (2019) 5173-5195.
[140] N.A. Rosli, I. Ahmad, F.H. Anuar, I. Abdullah, Application of polymethylmethacrylate-grafted cellulose as reinforcement for compatibilised polylactic acid/natural rubber blends, Carbohydrate Polymers 213 (2019) 50-58.
[141] K. Sharma, V. Kumar, B. Kaith, V. Kumar, S. Som, S. Kalia, H. Swart, Synthesis, characterization and water retention study of biodegradable Gum ghatti-poly (acrylic acid–aniline) hydrogels, Polymer Degradation and Stability 111 (2015) 20-31.

[142] D.K. Mandal, H. Bhunia, P.K. Bajpai, K.A. Dubey, L. Varshney, G. Madhu, Thermo-oxidative degradation kinetics of grafted polypropylene films, Radiation Effects and Defects in Solids 172(11-12) (2017) 878-895.
[143] J. Bandyopadhyay, A. Maity, B.B. Khatua, S.S. Ray, Thermal and rheological properties of biodegradable poly [(butylene succinate)-co-adipate] nanocomposites, Journal of Nanoscience and Nanotechnology 10(7) (2010) 4184-4195.
[144] P.H. Nam, P. Maiti, M. Okamoto, T. Kotaka, N. Hasegawa, A. Usuki, A hierarchical structure and properties of intercalated polypropylene/clay nanocomposites, Polymer 42(23) (2001) 9633-9640.
[145] H.Z. Tabari, A. Nourbakhsh, A. Ashori, Effects of nanoclay and coupling agent on the physico-mechanical, morphological, and thermal properties of wood flour/polypropylene composites, Polymer Engineering & Science 51(2) (2011) 272-277.
[146] N.T. Dintcheva, S. Al-Malaika, F.P. La Mantia, Effect of extrusion and photo-oxidation on polyethylene/clay nanocomposites, Polymer Degradation and Stability 94(9) (2009) 1571-1588.
[147] Y. Katoh, M. Okamoto, Crystallization controlled by layered silicates in nylon 6–clay nano-composite, Polymer 50(19) (2009) 4718-4726.
[148] T.D. Hapuarachchi, T. Peijs, E. Bilotti, Thermal degradation and flammability behavior of polypropylene/clay/carbon nanotube composite systems, Polymers for Advanced Technologies 24(3) (2013) 331-338.
[149] T. Kumanayaka, R. Parthasarathy, M. Jollands, Accelerating effect of montmorillonite on oxidative degradation of polyethylene nanocomposites, Polymer Degradation and Stability 95(4) (2010) 672-676.
[150] F.B. Dhieb, E.J. Dil, S.H. Tabatabaei, F. Mighri, A. Ajji, Effect of nanoclay orientation on oxygen barrier properties of LbL nanocomposite coated films, RSC Advances 9(3) (2019) 1632-1641.
[151] S. Kumar, P. Maiti, Controlled biodegradation of polymers using nanoparticles and its application, RSC Advances 6(72) (2016) 67449-67480.
[152] F. Bensaad, N. Belhaneche-Bensemra, Effects of calcium stearate as pro-oxidant agent on the natural aging of polypropylene, Journal of Polymer Engineering 38(8) (2018) 715-721.
[153] S. Fontanella, S. Bonhomme, J.-M. Brusson, S. Pitteri, G. Samuel, G. Pichon, J. Lacoste, D. Fromageot, J. Lemaire, A.-M. Delort, Comparison of biodegradability of various polypropylene films containing pro-oxidant additives based on Mn, Mn/Fe or Co, Polymer Degradation and Stability 98(4) (2013) 875-884.
[154] L. Contat-Rodrigo, Thermal characterization of the oxo-degradation of polypropylene containing a pro-oxidant/pro-degradant additive, Polymer Degradation and Stability 98(11) (2013) 2117-2124.
[155] A. Arkatkar, J. Arutchelvi, M. Sudhakar, S. Bhaduri, P.V. Uppara, M. Doble, Approaches to enhance the biodegradation of polyolefins, The Open Environmental Engineering Journal 2(1) (2009) 68-80.
[156] F.J. Arráez, M.L. Arnal, A.J. Müller, Thermal and UV degradation of polypropylene with pro-oxidant. Abiotic characterization, Journal of Applied Polymer Science 135(14) (2018) 46088.
[157] A. Santhoskumar, K. Palanivelu, A new additive formulation to enhance photo and biodegradation characteristics of polypropylene, International Journal of Polymeric Materials 61(10) (2012) 793-808.
[158] A. Arkatkar, J. Arutchelvi, S. Bhaduri, P.V. Uppara, M. Doble, Degradation of unpretreated and thermally pretreated polypropylene by soil consortia, International Biodeterioration & Biodegradation 63(1) (2009) 106-111.
[159] M. Sudhakar, M. Doble, P.S. Murthy, R. Venkatesan, Marine microbe-mediated biodegradation of low-and high-density polyethylenes, International Biodeterioration & Biodegradation 61(3) (2008) 203-213.
[160] F. Hayoune, S. Chelouche, D. Trache, S. Zitouni, Y. Grohens, Thermal decomposition kinetics and lifetime prediction of a PP/PLA blend supplemented with iron stearate during artificial aging, Thermochimica Acta 690 (2020) 178700.
[161] A.C. Albertsson, C. Barenstedt, S. Karlsson, Abiotic degradation products from enhanced environmentally degradable polyethylene, Acta Polymerica 45(2) (1994) 97-103.

[162] A.C. Albertsson, S. Karlsson, Degradable polymers for the future, Acta Polymerica 46(2) (1995) 114-123.
[163] M.C. Antunes, J.A. Agnelli, A.S. Babetto, B.C. Bonse, S.H. Bettini, Correlating different techniques in the thermooxidative degradation monitoring of high-density polyethylene containing pro-degradant and antioxidants, Polymer Testing 69 (2018) 182-187.
[164] C. Marcela, S. Alex, C. Baltus, H. SÃlvia, Abiotic thermo-oxidative degradation of high density polyethylene: Effect of manganese stearate concentration, Polymer Degradation and Stability 143 (2017) 95-103.
[165] D.K. Mandal, H. Bhunia, P.K. Bajpai, A. Kumar, G. Madhu, G.B. Nando, Biodegradation of Pro-oxidant Filled Polypropylene Films and Evaluation of the Ecotoxicological Impact, Journal of Polymers and the Environment 26(3) (2018) 1061-1071.
[166] P.K. Roy, M. Hakkarainen, A.-C. Albertsson, Exploring the biodegradation potential of polyethylene through a simple chemical test method, Journal of Polymers and the Environment 22(1) (2014) 69-77.
[167] L.S. Montagna, M.M. da Camargo Forte, R.M.C. Santana, Induced degradation of polypropylene with an organic pro-degradant additive, Journal of Materials Science and Engineering. A 3(2A) (2013) 123.
[168] P. Roy, P. Surekha, C. Rajagopal, V. Choudhary, Thermal degradation studies of LDPE containing cobalt stearate as pro-oxidant, Express Polymer Letters 1(4) (2007) 208-216.
[169] B. Suresh, S. Maruthamuthu, A. Khare, N. Palanisamy, V. Muralidharan, R. Ragunathan, M. Kannan, K.N. Pandiyaraj, Influence of thermal oxidation on surface and thermo-mechanical properties of polyethylene, Journal of Polymer Research 18(6) (2011) 2175-2184.
[170] S. Fontanella, S. Bonhomme, M. Koutny, L. Husarova, J.-M. Brusson, J.-P. Courdavault, S. Pitteri, G. Samuel, G. Pichon, J. Lemaire, Comparison of the biodegradability of various polyethylene films containing pro-oxidant additives, Polymer Degradation and Stability 95(6) (2010) 1011-1021.
[171] M. Koutný, T. Václavková, L. Matisová-Rychlá, J. Rychlý, Characterization of oxidation progress by chemiluminescence: A study of polyethylene with pro-oxidant additives, Polymer Degradation and Stability 93(8) (2008) 1515-1519.
[172] L.S. Montagna, A.L. Catto, M.M. de Camargo Forte, E. Chiellini, A. Corti, A. Morelli, R.M.C. Santana, Comparative assessment of degradation in aqueous medium of polypropylene films doped with transition metal free (experimental) and transition metal containing (commercial) pro-oxidant/pro-degradant additives after exposure to controlled UV radiation, Polymer Degradation and Stability 120 (2015) 186-192.
[173] M. Hakkarainen, A.-C. Albertsson, S. Karlsson, Weight losses and molecular weight changes correlated with the evolution of hydroxyacids in simulated in vivo degradation of homo-and copolymers of PLA and PGA, Polymer Degradation and Stability 52(3) (1996) 283-291.
[174] J. Šerá, L. Serbruyns, B. De Wilde, M. Koutný, Accelerated biodegradation testing of slowly degradable polyesters in soil, Polymer Degradation and Stability 171 (2019) 109031.
[175] J. Arutchelvi, M. Sudhakar, A. Arkatkar, M. Doble, S. Bhaduri, P.V. Uppara, Biodegradation of polyethylene and polypropylene, Indian Journal of Biotechnology 7(1) (2008) 9-22.
[176] C.L. D. Carvalho, A.F. Silveira, D. dos Santos Rosa, A study of the controlled degradation of polypropylene containing pro-oxidant agents, SpringerPlus 2(1) (2013) 623.
[177] L. Montagna, A.L. Catto, M.M. Forte, R.M. Santana, Biodegradation of PP films modified with organic pro-degradant: Natural ageing and biodegradation in soil in respirometric test, Polyolefins Journal 3(1) (2016) 59-68.
[178] K. Trongtorsak, P. Supaphol, S. Tantayanon, Effect of calcium stearate and pimelic acid addition on mechanical properties of heterophasic isotactic polypropylene/ethylene–propylene rubber blend, Polymer Testing 23(5) (2004) 533-539.
[179] C. de Carvalho, D. Rosa, Thermal oxidative degradation of polypropylene-containing pro-oxidants, Journal of Thermal Analysis and Calorimetry 115(2) (2014) 1627-1632.

[180] T. Muthukumar, A. Aravinthan, D. Mukesh, Effect of environment on the degradation of starch and pro-oxidant blended polyolefins, Polymer Degradation and Stability 95(10) (2010) 1988-1993.
[181] D. Rosa, M. Bardi, L. Machado, D. Dias, L. Silva, Y. Kodama, Starch plasticized with glycerol from biodiesel and polypropylene blends: mechanical and thermal properties, Journal of Thermal Analysis and Calorimetry 102(1) (2010) 181-186.
[182] M. Sedničková, S. Pekařová, P. Kucharczyk, J. Bočkaj, I. Janigová, A. Kleinová, D. Jochec-Mošková, L. Omaníková, D. Perďochová, M. Koutný, Changes of physical properties of PLA-based blends during early stage of biodegradation in compost, International Journal of Biological Macromolecules 113 (2018) 434-442.
[183] D.P. Komilis, R.K. Ham, A laboratory method to investigate gaseous emissions and solids decomposition during composting of municipal solid wastes, Compost Science & Utilization 8(3) (2000) 254-265.
[184] P. Stloukal, S. Pekařová, A. Kalendova, H. Mattausch, S. Laske, C. Holzer, L. Chitu, S. Bodner, G. Maier, M. Slouf, Kinetics and mechanism of the biodegradation of PLA/clay nanocomposites during thermophilic phase of composting process, Waste Management 42 (2015) 31-40.
[185] P. Stloukal, A. Kalendová, H. Mattausch, S. Laske, C. Holzer, M. Koutny, The influence of a hydrolysis-inhibiting additive on the degradation and biodegradation of PLA and its nanocomposites, Polymer Testing 41 (2015) 124-132.
[186] P. Stloukal, G. Jandíková, M. Koutny, V. Sedlařík, Carbodiimide additive to control hydrolytic stability and biodegradability of PLA, Polymer Testing 54 (2016) 19-28.
[187] P. Stloukal, P. Kucharczyk, Acceleration of polylactide degradation under biotic and abiotic conditions through utilization of a new, experimental, highly compatible additive, Polymer Degradation and Stability 142 (2017) 217-225.
[188] S. Mallakpour, M. Dehghani, M.R. Sabzalian, Green step-grow polymerization of biodegradable amino acid based diacids with 3, 5-diamino-N-(thiazole-2-yl) benzamide: characterization and study on bioactivity, Journal of Polymer Research 20(2) (2013) 1-6.
[189] M.P. Das, S. Kumar, Comparative study of germination rate and plant growth by secondary metabolites and in vitro LDPE biodegraded fragments by microbes, International Journal of Pharmaceutical Sciences Review & Research 21(2) (2013) 134-136.
[190] S. Mallakpour, F. Zeraatpisheh, M.R. Sabzalian, Biological activity of the nanostructure poly (ester-imide) s containing a tyrosine-based diol: wheat seedling growth and fungal biodegradation, Polymer-Plastics Technology and Engineering 53(5) (2014) 459-464.
[191] S. Mallakpour, M.R. Sabzalian, In vitro degradation assessment of optically active poly (urethane-imide) s based on α-amino acids, Polymer Bulletin 70(12) (2013) 3425-3441.
[192] A.S. Jarvis, V.A. McFarland, M.E. Honeycutt, Assessment of the effectiveness of composting for the reduction of toxicity and mutagenicity of explosive-contaminated soil, Ecotoxicology and Environmental Safety 39(2) (1998) 131-135.
[193] V. Ducrocq, P. Pandard, S. Hallier-Soulier, E. Thybaud, N. Truffaut, The use of quantitative PCR, plant and earthworm bioassays, plating and chemical analysis to monitor 4-chlorobiphenyl biodegradation in soil microcosms, Applied Soil Ecology 12(1) (1999) 15-27.
[194] C.L. Potter, J.A. Glaser, L.W. Chang, J.R. Meier, M.A. Dosani, R.F. Herrmann, Degradation of polynuclear aromatic hydrocarbons under bench-scale compost conditions, Environmental Science & Technology 33(10) (1999) 1717-1725.
[195] P. Rychter, R. Biczak, B. Herman, A. Smylla, P. Kurcok, G. Adamus, M. Kowalczuk, Environmental degradation of polyester blends containing atactic poly (3-hydroxybutyrate). Biodegradation in soil and ecotoxicological impact, Biomacromolecules 7(11) (2006) 3125-3131.
[196] L. Martin-Closas, R. Botet, A. Pelacho, An in vitro crop plant ecotoxicity test for agricultural bioplastic constituents, Polymer Degradation and Stability 108 (2014) 250-256.
[197] I.O.C.L. Ltd., https://propel.indianoil.in/ProductGradeInfo/1030FG.pdf, Product Technical Data Sheet (1030 FG pdf) (2018) Accessed 15 March, 2020.

[198] L.S.G. Clesceri, A.E.; Trussell, R.R., (Eds.) Standard methods for the examination of water and wastewater; American Public Health Association (APHA), American Water Works Association (AWWA), Water Pollution Control Federation (WPCF), 17th Ed., Washington, DC1989.
[199] G. Singh, N. Kaur, H. Bhunia, P.K. Bajpai, U.K. Mandal, Degradation behaviors of linear low-density polyethylene and poly (L-lactic acid) blends, Journal of Applied Polymer Science 124(3) (2012) 1993-1998.
[200] ASTM D 4329-05. Standard practice for fluorescent uv exposure of plastics, West Conshohocken, 2005.
[201] N. Anjum, B. Gupta, A.M. Riquet, Surface designing of polypropylene by critical monitoring of the grafting conditions: Structural investigations, Journal of Applied Polymer Science 101(1) (2006) 772-778.
[202] N.M. Moo-Tun, A. Valadez-González, J.A. Uribe-Calderon, Thermo-oxidative aging of low density polyethylene blown films in presence of cellulose nanocrystals and a pro-oxidant additive, Polymer Bulletin 75(7) (2018) 3149-3169.
[203] M. Salomez, M. George, P. Fabre, F. Touchaleaume, G. Cesar, A. Lajarrige, E. Gastaldi, A comparative study of degradation mechanisms of PBSA and PHBV under laboratory-scale composting conditions, Polymer Degradation and Stability 167 (2019) 102-113.
[204] ASTM D4338-15. Standard test method for determining aerobic biodegradation of plastic materials under controlled composting conditions, incorporating thermophilic temperatures, (2011).
[205] I. Petric, V. Selimbašić, Development and validation of mathematical model for aerobic composting process, Chemical Engineering Journal 139(2) (2008) 304-317.
[206] G. Madhu, H. Bhunia, P.K. Bajpai, G.B. Nando, Physico-mechanical properties and biodegradation of oxo-degradable HDPE/PLA blends, Polymer Science Series A 58(1) (2016) 57-75.
[207] C. Narayan, G. Madhu Dr, K. Ms, B. Diksha, Evaluation of biodegradability characteristics of cellulose-based film as per IS/ISO 14855-1, Journal of Applied Packaging Research 11(3) (2019) 2.
[208] S. Ahuja, R.K. Arya, Laplace transform treatment for chemical engineering systems: whether to use 0− or 0+, Chemical Engineering & Technology 41(4) (2018) 875-882.
[209] S. Ahuja, Discontinuity analysis for the treatment of nonlinear lumped-parameter systems for singular inputs, Theoretical Foundations of Chemical Engineering 49(5) (2015) 612-621.
[210] S. Ahuja, R.K. Arya, Comparison of the performances of different reduced forms of a condenser model, Chemical Engineering & Technology 40(9) (2017) 1630-1637.
[211] OCED 207. Earthworm acute toxicity test, OECD guideline for testing chemicals (1984).
[212] M. Sudhakar, A. Trishul, M. Doble, K.S. Kumar, S.S. Jahan, D. Inbakandan, R. Viduthalai, V. Umadevi, P.S. Murthy, R. Venkatesan, Biofouling and biodegradation of polyolefins in ocean waters, Polymer Degradation and Stability 92(9) (2007) 1743-1752.
[213] G. Fechine, D. Rosa, M. Rezende, N. Demarquette, Effect of UV radiation and pro-oxidant on PP biodegradability, Polymer Engineering & Science 49(1) (2009) 123-128.
[214] N.Z.M. Islam, N. Othman, Z. Ahmad, Z. Ismail, Effect of pro-degradant additive on photo-oxidative aging of polypropylene film, Sains Malaysiana 40(7) (2011) 803-808.
[215] R.N. Darie, R. Bodirlau, C.A. Teaca, J. Macyszyn, M. Kozlowski, I. Spiridon, Influence of accelerated weathering on the properties of polypropylene/polylactic acid/eucalyptus wood composites, International Journal of Polymer Analysis and Characterization 18(4) (2013) 315-327.
[216] W. Liu, B. Liu, X. Wang, Morphology, rheological properties, and crystallization behavior of polypropylene/clay nanocomposites, International Journal of Polymeric Materials 62(3) (2013) 164-171.
[217] A. Constantinou, A. Antelava, A. Bumajdad, G. Manos, R. Dewil, S. Al-Salem, Identification of commercial oxo-biodegradable plastics: Study of UV induced degradation in an effort 1 to combat plastic waste accumulation, Journal of Polymers and the Environment 28 (2020) 2364-2376.
[218] S. Ahuja, D. Singh, A Kinetic model of alkali catalyzed phenol-furfural novalac resinification, Polymers & Polymer Composites 19(7) (2011) 581-586.

[219] A. Constantinou, A. Antelava, A. Bumajdad, G. Manos, R. Dewil, S. Al-Salem, Identification of Commercial Oxo-Biodegradable Plastics: Study of UV Induced Degradation in an Effort 1 to Combat Plastic Waste Accumulation, Journal of Polymers and the Environment 28 (2020).
[220] M.P. Das, S. Kumar, Comparative study of germination rate and plant growth by secondary metabolites and in vitro LDPE biodegraded fragments by microbes, International Journal Pharmaceutical Science Review Research 21(2) (2013) 134-136.
[221] J. Pablos, C. Abrusci, I. Marín, J. López-Marín, F. Catalina, E. Espí, T. Corrales, Photodegradation of polyethylenes: Comparative effect of Fe and Ca-stearates as pro-oxidant additives, Polymer Degradation and Stability 95(10) (2010) 2057-2064.
[222] V. Sugumaran, H. Bhunia, A.K. Narula, Evaluation of biodegradability of potato peel powder based polyolefin biocomposites, Journal of Polymers and the Environment 26(5) (2018) 2049-2060.
[223] M. El-Arnaouty, A. Abdel Ghaffar, H. El Shafey, Radiation-induced graft copolymerization of acrylic acid/acrylonitrile onto LDPE and PET films and its biodegradability, Journal of Applied Polymer Science 107(2) (2008) 744-754.
[224] H. Marschner, Functions of mineral nutrients: Macronutrients mineral nutrition of higher plants, 2nd ed., Academic Press: UK, 1995 pp. 299-312.

Publications

I In Peer Reviewed (SCI) Journals

1.1 Publications Related to Ph.D. Work

1. **Sunil Sable**, Sanjeev Ahuja, and Haripada Bhunia "Studies on biodegradability of cobalt stearate filled polypropylene after abiotic treatment" *Journal of Polymers and the Environment*. 2020, 28:2236-2252 (Impact Factor: 2.572).

2. **Sunil Sable**, Sanjeev Ahuja, and Haripada Bhunia "Effect of pro-oxidant concentration on characteristics of packaging films of cobalt stearate filled polypropylene" *Journal of Polymer Engineering*. 2020, 40(8):637-64 (Impact Factor: 1.126).

3. **Sunil Sable**, Sanjeev Ahuja, and Haripada Bhunia "Preparation and characterization of oxo-degradable polypropylene composites containing a modified pro-oxidant" *Journal of Polymers and the Environment*. 2021, 29 (3):721-733 (Impact Factor: 2.572).

4. **Sunil Sable**, Sanjeev Ahuja, and Haripada Bhunia "Biodegradation kinetic modeling of pro-oxidant filled polypropylene composites during thermophilic phase of aerobic composting after abiotic treatment" *Environmental Science and Pollution Research*, 2021, (https://doi.org/10.1007/s11356-020-11766-0) (Impact Factor: 3.052).

1.2 Other Publications in the Related Area

1. **Sunil Sable**, Dev K. Mandal, Sanjeev Ahuja, and Haripada Bhunia "Biodegradation kinetic modelling of PP/PLA blends and composites under controlled composting conditions" *Journal of Environmental Management*. 2019, 249,109186 (Impact Factor: 5.647).

2. **Sunil Sable**, Sanjeev Ahuja, and Haripada Bhunia "Biodegradation kinetic modelling of acrylic acid grafted on polypropylene film" *Iranian Polymer Journal*. 2020, 29:735-747 (Impact Factor: 1.707).

1.3 Publications under review/communicated

1. Sunil Sable, Sanjeev Ahuja, and Haripada Bhunia "Characterization of polypropylene composites containing modified pro-oxidant after abiotic pretreatment" *Journal of Polymer Research*. 2021, (Revision submitted) (Impact Factor: 2.426).

2. Sunil Sable, Sanjeev Ahuja, and Haripada Bhunia "Biodegradation kinetic modelling of pro-oxidant filled polypropylene composites during thermophilic phase of aerobic

composting" *Journal of Environmental Science and Pollution Research*. 2021, (Under Review) (Impact Factor: 3.052).

3. **Sunil Sable**, Sanjeev Ahuja, and Haripada Bhunia "Biodegradation kinetic modelling of modified pro-oxidant containing polypropylene films under simulated aerobic composting conditions" *Science of the Total Environment*. 2021, (Communicated) (Impact Factor: 6.551).

4. **Sunil Sable**, Sanjeev Ahuja, and Haripada Bhunia "Biodegradation kinetic modelling of modified pro-oxidant containing polypropylene films under controlled composting conditions after abiotic pretreatment" *Journal of Environmental Management.* 2021, (Communicated) (Impact Factor: 5.647).

II In Conferences

2.1 International Conference

Oral presentations

1. **Sunil Sable,** Sanjeev Ahuja, and Haripada Bhunia "An overview of biodegradable polyolefins with pro-oxidants" Proceedings *of International Conference on Seamless Chemical Engineering in Service of Humanity: Innovations, Opportunities & Challenges,* Dr. B. R. Ambedkar National Institute of Technology Jalandhar, India, December 27 – 30, 2018, p. 30.

Poster presentations

1. **Sunil Sable,** Sanjeev Ahuja, and Haripada Bhunia "Biodegradation kinetic modelling of grafted and ungrafted blends and composites of polypropylene in composting conditions" *Proceedings of International Conference on 107th Indian Science Congress on Science and Technology: Rural Development,* University of Agricultural Sciences, Bangalore, India, January 3-7, 2020, p.171.

2.2 National Conference

Poster presentations

1. **Sunil Sable,** Sanjeev Ahuja, and Haripada Bhunia **"**Biodegradability of polypropylene for flexible packaging applications" *Proceedings of National Conference on Shaping the Energy Future: Challenges & Opportunities,* CSIR-Indian Institute of Petroleum, Dehradun, India, May 10-11, 2019, p.21.

REPRINTS OF PUBLISHED ARTICLES

Journal of Polymers and the Environment (2020) 28:2236–2252
https://doi.org/10.1007/s10924-020-01762-3

ORIGINAL PAPER

Studies on Biodegradability of Cobalt Stearate Filled Polypropylene After Abiotic Treatment

Sunil Sable[1] · Sanjeev Ahuja[1] · Haripada Bhunia[1]

Published online: 27 May 2020

Abstract
This study aims to investigate the effect of abiotic treatment (accelerated weathering) of cobalt stearate (CoSt) filled polypropylene (PP) composite films on their biodegradability. The PP composite films, after abiotic treatment, were characterized by different techniques and the results were compared with those of untreated films. After biodegradation (biotic treatment) of abiotically treated composite PP films, the degradation intermediates were evaluated for their ecotoxicological impact. The presence of oxygen products after degradation of composite PP by abiotic treatment was confirmed by FTIR. The carbonyl index of abiotically treated composite films was improved with CoSt loading and with the time of abiotic treatment. After abiotic treatment, the thermal stability of the modified PP sample decreased as shown by thermogravimetric analysis (TGA). The crystallinity of CoSt filled PP decreased with increase in CoSt, as revealed by DSC and XRD, which led to enhanced degradation of PP. The highest biodegradation of abiotically treated composite PP films was shown to be 36.42% having 2 phr CoSt in it. SEM results of biotically treated films also showed erosion, several small pits and increased roughness on the modified PP films. The overall results indicate that the addition of CoSt and abiotic treatment significantly enhanced the biodegradation of PP. Eco-toxicity tests of the degraded material, namely microbial test, plant growth test, and earthworm acute-toxicity test demonstrated that the degradation intermediates were nontoxic. Hence, CoSt filled PP has high industrial potential to make biodegradable flexible packaging.

Keywords Biodegradation · Degradation · Photo-oxidation · Pro-oxidant · UV exposure

Introduction

Polypropylene (PP) is the thermoplastics that is extensively utilized for manufacturing of grocery bags, films, sheets, containers, toys, pipes, cable jacketing, etc. for different and low density and performance, like excellent ductility, chemical resistance, water barrier properties, etc. [4]. PP in a film form is used for flexible packaging applications [2, 5]. Currently, the global production capacity of PP is significantly growing because of the increasing global popu-

Unsolicited original article

Sunil Sable, Sanjeev Ahuja and Haripada Bhunia*

Effect of pro-oxidant concentration on characteristics of packaging films of cobalt stearate filled polypropylene

https://doi.org/10.1515/polyeng-2020-0065
Received March 26, 2020; accepted June 6, 2020; published online xxx

Abstract: In this work, polypropylene (PP) filled with different proportions of CoSt were prepared in a twin-screw extruder by compounding technique. Eight films of these compounds were prepared using compression moulding. The modified PP films were characterized for chemical, physical, thermal, and morphological properties (before and after biodegradation). The biodegradation of the CoSt filled PP films was studied under controlled composting conditions, and the degradation intermediates were evaluated for their ecotoxicological impact. The CoSt present in the PP film was confirmed by Fourier transform infrared spectroscopy. As the addition of CoSt was progressively increased, the tensile strength and thermal stability decreased as shown by UTM and thermogravimetric analysis. The compounding of CoSt in PP reduced its crystallinity as revealed by the differential scanning calorimetry and X-ray diffraction analysis, and this led to enhanced degradation of PP. After biodegradation, SEM results of modified PP films showed rougher morphology than before biodegradation. The maximum biodegradation (19.78%) was shown by the film having 2 phr CoSt. The ecotoxicity tests of the degraded material, namely, microbial test, plant growth test, and earthworm acute-toxicity test demonstrated that the biodegradation intermediates were nontoxic. Hence, CoSt filled PP has high industrial poten-

1 Introduction

Polyolefins like polypropylene (PP) are one of the most inexpensive and widely used commercial thermoplastic polymers [1]. PP is extensively used in flexible packaging films due to its properties, including durability, low cost, mechanical integrity, hydrophobic nature, chemical resistance, mouldability, transparency, flexibility, and effective gas and water barrier properties [2–6]. The overall consumption of flexible packaging is expected to increase from 27.4 million tons in 2017 to 33.5 million tons in 2022 [7, 8]. However, the global production capacity of degradable plastics was very small, estimated at 0.91 million tonnes in 2018 [9] when compared with the 348 million tonnes of entire plastics generated in the world in 2017 [5, 10]. The plastics create a hazardous risk to living things and natural system for its high molecular weight, hydrophobic nature, resistance to microbial attack, increased shelf-life, unavailability of functional groups, discarding issues, and lack of degradability [11–13]. The deposition of PP in different land areas leads to environment-related, economical, and waste disposal problems [14–16]. Therefore, the new material formulations that can improve the PP degradation through different ways have been very challenging for the management of environmental problems [17–20].

The addition of pro-oxidants in polyolefins like PP and polyethylene (PE) makes themoxo-degradable through a

Journal of Polymers and the Environment (2021) 29:721–733
https://doi.org/10.1007/s10924-020-01910-9

ORIGINAL PAPER

Preparation and Characterization of Oxo-degradable Polypropylene Composites Containing a Modified Pro-oxidant

Sunil Sable[1] · Sanjeev Ahuja[1] · Haripada Bhunia[1]

Accepted: 29 September 2020 / Published online: 9 October 2020

Abstract

In this study, the changes in the properties of polypropylene (PP) after loading of modified pro-oxidant were studied. Different proportions of modified-cobalt stearate (CoSt) pro-oxidant were filled in PP, and composites were prepared in a twin-screw extruder through compounding technique. Five films of these composites were prepared using hot press moulding. The modified pro-oxidant loaded PP films were characterized for chemical, physical, thermal, and morphological properties (before and after the biodegradation test). The biodegradability of the modified pro-oxidant loaded PP films was measured according to ASTM D 5338, and the biodegradation intermediate products were evaluated for their eco-toxicological effect. The changes (with respect to PP) in FTIR spectra of modified pro-oxidant loaded PP were noticed before and after accelerated ageing. The tensile properties and thermal stability of modified pro-oxidant loaded PP films decreased as confirmed by universal testing machine (UTM) and thermogravimetric analysis (TGA). Using differential scanning calorimetry (DSC) and XRD analysis, it was found that the percentage crystallinity of modified pro-oxidant loaded PP films has decreased and this led to increased degradability of PP. After the biodegradability test, SEM results of modified pro-oxidant loaded PP films revealed rougher morphology than before the biodegradability test. The highest biodegradability (28.87%) was obtained in PP100T30 film containing 30 phr of modified pro-oxidant. All the eco-toxicity tests of the degraded product materials demonstrated that the degraded products were nontoxic. Hence, the prepared composites can be effectively used as biodegradable flexible packaging materials.

Environmental Science and Pollution Research
https://doi.org/10.1007/s11356-020-11766-0

RESEARCH ARTICLE

Biodegradation kinetic modeling of pro-oxidant filled polypropylene composites under thermophilic composting conditions after abiotic treatment

Sunil Sable[1] · Sanjeev Ahuja[1] · Haripada Bhunia[1]

Received: 30 March 2020 / Accepted: 18 November 2020

Abstract
This work aims at modeling and characterizing the kinetics of biodegradation of polypropylene loaded with cobalt stearate as pro-oxidant after abiotic treatment. Eight films of these composites were prepared using different pro-oxidant loadings. These films were treated abiotically using accelerated weathering for 40 h, and biotically using aerobic composting as per ASTM D 5338. The experimental data were analyzed using an eight-parameter Komilis model containing a flat lag phase. The model formulations involved hydrolysis of primary solid carbon and its subsequent mineralization. The first step was rate controlling and it included hydrolysis of slowly (C_s), moderately (C_m), and readily (C_r) hydrolyzable carbon fractions in parallel. The model parameters were evaluated by means of nonlinear regression technique. The surface morphology of the films before and after the biodegradability test supported the biodegradation results. The model parameters and undegraded/hydrolyzable/mineralizable carbon evolutions involved moderately and readily hydrolyzable carbons but with the absence of slowly hydrolyzable carbon. These exhibit degradability in the range of 11.20-36.42% in 45 days. Biodegradability increases with progressive increase in pro-oxidant loading. The rate of degradation reaches maximum (0.322-0.897% per day) at around the 39th-12th day. For all the films, readily hydrolyzable carbon fractions and their hydrolysis rate constants (k_r) are appreciably increased with increasing pro-oxidant loading. All the films show the presence of growth phase because of their high initial readily hydrolyzable carbon fractions. The SEM images after the abiotic and subsequently biotic treatments were progressively rougher. The methods presented here can be used for the design and control of other similar systems.

Keywords Biodegradability · Composting · Hydrolysis · Nonlinear regression · Polypropylene

Journal of Environmental Management 249 (2019) 109186

Contents lists available at ScienceDirect

Journal of Environmental Management

journal homepage: www.elsevier.com/locate/jenvman

Research article

Biodegradation kinetic modeling of oxo-biodegradable polypropylene/polylactide/nanoclay blends and composites under controlled composting conditions

Sunil Sable[a], Dev K. Mandal[b], Sanjeev Ahuja[b,*], Haripada Bhunia[a]

[a] Department of Chemical Engineering, Thapar Institute of Engineering & Technology, (Deemed to be University), Bhadson Road, Patiala, 147004, Punjab, India
[b] Department of Chemical Engineering, Sant Longowal Institute of Engineering and Technology, Deemed to Be University Under MHRD, Govt of India, Longowal, 148106, Punjab, India

ARTICLE INFO

Keywords:
Biodegradation
Blend
Kinetic modeling
Polypropylene
Polylactide
Pro-oxidant

ABSTRACT

Polypropylene/polylactide/nanoclay blend/composite films with/without pro-oxidants/compatibilizer were prepared and aerobically degraded to measure the CO_2 evolution under controlled composting conditions as per ASTM D 5338. A first-order Komilis model in series with a flat lag phase was postulated involving two stages; hydrolysis of solid carbon followed by its rapid mineralization. The first, rate-limiting stage further comprised of three possible parallel paths: the solid hydrolysis of readily, moderately, and slowly hydrolyzable carbon fractions. The model parameters were computed after correlating with the experimental data using nonlinear regression analysis. The results of the model characteristic parameters, un-degraded/hydrolyzable/mineralisable-intermediate carbon kinetics, and degradation curves exhibit two distinct kinetic regimes. The first regime comprising of slowly and moderately hydrolyzable carbon is shown by the first four films without pro-oxidants. This causes low degradability and degradation rate. The second regime comprising of the readily and moderately hydrolyzable carbon is shown by another four films containing pro-oxidants. They exhibit relatively high degradability and degradation rate, which peaks at around 11–14th day in the range of 0.219–0.268% per day. The values of their moderately hydrolyzable carbon fractions and the corresponding hydrolysis rates are significantly higher than that of the first regime. For the first regime, the degradability and degradation rate decreases with increase in the slowly hydrolyzable carbon impervious to microbial attack. Their degradation rate profiles show an absence of growth phase due to the absence of readily hydrolyzable carbon. The rate decreases monotonously starting from the maximum value ranging from 0.043 to 0.180% per day. The approach presented can also be implemented to model and design equipment for other waste biodegradation systems.

1. Introduction

Polyolefins like polypropylene (PP) are widely used plastic materials and fastest growing thermoplastics in the area of packaging, medical, and automotive industries (Al-Salem et al., 2017; Holcapkova

Polylactide (PLA) is one of the most widely used biodegradable biopolymers (Hamad et al., 2018; Lv et al., 2017). However, its high cost, brittleness, and limited shelf life restrict its use in packaging applications. Several types of researches have been published on the blending of PLA with polypropylene (PP) (Choudhary et al., 2011; Jain

Iranian Polymer Journal (2020) 29:735–747
https://doi.org/10.1007/s13726-020-00834-4

ORIGINAL RESEARCH

Biodegradation kinetic modeling of acrylic acid-grafted polypropylene during thermophilic phase of composting

Sunil Sable[1] · Sanjeev Ahuja[1] · Haripada Bhunia[1]

Received: 17 February 2020 / Accepted: 30 May 2020 / Published online: 12 June 2020

Abstract

This work aims at modelling and characterizing the kinetics of biodegradation of acrylic acid-grafted polypropylene. Different films of acrylic acid-grafted polypropylene were prepared. These films were degraded aerobically during thermophilic phase of composting process for measurement of carbon dioxide evolution as per ASTM D 5338. The experimental data were analyzed using an eight-parameter Komilis model containing a flat lag phase. The model formulations involved hydrolysis of primary solid carbon and its subsequent mineralization. The first step was rate controlling and it included hydrolysis of primary slowly, moderately, and readily hydrolyzable carbon fractions in parallel. The model parameters were evaluated by means of nonlinear regression technique. The model parameters, undegraded/hydrolyzable/mineralizable carbon evolutions and morphology revealed two typical kinetic regimes. The first five films exhibited slow degradation in the first regime involving slowly and moderately hydrolyzable carbons. They exhibited low degradability value in the range of 1.5–3.7% in 45 days. Their degradability decreased with an increase in the slowly hydrolyzable carbon refractory in nature. The remaining three films exhibited the second regime involving the moderately and readily hydrolyzable carbons. These showed relatively high degradability in the range of 4.7–5.6% in 45 days. The magnitudes of their moderately hydrolyzable carbon fractions were substantially higher than those of the first regime. All the eight films showed the absence of growth phase because of their small initial readily hydrolyzable carbon fractions. The study shows progressive enhancement in the biodegradation of effectively non-biodegradable polypropylene with an increase in degree of acrylic acid grafting. The methods presented here can be used for the design and control of other similar systems.

Keywords Biodegradability · Hydrolysis · Nonlinear regression · Polypropylene · Radiation grafting

Introduction

Plastics have become an essential part of our lifestyle and plastic production worldwide has exceeded 150 MT per year [1, 2]. Synthetic polymeric materials like polypropylene (PP) are extensively used for packaging applications However, the polymers like PP are not eco-friendly because of the lack of hydrophilic nature and absence of functional groups. Consequently, their disposal and management at the end of their service life are a cause of significant global concern [7–9]. These factors have led to the development of environmentally degradable polymeric material that can